Steric exclusion chromatography:

Advancement of a laboratory-based platform technology into a key component of viral vector and vaccine production processes

Dissertation

Zur

Erlangung des akademischen Grades des Doktors der Ingenieurwissenschaften

(Dr.-Ing.)

Dem Promotionszentrum für Ingenieurwissenschaften

am Forschungscampus Mittelhessen

vorgelegt von

Keven Lothert, M.Sc.

Gießen, den 25.06.2021

Datum der Disputation: 16.03.2022

Acknowledgements

I would like to express my gratitude to all the people who helped and supported me during the recent years of this work, either directly or indirectly.

I want to thank my supervisors Prof. Dr. Michael Wolff and Prof. Dr Bernd Smarsly for taking the time to evaluate the outcome of the performed work and for the given feedback so far. Additionally, I want to thank Michael for the opportunity to work in his lab and be a part of his growing group, for the open door and always taking the time to discuss questions and results.

Another huge thank you to the people sharing the office with me, who supplied both fruitful discussions and leisure talking. While these people were changing over time and included Daniel Loewe, Hauke Dieken, Daniel Humpert and Carolin Lappöhn, I want to thank Friederike Eilts in particular. We shared most of the laughter (the real one and the cynical one), the thoughts and the frustration on joint and individual projects.

To my students, particularly to Felix Beyer, Arabi Sivanesapillai and Guiliano Lauria, whose studies significantly advanced this work. Guiding them to completing their degrees, helped a lot to learn one or another lesson on my own.

Many thanks also to all the collaboration partners, who helped driving this work by supplying (feed-) materials or technical assistance. In that regard I want to especially name Felix Pagallies and Ralf Amann from the University Hospital of Tübingen and Karl Pflanz and Jennifer Labisch from Sartorius Stedim Biotech GmbH.

Furthermore, I want to thank all the colleagues in the IBPT and especially the cell culture technology lab, who ensured a pleasant working atmosphere and always offered advice and support, either scientifically or for the everyday life.

Last but not least, I want to thank my family, especially my wife Ines for the love and motivation and my parents for financial and mental support throughout my studies.

Eidesstattliche Erklärung / Declaration of authorship

Ich erkläre: Ich habe die vorgelegte Dissertation selbstständig und ohne unerlaubte fremde Hilfe und nur mit den Hilfen angefertigt, die ich in der Dissertation angegeben habe. Alle Textstellen, die wörtlich oder sinngemäß aus veröffentlichten Schriften entnommen sind, und alle Angaben, die auf mündlichen Auskünften beruhen, sind als solche kenntlich gemacht. Ich stimme einer evtl. Überprüfung meiner Dissertation durch eine Antiplagiat-Software zu. Bei den von mir durchgeführten und in der Dissertation erwähnten Untersuchungen habe ich die Grundsätze guter wissenschaftlicher Praxis, wie sie in der entsprechenden Satzung der federführenden Hochschule niedergelegt sind und die mir ausgehändigt wurde, eingehalten.

I declare that I have completed this dissertation single-handedly without the unauthorized help of a second party and only with the assistance acknowledged therein. I have appropriately acknowledged and cited all text passages that are derived verbatim from or are based on the content of published work of others, and all information relating to verbal communications. I consent to the use of an anti-plagiarism software to check my thesis. I have abided by the principles of good scientific conduct laid down in the regulations of the leading University which were delivered to me in carrying out the investigations described in the dissertation.

Gießen, 25.6.21 ------  Keven Lothert

Abstract

Biological macromolecules, such as viruses, virus-like particles or extracellular vesicles represent an important and permanently growing element in the biopharmaceutical industry. These macromolecules applied as pharmaceutical products have proven suitable for prophylactic or therapeutic vaccination, oncolytic therapy or gene transfer, to name only a few. Beside the challenge of producing sufficient amounts of product, its purification during the downstream processing, for example from cell culture harvests, is of major importance to allow a safe and efficient application. A large variety of particles differing in their physicochemical properties, possibly affecting their stability and their interaction with surrounding molecules, requires multifaceted processing strategies. For this reason, purification process development can be a time and cost consuming element, which emphasizes the benefits of flexible techniques that can be applied to a variety of different products. Over the past ten years the steric exclusion chromatography (SXC) was introduced as a possible platform technique for a fast and effective purification of macromolecules and nanoplexes such as large proteins, bacteriophages, and viruses. The technique was derived from the principle of polymer induced crowding mechanisms, that are already known for several decades. Although the method highly depends on the size of the target product, all the influencing process parameters and mechanisms of the method are not yet thoroughly understood. The SXC has been applied as an independent process unit operation but has not been implemented in large scale biopharmaceutical production. The latter can be mainly attributed to the novelty of the principle, the lack of appropriate stationary phases suitable for industrial production, and an inherent skepticism against new approaches compared to established and regulatory accepted procedures. This work aims to bridge laboratory applications of the SXC with scaled approaches of up to 200 L by suggesting possible processing schemes employing that technique as a major purification backbone. Simultaneously, these studies provide further insight into critical process parameters to allow for an improvement of the mechanistic understanding concerning the method itself. In the chapters of this work the successive implementation of the SXC into complete downstream processing schemes for viral vectors and vaccines is shown. While Chapter 1 gives an overview to introduce the importance of improving and extending the existing portfolio of purification procedures, it also introduces the benefits of applying platform technologies. Particularly the principle and advantages of the SXC are described as well as the scope of this thesis is outlined. Chapter 2 summarizes the general approach for applying and optimizing the SXC using the baculovirus vector as a model and Chapter 3 shows a screening comparison of the SXC against and in combination with well-known purification techniques. Afterwards, in Chapter 4, the platform applicability in complete processing schemes is shown for Hepatitis C and Orf virus purification targeting potential applications in human or veterinary medicine. Finally, Chapter 5 gives a short summary, including an outlook on future prospects and remaining hurdles.

Zusammenfassung

Biologische Makromoleküle, wie Viren, Virus-ähnliche Partikel oder extrazelluläre Vesikel sind ein wichtiger und zunehmend größerer Bestandteil biopharmazeutischer Produktionsprozesse. Diese Makromoleküle eignen sich unter anderem für prophylaktische und therapeutische Impfungen, Tumortherapie oder Gentransfer. Neben der Herstellung von ausreichenden Produktmengen ist auch deren so genannte Aufreinigung („Downstream Processing“), zum Beispiel aus der Zellkulturernte, von besonderer Bedeutung, um eine sichere und effiziente Therapie zu gewährleisten. Die Aufreinigung von biologischen Nanoplexen sieht sich mit einer Vielzahl verschiedener Partikel konfrontiert, welche sich zum Teil stark in ihren physikochemischen Eigenschaften unterscheiden und dadurch individuelle Stabilitäten und Interaktionen mit ihrer Umgebung aufweisen. Dadurch ist die Entwicklung und Optimierung von Aufreinigungsprozessen oftmals sehr zeit- und kostenintensiv. Dies steigert den Wunsch nach flexiblen Methoden, welche mit geringfügigen Adaptionen für eine Vielzahl von Nanoplexen eingesetzt werden können. In den letzten zehn Jahren wurde die sterische Exklusionschromatographie (SXC) als mögliche Plattformtechnologie zur schnellen und effektiven Aufreinigung von Makromolekülen, wie beispielsweise großen Proteinen, Bakteriophagen und Viren entwickelt. Das hierfür genutzte Prinzip der Zusammenlagerung von Molekülen in einer Lösung durch Zugabe von Polymeren ist bereits seit einigen Jahrzehnten bekannt. Die Methode ist hauptsächlich von der Größe des Zielproduktes abhängig, jedoch sind zum jetzigen Stand nicht alle Einflussparameter und der zu Grunde liegende Mechanismus vollständig erforscht. Auch wurde die SXC noch nicht im großen Maßstab im Prozess der Herstellung eingesetzt. Grund hierfür ist vermutlich die Neuheit der Methode und damit eine geringere Akzeptanz, sowie das Fehlen von prozesstauglichen und qualifizierten stationären Phasen und eine aktuell noch geringe Datenlage. Die vorliegende Arbeit hat die Zielsetzung eine Verbindung zwischen der Prozessentwicklung im Labor und der industriellen Herstellung bis hin zum 200 L Maßstab zu finden, indem sie Prozesse darstellt, deren Schwerpunkt auf der SXC beruht. Gleichzeitig bietet sie einen tieferen Einblick in kritische Einflussfaktoren und kann so zum besseren Verständnis über den Mechanismus der Methode beitragen. Die Kapitel dieser Arbeit stellen die fortlaufende Entwicklung der SXC von der individuellen Anwendung bis hin zu ihrer Integrierung in vollständige Verfahrensabläufe zur Impfstoff- und Virusvektorherstellung dar. Kapitel 1 gibt dabei einen Überblick über vorhandene Reinigungsmethoden und veranschaulicht, warum diese permanent optimiert und erweitert werden müssen. Insbesondere das Prinzip der SXC sowie ein Überblick über die im Rahmen dieser Arbeit durchgeführten Versuche werden beschrieben. Kapitel 2 zeigt die allgemeine Herangehensweise bei der Verwendung und Optimierung der SXC am Beispiel von Baculovirusvektoren. Kapitel 3 beschreibt die Gegenüberstellung und Kombination der SXC mit bekannten chromatographischen Methoden. Weiterführend wird in Kapitel 4 die Plattformtauglichkeit für Prozessschemen auf Basis der SXC am Beispiel von Hepatitis C und Orf Viren beschrieben. Abschließend wird in Kapitel 5 der aktuelle Stand zusammengefasst und in einem Ausblick noch zu bewältigende Hürden aufgezeigt.

Table of contents

List of Abbreviations

AEX	Anion exchange chromatography
CEX	Cation exchange chromatography
CDMO	Contract development and manufacturing organization
DSP	Downstream processing
dsDNA	Double stranded DNA
EMA	European medicines agency
FDA	Food and drug administration
GMP	Good manufacturing practice
GRAS	Generally recognized as safe
HCV	*Hepatitis-C-virus*
HEK	Human embryonic kidney
HIC	Hydrophobic interaction chromatography
IEX	Ion exchange chromatography
MDCK	Madin-Darby kidney cells
ORFV	Orf virus (*Parapoxvirus ovis*)
PEG	Polyethylene glycol
pI	Isoelectric point
SEC	Size exclusion chromatography
SPF	Specific pathogen free
SXC	Steric exclusion chromatography
STR	Stirred tank reactor
TFF	Tangential flow filtration
USP	Upstream processing
VLP	Virus like particle

List of own publications, presentations and patents related to the dissertation

Paper

i. Lothert, Keven; Sprick, Gundula; Beyer, Felix; Lauria, Guiliano; Czermak, Peter; Wolff, Michael W. Membrane-based steric exclusion chromatography for the purification of a recombinant baculovirus and its application for cell therapy (2020) Journal of Virological Methods 275 113756 DOI: 10.1016/j.jviromet.2019.113756

ii. Lothert, Keven; Pagallies, Felix; Feger, Thomas; Amann, Ralf; Wolff, Michael W. A selection of possible chromatographic downstream processing unit operations for Orf virus purification (2020) *Journal of Biotechnology* 323 P. 62-72 DOI: 10.1016/j.jbiotec.2020.07.023

iii. Lothert, Keven; Pagallies, Felix; Eilts, Friederike; Sivanesapillai, Arabi; Hardt, Martin; Moebus, Anna; Feger, Thomas; Amann, Ralf; Wolff, Michael W. A scalable downstream process for the purification of Orf virus (2020) *Journal of Biotechnology* 323 P. 221-230 DOI: 10.1016/j.jbiotec.2020.08.014

iv. Lothert, Keven*; Offersgaard, Anna*; Pihl, Anne F.; Mathiesen, Christian K.; Jensen, Tanja B.; Alzua, Garazi P.; Fahnoe, Ulrik; Bukh, Jens; Gottwein, Judith M.$; Wolff, Michael W.$ Development of a downstream process for the production of an inactivated whole hepatitis C virus vaccine (2020) *Scientific Reports* 10 16261 DOI: 10.1038/s41598-020-72328-5
*,$ equal contributions

Book chapters

i. Hoffmann, Daniel; Leber, Jasmin; Loewe, Daniel; Lothert, Keven; Oppermann, Tobias; Zitzmann, Jan; Weidner, Tobias; Salzig, Denise; Wolff, Michael W.; Czermak, Peter Purification of new biologicals using membrane-based processes in Membrane Processes in the Pharmaceutical and Biotechnological Field (Editor: Angelo Basile) (2018) DOI: 10.1016/B978-0-12-813606-5.00005-1

ii. Lothert, Keven*; Dekevic, Gregor*; Loewe, Daniel; Salzig, Denise; Czermak, Peter; Wolff, Michael W. Up-Downstream processing of biological nanoplexes in Methods in Molecular Biology -Vaccine Delivery Technology (Editors.: Blaine Pfeifer, Andrew Hill) (2021) DOI: 10.1007/978-1-0716-0795-4_12
*equal contributions

Patents

i. Priority submission EPÜ, Method for Virus Production, Number: EP20159795, Day of submission: 27.02.2020, Inventors: Wolff, Michael W.; Lothert, Keven; Amann Ralf; Pagallies, Felix; Feger Thomas; Submitted by: Technische Hochschule Mittelhessen, Eberhard-Karls-Universität, Tübingen

ii. EP, Method of purifying whole virus particles: Number: EP20186549.0, Day of submission: 17.07.2020, Inventors: Wolff, Michael W.; Lothert, Keven; Gottwein, Judith M.; Offersgaard, Anna; Bugk, Jens; Pihl, Anne F.; Submitted by: Technische Hochschule Mittelhessen, Copenhagen University Hospital

Conference contributions

a. Talks

i. Marichal-Gallardo, Pavel; Lothert, Keven; Grein, Tanja; Reichl, Udo; Czermak, Peter; Wolff, Michael W. Purification of cell culture-based virus particles by steric exclusion chromatography, ACS 2018, 18.-22.03.2018 New Orleans, USA

ii. Lothert, Keven; Beyer, Felix; Sprick, Gundula; Czermak, Peter; Wolff, Michael W. Purification of insect cell culture derived recombinant baculovirus by steric exclusion chromatography for cell therapy application, INSECTA 2018, 5.-7.09.2018 Giessen, Germany

iii. Wolff, Michael W.; Lothert, Keven; Eilts, Friederike; Development of production processes for vaccines and viral vectors, BioSeparations Forum 1.10.2020, virtual

vii. Eilts, Friederike; Lothert, Keven; Pagallies, Felix; Amann, Ralf; Wolff, Michael W.; The impact of purification on the particle integrity of the Orf virus analyzed for an established downstream process, ACHEMA pulse 2021, 15.-16.06.2021, virtual

b. Posters

i. Lothert, Keven; Loewe, Daniel; Grein, Tanja A.; Czermak, Peter; Wolff; Michael W. Purification of cell culture-derived oncolytic measles virus by membrane chromatography, ACS 2018, 18.-22.03.2018 New Orleans, USA

ii. Lothert, Keven; Beyer, Felix; Sprick, Gundula; Czermak, Peter; Wolff, Michael W. Steric exclusion chromatography for recombinant baculovirus purification: Model for an affordable, fast and efficient capture platform, 3rd Bioprocessing of Advanced Cellular Therapies Congress 2018, 29.-30.05.2018, Frankfurt, Germany

iii. Lothert, Keven, Beyer, Felix; Sprick, Gundula; Czermak, Peter; Wolff, Michael W. Steric Exclusion Chromatography for the purification of recombinant baculovirus, Vaccine Technology VII 2018, 17.-22.06.2018 Mont Tremblant, Quebec, Canada

iv. Wolff, Michael W.; Marichal-Gallardo, Pavel; Lothert, Keven; Fortuna, Ana R.; Czermak, Peter; Reichl, Udo A step towards globally affordable vaccines & gene therapies: Steric exclusion chromatography as a capture platform, Recovery of Biological Products XVIII 7.-12.10.2018 Asheville, North Carolina, USA

v. Lothert, Keven; Feger, Thomas; Amann, Ralf; Wolff, Michael W. A fast and scalable purification technique for vaccines and viral vectors: Purification of parapoxvirus particles using steric exclusion chromatography, ISPPP 2018, 04.-07.11.2018, Berlin, Germany

vi. Eilts, Friederike; Harsy, Yasmina M.J.; Orbay, Sabri; Lothert, Keven; Pagallies, Felix; Amann, Ralf; Wolff, Michael W. Charge-dependent purification of nanoparticles by steric exclusion chromatography, Himmelfahrtstagung on Bioprocess Engineering 2021 - New Bioprocesses, New Bioproducts, 10.-12.05.2021, online-event

Chapter 1 - Introduction

Recurrent diseases, such as the annual Influenza A wave, have been the main driver for developing easily adjustable platform processes for decades. More prevailing, the SARS-Cov-2 pandemic has once again drawn attention to critical bottlenecks during vaccine production and stresses the importance of flexible, fast-in-place production technologies that can quickly be adapted to new targets. This production incorporates both major aspects of biopharmaceutical manufacturing, the upstream processing (USP) as well as the downstream processing (DSP). For the sake of completeness, in the following, an overview on pharmaceutical macromolecules and both phases of processing, USP and DSP, is given, focusing mainly on the DSP.

Nanoplexes as vaccines, gene- and onco-therapeutic vectors

More than 220 years have passed since Edward Jenner showed a successful smallpox vaccination using the vaccinia virus by the end of the 18th century.[1] Since that time, the knowledge on viruses has greatly advanced yielding a thorough insight into production and application possibilities. Jenner's approach is a first example for using live attenuated viruses for vaccination. Today numerous biopharmaceutical products based on viruses are available on the market addressing different therapeutic challenges.[2] Beside classical vaccination against infectious diseases, therapeutic targets include gene- and anti-tumor therapy in terms of vector technologies or oncolytic treatment.[3–7] For vaccination, oncolytic treatment or gene therapy a variety of different approaches are feasible with individual properties and possibilities.[1,8–11] With regard to biopharmaceutical products and nanoplexes, not considering proteins, these include the use of nucleic acids, for example in RNA/DNA vaccines, viruses, and virus-like particles (VLPs).[2,12–14] In contrast to whole virus particles, VLPs only comprise of structural subunits of a virus, but do not contain it's genomic information. While nucleic acid vaccines represent an effective way to carry a specific information without major immunogenic site effects (e.g. against a vector), site-specific targeting inside the patient and uptake into the respective cells are not easily achievable.[15,16] Here, nanoplexes, such as viruses, VLPs or extracellular vesicles, offer certain benefits. These include an enhanced activation of the immune system, additional protection of the contained genetic information, as well as a site-specific mode of action to name only a few.[4,17–20] The specific kind of application is dependent on the desired effect and might involve the use of the whole active (equals infective) or inactivated viruses[21,22], as well as the use of disintegrated viruses or VLP parts in terms of split- or subunit vaccines (Figure 1).[23,24]

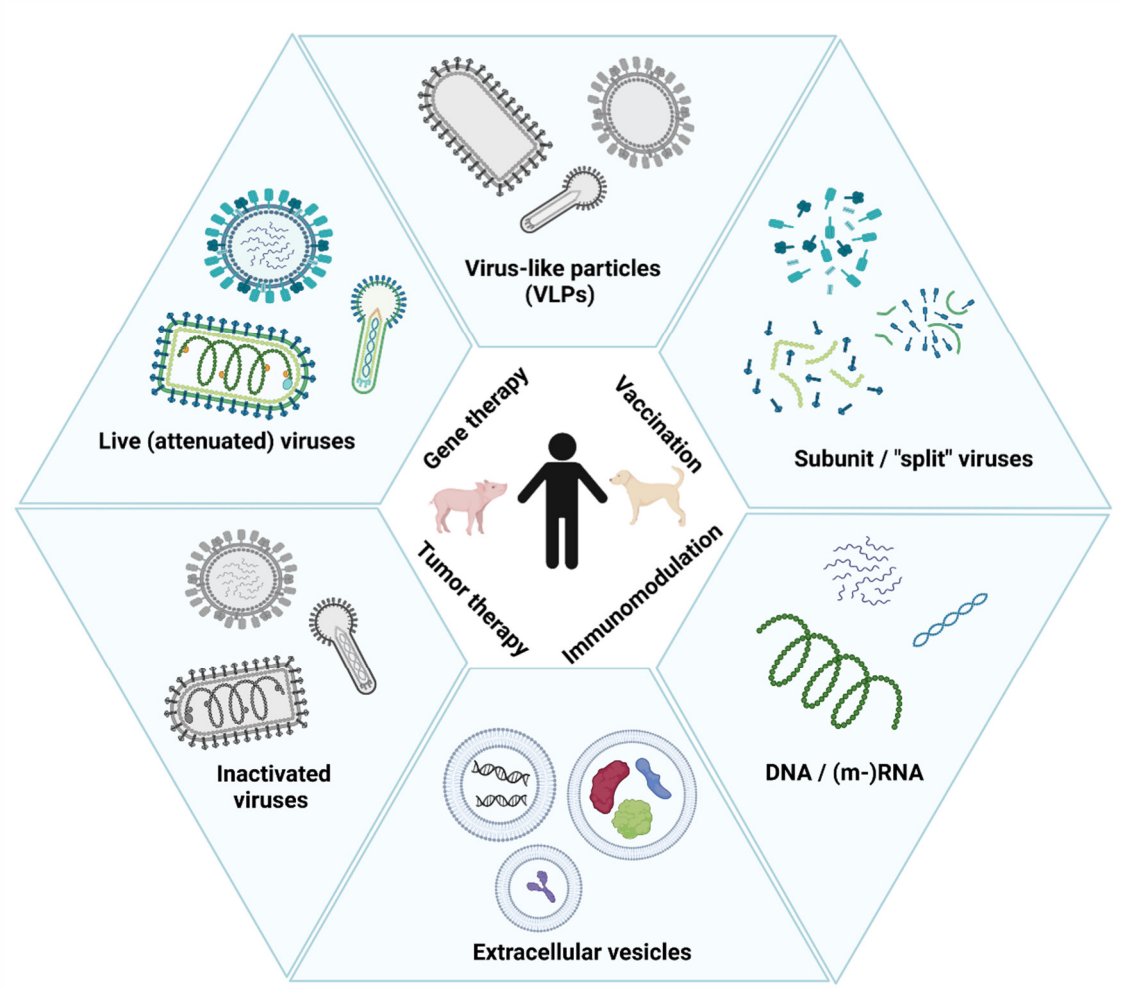

Figure 1 Different types of biological macromolecules and nanoplexes used for vaccination, as viral vectors or for tumor therapy. For therapeutic applications in humans and animals, various approaches are possible. Beside using whole and infective viral particles, these might as well be inactivated or mimicked by using virus-like particles (VLPs). Furthermore, the application of viral subunits ("split" vaccines) or of nucleic acids carrying the required information is feasible. Additionally, the use of extracellular vesicles facilitates the transport inside the host. (The figure was created using BioRender.com).

Consecutively novel approaches are developed in order to achieve the desired therapeutic goal. On the one hand this is driven by the desire to tackle unmet therapeutic tasks and find more effective approaches to already existing treatments.[25] On the other hand, in some cases a vector specific immunity might be developed, limiting its repeated usage to different applications.[26,27] Therefore, the identification of new nanoplexes does not only include viruses from human or animal origin, but potential products are derived from various sources, such as insects and plants.[28–31] In any case and independent of the nanoplex type and intended application form, the product has to be amplified in sufficient amounts, granting an economic provision of product harvest as starting material, which is the major responsibility of USP production.

USP production for product amplification

The main focus during USP processing of viruses is the maximization of product titers, while at the same time maintaining economic conditions using raw- and process materials, which are compliant to regulatory guidelines.[32–35] As viruses are unable to replicate on their own and per definition do not “live”, host cells are required that are capable of producing the individual components constituting the virus or the VLP.[36–39] Traditionally, vaccine generation was dependent on animals, for example by using lymph of infected calves, pigs or rabbits.[40] Later, virus production was also done in (chicken) eggs or embryos, as this displayed an easy and inexpensive alternative.[41] Even today a multitude of production processes are in place that utilize this technique, e.g. for Influenza vaccines.[42,43] The embryonated eggs are infected with the virus of interest and incubated for its propagation. Although, this approach offered a certain platform character, given by the premise of viruses being able to infect the embryoblast cells, it only has limited optimization potential in terms of product titers.[44] Only a few parameters, such as the compartment of inoculation in the embryonated egg or the incubation temperature and time might be adjusted depending on the virus of interest.[45–47] In consequence, the amplification in eggs is a rather uncontrolled procedure. Furthermore, the scalability is problematic, due to the large amount of specific-pathogen-free (SPF) eggs that are required and the resulting efforts for planning and logistics.[48] To overcome this limitation, virus production in cell-culture has been developed and optimized for several decades. The major advantage is to use virus-specific host cells, enabling a highly improved infection and replication efficiency and thus increasing product titers.[49,50] These host cells included on the one side naturally occurring and adapted cells lines, such as human embryonic and Madin-Darby canine kidney cells (HEK or MDCK) or vero cells derived from the African green monkey.[51,52] On the other side, specifically designed cells, such as AGE1.CR, EB66 or PER.C6 cells, were genetically modified to improve productivity and product titers, for example by enhancing the cellular metabolism.[53] In this respect, the development was less oriented for platform processes spanning over a variety of viruses but rather for optimization for one target virus, including its corresponding genotype variations. Beside the cell line itself, the employed cultivation strategy affects the resulting outcome. Early cultivations were mostly based on static virus production using adherent host cells. Over time this was carried forward to using stirred tank bioreactors (STRs) either with microcarriers for adherent cells, or directly with suspension cell culture. The application of STRs improved online process control, for example regarding pH and oxygen levels, and by that further optimized cell densities, nutrient supply and altogether viral yields.[54,55] Furthermore, the implementation of fed-batch or even continuous processing schemes became feasible.[56–58] Depending on the intended scale and the cultivated cells, other alternatives to the STR include the application of orbital shakers or wave bags,

offering different agitation modes and hence shear forces compared to the impellers used in the STR.[59,60] Most of these reaction systems are available in single use, reducing the risk of contamination and the required sterilization procedures.[61] Beside the cells and the cultivation system that is used for cell cultivation and product amplification, the utilized culture medium is another important aspect to alter the product yields. While serum containing media are tolerated by most of the cells, medium development towards serum-free or chemically defined media allows a reduced level of initial contaminant levels, such as proteins, higher process robustness and potentially increased product titers.[62–64] Nevertheless, the adaption to chemically defined medium is a time-consuming approach and the success rates are dependent on the demands of the respective cells.[53,65]

Although adaptions and improvements during USP allow an optimization of product yields, also the process-related contaminants are highly dependent on the selected production conditions.[66,67] Thus, increased product amounts in the cultivation might come hand in hand with an elevated burden of byproduct. The majority of these process-related contaminants comprise of host-cell derived debris highlighting especially the protein and DNA levels, which are particularly responsible for immunogenic side effects in the later patient.[68,69] Acceptable levels of residual protein and DNA levels are defined by the regulatory authorities, such as the United States' Food and Drug Administration (FDA) or the European Medicines Agency (EMA).[70–72] The choice of the virus amplification system defines the resulting type and degree of contamination. By adjustment of the cultivation conditions, e.g. time of harvest, impurity levels might be varied. In any case the USP process results in a rather heterogenous mixture of product and process related contaminants, which need to be removed, in order to enable a safe therapeutic treatment of both humans and animals. The removal of process-related contaminants is the main focus and challenge of the subsequent DSP strategies.[73,74] This dependency particularly indicates the importance of a directed and structured process development. Optimizing later DSP procedures, while at the same time changing USP parameters, greatly increases the required effort and results in recurring fine-tuning. Hence, USP production should be settled and robust, before starting the development of associated DSP procedures.

Common DSP purification techniques – possibilities and limitations

Standard DSP strategies comprise of a series of unit operations, each tackling another aim, including impurity removal, product concentration or adjustment of the buffer composition (Figure 2).[67,72–74]

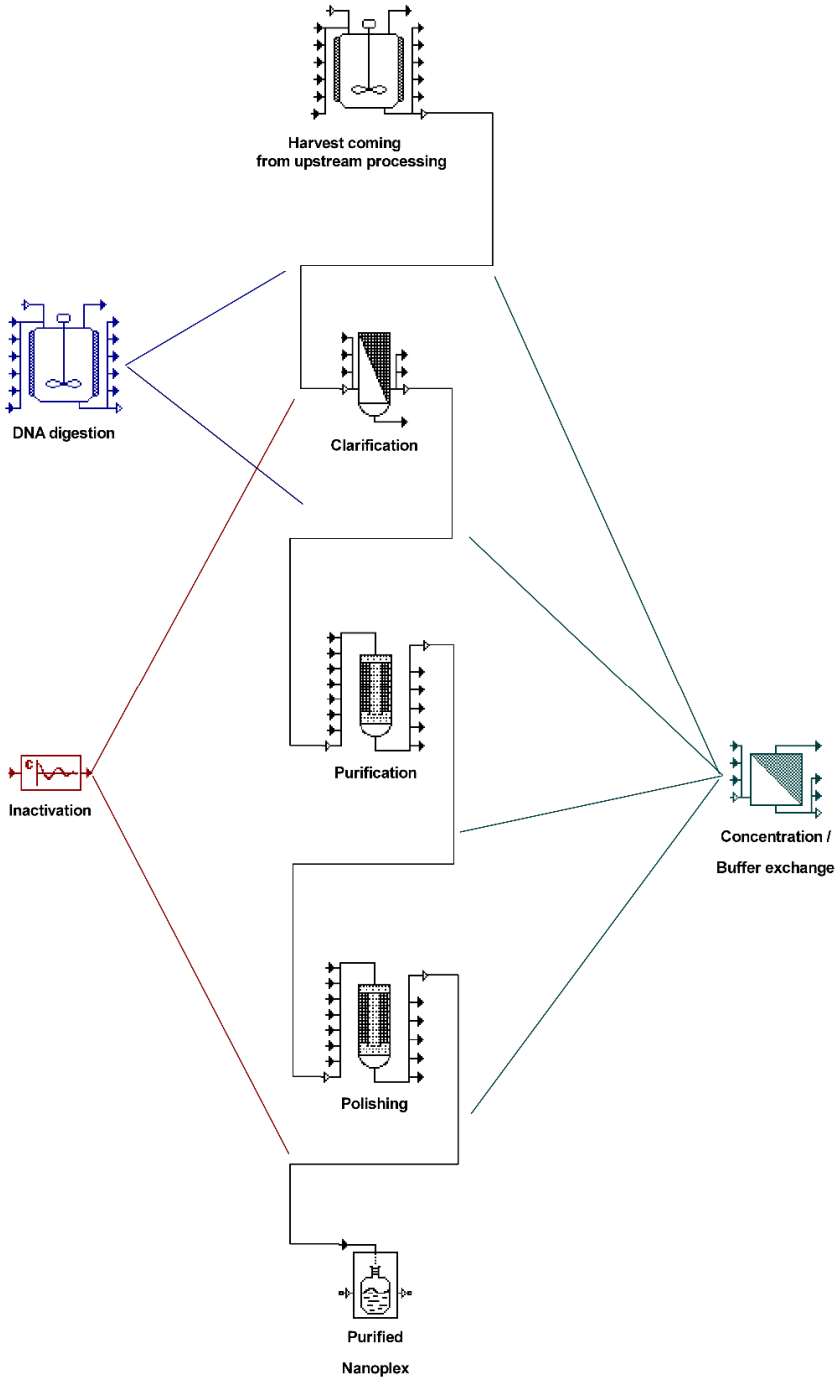

Figure 2 Example of a standard process scheme for a viral vaccine purification procedure. Generally spoken, the downstream processing (DSP) train can be divided into the different steps of clarification, purification and polishing. While the clarification aims to reduce the burden of larger particles, such as cells and cell debris, during purification and polishing host cell derived DNA and protein levels as well as other process-related impurities should be removed. Depending on the intended application and type of product, additionally nuclease treatments or inactivation procedures can be inserted at the indicated positions. Furthermore, concentration and buffer exchange, if for example required for subsequent unit operations or adequate formulation, are possible.

The first part of a DSP train after the harvest usually targets the removal of remaining host cells, cellular debris and larger aggregates formed during the USP. This is generally achieved by means of centrifugation, depth, ultra, or tangential flow filtration (TFF).[75–78] Depending on the respective product composition, a sequence of processing steps is often applied either by the sequential increase in centrifugation speed, or by the decrease of the filter pore size. Depending on the targeted production scale, however, the use of either filtration or centrifugation is more prevailing.[76] High investment costs when considering large scale centrifuges or such suitable for continuous processing have to be mentioned in that regard. Filtration applications, on the other side, are well scalable allowing a high throughput and also enabling single-use applications. Single-use is particularly beneficial, as it comes along with reduced costs and time for cleaning and sterilization procedures, including its validation.[79–81] Disadvantages using membrane filters for clarification might include, among others, the possible unspecific retention of product on the filter membranes, an increased shear stress for the product, and the recurrent costs of consumables. Despite the advantages of filtration-based techniques, the purification potential is limited. Especially when processing nanoplexes, ranging in sizes from a few up to several hundred nanometers, filters must enable an unhindered passage of these particles. Using appropriate filter cut-offs, consequently anything smaller, such as DNA and proteins will be co-purified, unless binding to larger cellular debris or being (un-)specifically retained, e.g. due to charge specific interactions. A useful variation in this regard is to perform a TFF instead of depth, or ultrafiltration, with the latter ones being generally considered as dead-end filtrations (Figure 3, left). A striking benefit of the TFF is that it can be used to retain the nanoplexes without directly filtering out the product as the filter membrane is overflown by the feed (Figure 3, right). Only the components smaller than the membrane cut-off are able to pass along with the solvent. Accordingly, the product in the retentate gets concentrated.[82,83] The continued addition of buffer to the retentate vessel, enables a simultaneous buffer exchange, pointing out the advantage of the TFF as a unit operation for a combined concentration and diafiltration.[51] While doing so the repeated circulation of the product through the TFF system has to be considered. This opposes an elevated shear stress, probably resulting in product losses, especially for sensitive nanoplexes, such as enveloped viruses. During the TFF, naturally, anything larger than the cut-off selected to concentrate the target product is equally concentrated in the retentate. Hence, the technique only offers limited applicability during clarification and although it is occasionally applied for the latter, this unit operation is most often placed after the clarification, prior to final formulation or a train of TFF units is used as a major purification step.[84,85] Regarding this, the TFF has a promising purification performance, however, molecules are not necessarily retained only according to their size and the membrane cut-off. Instead, a certain amount of the impurities

present in the starting material are co-concentrated. This holds especially true for the contained DNA, which might form complexes or aggregates with the product and its depletion reflects a common challenge. [86] To overcome these limitations a series of different TFF membranes might be applied or an additional nuclease digestion step included. Although in that manner, satisfactory purification results can be achieved, filtration-based clarification and concentration alone is not sufficient for pharmaceutical applications in many cases.

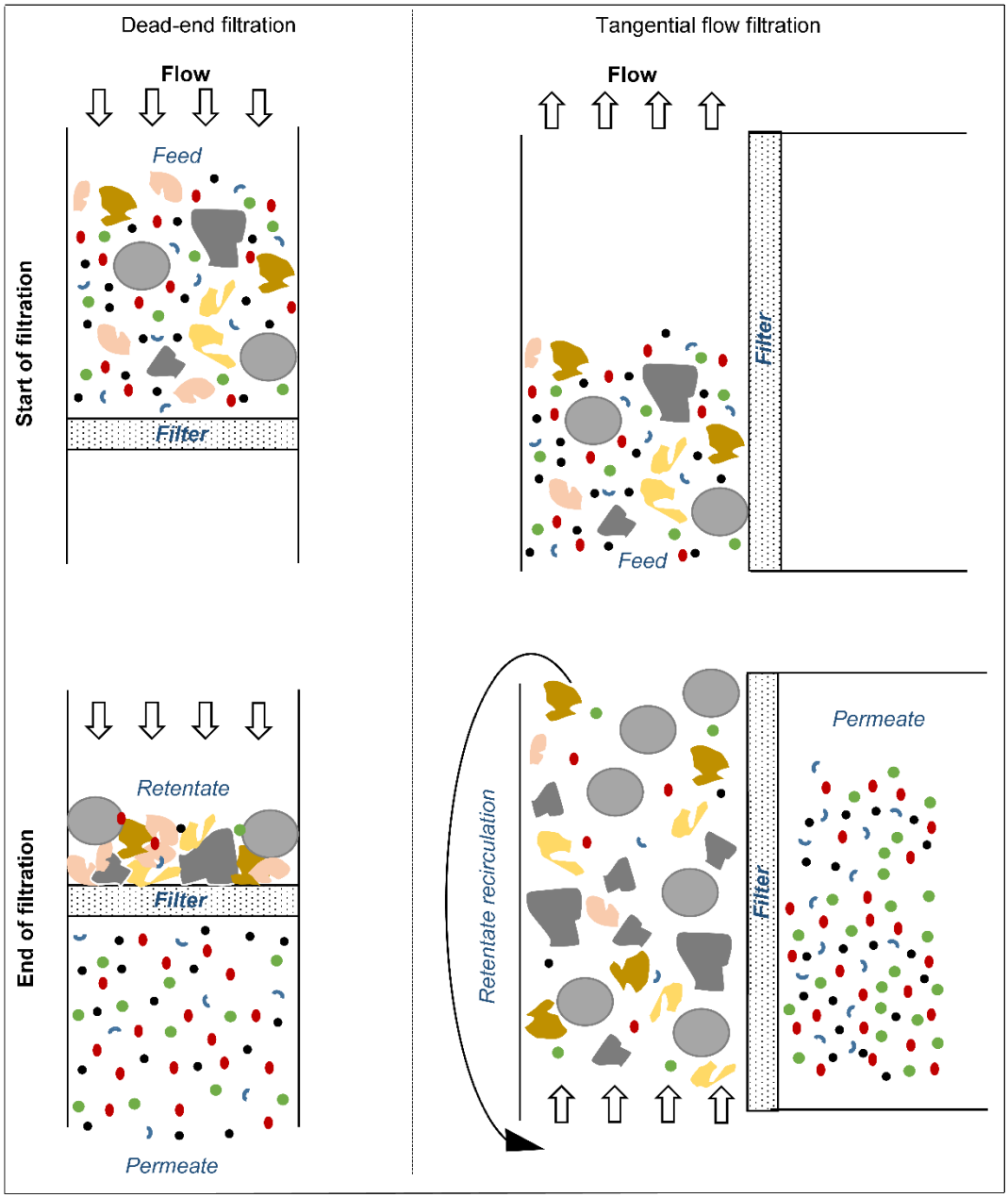

Figure 3 Working principles of the dead-end (left) and the tangential flow filtration (TFF, right) techniques. While dead-end technologies, such as ultra and depth filtration are well suited for retention of large particles (e.g. cell debris), letting the product and the majority of smaller contaminants pass, the TFF offers the possibility of product concentration, buffer exchange and impurity clearance in one step. Filter cake formation during dead-end filtration might lead to performance and product losses. However, cyclic recirculation during TFF might as well cause product disruption.

For the sake of completeness another approach to concentrate the product instead of using the TFF must be mentioned. This involves the use of density gradient (ultra-) centrifugation by use of, for example, sucrose-, CsCl or iodixanol gradients and centrifugation speeds in the range of 40,000 x g up to 100,000 x g[87–89]. As the separation is affected by the density of the molecules in solution, high purity levels can be obtained under more gentle conditions compared to TFF depending on the size of the target product. Nevertheless, the throughput is limited, and often requires a preceding concentration or accordingly large devices. The introduction of zonal centrifuges is a notable possibility in this regard.[90,91] However, as mentioned for the clarification, the investment costs for such devices are high, and expenses for cleaning and sterilization and respective validation procedures need additionally to be considered. Furthermore, as for the TFF a co-concentration of contaminants is possible.[92]

In terms of scalability, flexibility, and throughput, as well as for method specificity and, hence, purification performance, chromatography is still a key technology for nanoplex production processes.[93] Although there is a tendency to avoid chromatographic steps in the purification workflow, not at least due to high costs of chromatographic media[94,95], a vast range of methods was established and evaluated employing different chemistries and separation principles over the past decades. Figure 4 displays an overview on key technologies utilizing chromatography during the DSP. The method development for the chromatographic purification of nanoplexes was originally based on the knowledge of commonly applied DSP techniques used for proteins, particularly for antibody production.[73] Thus, mainly bead-based chromatography resins were applied in the beginning using ion exchange (IEX), for anion (AEX) or cation exchange (CEX)[96,97], hydrophobic interaction (HIC)[98] or size exclusion chromatography (SEC)[99,100]. However, especially for antibody production, affinity chromatography proved to be a superior possibility in terms of selectivity and hence in obtained purity levels.[101] Unfortunately, well established affinity methods, such as the popular Protein A resin for monoclonal antibody purification, are highly expensive. More importantly, also their application to nanoplexes, which differ a lot in their surface composition from single proteins was not possible and thus represents no straightforward approach.[102] Hence, specific affinity methods were developed for various types of viruses with its most prominent representative being the heparin affinity.[103–106]

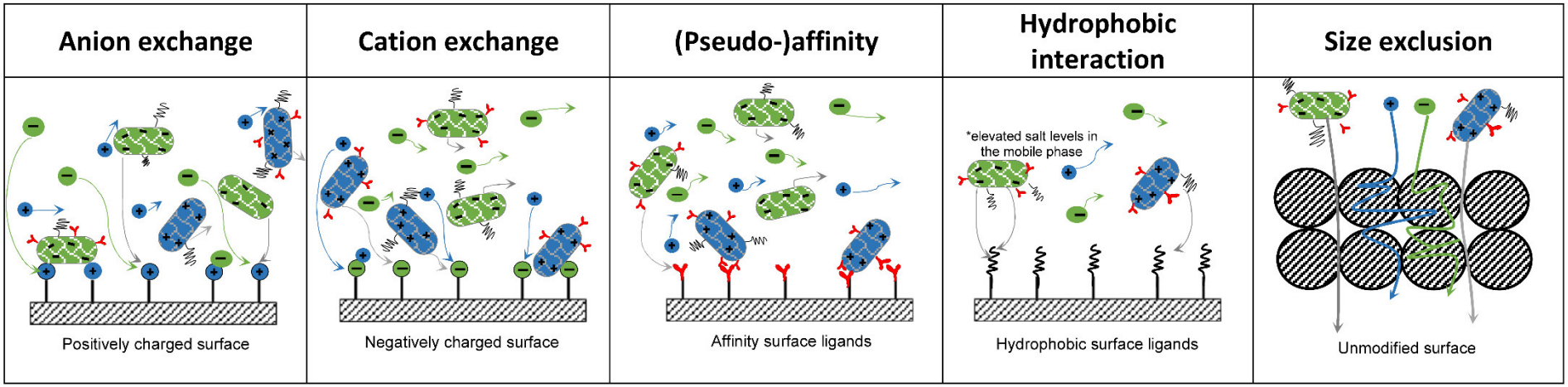

Figure 4 Principles of the most common chromatographic purification techniques applicable for the DSP of nanoplexes. In any case the individual components in the solution are separated by their distribution between surface of the stationary phase and the mobile phase. This distribution occurs due to binding of molecules to specific functional groups, or ligands on the surface. Each method has its specific mechanism and depending on the physico-chemical properties of the product, either the product or the impurities are retained. Thus, individual optimization and potentially a combination of two or more techniques is required. For ion exchange methods (anion or cation exchange) the pH of the surrounding buffer and the contained salt will influence the binding of molecules to the oppositely charged surface. During hydrophobic interaction chromatography, increasing salt levels will result in retention of more particles, whereas removing the salt from the system results in particle dissociation. During size exclusion chromatography, no binding occurs at all. Instead, molecules are passing through the stationary phase depending on their size, with larger particles eluting first. Although these basic principles are the main driver for the respective technique, other factors such as unspecific binding, or the formation of product-impurity-complexes and more might influence the actual performance.

As mentioned, these different chromatography techniques were originally mainly employed using bead-based resins and numerous DSP trains for nanoplexes have been developed or are still under investigation using this kind of stationary phase. However, it has been shown, that for large target molecules, such as viruses or bacteriophages, commonly applied resins exhibit certain shortcomings (Figure 5).[103]

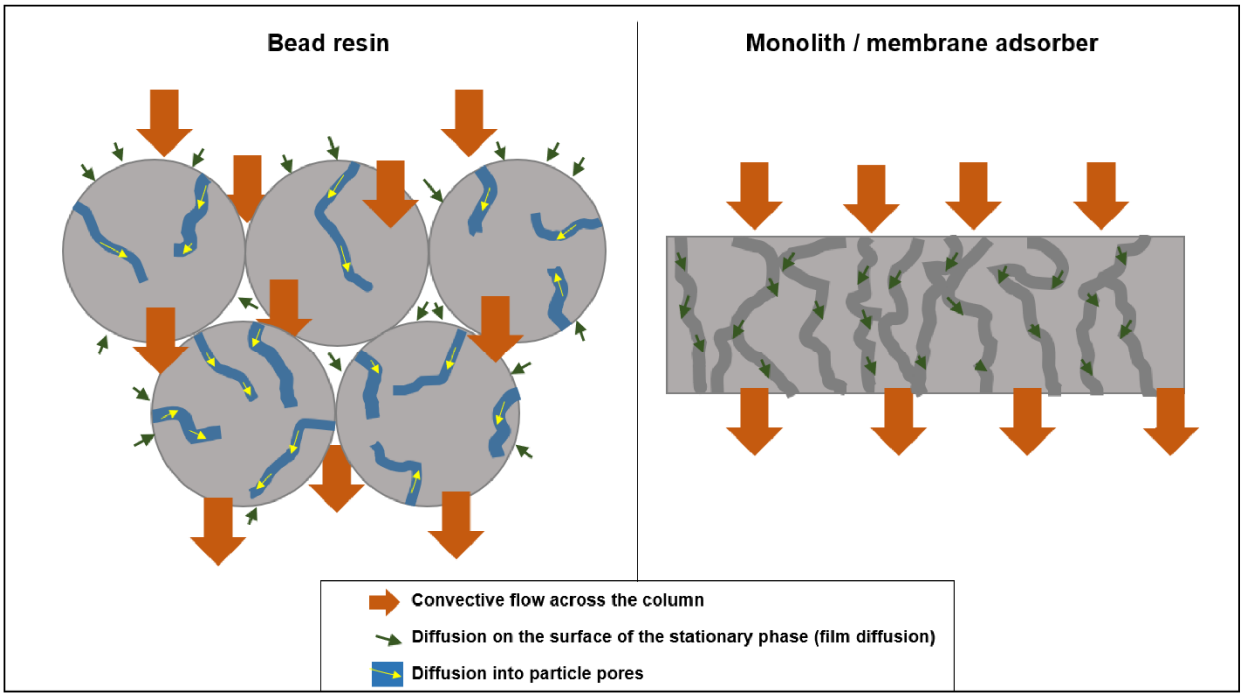

Figure 5 Flow properties in bead-based stationary phases (left) and convective flow materials, such as monoliths and membranes (right). While using chromatographic resins, the diffusion into the pores of the particles is of major importance. No pore diffusion exists when using monoliths and membranes (i.e., convective flow materials). When applying the latter materials, the film diffusion and the convective flow across the bed are the main driver of the separation. This enables higher flow rates and reduces the pressure drop across the column.

This is mainly attributed to higher pressure drops occurring in bead-based columns and an inaccessible surface area inside particle pores. The higher pressure drops are potentially leading to virus inactivation and degradation, whereas the limitation of the accessible surface area reduces the overall capacity. In general, the latter holds true rather for bind-and-elute methods, where the product is being retained, and not for flow-through methods, where the product is not supposed to bind to the stationary phase. In this regard, SEC as a flow-through method has a special position under the bead-based methods. Although it enables an efficient separation of nanoplexes and smaller contaminants, it is limited by reduced loading volume capacities and low flow rates.[107] Nevertheless, it has a high application potential for polishing and final formulation purposes. For earlier positions in the DSP train, and particularly for initial capture steps in the bind-and-elute mode, the SEC is not well suited. Here the use of monoliths and membranes displays promising alternative to resins. Monoliths on the one side, offer large binding capacities, but increase the overall costs drastically on the other side.[108] Furthermore, it was shown that monoliths are exceptionally susceptible to fouling, e.g. due to lipids, possibly

making a regeneration and reuse difficult.[109] When applied in single-use, these devices require a major share in the cost-of-goods and, if recycled, a validated cleaning and sterilization is necessary. Membrane-based approaches, on the contrary, promise the same benefits as monoliths at reduced costs of consumables, enabling single-use and thus avoiding excessive cleaning and sterilization procedures. Furthermore, the use of membrane systems implies an easier handling in terms of weight, size, and stability of the materials (e.g., allowing a backflushing of the stationary phase). Purifications of viruses and virus-like particles employing membranes have been established for various separation principles including, among others, ion exchange, hydrophobic interaction and (pseudo-) affinity. Table 1 gives a thorough overview on published studies conducted with membranes as stationary phase for the purification of viruses to the present. Several of the depicted approaches enable a high product recovery and/or a sufficient impurity removal.[110,111] However, they are often highly specific. This includes an extensive optimization for the individual target product, as for example pH values and ionic strengths during IEX methods. This specificity makes the process inflexible and the transfer to new or varying targets is difficult. However, as indicated in the beginning, the rage of possible target molecules is vast. This does not only include different kinds of nanoplexes, but also different virus classes, as well as variations within a certain virus species.[112] This also covers different genotypes of the same virus, for example, in the case of annual Influenza A deviations.[113] In contrast to individually optimizing processing approaches, platform technologies aim to increase process flexibility and thus are highly preferential.[33] These platform technologies are typically characterized by a high adaptability to various types of target products, while at the same time offering a sufficient specificity to successfully remove process-related contaminants. In addition to that, properties that span over a wide range of targets, such as the heparin binding affinity of various viruses due to their similar surface protein compositions can be utilized. Noteworthy in relation to this is the pseudo-affinity chromatography using sulfated cellulose membrane adsorbers.[114–117] This technique employs the heparin binding potential of various types of viruses, which allows for a feasible platform technology with broad application potential. By using sulfated cellulose as stationary phase, no requirement for using heparin itself remains. This modification eliminates the costs for the expensive heparin and, additionally, excludes the need for this animal-derived product, which is problematic from a regulatory point of view in pharmaceutical applications. However, as not all types of nanoplexes, have a heparin affinity, further platform approaches deserve an evaluation. In addition to common membrane adsorbers, table 1 lists chromatographic membrane applications with platform application potential as well.

Table 1 Overview on chromatographic purification strategies for viruses and virus-like particles using membranes as stationary phase (Updated in June 2021).

Virus / VLP Type	Type of membrane adsorber	Position in DSP and notes	Yield / Stage Recovery (%)	Dynamic binding capacity	Impurity depletion		Reference
					DNA	Protein	
Adenovirus 70-100 nm No envelope	AEX *Sartobind anion direct*	Purification (after clarification/ concentration) + nuclease	62% infective particles	N.A.	97% DNA reduction (13 ng/10^{11} total particles)	N.A. Only qualitative SDS-PAGE	Peixoto 2008[118]
	Adenopure kit - ion exchange membrane	Purification +nuclease	$4.2x10^{10}$- $1.26x10^{11}$ PFU	N.A.	N.A. *Not tested*	N.A. *Qualitative SDS-PAGE*	Duffy 2005[119]
	AEX Hydrogel grafted membranes low ligand density medium ligand density high ligand density Directly grafted membranes low ligand density medium ligand density high ligand density	Purification +nuclease	 90% 90% 25% ~20% ~25% ~30%	 3.02 mg_{virus} cm^{-2} 3.02 mg_{virus} cm^{-2} 4.70 mg_{virus} cm^{-2} N.A. N.A. N.A.	 0.1 µg mL^{-1} 0.35 µg mL^{-1} 0.25 µg mL^{-1} 0.2 µg mL^{-1} 0.4 µ mL^{-1} 0.5 µg mL^{-1}	 N.A. *(only total protein determination in the flow through, not in the eluate)* N.A. (only total protein determination in the flow through, not in the eluate)	Nestola 2014[120]
	AEX *Sartobind STIC*	Purification *(AEX in flow through mode) +nuclease*	<100%	5.43 mg_{DNA} mL^{-1} (no virus binding)	93% 4 LRV	70% 5 LRV	Nestola 2015[110]
	Affinity Membrane *Sartobind IDA 75, charged with Zn^{2+}*	Polishing +nuclease	87%	N.A.	<25 pg mL^{-1}	<0.3 ng mL^{-1} (<LOD)	Lee 2009[121]
	AEX Sartobind Q *Laterally-fed membrane*	Purification +nuclease	100% 100%	N.A. N.A.	90% 90%	90% 90%	Kawka 2019[111]
	AEX low ligand density (440 µmol/g) medium ligand density (750 µmol/g) high ligand density (1029 µmol/g)	Purification	50-90% depending on adsorption time	N.A.	N.A.	>95%	Turnbull 2019[122]
Adeno-associated virus (AAV) 18-26 nm No envelope	ViraKit™ - Ion exchange	Purification +nuclease	$9.3x10^{10}$ particles on average	N.A.	N.A. *Not tested*	N.A. *Only qualitative SDS-PAGE*	Duffy 2005[119]
	CEX *Mustang S* + AEX *Mustang Q*	Capture + polishing	AAV1: CEX (pH 6.5): 52% AEX (pH:8): 86% AAV8: Total: 49% (n=3)	N.A. N.A.	N.A. *Not tested*	N.A. *(90% purity based on SDA-PAGE)*	Okada 2009[123]
	SXC *Regenerated cellulose + PEG*	Capture	>95%	$3.1x10^{10}$ viral genomes cm^{-2}	>90%	>80%	Marichal-Gallardo 2021[124]

Aedes aegypti denso-nucleosis virus – VLP 20 nm No envelope	AEX *Sartobind Q*	Capture	N.A. Only adsorption isotherm measurement	1.35 x 10^{10} viruses mL^{-1}	N.A. Only adsorption isotherm measurement	N.A. Only adsorption isotherm measurement	Specht 2004[125]
	AEX *Sartobind Q* *Sartobind D* CEX *Sartobind S* *Sartobind C*	Capture/ purification	N.A. Only DBC and static binding analysis	$1.8x10^8$ viruses cm^{-1} $1.8x10^8$ viruses cm^{-1} No binding No binding	N.A. Only DBC and static binding analysis	N.A. Only DBC and static binding analysis	Han 2005[126]
	AEX *Sartobind Q* CEX *Sartobind S*	Capture	N.A. *Only DBC analysis*	$1.35x10^{10}$ viruses mL^{-1} $1.9x10^8$ viruses mL^{-1}	N.A. Only DBC analysis	N.A. Only DBC analysis	Wickramasinghe 2006[127]
	AEX *Sartobind Q* *Sartobind D* CEX *Sartobind S* *Sartobind C*	Purification / concentration after tangential flow filtration	N.A.	$1.8x10^8$ viruses cm^{-1} $1.8x10^8$ viruses cm^{-1} No binding of negative virus	N.A.	N.A.	Czermak 2008[128]
Baculovirus 30-60 x 250-300 nm Enveloped	AEX *Sartobind D*	Capture	65%	$7.7x10^{10}$ virus particles mL^{-1} $8.5x10^8$ virus particles cm^{-2}	5 µg x 10^9 virus $particles^{-1}$	66 µg x 10^9 virus $particles^{-1}$	Vicente 2009[129]
	AEX *Sartobind D*	Capture	85%	0.32 mg_{BSA} cm^{-2}	5-9 ng x 10^8 IP^{-1}	31-66 µg x 10^8 IP-1	Vicente 2011[130]
	CEX *Sartobind S15* CEX *Mustang S Acrodisc*	Capture	20% ~ 80%	N.A. *No DBC tested*	N.A. *Not tested*	N.A. *Only qualitative SDS-PAGE*	Wu 2007[131]
α-herpesvirus (pseudorabies virus PrV mutants)	CEX *S100 (sulfonic acid modified)*	Capture	85.6% *(PrV strain Kaplan)* 93% *(Bovine herpesvirus 1)* 99%	N.A. *No DBC tested*	N.A. *Not tested*	*N.A.* *Only qualitative PA-Gel*	Karger 1998[132]

			(PrV-GD⁻ Pass - lack of glycoprotein GD)				
Influenza A virus 80-120 nm Enveloped	SXC *Regenerated cellulose + PEG*	Capture	95%	DBC_5: 3.4 μg_{HA} cm^{-2} 906.7 μg_{HA} mL^{-1}	99.7% (2.5 LRV) 1324.5 ng total 88.3 ng mL^{-1}	92.4% (1.1 LRV) 524 µg 22.7 µg mL^{-1}	Marichal-Gallardo 2017[133]
	AEX *Sartobind Q*	Capture after ß-propriolactone inactivation	72% on average 256.74 kHAU (average)	2.23 mL cm^{-2} 3.12 kHAUcm^{-2} (Ex-Cell MDCK Medium) 4.72 mL cm^{-2} 5.19 kHAU cm^{-2} (GMEM)	Complete recovery in eluate 1.43 mg DNA (average)	77% total protein reduction 2.47 mg total protein (average)	Kalbfuss 2007[134]
	AEX *Q membrane*	Capture	<28%	10.8 kHAU cm^{-2}	N.A.	N.A.	Kalbfuss 2009[135]
	CEX S membrane	Capture	<22%	5.28 kHAU cm^{-2}	N.A.	N.A.	
	Glass fiber	Capture	4%	21.3 kHAU cm^{-2}	N.A.	N.A.	
	Iminodiacetic acid	Capture	<5%	2.70 kHAU cm^{-2}	N.A.	N.A.	
	Affinity Euonymus europaeus *Lectin – modified cellulose membrane*	Capture after ß-propriolactone inactivation	107.5% (A/Puerto Rico/8/34, H1N1)	9 kHAU cm^{-2}	99% (10.0 µg mL^{-1})	69.7% total protein reduction (55.9 µg mL^{-1})	Opitz 2007[136]
	IMAC *zinc-modified Sartobind® IDA*	Capture after ß-propriolactone inactivation	64% (A/Puerto Rico/8/34)	15.36 kHAU cm^{-2}	Ca. 93%	Ca. 74%	Opitz 2009[137]
	<u>Pseudo affinity</u> *Sulfated cellulose*	Capture after ß-propriolactone inactivation	82% (A/Puerto Rico/8/34) 94% (A/Wisconsin/67/2005) 73% (B/ Malaysia/2506/2004)	18 kHAU cm^{-2} or (14 μg_{HA} cm^{-2})	90% (23 ng dsDNA μg_{HA}^{-1}) 68% (59 ng dsDNA μg_{HA}^{-1}) 99% (30 ng dsDNA μg_{HA}^{-1})	84% (2.1 µg TP μg_{HA}^{-1}) 57% (2.3 µg TP μg_{HA}^{-1}) 58% (5.9 µg TP μg_{HA}^{-1})	Opitz 2009a[116]
	<u>CEX</u> *Sartobind C75*	Capture	63% (A/Puerto Rico/8/34)	N.A.	60%	84%	
	Sartobind S75		76% (A/Puerto Rico/8/34)	N.A.	61%	81%	

	Pseudo affinity *sulfated cellulose* + AEX *Satobind STIC*	Capture + Polishing	80% 100% 75% (total) A/PR/8/34 (H1/N1)	N.A. 17.5 μg_{DNA} cm^{-2}	97.5% 81% 99.5% (total) →1.2 ng_{DNA}/15 μg_{HA}	71% 36% 76% (total) →19.8 $\mu g_{protein}$/15 μg_{HA}	Weigel et 2016[138]
	Pseudo affinity *sulfated cellulose*	Capture after ß-propriolactone inactivation	57.4% A/PuertoRico/8/34	N.A.	5.1 ± 0.2 pg_{DNA} HAU^{-1}	1.2 ± 6 0.02 ng_{prot} HAU^{-1}	Fortuna 2017[139]
	AEX *ChromaSorb*	Polishing (flow through)	100% A/Wisconsin/N1H1	No quantification (flow through experiment)	100% (<10 ng)	80%	Iyer et al. 2012[140]
	Pseudo affinity *sulfated cellulose*	Capture + nuclease and EDTA-Protease Inhibitor Cocktail	64% A/PuertoRico/8/34		0.0038 μg_{DNA} μg_{HA}^{-1}	0.013 mg_{prot} μg_{HA}^{-1}	Carvalho 2018[114]
Influenza-VLP	Pseudo affinity – *sulfated cellulose* AEX *Sartobind Q* *Sartobind S*	Capture + nuclease and EDTA-Protease Inhibitor Cocktail	80% 47.4% 45.9%	$DBC_{20\%}$ 78 ng_{HA} mL^{-1} N.A. N.A.	80% <LOD <LOD	89% 0.07 $mg_{tot.prot.}$ μg_{HA}^{-1} 0.26 $mg_{tot.prot.}$ μg_{HA}^{-1} 0.18 $mg_{tot.prot.}$ μg_{HA}^{-1}	Carvalho 2018[114]
Lentivirus 80-130 nm *Enveloped*	AEX *Mustang Q*	Capture / concentration without prior clarification	76% ($2x10^8$ transduction units mL^{-1})	9.6×10^{10} transduction units $mL_{membrane}^{-1}$	7.22 µg mL^{-1}	3.03 mg mL^{-1}	Kutner 2009[141]
	AEX *LentiSELECT1000*	Capture / concentration +nuclease	43.6%	N.A.	N.A. *Only qualitative testing for protein and DNA content*		Zimmermann 2011[142]
	AEX *Mustang Q XT5*	Capture Two different lentiviral subtypes	33% 55%	N.A.	N.A.	N.A.	Bauler 2020[143]
	AEX *Mustang Q XT·*	Capture	N.A.	N.A.	N.A.	N.A.	Rout-Pitt 2018[144]
	AEX Mustang Q	Capture	N.A.	N.A.	N.A.	N.A.	Tinch 2019[145]

	AEX *Mustang Q Acrodisc*	Capture / concentration	80% (1 M NaCl elution) 65% (NaCl gradient)	N.A.	N.A.	N.A.	Marino 2015[146]
	AEX *Mustang Q*	Capture	60%	N.A.	N.A.	N.A.	Dropulic 2003[147]
	AEX *regenerated cellulose nanofibers derivatized with a quaternary amine*	Purification after tangential flow filtration	90%	N.A.	0%	2 LRV	Ruscic 2019[148]
	AEX *Sartobind Q* *(3 mL / 150 mL / 400 mL))* *Sartobind Phenyl* *Mustang Q*	Capture	30%/12.4%/22.4% N.A. N.A.	N.A.	N.A/98%/100 N.A. N.A.	N.A/100%/100% N.A. N.A.	Valkama 2020[149]
a) Murine leukemia virus 80-120 nm Enveloped	AEX a) *Mustang Q* b) *Mustang Q XT Acrodisc*	Capture + nuclease	51.8% ~1x10^{9} IFU mL^{-1} 48.3%	1.27 x 10^{8} infectious units mL$_{membrane}^{-1}$	2.21 LRV 45 µg total N.A. *Not tested*	3.51 LRV ~140 µg mL^{-1} N.A. *Not tested*	McNally 2014[150]
b)MoMLV-derived vectors (VSV.G pseudotyped)	AEX *LentiSELECT1000*	Capture / concentration + nuclease	38.5%	N.A.	N.A. *Only qualitative testing for coeluted DNA*	N.A. *Only qualitative testing for protein content*	Zimmermann 2011[142]
Murine polyomavirusV LP-Platform (VP1)	AEX *Sartobind Q*	Capture	69 ± 4%	N.A.	6 ng DNA per 100 µg VP1	Protein purity: 61%	Ladd Effio 2016a[151]
Human B19 Parvovirus-like particles 25-30 nm No envelope	AEX *Sartobind Q*	Capture	59%	5.7 mg mL^{-1}	8 ng DNA / 100 µg VLP	81.5% protein purity	Ladd Effio 2016b[152]
	AEX *Sartobind Q*	Initial purification	N.A. only feasibility study for interlaced size exclusion chromatography	N.A.	<20 ng/mL	81% protein purity	Ladd Effio 2016c[153]
Retro-VLPs Enveloped	AEX *Sartobind STIC*	Purification *(AEX flow through)*	45%	5.43 mg$_{DNA}$ mL$_{membrane}^{-1}$ (no virus binding)	2 LRVs (for whole train)	3.5 LRVs	Nestola 2015[110]
Rotavirus-VLPs 75-85 nm No envelope	AEX *Sartobind D 75*	Capture + Concentration	55.2% 97.6% total: 46%	N.A.	90% (1.3 LRV) ~100% (4.5 LRV) total: ~100% 1.4 mg$_{DNA}$/mg $_{VLP}$	45% (55% purity) 2% (98% purity) total: 2% (98% purity)	Vicente 2008[154]

Vaccinia virus / Modified vaccinia ankara virus 260 x 360 nm Enveloped	(Pseudo-) affinity *Heparin* *+AEX Q75* *Sulfated cellulose* *+AEX Q75* AEX *Q75* AEX *D75* CEX *C75*	Capture	56% *59%* 65% *58%* 77% 72% 21%		76% *95%* 90% *99.9%* 16% 30% 74%	99% *<LOQ (0.5 µg mL^{-1})* 99% *<LOQ (0.5 µg mL^{-1})* 99% 99% 99%	Wolff 2010a[155]
	Pseudo-affinity *a) Heparin* *b) Sulfated cellulose*	Capture	68% 75%		80% 95%	<LOQ (99.9%) <LOQ (99.9%)	Wolff 2010b[117]
Yellow fever virus 50 nm Enveloped	AEX *Q-membrane*	Capture	93.3%	170 µg cm^{-2}	0.9 ng/dose	317.6 ng_{HCP} mg^{-1}	Pato 2014[156]
	AEX *Q-membrane*	Capture	80.2%	170 µg cm^{-2}	1.3 ng/dose	86 ng_{HCP} mg^{-1}	Pato 2019[157]

AEX, anion exchange; CEX, cation exchanger; IMAC, Immobilized metal affinity chromatography; SXC, steric exclusion chromatography; LOQ, limit of quantification; LRV, Log reduction volume; VLP, Virus-like particle; N.A., Not applicable (i.e., not stated or not tested)

Steric exclusion chromatography as platform technology

One approach for a purification technique spanning over a wide range of possible targets is the steric exclusion chromatography (SXC).[158] Similar to the SEC it is mainly driven by the target particles' size. The major difference between both methods, however, is the mode of action. Whereas the SEC is performed as a flow through method, the SXC is implementable as a capture step, allowing larger loading volumes, an increased throughput, and a concentration of the target molecules at the same time. Although the underlying mechanism is not yet fully characterized (e.g., concerning adsorption constants), it is known that the SXC combines elements of precipitation with a size depending retention on a stationary phase, while at the same time avoiding an actual precipitation. Because of this, the separation is not driven by filtration in the first place. To clarify this relation, in the following the basic principle of macromolecular crowding and its application to the SXC is described.

The major driver of the SXC is an accelerated crowding of the molecules in solution due to the addition of a cosmotropic agent, such as the non-ionic polymer polyethylene glycol (PEG)[159–161]. The crowding is induced due to the hydrodynamic radius of the PEG, which is limiting its approximation to other particles in solution (Figure 6). This results in reduced PEG concentrations near the surface of the respective macromolecules (or the stationary phase, if present) compared to higher concentrations in the surrounding bulk solution. The arising concentration gradient leads to a thermodynamical destabilization of the system. This unfavored state is resolved by an association of the macromolecules to each other and by that, reducing the overall liquid volume not accessible for the crowding agent. Additionally, excess water is transferred to the bulk solvent during association, thus reducing the actual PEG concentration in the surrounding and strengthening the interaction between the associated macromolecules.

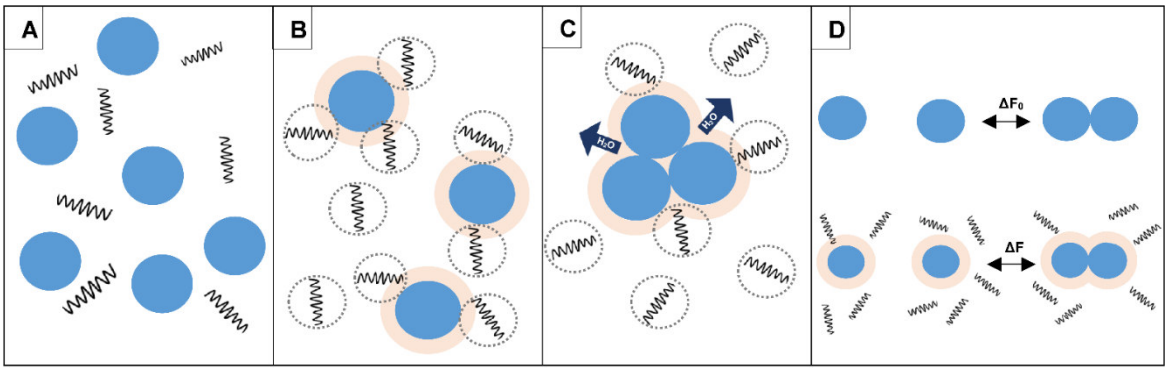

Figure 6 Polyethylene glycol (PEG) induced crowding effects of molecules in solution. In a solution containing macromolecules and a crowding agent, such as the coiled PEG (A) the hydrodynamic radii of the polymer determine the approximation of the PEG to the macromolecule (B) resulting in zones inaccessible to the PEG (yellow areas around the circles). This causes a concentration gradient between these PEG deficient zones and the surrounding solution. Due to an association of the macromolecules to each other, the surface area between these two phases is reduced. Furthermore, during the association excess water is transferred to the bulk, thus reducing the polymer concentration in the surrounding liquid. The high concentration of a crowding agent in the bulk solvent affects the free energy changes ΔF (instead of ΔF_0) and enables the association in the first place (D).

Depending on the size and concentration of the polymer, these effects might be adjusted and enable the selective exclusion of macromolecules of varying molecular weights. For decades, this has mainly been applied to entirely precipitate proteins and viruses with subsequent separation by centrifugation.[162–165] In this approach varying PEG concentrations between 4% and 40% were used and then incubated (usually under cold conditions) for at least about an hour before centrifugation.[166–168] Additionally, it was combined with high salt levels, e.g., >0.5 M NaCl to facilitate the precipitation. The method, however, was limited by a poor selectivity, bad recovery rates, and most of all, the high time-investment and difficult scalability. Besides protein purification, the effects of polyethylene glycole in a solution enable cell fusion, for example using hybridoma cells with the aim of immunoglobulin production.[169–172]

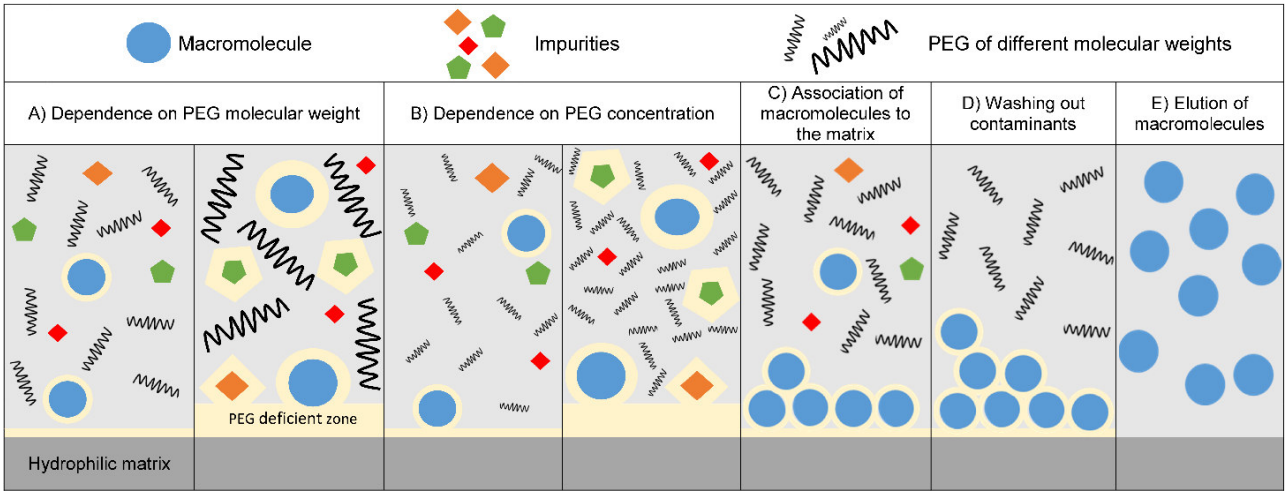

Figure 7 PEG induced crowding effects during the chromatographic purification of nanoplexes by steric exclusion chromatography (SXC). The particle association described in Figure 7 can be adjusted by varying the size and concentration of the PEG (A, B). Furthermore, particles do not only associate to each other but in presence of a hydrophilic surface also to this stationary phase (C). Maintaining the concentration of the crowding agents under flow conditions allows a removal of smaller contaminants (D). Finally, a removal of the PEG from the solution results in a subsequent dissociation of the particles and enables an elution of the latter. *Image reprinted from "Vaccine Delivery technology, Chapter 12 - Upstream and Downstream Processes for Viral Nanoplexes as Vaccines", authored by Keven Lothert, Gregor Dekevic, Daniel Loewe et al. with permission from Springer Nature, License number: 5053010802573.*

The SXC as a chromatography method (Figure 7), on the contrary, is performed at PEG concentrations below <15%, without holding times after adding the PEG, and under physiological salt conditions. It was primarily described for the purification of large proteins and bacteriophages using monoliths by the group of Pete Gagnon.[158,173,174] In the following the stationary phase was varied by using for example cryogel monoliths with differing surface characteristics[175,176], or starch-coated magnetic nanoparticles[177], optimizing the (selective) retention of still the same target molecules, such as serum proteins. A later application of the original monoliths successfully extended the range of targets to the separation of DNA and RNA molecules.[178] However, as indicated in the previous section, for larger nanoplexes, from the available convective flow materials, monoliths display major disadvantages such as pressure restrictions, limited single-usability, and high production costs. Furthermore, an implementation into aseptic processing is limited as the required monoliths are difficult to

autoclave due to their weight and sterilization by radiation is not possible. Thus in 2016 the SXC method was carried forward, by applying single-use cellulose membranes in custom-made housings for the purification of Influenza A viruses.[133,179,180] Initial proof-of concept studies following these findings indicated a high product recovery as well as a promising impurity removal.[179,180] Later the platform character was further underlined by the purifying adeno-associated viruses.[181] Hence the SXC's implementation into vaccine production schemes was a reasonable perspective still requiring a reliable confirmation, and a close study of the pitfalls associated with the technique. This can be considered as the starting point for the herein presented studies.

Directly linked to the works concerning the SXC so far, the aim of the studies conducted in the present work was to further evaluate a possible development of the SXC. The aim was to advance the method from laboratory-scaled platform approach to its incorporation into complete DSP process trains. These should enable a scalable processing to obtain products suitable for human or veterinary applications.

Scope of the presented studies

For a start, the SXC was established in the laboratory at first, using a rather large-sized model virus, the baculovirus, capable for applications in cell and gene therapy (chapter 2). By applying this model virus, the study revealed the impact of different process conditions, such as PEG concentration and flow rate on the method's performance, that can, however, be optimized in a design of experiments approach. The outcome was a virus recovery above 90%, virtually complete protein removal, and a high DNA depletion of 85% confirming the performance that other groups achieved with the SXC using other viruses of smaller size.[124,133] Furthermore, this initial study evaluated the application of different membrane types as stationary phase for the SXC and the influence of batch-to-batch variations for the same virus genotype. It was shown that the application of plain cellulose membranes, as already done in past studies, is the most promising approach. Other membranes showed a reduced virus recovery or impurity removal (e.g. polyamide membranes) or presented a lower stability during loading of the SXC (e.g. glass microfiber membranes). Although stabilizing these membranes by a binder or adjusting the pore size could improve the stability and enable efficient process scale applications, the use of plain cellulose is straightforward and economical. The batch-to-batch variation in this study was negligible, suggesting a robust method performance, provided a consistent USP procedure is available. Although this was already indicated in literature using Influenza A viruses[133] it was proven for larger model viruses, such as the baculovirus. The impurity removal was sufficient for certain cell therapy applications, however, in this first study the SXC was performed as a stand-alone procedure after an initial clarification by centrifugation. An

additional nuclease step or a subsequent polishing was not implemented. Thus, DNA levels were still higher than acceptable for human pharmaceutical applications that allow a maximum DNA amount of 10 ng/dose and DNA sizes below 200 bp.[70,71,182] As a matter of course, for a human pharmaceutical product fulfilling regulatory product requirements, a complete DSP needed to be developed, including the SXC as one of the chromatographic methods. Consequently, the SXC was implemented into two production processes for the purification of Hepatitis-C-virus (HCV) as well as for the Orf virus (ORFV). For the reasons below, both virus types are particularly interesting for evaluations. For HCV currently no vaccination is available and therapeutic approaches are based on antiviral agents, with limited success.[183,184] ORFV on the other side, represents a promising platform technology as a viral vector, for oncolytic treatment and is currently under evaluation for a SARS-Cov-2 vaccination at the time of writing this thesis.[185] Hence for neither of these viruses an existing DSP procedure was available. Accordingly, the process development was completely open and not directed by historical data, making it particularly interesting and suitable for novel approaches. As the HCV family comprises of six genotypes with various subsets and the ORFV itself represents a platform technology with potentially unlimited subtypes, the implementation of a DSP platform approach using the SXC was reasonable. Although both viruses are enveloped, they are representatives of different nanoplex appearances with entirely divergent surface compositions.[186] Additionally, HCV displays a rather small (30 - 80 nm) spherical particle, whereas the ORFV is rather large (150 x 250) and rod shaped.[186,187]

For the ORFV, a screening approach was evaluated (chapter 3). Here along the way of process development, the SXC was benchmarked against commonly applied stationary phases, such as IEX or pseudo-affinity membranes. Although some of these alternatives were equally suitable for virus retention and recovery, superior performance with regard to a simultaneous removal of impurities was observed for the SXC. Without rigorous method optimization more than 85% of the loaded virus amounts could be recovered, while, at the same time, reducing the remaining dsDNA and protein levels to 37% and below 1%, respectively. To set-up a complete processing scheme, subsequently, secondary purification techniques were evaluated following the initial SXC capture. Among these were again different IEX membranes, pseudo-affinity and HIC membranes, as well the Capto™ Core 700 resin. It could be determined that the main focus of the secondary chromatography after the SXC was to remove residual DNA and maintain the virus concentration as most of the proteins were already eliminated at that stage. For this reason, the benefit of the evaluated AEX membranes was negligible, as the remaining DNA was co-eluting. Also, the sulfated cellulose membrane adsorbers only had a limited applicability, due to high viral losses in secondary as well as in primary purification. Despite the theoretical feasibility of this pseudo affinity technique, the pore

size of the device (~0.8 µm) might not be optimum for the large ORFV. As optimization of this technique was beyond the scope of this project, the most promising methods after an initial SXC capture step were the use of a mixed-mode size exclusion chromatography and a HIC membrane. For the sake of viral integrity and unhindered product recovery, the Capto™ Core 700 flow-through method was more promising than the bind-and-elute principle of the HIC, which generally requires high amounts of salt during loading.

To complete the downstream purification scheme, subsequently the DSP procedure was optimized by integrating a clarification train comprising of two filter units with sequentially decreasing pore sizes and a nuclease treatment (chapter 4, part A). While the clarification was mainly used to remove larger cells and cell debris, the chromatography set up was primarily responsible for impurity removal and concentration, with the latter one being achieved during the SXC. An additional advantage of this set-up was that not only process-related impurities from the USP were successfully removed but also supplements arising from the DSP. Of these the most notable is the nuclease enzyme, which is used for DNA digestion, but must be removed from the final pharmaceutical composition. As the SXC eliminates more than 98% and the Capto™ Core 700 the residual amounts of proteins, the resulting products can be considered nuclease free. The second major process-related contaminant, added during the DSP, is the PEG. Although final PEG levels could only be estimated based on theoretical calculation (<2%), PEG is “generally recognized as safe” (GRAS) and thus no critical aspect of the final product. In conclusion, using the derived DSP process, for two different Vero cell-derived ORFV virus genotypes, the final product specifications were within regulatory limitations of 10 ng_{DNA}/dose for doses of up to 1.0E+7 viruses/mL. In total, the virus recovery was ~64% for the entire process and above 90% for the SXC step alone. This extends the earlier statements, showing the method’s robustness not only for different USP batches, but also for different variations, i.e. genotypes, of the same product within the utilized chromatographic set-up and scale. These findings confirmed earlier results for different Influenza A strains using the SXC[133] and, furthermore, proves the applicability to a whole process train for the production of human pharmaceuticals.

The platform character of the SXC in DSP processing schemes was shown for the HCV, afterwards (chapter 4, part B). Here, no evaluation of different alternative unit operations was conducted. The process scheme was settled in the beginning and unit operations were subsequently optimized. By this approach, a process was developed that started with an initial clarification and concentration by depth and crossflow filtration approaches. Afterwards, the feed was nuclease digested and directly applied to the SXC. First experiments with standard SXC process conditions derived from literature[133] and from the results obtained in chapter 2

and 3, however, resulted in a complete product loss in the flow-through fraction. A variation of the previously identified critical process parameters could not resolve this issue. Hence, for this particular product and procedure some critical process parameters might differ. The SXC performance was described in the literature to be optimal for pH values near the isoelectric point (pI) of the product[158]. Hence the pI was determined for the evaluated HCV showing a rather alkaline condition. Following this result, it could be shown for virus particles for the first time, that for rather alkaline pIs (>9), a pH difference of already one unit can crucially affect the methods' performance. While the SXC was inoperative at neutral (pH 7.4) conditions, for values above a pH of 8.5 the outcome was highly improved. By applying the elevated pH conditions a full virus recovery was achieved. In combination with the initial clarification and a subsequent polishing step using sulfated cellulose membrane adsorbers, the impurity clearance was sufficient to allow therapeutic applications in humans for doses of up to 1.0E+8 viruses/mL. The feasibility was proven for two major HCV genotypes. Using sulfated cellulose membrane adsorbers, a (pseudo-) affinity technique described earlier, for the polishing step, ensures the removal of remaining nuclease and PEG as both are theoretically unable to bind to the stationary phase. Hence, as compared to the results of ORFV (chapter 4, part A), a clearance of process-related impurities can be assumed in that case as well.

In summary, the studies showed, that the inclusion of the SXC is suitable for an integration as a capture step into DSP processing schemes. The SXC then is the major cause for impurity clearance and product concentration, while at the same time allowing high recoveries. Nevertheless, the combination with further unit operations is required, in order to allow a separation of larger cellular contaminants as well as a final polishing. As a result, the purification train can be reduced to its most basic framework of clarification, capture (SXC) and a final polishing step and to meet the purity requirements. This low number of processing steps minimizes overall losses and enables an intensified productivity.

References

1. Plotkin, S. History of vaccination. *Proceedings of the National Academy of Sciences of the United States of America* **111,** 12283–12287; 10.1073/pnas.1400472111 (2014).
2. Jeong, H. & Seong, B. L. Exploiting virus-like particles as innovative vaccines against emerging viral infections. *Journal of microbiology (Seoul, Korea)* **55,** 220–230; 10.1007/s12275-017-7058-3 (2017).
3. Kaufman, H. L., Kohlhapp, F. J. & Zloza, A. Oncolytic viruses. A new class of immunotherapy drugs. *Nature reviews. Drug discovery* **14,** 642–662; 10.1038/nrd4663 (2015).
4. Pastoret, P.-P. & Vanderplasschen, A. Poxviruses as vaccine vectors. *Comparative Immunology, Microbiology and Infectious Diseases* **26,** 343–355; 10.1016/S0147-9571(03)00019-5 (2003).
5. Qian, C. *et al.* Recent Progress on the Versatility of Virus-Like Particles. *Vaccines* **8**; 10.3390/vaccines8010139 (2020).
6. Roldão, A., Silva, A. C., Mellado, M., Alves, P. M. & Carrondo, M. in *Reference Module in Life Sciences* (Elsevier2017), p. 675.
7. Lawler, S. E., Speranza, M.-C., Cho, C.-F. & Chiocca, E. A. Oncolytic Viruses in Cancer Treatment. A Review. *JAMA oncology* **3,** 841–849; 10.1001/jamaoncol.2016.2064 (2017).
8. Dunbar, C. E. *et al.* Gene therapy comes of age. *Science (New York, N.Y.)* **359**; 10.1126/science.aan4672 (2018).
9. Casanova, I. *et al.* Protein-driven nanomedicines in oncotherapy. *Current opinion in pharmacology* **47,** 1–7; 10.1016/j.coph.2018.12.004 (2019).
10. Rawal, S. & Patel, M. M. Threatening cancer with nanoparticle aided combination oncotherapy. *Journal of controlled release : official journal of the Controlled Release Society* **301,** 76–109; 10.1016/j.jconrel.2019.03.015 (2019).
11. Wei, M.-M., Wang, Y.-S. & Ye, X.-S. Carbohydrate-based vaccines for oncotherapy. *Medicinal research reviews* **38,** 1003–1026; 10.1002/med.21493 (2018).
12. Gilbert, C. & Cordaux, R. Viruses as vectors of horizontal transfer of genetic material in eukaryotes. *Current opinion in virology* **25,** 16–22; 10.1016/j.coviro.2017.06.005 (2017).
13. Lundstrom, K. Latest development on RNA-based drugs and vaccines. *Future science OA* **4,** FSO300; 10.4155/fsoa-2017-0151 (2018).
14. Russell, S. J. & Barber, G. N. Oncolytic Viruses as Antigen-Agnostic Cancer Vaccines. *Cancer cell* **33,** 599–605; 10.1016/j.ccell.2018.03.011 (2018).
15. Cimolai, N. Do RNA vaccines obviate the need for genotoxicity studies? *Mutagenesis*; 10.1093/mutage/geaa028 (2020).
16. Le, T. K. *et al.* Nucleic Acid-Based Technologies Targeting Coronaviruses. *Trends in biochemical sciences* **46,** 351–365; 10.1016/j.tibs.2020.11.010 (2021).
17. György, B., Hung, M. E., Breakefield, X. O. & Leonard, J. N. Therapeutic applications of extracellular vesicles: clinical promise and open questions. *Annual review of pharmacology and toxicology* **55,** 439–464; 10.1146/annurev-pharmtox-010814-124630 (2015).
18. Rodríguez-Limas, W. A., Sekar, K. & Tyo, K. E. J. Virus-like particles: the future of microbial factories and cell-free systems as platforms for vaccine development. *Current opinion in biotechnology* **24,** 1089–1093; 10.1016/j.copbio.2013.02.008 (2013).
19. Lauring, A. S., Jones, J. O. & Andino, R. Rationalizing the development of live attenuated virus vaccines. *Nature biotechnology* **28,** 573–579; 10.1038/nbt.1635 (2010).
20. Krammer, F. & Palese, P. Advances in the development of influenza virus vaccines. *Nature reviews. Drug discovery* **14,** 167–182; 10.1038/nrd4529 (2015).

21. Abente, E. J. *et al.* Comparison of Adjuvanted-Whole Inactivated Virus and Live-Attenuated Virus Vaccines against Challenge with Contemporary, Antigenically Distinct H3N2 Influenza A Viruses. *Journal of virology* **92**; 10.1128/JVI.01323-18 (2018).
22. David, S. C. *et al.* The effect of gamma-irradiation conditions on the immunogenicity of whole-inactivated Influenza A virus vaccine. *Vaccine* **35,** 1071–1079; 10.1016/j.vaccine.2016.12.044 (2017).
23. Moyle, P. M. & Toth, I. Modern subunit vaccines: development, components, and research opportunities. *ChemMedChem* **8,** 360–376; 10.1002/cmdc.201200487 (2013).
24. Schiller, J. T. & Lowy, D. R. Raising expectations for subunit vaccine. *The Journal of infectious diseases* **211,** 1373–1375; 10.1093/infdis/jiu648 (2015).
25. Humphreys, I. R. & Sebastian, S. Novel viral vectors in infectious diseases. *Immunology* **153,** 1–9; 10.1111/imm.12829 (2018).
26. Nidetz, N. F. *et al.* Adeno-associated viral vector-mediated immune responses: Understanding barriers to gene delivery. *Pharmacology & therapeutics* **207,** 107453; 10.1016/j.pharmthera.2019.107453 (2020).
27. Vries, R. D. de & Rimmelzwaan, G. F. Viral vector-based influenza vaccines. *Human vaccines & immunotherapeutics* **12,** 2881–2901; 10.1080/21645515.2016.1210729 (2016).
28. Balke, I. & Zeltins, A. Use of plant viruses and virus-like particles for the creation of novel vaccines. *Advanced drug delivery reviews* **145,** 119–129; 10.1016/j.addr.2018.08.007 (2019).
29. Vet, L. J. *et al.* Protective Efficacy of a Chimeric Insect-Specific Flavivirus Vaccine against West Nile Virus. *Vaccines* **8**; 10.3390/vaccines8020258 (2020).
30. Hobson-Peters, J. *et al.* A recombinant platform for flavivirus vaccines and diagnostics using chimeras of a new insect-specific virus. *Science translational medicine* **11**; 10.1126/scitranslmed.aax7888 (2019).
31. Cañizares, M. C., Nicholson, L. & Lomonossoff, G. P. Use of viral vectors for vaccine production in plants. *Immunology and cell biology* **83,** 263–270; 10.1111/j.1440-1711.2005.01339.x (2005).
32. Sinclair, A. & Latham, P. in *Vaccine Development and Manufacturing,* edited by E. P. Wen, R. Ellis & N. S. Pujar (Wiley2014), pp. 413–435.
33. Gränicher, G. *et al.* Production of Modified Vaccinia Ankara Virus by Intensified Cell Cultures: A Comparison of Platform Technologies for Viral Vector Production. *Biotechnology journal* **16,** e2000024; 10.1002/biot.202000024 (2021).
34. Ungerechts, G. *et al.* Moving oncolytic viruses into the clinic: clinical-grade production, purification, and characterization of diverse oncolytic viruses. *Molecular therapy. Methods & clinical development* **3,** 16018; 10.1038/mtm.2016.18 (2016).
35. Smith, J., Lipsitch, M. & Almond, J. W. Vaccine production, distribution, access, and uptake. *The Lancet* **378,** 428–438; 10.1016/S0140-6736(11)60478-9 (2011).
36. Genzel, Y. & Reichl, U. in *Animal Cell Biotechnology,* edited by J. M. Walker & R. Pörtner (Humana Press, Totowa, NJ, 2007), pp. 457–473.
37. Forterre, P. & Prangishvili, D. The origin of viruses. *Research in microbiology* **160,** 466–472; 10.1016/j.resmic.2009.07.008 (2009).
38. Ruiz-Mirazo, K., Peretó, J. & Moreno, A. A universal definition of life: autonomy and open-ended evolution. *Origins of life and evolution of the biosphere : the journal of the International Society for the Study of the Origin of Life* **34,** 323–346; 10.1023/B:ORIG.0000016440.53346.dc (2004).
39. Fuenmayor, J., Gòdia, F. & Cervera, L. Production of virus-like particles for vaccines. *New biotechnology* **39,** 174–180; 10.1016/j.nbt.2017.07.010 (2017).
40. Jana, L. A. & Osborn, J. E. in *Vaccinophobia and Vaccine Controversies of the 21st Century,* edited by A. Chatterjee (Springer New York, New York, NY, 2013), pp. 1–13.

41. Gerdil, C. The annual production cycle for influenza vaccine. *Vaccine* **21,** 1776–1779; 10.1016/S0264-410X(03)00071-9 (2003).
42. Chen, J.-R., Liu, Y.-M., Tseng, Y.-C. & Ma, C. Better influenza vaccines: an industry perspective. *Journal of biomedical science* **27,** 33; 10.1186/s12929-020-0626-6 (2020).
43. Farzaneh, M., Hassani, S.-N., Mozdziak, P. & Baharvand, H. Avian embryos and related cell lines: A convenient platform for recombinant proteins and vaccine production. *Biotechnology journal* **12**; 10.1002/biot.201600598 (2017).
44. Manini, I. *et al.* Egg-Independent Influenza Vaccines and Vaccine Candidates. *Vaccines* **5**; 10.3390/vaccines5030018 (2017).
45. van Rooyen, P. J., Munz, E. K. & Weiss, K. E. The optimal conditions for the multiplication of Neethling-type lumpy skin disease virus in embryonated eggs. *The Onderstepoort journal of veterinary research* **36,** 165–174 (1969).
46. Gentry, R. F. Cultivation of Infectious Laryngotracheitis Virus in Embryonated Chicken Eggs by Various Routes of Inoculation. *Avian Diseases* **7,** 31; 10.2307/1587986 (1963).
47. Manders, T. T. M., Matthijs, M. G. R., Veraa, S., van Eck, J. H. H. & Landman, W. J. M. Success rates of inoculation of the various compartments of embryonated chicken eggs at different incubation days. *Avian pathology : journal of the W.V.P.A* **50,** 61–77; 10.1080/03079457.2020.1834503 (2021).
48. Tree, J. A., Richardson, C., Fooks, A. R., Clegg, J. & Looby, D. Comparison of large-scale mammalian cell culture systems with egg culture for the production of influenza virus A vaccine strains. *Vaccine* **19,** 3444–3450; 10.1016/S0264-410X(01)00053-6 (2001).
49. Genzel, Y., Rödig, J., Rapp, E. & Reichl, U. Vaccine production: upstream processing with adherent or suspension cell lines. *Methods in molecular biology (Clifton, N.J.)* **1104,** 371–393; 10.1007/978-1-62703-733-4_23 (2014).
50. Vicente, T., Roldão, A., Peixoto, C., Carrondo, M. J. T. & Alves, P. M. Large-scale production and purification of VLP-based vaccines. *Journal of invertebrate pathology* **107 Suppl,** S42-8; 10.1016/j.jip.2011.05.004 (2011).
51. Kotin, R. M. Large-scale recombinant adeno-associated virus production. *Human molecular genetics* **20,** R2-6; 10.1093/hmg/ddr141 (2011).
52. Grein, T. A. *et al.* High titer oncolytic measles virus production process by integration of dielectric spectroscopy as online monitoring system. *Biotechnology and bioengineering* **115,** 1186–1194; 10.1002/bit.26538 (2018).
53. Genzel, Y. Designing cell lines for viral vaccine production: Where do we stand? *Biotechnology journal* **10,** 728–740; 10.1002/biot.201400388 (2015).
54. Genzel, Y., Dietzsch, C., Rapp, E., Schwarzer, J. & Reichl, U. MDCK and Vero cells for influenza virus vaccine production: a one-to-one comparison up to lab-scale bioreactor cultivation. *Applied microbiology and biotechnology* **88,** 461–475; 10.1007/s00253-010-2742-9 (2010).
55. Nikolay, A., Léon, A., Schwamborn, K., Genzel, Y. & Reichl, U. Process intensification of EB66® cell cultivations leads to high-yield yellow fever and Zika virus production. *Applied microbiology and biotechnology* **102,** 8725–8737; 10.1007/s00253-018-9275-z (2018).
56. Tapia, F., Vázquez-Ramírez, D., Genzel, Y. & Reichl, U. Bioreactors for high cell density and continuous multi-stage cultivations: options for process intensification in cell culture-based viral vaccine production. *Applied microbiology and biotechnology* **100,** 2121–2132; 10.1007/s00253-015-7267-9 (2016).
57. Gutiérrez-Granados, S., Gòdia, F. & Cervera, L. Continuous manufacturing of viral particles. *Current Opinion in Chemical Engineering* **22,** 107–114; 10.1016/j.coche.2018.09.009 (2018).
58. Vázquez-Ramírez, D., Jordan, I., Sandig, V., Genzel, Y. & Reichl, U. High titer MVA and influenza A virus production using a hybrid fed-batch/perfusion strategy with an ATF

system. *Applied microbiology and biotechnology* **103,** 3025–3035; 10.1007/s00253-019-09694-2 (2019).
59. Zhang, X. *et al.* Use of orbital shaken disposable bioreactors for mammalian cell cultures from the milliliter-scale to the 1,000-liter scale. *Advances in biochemical engineering/biotechnology* **115,** 33–53; 10.1007/10_2008_18 (2009).
60. Negrete, A. & Kotin, R. M. Production of recombinant adeno-associated vectors using two bioreactor configurations at different scales. *Journal of virological methods* **145,** 155–161; 10.1016/j.jviromet.2007.05.020 (2007).
61. Eibl, R., Kaiser, S., Lombriser, R. & Eibl, D. Disposable bioreactors: the current state-of-the-art and recommended applications in biotechnology. *Applied microbiology and biotechnology* **86,** 41–49; 10.1007/s00253-009-2422-9 (2010).
62. Rourou, S., Ben Zakkour, M. & Kallel, H. Adaptation of Vero cells to suspension growth for rabies virus production in different serum free media. *Vaccine* **37,** 6987–6995; 10.1016/j.vaccine.2019.05.092 (2019).
63. Tanaka, T., Takahashi, M., Kusano, E. & Okamoto, H. Development and evaluation of an efficient cell-culture system for Hepatitis E virus. *The Journal of general virology* **88,** 903–911; 10.1099/vir.0.82535-0 (2007).
64. Grein, T. A. *et al.* Aeration and Shear Stress Are Critical Process Parameters for the Production of Oncolytic Measles Virus. *Frontiers in bioengineering and biotechnology* **7,** 78; 10.3389/fbioe.2019.00078 (2019).
65. van der Valk, J. *et al.* Optimization of chemically defined cell culture media--replacing fetal bovine serum in mammalian in vitro methods. *Toxicology in vitro : an international journal published in association with BIBRA* **24,** 1053–1063; 10.1016/j.tiv.2010.03.016 (2010).
66. Josefsberg, J. O. & Buckland, B. Vaccine process technology. *Biotechnology and bioengineering* **109,** 1443–1460; 10.1002/bit.24493 (2012).
67. Nestola, P. *et al.* Improved virus purification processes for vaccines and gene therapy. *Biotechnology and bioengineering* **112,** 843–857; 10.1002/bit.25545 (2015).
68. Nooraei, S. *et al.* Virus-like particles: preparation, immunogenicity and their roles as nanovaccines and drug nanocarriers. *Journal of nanobiotechnology* **19,** 59; 10.1186/s12951-021-00806-7 (2021).
69. Konrad, M. Immunogenicity of proteins administered to humans for therapeutic purposes. *Trends in Biotechnology* **7,** 175–179; 10.1016/0167-7799(89)90095-4 (1989).
70. European Pharmacopoeia. *Ed. 10.2* (2020).
71. FDA. *Characterization and Qualification of Cell Substrates and Other Biological Materials Used in the Production of Viral Vaccines for Infectious Disease Indications. Guidance for Industry* (2010).
72. Effio, C. L. & Hubbuch, J. Next generation vaccines and vectors: Designing downstream processes for recombinant protein-based virus-like particles. *Biotechnology journal* **10,** 715–727; 10.1002/biot.201400392 (2015).
73. Wolf, M. W. & Reichl, U. Downstream processing of cell culture-derived virus particles. *Expert review of vaccines* **10,** 1451–1475; 10.1586/erv.11.111 (2011).
74. Morenweiser, R. Downstream processing of viral vectors and vaccines. *Gene therapy* **12 Suppl 1,** S103-10; 10.1038/sj.gt.3302624 (2005).
75. Besnard, L. *et al.* Clarification of vaccines: An overview of filter based technology trends and best practices. *Biotechnology advances* **34,** 1–13; 10.1016/j.biotechadv.2015.11.005 (2016).
76. Felo, M., Christensen, B. & Higgins, J. Process cost and facility considerations in the selection of primary cell culture clarification technology. *Biotechnol Progress* **29,** 1239–1245; 10.1002/btpr.1776 (2013).

77. Negrete, A., Pai, A. & Shiloach, J. Use of hollow fiber tangential flow filtration for the recovery and concentration of HIV virus-like particles produced in insect cells. *Journal of virological methods* **195,** 240–246; 10.1016/j.jviromet.2013.10.017 (2014).
78. Carvalho, S. B. *et al.* Efficient filtration strategies for the clarification of influenza virus-like particles derived from insect cells. *Separation and Purification Technology* **218,** 81–88; 10.1016/j.seppur.2019.02.040 (2019).
79. Eibl, D. & Eibl, R. in *Single-Use Technology in Biopharmaceutical Manufacture,* edited by R. Eibl & D. Eibl (Wiley2019), pp. 1–11.
80. Langer, E. S. & Rader, R. A. Single-use technologies in biopharmaceutical manufacturing: A 10-year review of trends and the future. *Eng. Life Sci.* **14,** 238–243; 10.1002/elsc.201300090 (2014).
81. Shukla, A. A. & Gottschalk, U. Single-use disposable technologies for biopharmaceutical manufacturing. *Trends in Biotechnology* **31,** 147–154; 10.1016/j.tibtech.2012.10.004 (2013).
82. Loewe, D. *et al.* Tangential Flow Filtration for the Concentration of Oncolytic Measles Virus: The Influence of Filter Properties and the Cell Culture Medium. *Membranes* **9**; 10.3390/membranes9120160 (2019).
83. Wickramasinghe, S. R., Kalbfuss, B., Zimmermann, A., Thom, V. & Reichl, U. Tangential flow microfiltration and ultrafiltration for human influenza A virus concentration and purification. *Biotechnology and bioengineering* **92,** 199–208; 10.1002/bit.20599 (2005).
84. Cooper, A. R. *et al.* Highly efficient large-scale lentiviral vector concentration by tandem tangential flow filtration. *Journal of virological methods* **177,** 1–9; 10.1016/j.jviromet.2011.06.019 (2011).
85. Carvalho, S. B. *et al.* Membrane-Based Approach for the Downstream Processing of Influenza Virus-Like Particles. *Biotechnology journal* **14,** e1800570; 10.1002/biot.201800570 (2019).
86. Konz, J. O., Lee, A. L., Lewis, J. A. & Sagar, S. L. Development of a purification process for adenovirus: controlling virus aggregation to improve the clearance of host cell DNA. *Biotechnol Progress* **21,** 466–472; 10.1021/bp049644r (2005).
87. Hermens, W. T. *et al.* Purification of recombinant adeno-associated virus by iodixanol gradient ultracentrifugation allows rapid and reproducible preparation of vector stocks for gene transfer in the nervous system. *Human gene therapy* **10,** 1885–1891; 10.1089/10430349950017563 (1999).
88. Killington, R. A., Stokes, A. & Hierholzer, J. C. in *Virology Methods Manual* (Elsevier1996), pp. 71–89.
89. Nasukawa, T. *et al.* Virus purification by CsCl density gradient using general centrifugation. *Archives of virology* **162,** 3523–3528; 10.1007/s00705-017-3513-z (2017).
90. Reimer, C. B. *et al.* Purification of large quantities of influenza virus by density gradient centrifugation. *Journal of virology* **1,** 1207–1216; 10.1128/JVI.1.6.1207-1216.1967 (1967).
91. Plüisch, C. S., Bössenecker, B., Dobler, L. & Wittemann, A. Zonal rotor centrifugation revisited: new horizons in sorting nanoparticles. *RSC Adv.* **9,** 27549–27559; 10.1039/C9RA05140F (2019).
92. McCarron, A., Donnelley, M. & Parsons, D. Scale-up of lentiviral vectors for gene therapy: advances and challenges. *Cell Gene Therapy Insights* **3,** 719–729; 10.18609/cgti.2017.072 (2017).
93. Rathore, A. S., Kumar, D. & Kateja, N. Recent developments in chromatographic purification of biopharmaceuticals. *Biotechnology letters* **40,** 895–905; 10.1007/s10529-018-2552-1 (2018).
94. Roque, A. C. A. *et al.* Anything but Conventional Chromatography Approaches in Bioseparation. *Biotechnology journal* **15,** e1900274; 10.1002/biot.201900274 (2020).

95. Azevedo, A. M., Rosa, P. A. J., Ferreira, I. F. & Aires-Barros, M. R. Chromatography-free recovery of biopharmaceuticals through aqueous two-phase processing. *Trends in Biotechnology* **27,** 240–247; 10.1016/j.tibtech.2009.01.004 (2009).
96. Trilisky, E. I. & Lenhoff, A. M. Sorption processes in ion-exchange chromatography of viruses. *Journal of Chromatography A* **1142,** 2–12; 10.1016/j.chroma.2006.12.094 (2007).
97. Koho, T. *et al.* Purification of norovirus-like particles (VLPs) by ion exchange chromatography. *Journal of virological methods* **181,** 6–11; 10.1016/j.jviromet.2012.01.003 (2012).
98. Weigel, T., Soliman, R., Wolff, M. W. & Reichl, U. Hydrophobic-interaction chromatography for purification of influenza A and B virus. *Journal of chromatography. B, Analytical technologies in the biomedical and life sciences* **1117,** 103–117; 10.1016/j.jchromb.2019.03.037 (2019).
99. Transfiguracion, J., Jorio, H., Meghrous, J., Jacob, D. & Kamen, A. High yield purification of functional baculovirus vectors by size exclusion chromatography. *Journal of virological methods* **142,** 21–28; 10.1016/j.jviromet.2007.01.002 (2007).
100. Kalbfuss, B., Wolff, M., Morenweiser, R. & Reichl, U. Purification of cell culture-derived human influenza A virus by size-exclusion and anion-exchange chromatography. *Biotechnology and bioengineering* **96,** 932–944; 10.1002/bit.21109 (2007).
101. Ayyar, B. V., Arora, S., Murphy, C. & O'Kennedy, R. Affinity chromatography as a tool for antibody purification. *Methods (San Diego, Calif.)* **56,** 116–129; 10.1016/j.ymeth.2011.10.007 (2012).
102. Hober, S., Nord, K. & Linhult, M. Protein A chromatography for antibody purification. *Journal of chromatography. B, Analytical technologies in the biomedical and life sciences* **848,** 40–47; 10.1016/j.jchromb.2006.09.030 (2007).
103. Pereira Aguilar, P. *et al.* Capture and purification of Human Immunodeficiency Virus-1 virus-like particles: Convective media vs porous beads. *Journal of chromatography. A* **1627,** 461378; 10.1016/j.chroma.2020.461378 (2020).
104. Zahn, A. & Allain, J.-P. Hepatitis C virus and hepatitis B virus bind to heparin: purification of largely IgG-free virions from infected plasma by heparin chromatography. *The Journal of general virology* **86,** 677–685; 10.1099/vir.0.80614-0 (2005).
105. Segura, M. d. l. M., Kamen, A., Trudel, P. & Garnier, A. A novel purification strategy for retrovirus gene therapy vectors using heparin affinity chromatography. *Biotechnology and bioengineering* **90,** 391–404; 10.1002/bit.20301 (2005).
106. Hu, J., Ni, Y., Dryman, B. A., Meng, X. J. & Zhang, C. Purification of porcine reproductive and respiratory syndrome virus from cell culture using ultrafiltration and heparin affinity chromatography. *Journal of chromatography. A* **1217,** 3489–3493; 10.1016/j.chroma.2010.03.023 (2010).
107. Weigel, T. *et al.* A flow-through chromatography process for influenza A and B virus purification. *Journal of virological methods* **207,** 45–53; 10.1016/j.jviromet.2014.06.019 (2014).
108. Rajamanickam, V., Herwig, C. & Spadiut, O. Monoliths in Bioprocess Technology. *Chromatography* **2,** 195–212; 10.3390/chromatography2020195 (2015).
109. Burden, C. S., Jin, J., Podgornik, A. & Bracewell, D. G. A monolith purification process for virus-like particles from yeast homogenate. *Journal of chromatography. B, Analytical technologies in the biomedical and life sciences* **880,** 82–89; 10.1016/j.jchromb.2011.10.044 (2012).
110. Nestola, P. *et al.* Rational development of two flowthrough purification strategies for adenovirus type 5 and retro virus-like particles. *Journal of chromatography. A* **1426,** 91–101; 10.1016/j.chroma.2015.11.037 (2015).

111. Kawka, K. *et al.* Purification of therapeutic adenoviruses using laterally-fed membrane chromatography. *Journal of Membrane Science* **579,** 351–358; 10.1016/j.memsci.2019.02.056 (2019).
112. Domingo, E. & Perales, C. in *Encyclopedia of life sciences,* edited by J. W. &. S. Ltd (Wiley, Chichester, England, 2005).
113. Belongia, E. A. *et al.* Repeated annual influenza vaccination and vaccine effectiveness: review of evidence. *Expert review of vaccines* **16,** 1–14; 10.1080/14760584.2017.1334554 (2017).
114. Carvalho, S. B. *et al.* Purification of influenza virus-like particles using sulfated cellulose membrane adsorbers. *Journal of chemical technology and biotechnology (Oxford, Oxfordshire : 1986)* **93,** 1988–1996; 10.1002/jctb.5474 (2018).
115. Fortuna, A. R. *et al.* Use of sulfated cellulose membrane adsorbers for chromatographic purification of cell cultured-derived influenza A and B viruses. *Separation and Purification Technology* **226,** 350–358; 10.1016/j.seppur.2019.05.101 (2019).
116. Opitz, L., Lehmann, S., Reichl, U. & Wolff, M. W. Sulfated membrane adsorbers for economic pseudo-affinity capture of influenza virus particles. *Biotechnology and bioengineering* **103,** 1144–1154; 10.1002/bit.22345 (2009).
117. Wolff, M. W., Siewert, C., Hansen, S. P., Faber, R. & Reichl, U. Purification of cell culture-derived modified vaccinia ankara virus by pseudo-affinity membrane adsorbers and hydrophobic interaction chromatography. *Biotechnology and bioengineering* **107,** 312–320; 10.1002/bit.22797 (2010).
118. Peixoto, C., Ferreira, T. B., Sousa, M. F. Q., Carrondo, M. J. T. & Alves, P. M. Towards purification of adenoviral vectors based on membrane technology. *Biotechnology progress* **24,** 1290–1296; 10.1002/btpr.25 (2008).
119. Duffy, A. M., O'Doherty, A. M., O'Brien, T. & Strappe, P. M. Purification of adenovirus and adeno-associated virus: comparison of novel membrane-based technology to conventional techniques. *Gene therapy* **12 Suppl 1,** S62-72; 10.1038/sj.gt.3302616 (2005).
120. Nestola, P. *et al.* Impact of grafting on the design of new membrane adsorbers for adenovirus purification. *Journal of biotechnology* **181,** 1–11; 10.1016/j.jbiotec.2014.04.003 (2014).
121. Lee, D.-S., Kim, B.-M. & Seol, D.-W. Improved purification of recombinant adenoviral vector by metal affinity membrane chromatography. *Biochemical and biophysical research communications* **378,** 640–644; 10.1016/j.bbrc.2008.11.096 (2009).
122. Turnbull, J. *et al.* Adenovirus 5 recovery using nanofiber ion-exchange adsorbents. *Biotechnology and bioengineering* **116,** 1698–1709; 10.1002/bit.26972 (2019).
123. Okada, T. *et al.* Scalable purification of adeno-associated virus serotype 1 (AAV1) and AAV8 vectors, using dual ion-exchange adsorptive membranes. *Human gene therapy* **20,** 1013–1021; 10.1089/hum.2009.006 (2009).
124. Marichal-Gallardo, P. *et al.* Single-use capture purification of adeno-associated viral gene transfer vectors by membrane-based steric exclusion chromatography. *Human gene therapy*; 10.1089/hum.2019.284 (2021).
125. Specht, R. *et al.* Densonucleosis virus purification by ion exchange membranes. *Biotechnology and bioengineering* **88,** 465–473; 10.1002/bit.20270 (2004).
126. Han, B., Specht, R., Wickramasinghe, S. R. & Carlson, J. O. Binding Aedes aegypti densonucleosis virus to ion exchange membranes. *Journal of chromatography. A* **1092,** 114–124; 10.1016/j.chroma.2005.06.089 (2005).
127. WICKRAMASINGHE, S., CARLSON, J., TESKE, C., HUBBUCH, J. & ULBRICHT, M. Characterizing solute binding to macroporous ion exchange membrane adsorbers using confocal laser scanning microscopy. *Journal of Membrane Science* **281,** 609–618; 10.1016/j.memsci.2006.04.032 (2006).

128. Czermak, P. *et al.* Purification of the densonucleosis virus by tangential flow ultrafiltration and by ion exchange membranes. *Desalination* **224,** 23–27; 10.1016/j.desal.2007.04.074 (2008).
129. Vicente, T., Peixoto, C., Carrondo, M. J. T. & Alves, P. M. Purification of recombinant baculoviruses for gene therapy using membrane processes. *Gene therapy* **16,** 766–775; 10.1038/gt.2009.33 (2009).
130. Vicente, T., Fáber, R., Alves, P. M., Carrondo, M. J. T. & Mota, J. P. B. Impact of ligand density on the optimization of ion-exchange membrane chromatography for viral vector purification. *Biotechnology and bioengineering* **108,** 1347–1359; 10.1002/bit.23058 (2011).
131. Wu, C., Soh, K. Y. & Wang, S. Ion-exchange membrane chromatography method for rapid and efficient purification of recombinant baculovirus and baculovirus gp64 protein. *Human gene therapy* **18,** 665–672; 10.1089/hum.2007.020 (2007).
132. Karger, A., Bettin, B., Granzow, H. & Mettenleiter, T. C. Simple and rapid purification of alphaherpesviruses by chromatography on a cation exchange membrane. *Journal of virological methods* **70,** 219–224; 10.1016/S0166-0934(97)00200-0 (1998).
133. Marichal-Gallardo, P., Pieler, M. M., Wolff, M. W. & Reichl, U. Steric exclusion chromatography for purification of cell culture-derived influenza A virus using regenerated cellulose membranes and polyethylene glycol. *Journal of chromatography. A* **1483,** 110–119; 10.1016/j.chroma.2016.12.076 (2017).
134. Kalbfuss, B. *et al.* Direct capture of influenza A virus from cell culture supernatant with Sartobind anion-exchange membrane adsorbers. *Journal of Membrane Science* **299,** 251–260; 10.1016/j.memsci.2007.04.048 (2007).
135. Kalbfuss, B. (Dissertation, Version 1.5).
136. Opitz, L., Lehmann, S., Zimmermann, A., Reichl, U. & Wolff, M. W. Impact of adsorbents selection on capture efficiency of cell culture derived human influenza viruses. *Journal of biotechnology* **131,** 309–317; 10.1016/j.jbiotec.2007.07.723 (2007).
137. Opitz, L., Hohlweg, J., Reichl, U. & Wolff, M. W. Purification of cell culture-derived influenza virus A/Puerto Rico/8/34 by membrane-based immobilized metal affinity chromatography. *Journal of virological methods* **161,** 312–316; 10.1016/j.jviromet.2009.06.025 (2009).
138. Weigel, T. *et al.* A membrane-based purification process for cell culture-derived influenza A virus. *Journal of biotechnology* **220,** 12–20; 10.1016/j.jbiotec.2015.12.022 (2016).
139. Fortuna, A. R., Taft, F., Villain, L., Wolff, M. W. & Reichl, U. Optimization of cell culture-derived influenza A virus particles purification using sulfated cellulose membrane adsorbers. *Engineering in life sciences* **18,** 29–39; 10.1002/elsc.201700108 (2018).
140. Iyer, G. *et al.* Flow-Through Purification of Viruses- A Novel Approach to Vaccine Purification. *Procedia in Vaccinology* **6,** 106–112; 10.1016/j.provac.2012.04.015 (2012).
141. Kutner, R. H., Puthli, S., Marino, M. P. & Reiser, J. Simplified production and concentration of HIV-1-based lentiviral vectors using HYPERFlask vessels and anion exchange membrane chromatography. *BMC biotechnology* **9,** 10; 10.1186/1472-6750-9-10 (2009).
142. Zimmermann, K. *et al.* Highly efficient concentration of lenti- and retroviral vector preparations by membrane adsorbers and ultrafiltration. *BMC biotechnology* **11,** 55; 10.1186/1472-6750-11-55 (2011).
143. Bauler, M. *et al.* Production of Lentiviral Vectors Using Suspension Cells Grown in Serum-free Media. *Molecular therapy. Methods & clinical development* **17,** 58–68; 10.1016/j.omtm.2019.11.011 (2020).

144. Rout-Pitt, N., McCarron, A., McIntyre, C., Parsons, D. & Donnelley, M. Large-scale production of lentiviral vectors using multilayer cell factories. *Journal of biological methods* **5,** e90; 10.14440/jbm.2018.236 (2018).
145. Tinch, S., Szczur, K., Swaney, W., Reeves, L. & Witting, S. R. A Scalable Lentiviral Vector Production and Purification Method Using Mustang Q Chromatography and Tangential Flow Filtration. *Methods in molecular biology (Clifton, N.J.)* **1937,** 135–153; 10.1007/978-1-4939-9065-8_8 (2019).
146. Marino, M. P. *et al.* A scalable method to concentrate lentiviral vectors pseudotyped with measles virus glycoproteins. *Gene therapy* **22,** 280–285; 10.1038/gt.2014.125 (2015).
147. Dropulic, B. *et al.* Large-scale Purification of a Lentiviral Vector by Size Exclusion Chromatography or Mustang Q Ion Exchange Capsule. *BioProcess J* **2,** 89–95; 10.12665/J25.Dropulic (2003).
148. Ruscic, J., Perry, C., Mukhopadhyay, T., Takeuchi, Y. & Bracewell, D. G. Lentiviral Vector Purification Using Nanofiber Ion-Exchange Chromatography. *Molecular therapy. Methods & clinical development* **15,** 52–62; 10.1016/j.omtm.2019.08.007 (2019).
149. Valkama, A. J. *et al.* Development of Large-Scale Downstream Processing for Lentiviral Vectors. *Molecular therapy. Methods & clinical development* **17,** 717–730; 10.1016/j.omtm.2020.03.025. (2020).
150. McNally, D. J., Darling, D., Farzaneh, F., Levison, P. R. & Slater, N. K. H. Optimised concentration and purification of retroviruses using membrane chromatography. *Journal of chromatography. A* **1340,** 24–32; 10.1016/j.chroma.2014.03.023 (2014).
151. Ladd Effio, C. *et al.* High-throughput process development of an alternative platform for the production of virus-like particles in Escherichia coli. *Journal of biotechnology* **219,** 7–19; 10.1016/j.jbiotec.2015.12.018 (2016).
152. Ladd Effio, C. *et al.* Modeling and simulation of anion-exchange membrane chromatography for purification of Sf9 insect cell-derived virus-like particles. *Journal of chromatography. A* **1429,** 142–154; 10.1016/j.chroma.2015.12.006 (2016).
153. Ladd Effio, C., Oelmeier, S. A. & Hubbuch, J. High-throughput characterization of virus-like particles by interlaced size-exclusion chromatography. *Vaccine* **34,** 1259–1267; 10.1016/j.vaccine.2016.01.035 (2016).
154. Vicente, T. *et al.* Anion-exchange membrane chromatography for purification of rotavirus-like particles. *Journal of Membrane Science* **311,** 270–283; 10.1016/j.memsci.2007.12.021 (2008).
155. Wolff, M. W. *et al.* Capturing of cell culture-derived modified Vaccinia Ankara virus by ion exchange and pseudo-affinity membrane adsorbers. *Biotechnology and bioengineering* **105,** 761–769; 10.1002/bit.22595 (2010).
156. Pato, T. P. *et al.* Development of a membrane adsorber based capture step for the purification of yellow fever virus. *Vaccine* **32,** 2789–2793; 10.1016/j.vaccine.2014.02.036 (2014).
157. Pato, T. P. *et al.* Purification of yellow fever virus produced in Vero cells for inactivated vaccine manufacture. *Vaccine* **37,** 3214–3220; 10.1016/j.vaccine.2019.04.077 (2019).
158. Lee, J. *et al.* Principles and applications of steric exclusion chromatography. *Journal of chromatography. A* **1270,** 162–170; 10.1016/j.chroma.2012.10.062 (2012).
159. Chen, W.-Y. *et al.* Kosmotrope-like hydration behavior of polyethylene glycol from microcalorimetry and binding isotherm measurements. *Langmuir : the ACS journal of surfaces and colloids* **29,** 4259–4265; 10.1021/la304500w (2013).
160. Arakawa, T. & Gagnon, P. Excluded Cosolvent in Chromatography. *Journal of pharmaceutical sciences* **107,** 2297–2305; 10.1016/j.xphs.2018.05.006 (2018).

161. Phillip, Y., Sherman, E., Haran, G. & Schreiber, G. Common crowding agents have only a small effect on protein-protein interactions. *Biophysical journal* **97,** 875–885; 10.1016/j.bpj.2009.05.026 (2009).
162. Polson, A. A theory for the displacement of proteins and viruses with polyethylene glycol. *Preparative biochemistry* **7,** 129–154; 10.1080/00327487708061631 (1977).
163. Vajda, B. P. Concentration and purification of viruses and bacteriophages with polyethylene glycol. *Folia microbiologica* **23,** 88–96; 10.1007/BF02876605. (1978).
164. Adams, A. Concentration of Epstein-Barr virus from cell culture fluids with polyethylene glycol. *The Journal of general virology* **20,** 391–394; 10.1099/0022-1317-20-3-391 (1973).
165. Atha, D. H. & Ingham, K. C. Mechanism of precipitation of proteins by polyethylene glycols. Analysis in terms of excluded volume. *The Journal of biological chemistry* **256,** 12108–12117 (1981).
166. Ingham, K. C. in *Part C: Enzyme Purification and Related Techniques* (Elsevier1984), pp. 351–356.
167. Lewis, G. D. & Metcalf, T. G. Polyethylene glycol precipitation for recovery of pathogenic viruses, including hepatitis A virus and human rotavirus, from oyster, water, and sediment samples. *Applied and environmental microbiology* **54,** 1983–1988; 10.1128/AEM.54.8.1983-1988.1988 (1988).
168. Kanarek, A. D. & Tribe, G. W. Concentration of certain myxoviruses with polyethylene glycol. *Nature* **214,** 927–928; 10.1038/214927a0 (1967).
169. Yang, J. & Shen, M. H. Polyethylene glycol-mediated cell fusion. *Methods in molecular biology (Clifton, N.J.)* **325,** 59–66; 10.1385/1-59745-005-7:59 (2006).
170. Holzlöhner, P. & Hanack, K. Generation of Murine Monoclonal Antibodies by Hybridoma Technology. *Journal of visualized experiments : JoVE*; 10.3791/54832 (2017).
171. Gefter, M. L., Margulies, D. H. & Scharff, M. D. A simple method for polyethylene glycol-promoted hybridization of mouse myeloma cells. *Somatic cell genetics* **3,** 231–236; 10.1007/BF01551818 (1977).
172. Dubois, A. R. S. X. *et al.* High-resolution analysis of the B cell repertoire before and after polyethylene glycol fusion reveals preferential fusion of rare antigen-specific B cells. *Human antibodies* **24,** 1–15; 10.3233/HAB-150288 (2016).
173. Gagnon, P. *Purification of biological products by constrained cohydration chromatography. European Patent* (2012).
174. Gagnon, P. *Purification of biological productsby constrained cohydration chromatography. US Patent* (pending).
175. Wang, C., Bai, S., Tao, S.-P. & Sun, Y. Evaluation of steric exclusion chromatography on cryogel column for the separation of serum proteins. *Journal of chromatography. A* **1333,** 54–59; 10.1016/j.chroma.2014.01.059 (2014).
176. Tao, S.-P., Zheng, J. & Sun, Y. Grafting zwitterionic polymer onto cryogel surface enhances protein retention in steric exclusion chromatography on cryogel monolith. *Journal of chromatography. A* **1389,** 104–111; 10.1016/j.chroma.2015.02.051 (2015).
177. Gagnon, P., Toh, P. & Lee, J. High productivity purification of immunoglobulin G monoclonal antibodies on starch-coated magnetic nanoparticles by steric exclusion of polyethylene glycol. *Journal of chromatography. A* **1324,** 171–180; 10.1016/j.chroma.2013.11.039 (2014).
178. Levanova, A. & Poranen, M. M. Application of steric exclusion chromatography on monoliths for separation and purification of RNA molecules. *Journal of chromatography. A* **1574,** 50–59; 10.1016/j.chroma.2018.08.063 (2018).
179. Wolff, M. W., Pieler, M. M., Reichl, U. & Marichal-Gallardo, P. *Method for the separation of virus compositions including depletion and purification thereof. European Patent* (pending).

180. Wolff, M. W., Pieler, M. M., Reichl, U. & Marichal-Gallardo, P. *Method for the separation of virus compositions including depletion and purification thereof. US Patent* (pending).
181. Marichal-Gallardo, P. A. Chromatographic purification of biological macromolecules by their capture on hydrophilic surfaces with the aid of non-ionic polymers (2019).
182. *WHO Expert Committee on Biological Standardization. Fifty-fourth report* (World Health Organization, Geneva, 2005).
183. Bukh, J. The history of hepatitis C virus (HCV): Basic research reveals unique features in phylogeny, evolution and the viral life cycle with new perspectives for epidemic control. *Journal of hepatology* **65,** S2-S21; 10.1016/j.jhep.2016.07.035 (2016).
184. Naderi, M. *et al.* Hepatitis C virus and vaccine development. *International journal of molecular and cellular medicine* **3,** 207–215 (2014).
185. Wang, R., Wang, Y., Liu, F. & Luo, S. Orf virus: A promising new therapeutic agent. *Reviews in medical virology* **29,** e2013; 10.1002/rmv.2013 (2019).
186. Merz, A. *et al.* Biochemical and morphological properties of hepatitis C virus particles and determination of their lipidome. *The Journal of biological chemistry* **286,** 3018–3032; 10.1074/jbc.M110.175018 (2011).
187. Nagington, J., Newton, A. A. & Horne, R. W. The structure of orf virus. *Virology* **23,** 461–472; 10.1016/0042-6822(64)90230-2 (1964).

Chapter 2 – Initial evaluation of the SXC: Optimization of critical process parameters and screening of stationary phase membranes using as a model the baculovirus

This chapter demonstrates the general approach for virus purification by membrane-based SXC. By using the insect cell-derived baculovirus as a model, it is shown how critical process parameters, such as PEG concentration and process flow rate, can be optimized. It is also highlighted that such an optimization often includes a trade-off between virus recovery and impurity removal. Furthermore, attention is drawn to the importance of sufficient sample loading in terms of dynamic binding capacities, to reduce the susceptibility for unspecific losses, highly affecting the overall material balances and thus the estimated product recovery. The optimized SXC process presented in this chapter, allowed for a sufficient product purity for ex-vivo use as a gene transfer tool for human stromal cell transduction. To achieve this aim, no further process steps were included, despite an initial clarification by filtration or centrifugation. The presented manuscript further points out that the process conditions are suitable for different viral production batches of the same genotype without the need for additional adjustments.

Particularly new in this study is the examination of different stationary phase materials for the SXC application. To our knowledge no application other than regenerated cellulose, porous poly-methacrylate with OH-ligands and dextran beads are described in literature. In the following study a total of seven different membranes of four material classes were evaluated. The most promising ones, a kind of glass fiber and a polyamide membrane, were evaluated in more detail and benchmarked against regenerated cellulose membranes.

Journal of Virological Methods 275 (2020) 113756

Contents lists available at ScienceDirect

Journal of Virological Methods

journal homepage: www.elsevier.com/locate/jviromet

Membrane-based steric exclusion chromatography for the purification of a recombinant baculovirus and its application for cell therapy

Keven Lothert[a], Gundula Sprick[a], Felix Beyer[a], Guiliano Lauria[a], Peter Czermak[a,b,c], Michael W. Wolff[a,*]

[a] Institute of Bioprocess Engineering and Pharmaceutical Technology, University of Applied Sciences Mittelhessen (THM), Wiesenstr. 14, 35390, Giessen, Germany
[b] Bioresources, Fraunhofer Institute for Molecular Biology and Applied Ecology (IME), Winchesterstr. 2, 35394, Giessen, Germany
[c] Faculty of Biology and Chemistry, Justus-Liebig-University of Giessen, Ludwigstr. 23, 35390, Giessen, Germany

ARTICLE INFO

Keywords:
Downstream processing
Stem cells
Baculovirus
Design of experiments

ABSTRACT

The continuously increasing potential of stem cell treatments for various medical conditions has accelerated the need for fast and efficient purification techniques for individualized cell therapy applications. Genetic stem cell engineering is commonly done with viral vectors like the baculovirus. The baculovirus is a safe and efficient gene transfer tool, that has been used for the expression of recombinant proteins for many years. Its purification has been based mainly on ion exchange matrices. However, these techniques impair process robustness, if different genetically modified virus particles are applied. Here, we evaluated the membrane-based steric exclusion chromatography for the purification of insect cell culture-derived recombinant *Autographa californica* multicapsid nucleopolehydroviruses for an application in cell therapy. The method has already proven to be a powerful tool for the purification of Influenza A virus particles, using cellulose membranes.

Aside from the aforementioned cellulose, we evaluated alternative stationary phases, such as glass fiber and polyamide membranes. The highest dynamic binding capacitiy was determined for cellulose with 5.08E + 07 pfu per cm^2 membrane. Critical process parameters were optimized, using a design of experiments (DoE) approach. The determined process conditions were verified by different production batches, obtaining a mean virus yield of 91% ± 6.5%. Impurity depletion was > 99% and 85% for protein and dsDNA, without nuclease treatment. Due to the method's specificity, its application to other baculoviruses, with varying surface modifications, is conceivable without major process changes. The physiological buffer conditions enable a gentle handling of the virus particles without decreasing the transduction efficacy. The simple procedure with sufficient impurity removal enables the substitution of time-consuming ultra centrifugation steps and can serve as a first process unit operation to obtain higher purities.

1. Introduction

The improvement of purification techniques for biological nanoplexes, i.e. viral vaccines and gene therapy products, is of permanent interest, as the public health system faces the challenge to reduce costs and to improve product purity and productivity. Most of the current production processes are optimized to purifiy proteins, whereas the downstream part for the larger viruses, virus-like particles and viral vectors is often a bottleneck. To resolve this limitation for the chromatographic purification of viruses and virus particles, the application of membrane adsorbers has proven to be a fast and efficient alternative to resins, and less expensive than monolith-based applications (Kramberger et al., 2015; Trilisky and Lenhoff, 2007; Wu et al., 2013). In bead-based systems, the size exclusion of larger macromolecules from the pores leads to a reduced accessible surface for product adsorption. A further disadvantage of these materials is the limited flow rate due to a higher pressure drop across the column (Wolff and Reichl, 2011). By using membrane chromatography, the limitations of bead systems are avoided, thus reducing process times and costs (Nestola et al., 2015; Orr et al., 2013).

Abbreviations: *Ac*MNPV, *Autographa californica* multicapsid nucleopolyhedrovirus; CV, column volumes; DBC, dynamic binding capacity; DoE, design of experiments; GMF, glas microfiber filter; GFP, green fluorescent protein; HCM, hydrosart cellulose membranes; HMSC, human mesenchymal stromal cell; MF, mean fluorescence intensity; MOI, multiplicity of infection; PA, polyamide; PEG, polyethylene glycol; SXC, steric exclusion chromatography; VSV-G, vesicular stomatitis virus glycoprotein

* Corresponding author.
E-mail addresses: keven.lothert@lse.thm.de (K. Lothert), peter.czermak@lse.thm.de (P. Czermak), michael.wolff@lse.thm.de (M.W. Wolff).

https://doi.org/10.1016/j.jviromet.2019.113756
Received 27 June 2019; Received in revised form 7 October 2019; Accepted 16 October 2019
Available online 20 October 2019
0166-0934/

With regard to the baculovirus purification, a variety of different purification techniques have been described, including filtration approaches (Michalsky et al., 2009, 2010) as well as sucrose gradient ultracentrifugation (Airenne et al., 2000). Both techniques are limited, mainly due to high equipment costs, time-consuming procedures and a poor virus recovery and impurity depletion (Kwang et al., 2016). Bead-based chromatography methods, employing heparin affinity (Nasimuzzaman et al., 2016), immobilized metal affinity (Hu et al., 2003) or size exclusion (Transfiguracion et al., 2007) have been evaluated, but they just as are limited by the drawbacks stated above. Furthermore, several membrane chromatography purification processes have been reported, applying ion exchange membranes exclusively (Grein et al., 2012; Vicente et al., 2009; Wu et al., 2007). The limiting factor for these applications is the dependence on the viral surface composition to allow sufficient virus-binding. Thus, for varying virus genotypes, or changes in the upstream processing that alter the surface of the budded virus particles, the performance of these matrices must be re-evaluated.

The steric exclusion chromatography (SXC) represents a good alternative to the described procedures, as the technique focuses on the size of the target species, and not on a specific surface composition.

Initial reports on this chromatographic method were made by Lee et al. (2012) for the purification of IgM and bacteriophage M13K07, using OH-monoliths. Subsequently, the purification of y-globulin and albumin (purity: 79% and 94.7% resp. in a two-component system), using hydrophilic cryogel monoliths, was shown by the same group (Tao et al., 2015; Wang et al., 2014; Gagnon Peter, 2017 European Patent EP2720768B1Gagnon, 2012Gagnon Peter, 2017 European Patent EP2720768B1; Gagnon Peter US Patent US20170218011A1, pendingGagnon, 2017Gagnon Peter US Patent US20170218011A1, pending). Furthermore, the SXC was used in combination with starch-coated magnetic nanoparticles for the purification of IgG monoclonal antibodies (Gagnon et al., 2014). Marichal-Gallardo et al. (2017) recently showed the successful application of cellulose membranes for the purification of Influenza A virus particles by SXC (Marichal-Gallardo et al., 2017; Wolff et al. European Patent EP3371302A1, pending; Wolff et al. US Patent US20190085300A1, pending). This allowed a fast and cost-efficient purification of virus particles, that can furthermore be carried out with single-use materials, reducing the need for cleaning and sterilization procedures.

The method is based on a described effect, where polymers, such as polyethylene glycol (PEG) in high concentrations, induce molecular crowding and protein-protein associations (Arakawa and Timasheff, 2002; Atha and Ingham, 1981; Kuznetsova et al., 2014). This effect was intensely used for the purification of proteins and virus particles, as the precipitation of the macromolecules enabled an efficient separation from smaller molecules (Giese et al., 2013; Hönig and Kula, 1976; Sim et al., 2012). However, this means that proteins either need a preceeding purification, or they require distinct molecular weight differences, in order to be selectively precipitated. When using PEG during SXC, precipitation must be avoided to prevent filtration effects on the stationary phase as well as virus damage. Thus, PEG concentrations are chosen that lie below precipitation conditions (Lee et al., 2012).

For the SXC, a crude pre-clarified cell culture harvest is mixed with a PEG-containing solution, and afterwards applied to a hydrophilic stationary phase. The steric exclusion of PEG from both, the stationary phase and the macromolecules in the solution, leads to the formation of PEG-deficient zones. In order to reduce the surface between the PEG-deficient areas and the solvent with higher PEG concentrations, macromolecules associate with the stationary phase and with other macromolecules surrounded by PEG-deficient zones. Depending on the molecular weight and the concentration of PEG, particles of different size can be retained, whereas smaller impurities, unaffected by the PEG-deficient zones, are washed out. To elute the macromolecule of interest, the concentration of PEG in the mobile phase is reduced.

In the present work, vesicular stomatitis virus glycoprotein (VSV-G) pseudotyped *Autographa californica* multicapsid nucleopolyhedrovirus (*Ac*MNPV) particles were purified using membrane-based SXC. This virus can serve for gene transfer and the transduction of human mesenchymal stromal cells (hMSCs). The pseudotyping of the virus with VSV-G, as described by Sprick et al. (2017), allows an improved transduction efficacy of hMSCs compared to the native *Ac*MNPV. Certain advantages make the baculovirus a favourable tool for the application as a gene transfer tool or viral vector. Thereof most important to be named is that the main host of the baculoviridae are insects. As a consequence, they cannot replicate in mammalian cells despite their ability to transduce them, reducing the risk for possible immunogenic effects (Summers, 2006). Other viral vectors, such as the adeno- and adeno-associated virus or the lenti- or retrovirus vectors, show certain disadvantages, e. g. a high risk potential (immune responses, integration of viral genetic information into the hosts' genome) or a small genome size, limiting the modification possibilities (Liniger et al., 2007; Raper et al., 2003; Scott et al., 2016; Vannucci et al., 2013). In consequence, the herein presented method provides a fast and efficient method for the purification of a highly effective and safe tool for cell transduction and gene transfer.

Furthermore, the applied recombinant baculovirus served as a model for large rod-shaped virus particles (L: 200 nm–300 nm; D: 30 nm–60 nm) for the SXC, as currently no data on the method performace for this kind of particle is available.

It is of additional interest for size-dependent purification methods, that for VSV-G pseudotyped viruses slightly different particle sizes and a rather oval than rod shaped structure have been described previously (Barsoum et al., 1997). In this work, the optimization of the yield and product purity and the maintained efficacy of the viral vector after purification was confirmed.

2. Materials and methods

2.1. Used baculovirus

*Ac*MNPV, pseudotyped with the VSV-G, were used. Virus details and the pseudotyping have been described previously (Sprick et al., 2017). More detailed information can be found in the supplements.

2.2. Cell culture

The virus production was carried out in Sf9 cells, maintained in serum-free medium (Sf900 II SFM medium, #10902096; Life technologies) using spinner flasks (50 ml culture volume) or a stirred tank reactor (2.4 l culture volume), as reported by Sprick et al. (2017). Further details are given in the supplementary data, as this is not the focus of this work.

2.3. Virus harvest and initial clarification

Virus particles were harvested at a cell viability below 50%. For the initial clarification, the cell culture broth was either centrifuged (10 min at 250 x*g* and 3000 x*g*, 10 min; and 20 min at 4700 x*g*) or filtered using depth filtration. For the latter, polypropylen filters (Sartorius) were applied, that offer pore sizes of 3 and 0.65 µm and a filter area of 0.12 m^3 and 0.013 m^3, respectively. Filtration was done at a constant flow of 150 ml min^{-1}, using the SARTOFLOW® Slice 200 system (Sartorius). The clarified virus suspension was stored and light-protected at 4 °C until further usage.

2.4. Determination of AcMNPV titer

The virus amount in the harvest solution was determined by the $TCID_{50}$ method (Sprick et al., 2017). Briefly, Sf9 cells were infected in multiwell plates with dilutions ranging from 10^{-2} to 10^{-9} pfu ml^{-1}. The virus particles carried the gene encoding for the green fluorescent

protein (GPF), which was subsequently expressed in infected cells. Thus, wells emitting green fluorescent light were counted after 5 to 7 days of incubation at 27 °C, using a fluorescence microscope (Wilovert AFL 20 microscope, supplied by Hund GmbH) with a SYBR-Green fluorescence emission filter (Hund GmbH).

2.5. SXC purification of virus particles

The chromatographic separations were done on an Äkta Pure 25 liquid chromatography system (GE Healthcare) with UV (280 nm), and by conductivity monitoring at room temperature. Furthermore, a 90° light-scattering detector (Nano DLS Particle Size Analyzer, Brookhaven Instruments) was integrated into the flow path. Hydrosart cellulose membranes (HCM) with a nominal pore size of 3–5 µm were kindly provided by Sartorius Stedim Biotech GmbH. Following an optimization of critical process parameters (see Section 2.6), additionally glass microfiber filters with a nominal pore size of 1.6 µm (GMF, #516-0862, VWR Collection) and polyamide membranes with a nominal pore size of 5 µm (PA, "Ultipor®" #NCG047100 Pall Laboratory) were used. The membranes were prepared by punching discs of 13 mm in diameter, and by stacking 15 slices. The membrane stack was framed by support screens in a 13 mm stainless steel filter holder (#4042; PALL Life Sciences). For a stack of 15 membranes, a total surface of 19.9 cm^2 and a column volume of 0.14 ml (HCM, PA) or 0.13 ml (GMF) was given. The column volume was calculated from diameter, height and the number of membranes, and was therefore considered as the theoretical column volume. With small changes, the chromatographic runs were performed as described by Marichal-Gallardo et al. (2017). Briefly, the membranes were washed with MilliQ water and equilibrated using PBS containing the desired concentration of PEG (see Section 2.6). The preclarified virus harvest was diluted 1:2 with a PBS/PEG solution to equal the conditions of the running buffer, and loaded using a 10 ml or 150 ml superloop (GE Healthcare). Following sample loading, the column was washed with equilibration buffer until the UV signal dropped to the baseline. Finally, the virus particles were eluted using PBS without PEG.

The elution efficiency concerning virus recovery was tested, using both downward flow (normal flow direction) and upward flow (backflushing the column), in order to evaluate a possible filtration effect. Although the membranes can be operated as single-use materials, here the column was regenerated using 0.5 M NaOH and 1 M NaCl in ultrapure water to allow a reuse of the membrane stack. All buffers used were filtered, using a 0.2 µm bottletop filter (#431118, Corning), and degassed in an ultrasonic bath (Ultrasonic cleaner, VWR).

2.6. Optimization of critical process parameters

A design of experiments (DoE)-based approach was performed in order to optimize the virus yield, total protein and dsDNA reduction, respectively. Therefore, the critical process parameters, i.e. the PEG concentration, the PEG molecular weight and the NaCl concentration in the elution step were varied within the design space provided in Table 1. The experiments were planned and evaluated using the Design Expert® software (Version 11, Stat Ease). A response surface design was used with a total of 28 randomized runs.

Table 1
Experimental factors and levels used for the optimization of the SXC for the purification of VSV-G pseudotyped recombinant AcMNPV. These values determine the design space.

Factor	Unit	Level		
		Low	Center	High
Polyethylene glycol concentration (w/v)	[%]	4	8.52	12
Polyethylene glycol molecular weight	[g mol^{-1}]	6000	8000	12000
NaCl concentration in the elution step	[M]	0	1	2
Flow rate	[ml min^{-1}]	0.5	3.75	7

2.7. Dynamic binding capacity determination at optimum process conditions

The dynamic binding capacity (DBC) was determined, using the 13 mm filter holder, and a stack of fifteen membranes prepared as stated in Section 2.5. The HCM, GMF and PA membranes were tested with regard to their DBC. The virus feed of a known concentration was loaded onto the column, until a complete breakthrough was observed, based on a light-scattering detection. The amount of virus at a 10% breakthrough was then calculated in relation to the maxium signal. All three membrane types were tested for their binding capacity.

For the calculation of mass balances, all DBC runs were additionally washed and eluted as described in Section 2.5.

2.8. Analytics of purified virus particles

2.8.1. Dialysis of SXC fractions

All samples were dialized against PBS, prior to the qPCR and dsDNA assays. The dialysis tubing with a molecular weight cut-off of 14 kDa (#D9777-100FT; Sigma-Aldrich) was prepared as follows: The tubes were cut into segments of appropriate length and washed at 70 °C for 4 h under stirring with 0.1 M $NaHCO_3$ (pH 7.0) containing 0.01 M EDTA. After 2 h of incubation, the buffer was exchanged by a fresh prewarmed $NaHCO_3$ buffer. Afterwards the tubings were washed with MilliQ water at room temperature - under stirring over night, exchanging the water three times within the first three hours. The prepared tubings were used for the dialyis of the individual SXC fractions. The dialysis was done over night at 4 °C under stirring with a 1000-fold buffer exchage to PBS.

2.8.2. Quantitative real-time PCR for viral DNA amplification

Viral dsDNA was isolated from dialized samples using the PureLink™ Viral RNA/DNA Mini Kit (#12280050, Thermo Fisher Scientific) according to the manufacturers instructions. The isolated DNA was directly used for quantitative PCR (qPCR). The qPCR was performed with the QuantiNova™ SYBR® Green PCR Kit (#208054, Quiagen), as described in the manual, in order to quantify the VSV-G. A master mix comprising 2x SYBR Green PCR Master Mix, nuclease-free water as well as forward and reversed primers (final concentration 1 µM, *Sigma Aldrich*) was prepared. In a 96 well twin.tec® PCR plate (Eppendorf), 4 µl extracted DNA sample were mixed with 16 µl master mix and amplification was done with a Mastercycler ep gradient S realplex^2 (Eppendorf). The following program was applied: (1) 2 min 75 °C pre-incubation, (2) 40 cycles of (i) 15 s 95 °C denaturation, (ii) 10 s 60 °C annealing, (iii) 10 s 72 °C elongation (3) melting curve analysis from 72 °C to 90 °C within 20 min. After each cycle, and during the melting gradient, the fluorescence signal was measured. The total viral DNA was quantified against a standard calibration curve in the range of 10^3 to 10^8 copy numbers (cn) per ml. The virus recovery was calculated, based on the viral DNA amount in all chromatographic fractions (flow through, wash, elution) and the amount contained in the injected feed with a standard deviation $\leq$15%.

2.8.3. Total protein assay

The content of total protein was evaluated, using non-dialized chromatographic samples and the Pierce™ BCA Protein Assay Kit (#23225; Thermo Scientific) according to the manufacturers instructions. Briefly, in a 96-well microplate, 25 µl of each sample were mixed with 200 µl working reagent and incubated at 37 °C for 30 min. Afterwards, absorbance was measured at 562 nm, using a plate reader (BioTek™ Cytation™ 3, BioTek). Bovine gamma globulin (kit contained) was used to produce a standard calbibration curve in the range of 20–2000 µg ml^{-1}. The relative standard deviation of technical triplicates was 10%.

2.8.4. dsDNA assay

The total dsDNA content was evaluated using the Quant-iT™ PicoGreen® dsDNA Kit (#P11496, Thermo Fisher Scientific) according to the instructions. Dialized samples were analyzed in a 96-well format, using the plate reader (Cytation™ 3, BioTek). Each plate contained two standard calibration curves, prepared from λ-DNA of the above mentioned kit in the range of 0.025 ng ml^{-1} to 25 ng ml^{-1} (low-range) and 1 ng ml^{-1} to 1000 ng ml^{-1} (high-range), respectively. Fluorescence excitation was at 480 nm and the emission intensity was measured at 520 nm. The assays' standard deviation was 15%.

2.8.5. Particle size distribution measurements

Virus harvests and chromatographic elution samples were analyzed at room temperature with a Zetasizer Nano ZS90 (Malvern), equipped with a He-Ne laser (633 nm) and the use of disposable cuvettes (100 µl, 1 ml). Size distribution measurement was performed, using a 90° light scattering detector angle. Data analysis was done with the Malvern Zetasizer Software (version 7.12) and multiple narrow modes as a data processing option. Dispersant refractive index and viscosity of the dispersant were determined in advance by measuring buffer and medium, and were set to 1.45 (refractive index) and 0.954 cP (viscosity) for all experiments. All samples were measured in undiluted form, with 1:5 and 1:10 dilutions in PBS.

2.8.6. Efficacy verification of the purified AcMNPVs by Transduction of hMSC

For the transduction experiments, mesenchymal stromal cells were seeded in 24 well plates (TPP) at a density of 15,000 cells cm^{-2}, and cultivated overnight in a growth medium (Dulbecco's Modified Eagle's Medium, Merck) + 10% FCS (Merck) + 1% Ala-Gln (Merck). After the removal of the supernatant, 75 virus particles per cell were added. The volume was adjusted to 500 µl with PBS + Ca^{2+}, Mg^{2+} and the cells and viruses were incubated at 37 °C in a 5% CO_2 humidified atmosphere. After 24 h of incubation, the supernatant was discarded, followed by a washing of the wells with PBS and by detaching the cells using trypsin/EDTA in a final concentration of 0.05% trypsin and 0.02% EDTA, respectively. The trypsin activity was stopped after a complete cell detachment by adding 100 µl of a soybean trypsin inhibitor to a final concentration of 0.1 mg ml^{-1} (Sigma-Aldrich). The cell suspension was finally analyzed for the GFP expression, using a flow cytometer (Guava easyCyte HT-2 L, Merck Milipore).

3. Results

3.1. Optimization of critical process parameters

Scouting experiments (data not shown) were carried out to verify the critical process parameters, such as the PEG concentration and molecular weight, as shown in literature (Lee et al., 2012; Marichal-Gallardo et al., 2017). Furthermore, the applied flow rate, the number of membrane layers as well as the NaCl concentration of the elution buffer were determined as critical, and subsequently optimized. Based on a quadratic model, viral recovery values ranged from 4 to 100% within the design space (see Table 1) as shown in the surface response plots (Fig. 1). Varying the PEGs' molecular weight and concentration itself, resulted in virus recoveries between 20 to 80% (Fig. 1, A). The maximum recovery of ~80% for an optimal virus retention and recovery, was observed at about 8% PEG 8000. Considering the applied flow rate, it is depicted, that virus recovery dropped to zero for flow rates above 6 ml min^{-1} at low polymer concentrations (Fig. 1, D), but also in combination with PEG of a higher molecular weight (Fig. 1, B). Furthermore, a decreased recovery at lower flow rates, using 12% PEG, could be observed (Fig. 1, D). A flow rate optimum for each individual polymer molecular weight was visible. For the PEG with the highest molecular weight, the lowest flow rates resulted in a nearly complete virus recovery.

In contrast, using smaller PEG molecular weights of 6000 and 8000 g mol^{-1} and intermediate flow rates between 3 and 7 ml min^{-1} resulted in a higher virus recovery.

Varying the NaCl concentration in the elution buffer (Fig. 1, C/E/F), causes changes in the recovery within 10–15% with, in general, an increased recovery for higher NaCl concentrations.

For the optimization of DNA and protein depletion, a linear model was applied. It was observed, that the contaminant depletion decreased in relation to an increase of PEG concentrations and molecular weights (Fig. 2, A and D). The best contaminant removal could be achieved at the lowest PEG concentration and molecular weight with 100% and 85% for protein and dsDNA, respectively, whereas at 12% of PEG 12,000 only 76% of the total protein and 49% of the DNA could be removed. The high impact of the flow rate on the virus retention could not be observed for impurity removal. Changes in impurity recovery only account for less than 5% for varying flow rates (Fig. 2, B,C,E,F). An adjustment of the salt concentration during the elution did not affect the impurity depletion (data not shown).

Following an optimization, the "sweet spot" conditions stated in Table 2 were determined. These parameters were selected in order to achieve a recovery above 75%, as well as a DNA and protein removal of at least 60% and 95%, respectively. The salt concentration in the product buffer was settled to 0.5 M in order to benefit from its positive effect, while not burdening the virus particles with an increased osmotic pressure. These conditions were applied for all subsequent experiments.

3.2. Dynamic binding capacity at optimum process conditions

Using cellulose membranes (3–5 µm pore size), the viral DNA concentration in the feed solution was 1.26E + 07 cn ml^{-1} and the amount of infective particles was determined with 9.45E + 06 pfu ml^{-1}. For a complete breakthrough, 80.3 ml of the feed solution could be applied to the membrane stack, equaling a total amount of 1.01E + 09 cn or 7.59E + 08 pfu. A breakthrough of 10% was observed after 26 ml, allowing an application of 2.46E + 08 pfu to a 15 membrane stack, equaling a capacity of 1.23E + 07 pfu per cm^2 membrane (1.64E + 07 cn cm^{-2}). In comparison to that, a total of 7.91E + 06 pfu (8.69E + 06 cn) could be loaded per cm^2 GMF membrane (Fig. 3) and 9.38E + 05 pfu (1.03E + 06 cn) per cm^2 of PA membranes.

3.3. Verification of the optimum process conditions

3.3.1. Virus recovery

After performing triplicate SXC runs for each virus production batch under the same process conditions, mean virus yields of 90.9% ± 13.8% were achieved (Fig. 4), based on viral DNA determination. Less than 10% of the applied virus were not retained, with about 2% recovered in the flow-through, and an additional 6.5% in the wash fraction, respectively. Varying the flow direction of the elution, did not result in significant differences concerning virus recovery, determined by a students' *t*-test. For nine purifications of three different production batches, virus yields in the product fraction differed in less than 8%, which is within the range of the analytical error (data not shown).

The size distribution analysis before and after chromatographic separation is shown in Table 3, presenting two main size populations for the length and the diameter of the virus. The elution pool mainly shows particles with a mean size of 322 x 63 nm, comparable to the values measured for the feed. No other size populations or larger aggregates could be found.

3.3.2. Impurity removal

For three different production batches with triplicate SXC purifications performed for each batch, a remaining dsDNA amount of 15–38 % in the elution fraction was found, depending on the production batch

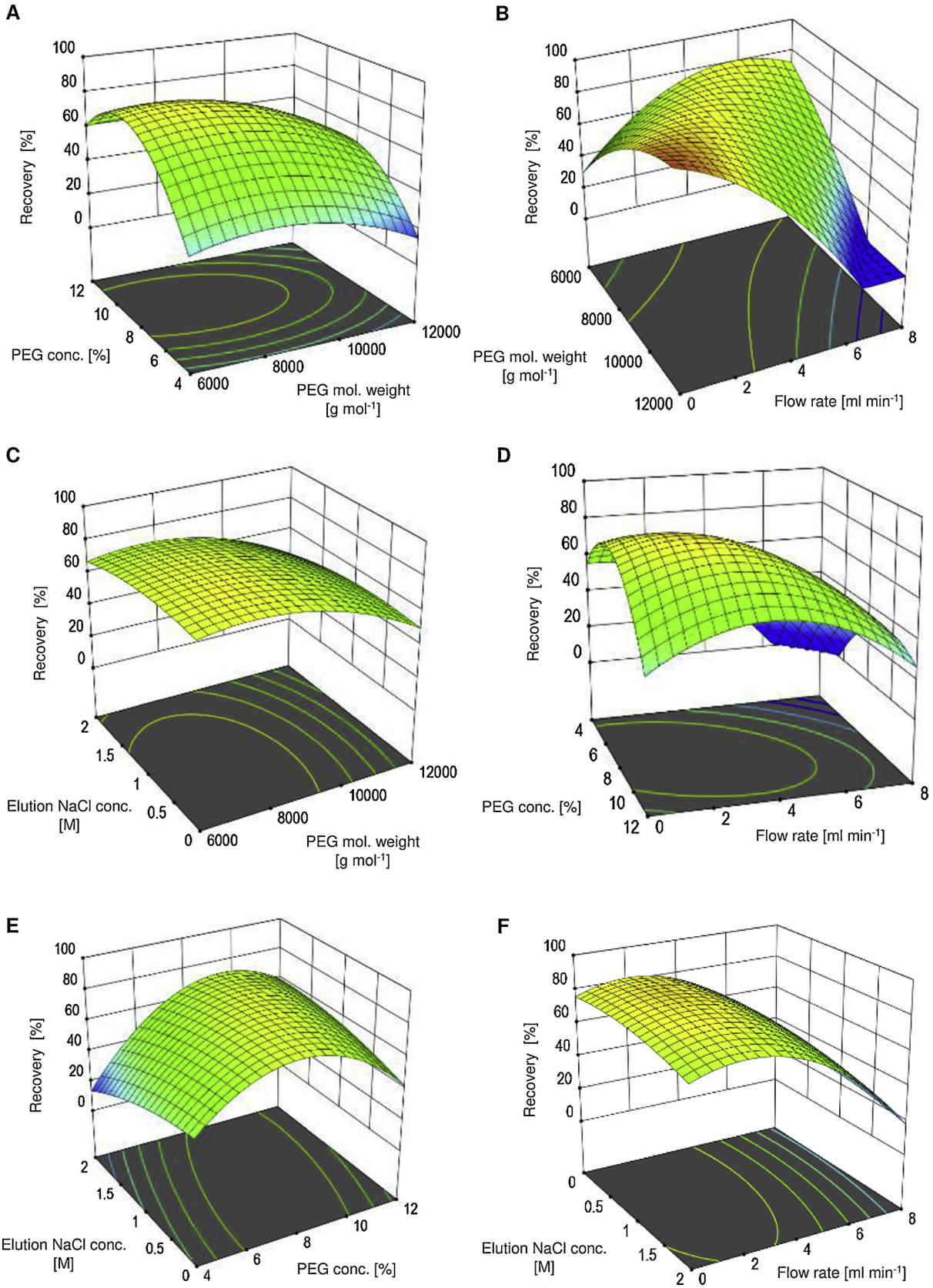

Fig. 1. Virus recoveries under varying process conditions: Elution yields in relation to the PEG concentration and the molecular weight, the flow rate and the NaCl concentration in the elution, respectively. The biggest influence is caused by the polymer concentration and the applied flow rate. However, the recovery is also affected by the PEGs molecular weight and, to a lesser extent by the amount of salt during elution. Process parameters not shown in the individual graphs were set to their medium value. Blue areas show recoveries below 40%, green areas stand for 40–80% and yellow to red areas are above 80 and 90%, respectively. (For interpretation of the references to colour in this figure legend, the reader is referred to the web version of this article).

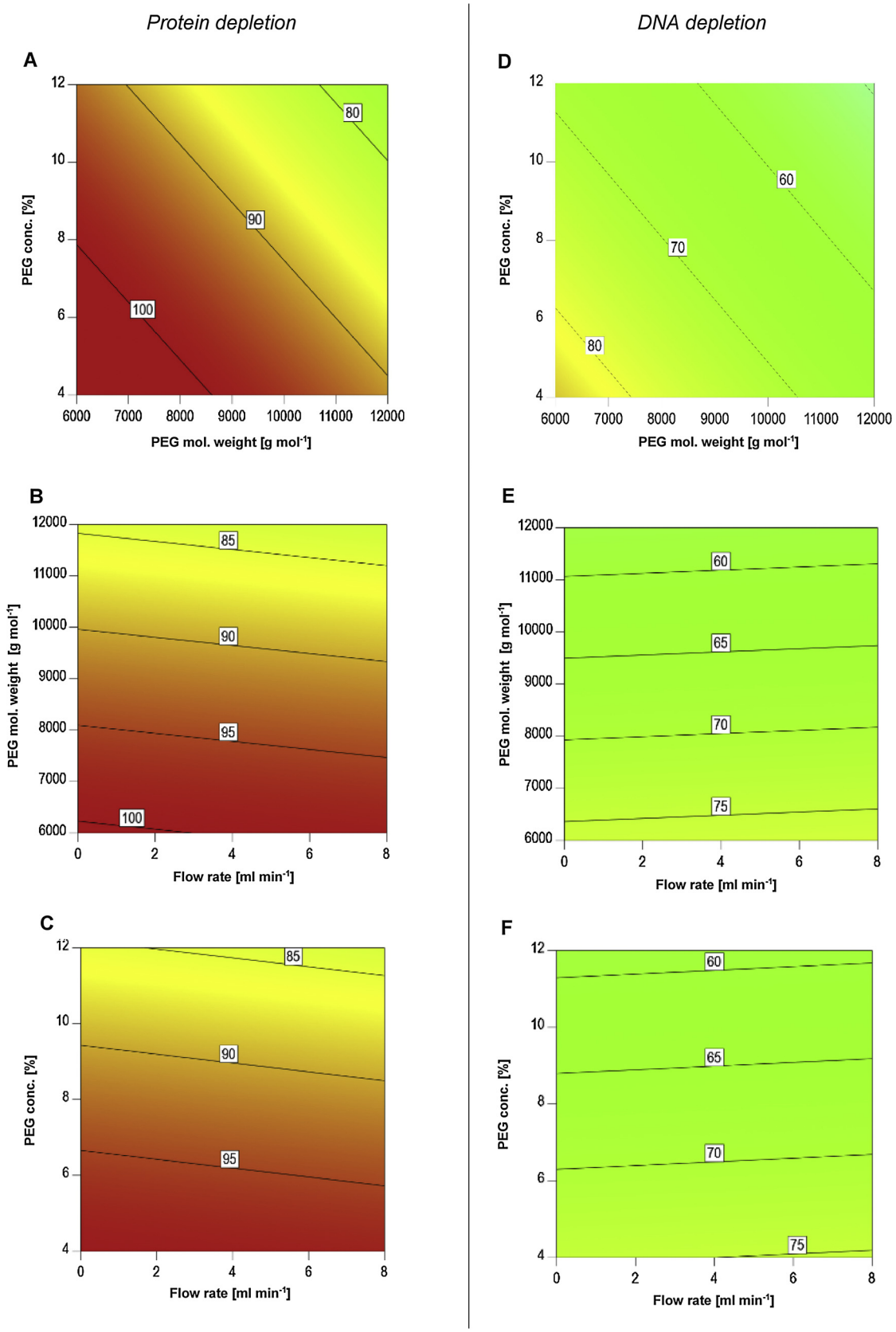

Fig. 2. Optimization of the impurity removal: Protein (left) and DNA (right) depletion in dependance on varying conditions for PEG concentration and molecular weight as well as flow rate. A significant influence was observed for the impurity depletion, when the PEG concentration and molecular weight changed. A minor impact was observed for different flow rates (< 5%). Process parameters not shown in the individual graphs were set to their medium value. Red are impurity depletions above 90%, green are values below 80 and yellow to orange show the range in between. (For interpretation of the references to colour in this figure legend, the reader is referred to the web version of this article).

Table 2
Optimum SXC parameters and expected responses resulting from the DoE optimization. Special focus was set on a high virus recovery while obtaining sufficient impurity removal values.

Selected optimum parameters ("Sweet spot")				Predicted responses		
PEG mol. weight	PEG conc.	NaCl conc. (Elution)	Flow Rate	Recovery	Protein depletion	DNA depletion
[g mol^{-1}]	[%]	[M]	[ml min^{-1}]	[%]	[%]	[%]
8000	8	0.5	3.24	81.24 ± 9.05	95.40 ± 2.18	66.21 ± 6.09

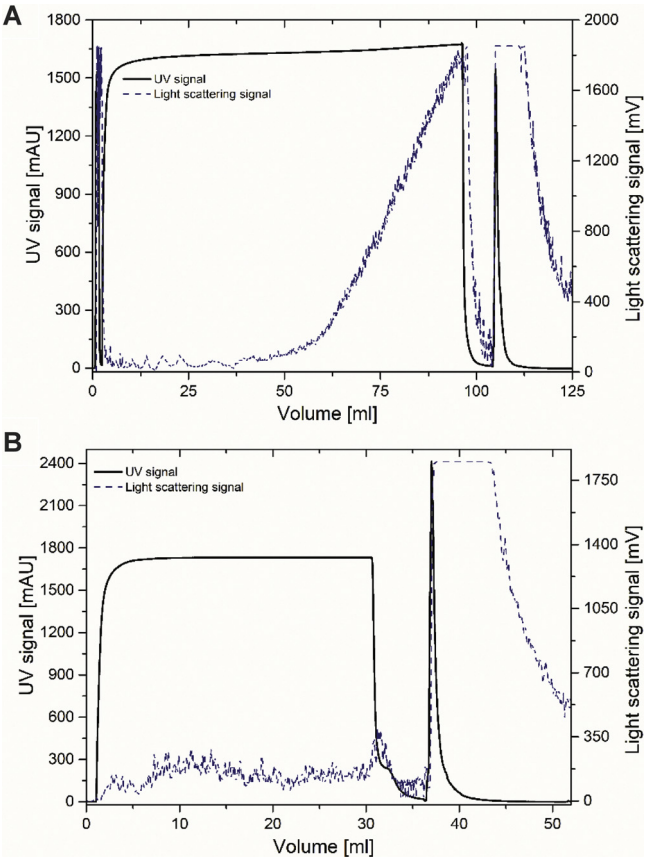

Fig. 3. Chromatograms for the dynamic binding capacity of GMF membranes (A) and HCM SXC purification using a loading volume at $DBC_{10\%}$ (B): A). Shown are the UV (280 nm) and the light scattering signal (90° light scattering) for the SXC purification, using 10 layers of GMF membranes and a 13 mm filter holder. From 0–3 ml the 100% breakthrough signal is shown without the membranes in the flow path. Afterwards a sample was loaded (3–97 ml) until complete breakthrough occured. Subsequently the membranes were washed until 105 ml and then the virus was eluted. The $DBC_{10\%}$ was reached after loading of about 55 ml. The feed contained approximately 1.67×10^6 pfu (1.83×10^6) per ml. B). The loading of a 30 ml virus feed containing 8.2×10^6 pfu ml^{-1} to a stack of 15 cellulose membranes was followed by a similar procedure of washing and elution.

(Fig. 5, A). This resulted in a mean DNA depletion of 84.9% ± 13.75%. Altogether, the elution pool contained about 199 ng ml^{-1} dsDNA at viral DNA titers of about 2.2E + 07 cn ml^{-1}.

With regard to the total protein contamination in the samples, literally a complete removal could be seen. For three different production batches, less than 1% of the initially contained protein amount was detected in the product fraction, assuming a protein depletion above 99% (Fig. 5, B). Most of the protein was already removed during sample application with about 92%, and an additional 13% were found in the wash fraction. On average, the feed solution contained 15 µg total protein, whereas less than 50 ng remained in the product fraction.

The recovery of both, dsDNA and total protein in the product fraction, was independent from the used elution flow direction (data not shown).

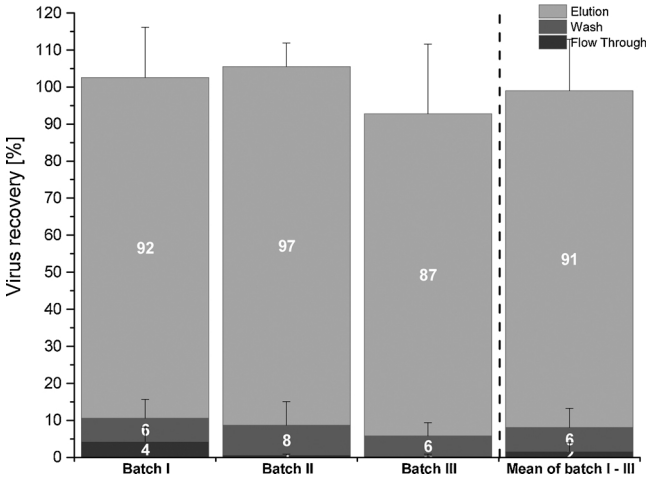

Fig. 4. Baculovirus recoveries based on DNA-titer quantified using qPCR: To determine the reproducibility of the method, biological replicates (three different virus cultivation batches) as well as technical replicates (three SXC purifications for each batch) were evaluated. The mean recovery of the three batches was calculated.

Table 3
Particle size distribution for crude virus harvest and for the elution fraction as determined by dynamic light scattering. Shown is the mean and standard deviation of the two most abundant size populations of repeated measurements.

Apparent hydrodynamic radius [nm]			
Harvest solution (feed)		Elution	
Size population I	Size population II	Size population I	Size population II
319.16 ± 32.91	54.788 ± 5.88	322.73 ± 22.04	62.97 ± 5.82

3.4. Alternative stationary phases

Using the GMF for a triplicate SXC of one cultivation batch, a virus recovery of 73% ± 11% was obtained with about 10% of the virus found in the flow-through and 1% in the wash fraction. Approximately 3% of the initial protein amount was found in the elution and 55% of the contained DNA, suggesting a contaminant depletion of 93% and 45% for proteins and DNA, respectively.

For the PA membrane, a virus recovery of 81% ± 17% in the elution could be determined, whereas about 15% ± 10% were removed in the flow-through and wash fractions. No proteins remained in the product fraction, whereas the dsDNA depletion was about 81%.

3.5. Efficacy verification of the purified AcMNPVs by Transduction of hMSC

To verify the viral capability of transducing mammalian cells after

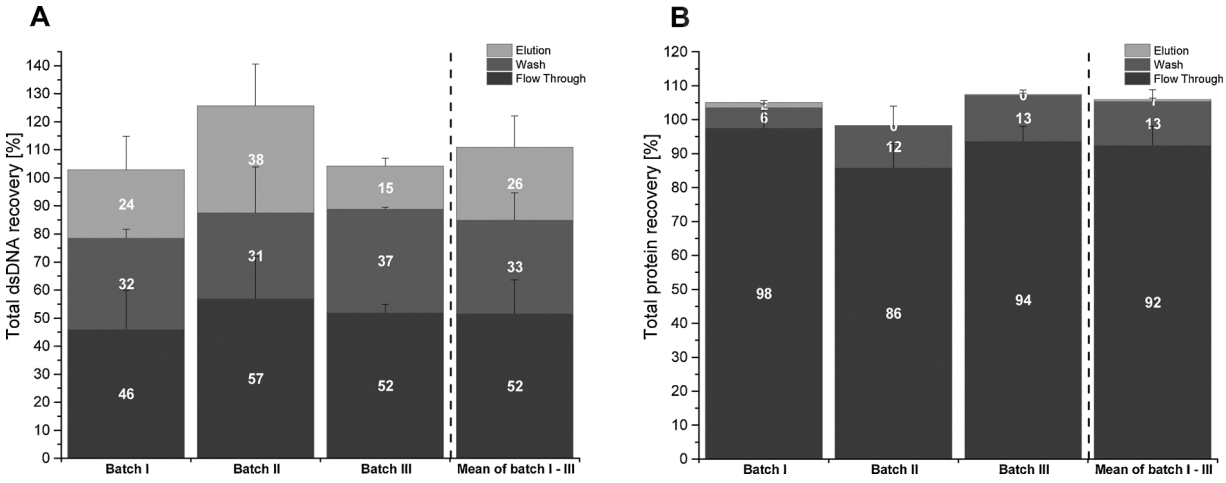

Fig. 5. Confirmation of the impurity removal under optimum conditions: The recovery of double stranded DNA (A) and the total protein amount (B) in individual chromatographic fractions was evaluated for both biological (different cultivation batches) and technical triplicates in downward and upward flow conditions. Additionally, the mean recovery was determined in all 18 runs of different production batches and elution modes and depicted for each contaminant.

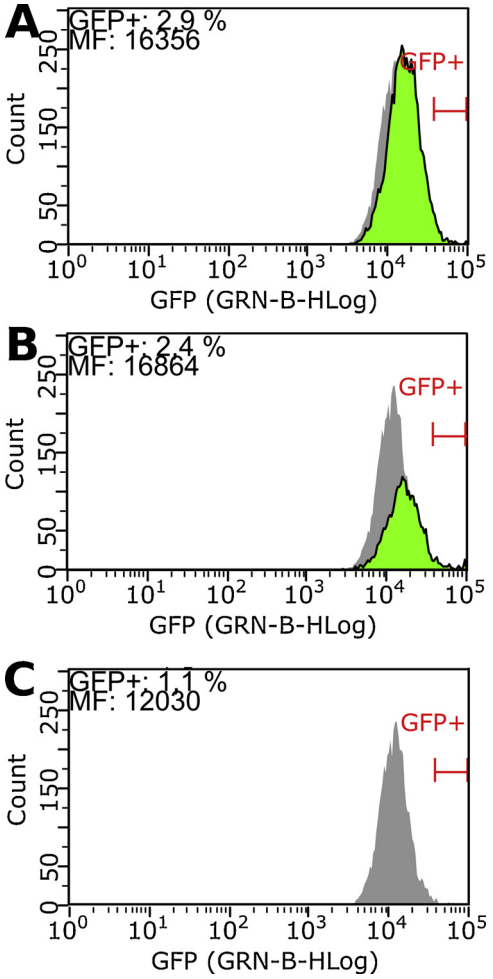

Fig. 6. Evaluation of the transduction efficiency: The determination of GFP + hMSCs after the transduction of purified (A) and unpurified (B) baculoviruses. C) shows the control of non-transduced cells. MF is the mean fluorescence intensity of all cells measured given in relative units. (For interpretation of the references to colour in this figure legend, the reader is referred to the web version of this article).

the purification using SXC, primary hMSCs were transduced and the amount of GFP + cells was measured afterwards, using flow cytomertry. As shown in Fig. 6, the purification did not lead to intense viral inactivation, as the amount of GFP + cells after (2.9% Fig. 6, A) and before (2.4% Fig. 6, B) were comparable. Mean fluorescence intensities (MF) for the transduced cells were at 16,356 U (Fig. 6, A) and 16,864 U (Fig. 6, B) and only 12,030 U for the control (Fig. 6, C).

4. Discussion

4.1. Optimization of critical SXC parameters

In theory, the retention of viruses and smaller impurities should increase continuously with an increase of the polymer concentration, due to an enhanced association of molecules for higher PEG concentrations (Marichal-Gallardo et al., 2017). This effect is supported by the given data. Not only retention is enhanced, but also smaller molecules are progressively retained. This is visible in the reduced impurity removal for the highest PEG concentration and molecular weight. The completely diminished virus recovery at flow rates above 6 ml min^{-1} might be caused by the short residence time in the membrane stack. Hence, the virus association was insufficient or disabled, especially at very low (4%) polymer concentrations. A reduced virus recovery for low flow rates and a high molecular weight, might be caused by an increased virus aggregation and thus by possible additional filtration effects. The effect of salt on the SXC has been described previously (Lee et al., 2012; Marichal-Gallardo et al., 2017), as salts weaken the retention in relation to their concentration and the Hofmeister series. Therefore, it is not surprising, that the addition of salt during the elution step allows a faster dissociation of virus particles and an enhanced elution. The observed effect of a 10–15% increased virus elution, using higher salt concentrations, might be explained by that effect, but are also within the analytical error. As the virus activity should not be affected for the sake of a complete virus elution, an appropriate tradeoff is required. To conclude, the elution NaCl concentration is optimally adjusted between 0 and 1 M.

4.2. Dynamic binding capacities

Cellulose membranes offered the highest dynamic binding capacities per cm^2, closely followed by GMF and the PA membranes, offering the lowest capacity. However, the three membrane types show varying pore size distributions. The used cellulose membranes show pore sizes between 3–5 µm, whereas the GMF membrane has smaller pores with only 1.6 µm, and the PA membrane has slightly larger pores with a nominal pore size of 5 µm. As for the 5 µm pores of the PA membrane,

the total accessible surface might be reduced, allowing less interaction between the macromolecules and the stationary phase, leading to a decreased capacity.

4.3. Verification of optimum process conditions

The values for the mean yield are in accordance with the predictions of the optimization experiments (see paragraph 3.1) within the margin of deviation. Obviously, the recovery is at the higher limit of the predicted values. This can be explained, as optimization experiments were not conducted at $DBC_{10\%}$ conditions. This is due to an iterative process to find optimum process parameters, and to determine the binding capacity for these afterwards. The confirmation runs were performed after determining the $DBC_{10\%}$ and optimzing and increasing the loading volume accordingly, to reduce virus losses. For other described membrane-based (anion exchange) processes, recoveries of 78% (*Wu et al.*, 2007), 65% (Vicente et al., 2009) or close to 100% (Grein et al., 2012) have been described. Recoveries of sucrose gradient-, tangetial flow ultrafiltration and centrifugation techniques were generally even lower (50–70%, Kwang et al., 2016). This shows a comparable and even superior performance of the SXC method.

The determined baculovirus size distribution is in good alignment with the described particle sizes for VSV-G pseudotyped *Ac*MNPV (Barsoum et al., 1997), being slightly larger than without pseudotyping (Ihalainen et al., 2010). For SXC applications, the formation of protein aggregates, directly after mixing the crude sample with the PEG solution, has been described previously (Lee et al., 2012; Wang et al., 2014). However, no aggregates or varying size populations were observed in the elution. Possible occuring aggregates of virus particles seem to disengage, once the PEG is removed from the system, which was also reported for the influenza virus by Marichal-Gallardo et al. (2017). Furthermore, also the virus itself does not show a change in size and shape as a result of a SXC purification, as the determined size values of the virus in the elution fraction equal the measured starting material.

The DNA and protein removal showed a slightly better performance than predicted (see paragraph 3.1). However, the results are in accordance with the expected values of the design optimization (see paragraph 3.1.) with about 85% compared to 66% for dsDNA, and more than 99% in comparison to 95% for total protein. As already described above for the virus recovery, this issue might occur due to a higher amount of virus suspension being loaded to the column during the confirmation runs. These were performed after the DBC determination in contrast to the DoE runs, which were operated below a $DBC_{10\%}$ loading volume.

Under these conditions the protein removal was nearly complete. However, a further reduction of the DNA content is desirable. The remaining 15% of the DNA content could have been caused either by withhold DNA due to the process conditions, e.g. DNA being sterically excluded by the PEG and retained. Or it could have resulted from the DNA binding to the virus particles, as it has already been described for Influenza A particles (Weigel et al., 2016). Although these are virus particles of a different kind, a binding of the DNA to the surface is also conceivable. Further possible explanations have been discussed recently, and include the co-purification of extracellular vesicles, such as exo- or ectosomes containing nucleic acids or the presence of residual chromatin (Marichal-Gallardo et al., 2017). Additionally, it has to be discussed, that the baculovirus is a DNA virus. This might explain total DNA recoveries above 100% (e.g. batch II with 126%), as it is possible, that some additional DNA is released, due to virus degradation. However, the assays' error of about 15%, which applies for each measured fraction, also needs to be kept in mind. Although it could not be resolved, which of these explanations contributed the most, or at all, to the remaining DNA levels in the elution pool, they give indications for future optimization and detailed characterization trials. Concerning the SXC performance, it was previously shown, that for Influenza A virus particles, the DNA reduction without an additional nuclease treatment was 99.7% and only 76.5 to 89.2% for purifications including a nuclease incubation step (Marichal-Gallardo et al., 2017). Lee et al. (2012) achieved a DNA reduction of 93% when using OH-monoliths for the SXC purification of bacteriopage M13K07 without additional nuclease digestion. For the present application of the membrane-based SXC, the application of an additional nuclease step might be tested, in order to further reduce the amount of the remaining DNA contamination, in case this is desired. Furthermore, an additional purification step could be performed, for example using sulfated cellulose membrane adsorbers (Carvalho et al., 2018; Fortuna et al., 2018). Since baculovirus particles show a heparin affinity (Nasimuzzaman et al., 2016; Wu and Wang, 2012), this method could also have a high potential as an orthogonal purification step to the SXC. As the total virus recovery was less than 100% in some cases, different elution modes were tested in order to exclude a possible filtration effect on the membrane stack and to increase the robustness of the method. However, for neither of the analyzed species a significant effect could be observed, according to students' *t*-test. This excludes the possibility of virus filtration.

For the process contaminants, a change in the elution flow direction was not promising, as most of the contaminating proteins and DNA were washed out during sample application, and were not affected by the process conditions during the elution.

4.4. Alternative stationary phases

Comparing the results for the alternative stationary phases, it can be concluded, that cellulose exhibits a superior performance over GMF and PA membranes. GMF membranes show a comparable binding capacity, but a slightly lower virus recovery and a poor impurity removal, with most of the DNA and higher protein amounts remaining in the product. Additionally, the GMF membranes seem to collapse during the purification process, leading to a dense accumulation GMF. In contrast to the other membranes used, for this GMF bulk, individual membranes could not be segregated anymore. As a result, the purification will most probably not resemble a membrane-, but a bead-based system. For the latter, neither an equal pore distribution, nor a convective flow can be assumed. Due to the collapse, particles and impurities are filtered additionally, leading to a higher contamination amount in the product fraction. For PA membranes, both virus recovery and impurity removal were comparable to that of cellulose. However, the highly reduced binding capacity displays a major disadvantage. For applications where cellulose cannot be used, e.g. due to an unspecific binding of the target molecules, as observed for measles virus (data not shown), PA membranes could present a suitable alternative. To overcome the reduced binding capacity, an increase of the membrane diameter and the effective membrane area, could be appropriate.

4.5. Efficacy verification of the purified AcMNPVs by Transduction of hMSC

The applied purification methods did not seem to impact the transduction ability of the virus particles considerably. The amounts of GFP positive cells and the MF were comparable for transduced cells, using purified and unpurified virus, whereas both values were considerably lower for the control. Although the difference between the purified and unpurified virus is not very high, the transduction efficacy slightly increased with 2.9% GPF-positive cells compared to 2.5% before the purification. This indicates an additional removal of interfering contaminants which influence the transduction.

As a result, SXC might be a potential method to purify AcMNPV, used for cell therapy applications. Furthermore, the achieved purity by SXC was sufficent for a successful transduction of hMSC cells.

5. Conclusion

*Ac*MNPV VSV-G pseudotyped virus particles were efficiently

purified using membrane-based steric exclusion chromatography with recovery yields of about > 90% and impurity removals for host cell proteins and DNA of more than 99% and 85%, respectively. The method provides a superiour binding capacity for viral particles and, theoretically, allows an easy scalability by an increase of the membrane diameter. Depending on the desired application, the use of PA membranes or glass fiber is feasible. The infectivity of the virus particles was not considerably affected by the chromatographic procedure, as the purified virus was capable of transducing hMSCs. However, limiting factors factors might include the evaluation of the infective to non-infective particle ratio, as well as the uncertainty of co-purified vesicles and their possible impact on the intended use, which was not evaluated here. A further DNA reduction would be possible, if required for the application, and would include an additional nuclease digestion or an orthogonal process unit operation. The achieved purity levels and the simplicity of the method make it a great alternative for laborious ultracentrifugation steps or expensive ion exchange membrane chromatography. This allows for an easy local implementation, e.g. for individualized medications.

Declaration of Competing Interest

None.

Acknowledgements

The authors acknowledge the Technische Hochschule Mittelhessen for the initial financial support. Furthermore the authors want to thank Friederike Eilts and Carolin Lappöhn for proofreading of the manuscript.

Appendix A. Supplementary data

Supplementary material related to this article can be found, in the online version, at doi:https://doi.org/10.1016/j.jviromet.2019.113756.

References

Airenne, K.J., Hiltunen, M.O., Turunen, M.P., Turunen, A.M., Laitinen, O.H., Kulomaa, M.S., Ylä-Herttuala, S., 2000. Baculovirus-mediated periadventitial gene transfer to rabbit carotid artery. Gene Ther. 7 (17), 1499–1504. https://doi.org/10.1038/sj.gt.3301269.

Arakawa, T., Timasheff, S.N., 2002. Mechanism of polyethylene glycol interaction with proteins. Biochemistry 24 (24), 6756–6762. https://doi.org/10.1021/bi00345a005.

Atha, D.H., Ingham, K.C., 1981. Mechanism of precipitation of proteins by polyethylene glycols. Analysis in terms of excluded volume. J. Biol. Chem. 256 (23), 12108–12117. https://doi.org/10.1002/bit.25615.

Barsoum, J., Brown, R., McKee, M., Boyce, F.M., 1997. Efficient transduction of mammalian cells by a recombinant baculovirus having the vesicular stomatitis virus G glycoprotein. Hum. Gene Ther. 8 (17), 2011–2018. https://doi.org/10.1089/hum.1997.8.17-2011.

Carvalho, S., Fortuna, A.R., Wolff, M.W., Peixoto, C.M., Alves, P., Reichl, U., Jt Carrondo, M., 2018. Purification of influenza virus-like particles using sulfated cellulose membrane adsorbers. J. Chem. Technol. Biotechnol. 93 (7), 1988–1996. https://doi.org/10.1002/jctb.5474.

Fortuna, A.R., Taft, F., Villain, L., Wolff, M.W., Reichl, U., 2018. Optimization of cell culture-derived influenza A virus particles purification using sulfated cellulose membrane adsorbers. Eng. Life Sci. 18, 29–39. https://doi.org/10.1002/elsc.201700108.

Gagnon, P., Toh, P., Lee, J., 2014. High productivity purification of immunoglobulin G monoclonal antibodies on starch-coated magnetic nanoparticles by steric exclusion of polyethylene glycol. J. Chrom. A 1324, 171–180. https://doi.org/10.1016/j.chroma.2013.11.039.

Gagnon, P.S. (2012) Purification of biological products by constrained cohydration chromatography European Patent EP2720768B1.

Gagnon, P.S. (pending) Purification of biological products by constrained cohydration chromatography, US Patent US20170218011A1.

Giese, G., Myrold, A., Gorrell, J., Persson, J., 2013. Purification of antibodies by precipitating impurities using Polyethylene Glycol to enable a two chromatography step process. J Chromatogr B Analyt Technol Biomed Life Sci. 938, 14–21. https://doi.org/10.1016/j.jchromb.2013.08.029.

Grein, T.A., Michalsky, R., Vega López, M., Czermak, P., 2012. Purification of a recombinant baculovirus of Autographa californica M nucleopolyhedrovirus by ion exchange membrane chromatography. J. Virol. Methods 183 (2), 117–124. https://doi.org/10.1016/j.jviromet.2012.03.031.

Hönig, W., Kula, M.R., 1976. Selectivity of protein precipitation with polyethylene glycol fractions of various molecular weights. Anal. Biochem. 72, 502–512. https://doi.org/10.1016/0003-2697(76)90560-1.

Hu, Y.-C., Tsai, C.-T., Chung, Y.-C., Lu, J.-T., Hsu, J.T.-A., 2003. Generation of chimeric baculovirus with histidine-tags displayed on the envelope and its purification using immobilized metal affinity chromatography. Enzyme Microb. Technol. 33 (4), 445–452. https://doi.org/10.1016/S0141-0229(03)00143-1.

Ihalainen, T.O., Laakkonen, J.P., Paloheimo, O., Ylä-Herttuala, S., Airenne, K.J., Vihinen-Ranta, M., 2010. Morphological characterization of baculovirus Autographa californica multiple nucleopolyhedrovirus. Virus Res. 148 (1-2), 71–74. https://doi.org/10.1016/j.virusres.2009.11.017.

Kramberger, P., Urbas, L., Štrancar, A., 2015. Downstream processing and chromatography based analytical methods for production of vaccines, gene therapy vectors, and bacteriophages. Hum. Vaccin. Immunother. 11 (4), 1010–1021. https://doi.org/10.1080/21645515.2015.1009817.

Kuznetsova, I.M., Turoverov, K.K., Uversky, V.N., 2014. What macromolecular crowding can do to a protein. Int. J. Mol. Sci. 15 (12), 23090–23140. https://doi.org/10.3390/ijms151223090.

Kwang, T.W., Zeng, X., Wang, S., 2016. Manufacturing of *Ac*MNPV baculovirus vectors to enable gene therapy trials. Mol. Ther. Methods Clin. Dev. 3, 15050. https://doi.org/10.1038/mtm.2015.50.

Lee, J., Gan, H.T., Latiff, S.M.A., Chuah, C., Lee, W.Y., Yang, Y.-S., Loo, B., Ng, S.K., Gagnon, P., 2012. Principles and applications of steric exclusion chromatography. J. Chrom. A 1270, 162–170. https://doi.org/10.1016/j.chroma.2012.10.062.

Liniger, M., Zuniga, A., Naim, H.Y., 2007. Use of viral vectors for the development of vaccines. Expert Rev. Vaccines 6 (2), 255–266. https://doi.org/10.1586/14760584.6.2.255.

Marichal-Gallardo, P., Pieler, M.M., Wolff, M.W., Reichl, U., 2017. Steric exclusion chromatography for purification of cell culture-derived influenza A virus using regenerated cellulose membranes and polyethylene glycol. J. Chrom. A 1483, 110–119. https://doi.org/10.1016/j.chroma.2016.12.076.

Michalsky, R., Passarelli, A.L., Pfromm, P.H., Czermak, P., 2009. Purification of the baculovirus Autographa californica M nucleopolyhedrovirus by tangential flow ultrafiltration. Desalination 245 (1-3), 694–700. https://doi.org/10.1016/j.desal.2009.02.039.

Michalsky, R., Passarelli, A.L., Pfromm, P.H., Czermak, P., 2010. Concentration of the baculovirus Autographa californica M nucleopolyhedrovirus (AcMNPV) by ultrafiltration. Desalination 250 (3), 1125–1127. https://doi.org/10.1016/j.desal.2009.09.123.

Nasimuzzaman, M., Lynn, D., van der Loo, J.C., Malik, P., 2016. Purification of baculovirus vectors using heparin affinity chromatography. Mol. Ther. Methods Clin. Dev. 3, 16071. https://doi.org/10.1038/mtm.2016.71.

Nestola, P., Peixoto, C., Silva, R.R.J.S., Alves, P.M., Mota, J.P.B., Carrondo, M.J.T., 2015. Improved virus purification processes for vaccines and gene therapy. Biotechnol. Bioeng. 112 (5), 843–857. https://doi.org/10.1002/bit.25545.

Orr, V., Zhong, L., Moo-Young, M., Chou, C.P., 2013. Recent advances in bioprocessing application of membrane chromatography. Biotechnol. Adv. 31 (4), 450–465. https://doi.org/10.1016/j.biotechadv.2013.01.007.

Raper, S.E., Chirmule, N., Lee, F.S., Wivel, N.A., Bagg, A., Gao, G.-p., Wilson, J.M., Batshaw, M.L., 2003. Fatal systemic inflammatory response syndrome in a ornithine transcarbamylase deficient patient following adenoviral gene transfer. Mol. Genet. Metab. 80 (1-2), 148–158. https://doi.org/10.1016/J.YMGME.2003.08.016.

Scott, M.K., Chommanard, C., Lu, X., Appelgate, D., Grenz, L., Schneider, E., Gerber, S.I., Erdman, D.D., Thomas, A., 2016. Human adenovirus associated with severe respiratory infection, Oregon, USA, 2013-2014. Emerging Infect. Dis. 22 (6), 1044–1051. https://doi.org/10.3201/eid2206.151898.

Sim, S.-L., He, T., Tscheliessnig, A., Mueller, M., Tan, R.B.H., Jungbauer, A., 2012. Protein precipitation by polyethylene glycol: a generalized model based on hydrodynamic radius. J. Biotechnol. 157 (2), 315–319. https://doi.org/10.1016/j.jbiotec.2011.09.028.

Sprick, G., Weidner, T., Salzig, D., Czermak, P., 2017. Baculovirus-induced recombinant protein expression in human mesenchymal stromal stem cells: a promoter study. New Bioeth. 39 (Pt B), 161–166. https://doi.org/10.1016/j.nbt.2017.08.006.

Summers, M.D., 2006. Milestones leading to the genetic engineering of baculoviruses as expression vector systems and viral pesticides. Insect Viruses: Biotechnological Applications 68. Elsevier, pp. 3–73. https://doi.org/10.1016/S0065-3527(06)68001-9.

Tao, S.-P., Zheng, J., Sun, Y., 2015. Grafting zwitterionic polymer onto cryogel surface enhances protein retention in steric exclusion chromatography on cryogel monolith. J. Chrom. A 1389, 104–111. https://doi.org/10.1016/j.chroma.2015.02.051.

Transfiguracion, J., Jorio, H., Meghrous, J., Jacob, D., Kamen, A., 2007. High yield purification of functional baculovirus vectors by size exclusion chromatography. J. Virol. Methods 142 (1-2), 21–28. https://doi.org/10.1016/j.jviromet.2007.01.002.

Trilisky, E.I., Lenhoff, A.M., 2007. Sorption processes in ion-exchange chromatography of viruses. J. Chrom. A 1142 (1), 2–12. https://doi.org/10.1016/j.chroma.2006.12.094.

Vannucci, L., Lai, M., Chiuppesi, F., Ceccherini-Nelli, L., Pistello, M., 2013. Viral vectors: a look back and ahead on gene transfer technology. New Micobiol. 36 (1), 1–22.

Vicente, T., Peixoto, C., Carrondo, M.J.T., Alves, P.M., 2009. Purification of recombinant baculoviruses for gene therapy using membrane processes. Gene Ther. 16 (6), 766–775. https://doi.org/10.1038/gt.2009.33.

Wang, C., Bai, S., Tao, S.-P., Sun, Y., 2014. Evaluation of steric exclusion chromatography on cryogel column for the separation of serum proteins. J. Chrom. A 1333, 54–59. https://doi.org/10.1016/j.chroma.2014.01.059.

Weigel, T., Solomaier, T., Wehmeyer, S., Peuker, A., Wolff, M.W., Reichl, U., 2016. A

membrane-based purification process for cell culture-derived influenza A virus. J. Biotechnol. 220, 12–20. https://doi.org/10.1016/j.jbiotec.2015.12.022.
Wolff, M.W., Reichl, U., 2011. Downstream processing of cell culture-derived virus particles. Expert Rev. Vaccines 10 (10), 1451–1475. https://doi.org/10.1586/erv.11.111.
Wolff, M.W., Pieler, M.M., Reichl, U., Marichal-Gallardo, P. (pending), Method for the separation of virus compositions including depletion and purification thereof, European Patent EP3371302A1.
Wolff, M.W., Pieler, M.M., Reichl, U., Marichal-Gallardo, P. (pending), Method for the separation of virus compositions including depletion and purification thereof, US Patent US20190085300A1.
Wu, C., Soh, K.Y., Wang, S., 2007. Ion-exchange membrane chromatography method for rapid and efficient purification of recombinant baculovirus and baculovirus gp64 protein. Hum. Gene Ther. 18 (7), 665–672. https://doi.org/10.1089/hum.2007.020.
Wu, C., Wang, S., 2012. A pH-sensitive heparin-binding sequence from Baculovirus gp64 protein is important for binding to mammalian cells but not to Sf9 insect cells. J. Virol. 86 (1), 484–491. https://doi.org/10.1128/JVI.06357-11.
Wu, Y., Simons, J., Hooson, S., Abraham, D., Carta, G., 2013. Protein and virus-like particle adsorption on perfusion chromatography media. J. Chrom. A 1297, 96–105. https://doi.org/10.1016/j.chroma.2013.04.062.

Chapter 3 - ORFV vaccine process development: Benchmarking the SXC against commonly applied unit operations

In the following chapter the SXC was combined with several orthogonal purification techniques in order to subsequently set up an efficient and complete DSP procedure. To demonstrate the broad applicability of the SXC in vaccine manufacturing processes a different virus, the ORFV, was used. The ORFV, also referred to as *parapoxvirus ovis*, is an enveloped virus, which has a high potential as vaccination and gene therapy tool. Up to the date no purification procedure was available, allowing an elaborate process development.

In the first step the SXC was compared to different membrane-based chromatographic techniques, which are commonly applied in viral vector and vaccine DSP procedures, i.e., ion exchangers or hydrophobic interaction chromatography. Furthermore, second-step chromatographic purification methods were evaluated for subsequent removal of the remaining impurity levels after SXC. The optimization of the SXC using the ORFV regarding critical process parameters, resulting recoveries and impurity levels was done comparable to the approach presented in chapter 2. The resulting data suggests not only the feasible inclusion of the SXC into a DSP process train, but also indicates its superior performance regarding product recovery and impurity depletion, while at the same time offering milder process conditions than the other tested approaches. The latter especially accounts for the high salt concentrations that are required for loading buffers during hydrophobic interaction chromatography and elution buffers when using ion exchangers. Additionally, the benefits of the SXC, by using virtually any PEG-free buffer of choice for elution is indicated. Due to this, an additional diafiltration step by TFF can be omitted. However, the study also clearly pointed out, that the mere inclusion of the SXC into a downstream processing scheme is not sufficient to satisfy regulatory requirements for medical applications concerning residual contaminant concentrations, primarily due to the remaining DNA levels. As in other production processes an additional nuclease digestion is therefor required and also commonly applied.

Journal of Biotechnology 323 (2020) 62–72

Contents lists available at ScienceDirect

Journal of Biotechnology

journal homepage: www.elsevier.com/locate/jbiotec

Selection of chromatographic methods for the purification of cell culture-derived Orf virus for its application as a vaccine or viral vector

Keven Lothert[a], Felix Pagallies[b], Thomas Feger[b], Ralf Amann[b], Michael W. Wolff[a,c,*]

[a] Institute of Bioprocess Engineering and Pharmaceutical Technology, University of Applied Sciences Mittelhessen (THM), Giessen, Germany
[b] Department of Immunology, University of Tuebingen, Tuebingen, Germany
[c] Fraunhofer Institute for Molecular Biology and Applied Ecology (IME), Giessen, Germany

ARTICLE INFO

Keywords:
Parapoxvirus
Viral vector
Steric exclusion chromatography
Isoelectric point

ABSTRACT

In recent years, the Orf virus has become a promising tool for protective recombinant vaccines and oncolytic therapy. However, suitable methods for an Orf virus production, including up- and downstream, are very limited. The presented study focuses on downstream processing, describing the evaluation of different chromatographic unit operations. In this context, ion exchange-, pseudo-affinity- and steric exclusion chromatography were employed for the purification of the cell culture-derived Orf virus, aiming at a maximum in virus recovery and contaminant depletion. The most promising chromatographic methods for capturing the virus particles were the steric exclusion- or salt-tolerant anion exchange membrane chromatography, recovering 84 % and 86 % of the infectious virus. Combining the steric exclusion chromatography with a subsequent Capto™ Core 700 resin or hydrophobic interaction membrane chromatography as a secondary chromatographic step, overall virus recoveries of up to 76 % were achieved. Furthermore, a complete cellular protein removal and a host cell DNA depletion of up to 82 % was possible for the steric exclusion membranes and the Capto™ Core 700 combination.

The study reveals a range of possible unit operations suited for the chromatographic purification of the cell culture-derived Orf virus, depending on the intended application, i.e. a human or veterinary use, and the required purity.

1. Introduction

The first viral vector-based therapy drugs have already received marketing approval, and numerous products are at different stages of clinical and preclinical testing to treat a variety of both inherited and acquired diseases (Shirley et al., 2020). Among the currently used viral vectors for gene therapy and vaccines, recombinant poxviruses have a large packaging capacity and a favorable safety and efficacy (Pastoret and Vanderplasschen, 2003; Verheust et al., 2012). One example of these viral vectors is the Orf virus (ORFV), a member of the genus *Parapoxvirus* of the family *Poxviridae*. It contains a linear double-stranded DNA genome of approx. 140 kbp in length, and is an enveloped ovoid-shaped virus measuring approximately 260 nm x 160 nm (Nagington et al., 1964). The envelope is surrounded by a characteristic tubule-like structure in a spiral fashion, resembling a ball of wool (Spehner et al., 2004).

Previously, we reported the successful use of the attenuated ORFV for the generation of different recombinants with diverse modifications able to protect against various infectious viral diseases (Rohde et al., 2011, 2013; Rziha et al., 2016; van Rooij et al., 2010). Also other ORFV strains were successfully used for the generation of recombinant vaccines (Hain et al., 2016; Tan et al., 2012), and inactivated ORFV showed immunomodulatory properties in different preclinical models (Bergqvist et al., 2017; Fleming et al., 2015; Wang et al., 2019). Furthermore, Rintoul et al. demonstrated an oncolytic activity for the wild-type ORFV strain NZ2, causing a significantly reduced tumor growth in immune-competent and xenograft human tumor models (Rintoul et al., 2012). These and other reports show the excellent potential of the ORFV vector and its broad field of possible applications (Amann et al., 2013; Friebe et al., 2018; O'Leary et al., 2018).

Abbreviations: DBC, dynamic binding capacity; DLS, dynamic light scattering; HIC, hydrophobic interaction chromatography; HICP, HIC membrane adsorber with phenyl ligand; IEX, ion exchange chromatography; IEX-Q, strong anion exchanger (Quaternary ammonium); IEX-S, strong cation exchanger (Methyl sulfonate); IEX-STPA, salt tolerant polyamide anion exchanger; IU, infective units; MVA, Modified Vaccinia Ankara virus; PEG, polyethylene glycol; pI, isoelectric point; SCMA, sulfated cellulose membrane adsorber; SEC, size exclusion chromatography; SXC, steric exclusion chromatography; $TCID_{50}$, fifty-percent tissue culture infective dose

* Corresponding author at: University of Applied Sciences Mittelhessen (THM), Wiesenstr. 14, 35390, Giessen, Germany.
E-mail address: Michael.Wolff@lse.thm.de (M.W. Wolff).

https://doi.org/10.1016/j.jbiotec.2020.07.023
Received 26 May 2020; Received in revised form 23 July 2020; Accepted 31 July 2020
Available online 05 August 2020
0168-1656/

Knowledge on ORFV production processes is very limited and mainly focuses on upstream processing (Pohlscheidt et al., 2008; Wang et al., 2019). Downstream processing (DSP) procedures generally employ sucrose gradient ultracentrifugation (Rziha et al., 2016) and do not satisfy regulatory demands for the purity of vaccines and gene therapeutic products (European Pharmacopoeia, 2020; World Health Organization, 2017). In order to identify promising chromatographic methods for the purification of ORFV, a direct comparison of the methods used for the DSP of other poxviruses could indicate a feasible approach. For the Modified Vaccinia Ankara virus (MVA), the utilization of anion exchange chromatography (Wolff et al., 2010b) or hydrophobic interaction chromatography (Wolff et al., 2010a) has been reported and could be carried forward for the ORFV purification. Alternatively, Wolff et al. described the successful purification by pseudo-affinity stationary phases based on sulfated carbohydrates with virus yields exceeding 60 % (Wolff et al., 2010a, b) for MVA. Similar methods have previously been shown for the purification of Influenza A virus, using sulfated-cellulose membranes as a stationary phase (Carvalho et al., 2018; Fortuna et al., 2018, 2019) with recoveries of up to 81 %. As Scagliarini and co-workers described the affinity of ORFV to heparin (Scagliarini et al., 2004), the application of sulfated cellulose ligands appears possible, as sulfated carbohydrates are known to mimic heparin ligands (Gallagher et al., 2020; Paluck et al., 2016). Generally, as for nearly all larger macromolecules and nanoplexes, size-dependent chromatographic methods, e.g. size exclusion chromatography (SEC) or steric exclusion chromatography (SXC), should be applicable for ORFV. Examples for the purification of viruses by SEC are the turkey coronavirus (Loa et al., 2002), vesicular stomatitis virus-pseudotyped retrovial particles (Transfiguracion et al., 2003), and the Influenza virus (Heyward et al., 1977; Kalbfuss et al., 2007b; Nayak et al., 2005). More recently, SXC has also been proven to be a valuable tool for the purification of large proteins and bacteriophages (Gagnon et al., 2014; Lee et al., 2012; Tao et al., 2015; Wang et al., 2014). Furthermore, it was successfully applied for the purification of the Influenza A virus (Marichal-Gallardo et al., 2017) and baculovirus particles (Lothert et al., 2020), using regenerated cellulose membranes. Moreover, the Capto™ Core 700 resin (named CC700 hereafter) has also been described as an approach for the purification of infectious virus particles, allowing an efficient impurity removal (James et al., 2016).

Here, we describe the evaluation of different chromatographic applications that can be used for the purification of the ORFV strain D1701-V. One aim was to identify feasible unit operations that have a high specificity for the virus. Secondly, it is desired to use these methods, either individually or in a combination, for a virus purification with regard to product yields and respective purity requirements. Among the tested methods are the membrane-based ion exchange-, hydrophobic interaction-, pseudo-affinity-, and the steric exclusion chromatography, as well as CC700.

2. Materials and methods

2.1. Virus production and initial clarification

For all chromatographic capture steps, a clarified virus harvest was required. Virus amplification was done in an adherent cell culture. Briefly, Vero cells (ATCC, CCL-81) were seeded at 2×10^4 cells per cm^2 in T-225 CytoOne® flasks (STARLAB International). Infection was done at a multiplicity of infection of 0.05. After five days, the supernatant was harvested and frozen/thawed (−80 °C, 22 °C) for a cell disruption and a subsequent virus release. For an initial clarification, the supernatant was centrifuged at 4 °C and 6000 x *g* for 10 min. The clarified virus suspension was used for following chromatographic steps. For a reliable comparability, one production batch was used for all subsequent experiments.

2.2. Screening of feasible chromatographic process unit operations

The chromatographic experiments were done using an Äkta™ Pure 25 liquid chromatography system (GE Healthcare Life Sciences) with UV (280 nm), and conductivity monitoring was carried out at room temperature. Additionally, the light scattering signal was measured online with a Nano DLS Particle Size Analyzer (Brookhaven Instruments). All buffers were filtered with a 0.2 µm filter (Corning) and degassed by ultra-sonication (USC500 THD, VWR) prior to usage.

2.2.1. SXC

The SXC was performed exclusively as a capture step. Regenerated cellulose membranes with a nominal pore size of 1 µm (Whatman RC60, GE Healthcare Life Sciences) were applied as stationary phases. The membranes were punched to discs of 13 or 24 mm and assembled into stainless steel filter holders with 13 mm (#4042; PALL Life Sciences) or 25 mm diameter (XX4502500, Merck), respectively. For each device, 10 membrane layers were stacked, providing a total surface area of 13.3 cm^2 (~0.09 mL) for the 13 mm device, and 45.2 cm^2 (0.32 mL) for the 24 mm membranes. At first, the membrane stack was equilibrated, using either PBS (Thermo Fisher Scientific) or 20 mM TRIS-HCl (Carl Roth) at a pH of 7.4 containing 8 % polyethylene glycol (PEG) 8000 (Carl Roth). The TRIS buffer was additionally supplemented with 180 mM NaCl (Carl Roth). The clarified virus harvest was conditioned with PBS, or 20 mM TRIS-HCl buffer (pH 7.4, 180 mM NaCl) containing an appropriate PEG concentration to meet the criteria of the equilibration buffer. Samples were applied using either a 10 mL or a 150 mL super-loop, depending on the employed membrane volume. After sample application, the column was washed with equilibration buffer (at least 30 column volumes) and the virus was finally eluted using PBS, or 20 mM TRIS-HCl buffer pH 7.4 without PEG, but supplemented with 0.4 M NaCl (Carl Roth). A new stack of membranes was used for every chromatographic experiment. For the characterization of the SXC performance, the 13 mm filter holder was operated with a PBS buffer at a flow rate of 0.5 mL min^{-1}. To evaluate subsequent purification steps, larger amounts of SXC-purified material were prepared. Therefore, the 25 mm filter holder module was used, and TRIS-buffer was employed during loading, wash, and elution to reduce buffer exchanges between process units. Furthermore, these runs were conducted at a flow rate of 3 mL min^{-1} to reduce processing time. The chromatographic experiments were carried out three times, and the elutions were pooled, aliquoted, and frozen at −80 °C until further usage. In parallel, freeze/thaw stabilities in the elution buffer were evaluated for four freeze/thaw cycles after SXC purification (see Section 2.5).

2.2.2. Ion exchange chromatography (IEX)

The IEX was tested for both the capture and the second chromatographic purification step. Therefore, Sartobind® S devices were tested for the cation exchange chromatography (named IEX-S hereafter), and Sartobind® Q (IEX-Q) and Sartobind® STIC®-PA (IEX-STPA) were applied as an anion exchanger and salt-tolerant anion exchanger, respectively (all membrane devices were “pico”-scale modules obtained from Sartorius Stedim Biotech). For all IEX experiments, the columns were equilibrated with 20 mM TRIS-HCl pH 7.4, supplemented with 180 mM NaCl. The samples were mixed with the appropriate buffer to meet these conditions. Afterwards, the samples were applied and the columns subsequently washed with equilibration buffer, until the UV- and light scattering signal reached the baseline. Using 2 M NaCl in 20 mM TRIS-HCl pH 7.4, the bound fraction was finally eluted. In the case of the STPA membrane, an additional 150 mM sodium phosphate (Sigma-Aldrich) was added to the elution buffer. For all steps, a flow rate of 1 mL min^{-1} was applied. The Q and the STPA membranes were tested as a capture step. Furthermore, the SXC-purified material was processed with all described anion exchange membranes for a secondary purification step. All anion exchange experiments were performed in triplicates. Cation exchange experiments were performed

only once for both processing steps, as the isoelectric point (pI) of the ORFV (see Section 3.1) suggests a low binding potential for the virus with a high level of impurities in the flow-through fraction at the given buffer conditions.

2.2.3. Hydrophobic interaction chromatography (HIC)

Sartobind® Phenyl Pico membrane modules (Sartorius Stedim Biotech GmbH) were used for the secondary chromatography of SXC-purified material (named HICP hereafter). Using similar conditions as previously described for Modified Vaccinia Ankara virus (MVA, (Wolff et al., 2010a), the column was equilibrated with 20 mM TRIS-HCl pH 7.4, supplemented with 180 mM NaCl and 1.7 M ammonium sulfate (VWR International GmbH). SXC eluates were adjusted to these conditions by adding the required amounts of salts. After sample loading, the membrane stack was washed, maintaining the high salt concentration. The elution was achieved by removing the ammonium sulfate from the system, using 20 mM TRIS-HCl pH 7.4 and 180 mM NaCl. HICP-secondary chromatographic steps were performed in triplicates, using flow rates of 1 mL min^{-1}.

2.2.4. Pseudo-affinity chromatography (sulfated cellulose)

Sulfated cellulose membrane adsorbers (SCMA) were used in a bind-and-elute mode, and tested for capture and secondary purification. SCMA membranes were obtained as a DIN A4 format sheet (#94SC–04-001, Sartorius Stedim Biotech) and punched to discs of 13 mm diameter. The discs were assembled into the 13 mm stainless steel filter holder mentioned above, with stacks comprising 10 membrane layers. Both the clarified virus broth (capture) and SXC-purified material (secondary purification) were subjected to SCMA purification with triplicate runs for each case. Prior to chromatography, the respective sample was mixed with 20 mM TRIS-HCl pH 7.4 in order to reduce its conductivity below 5 mS cm^{-1}. Conductivities were in the range between 3–4.2 mS cm^{-1} for all runs. After the equilibration of the membrane stack with 20 mM TRIS-HCl pH 7.4, the sample was applied and subsequently washed with equilibration buffer. The elution was achieved by using an equilibration buffer supplemented with 2 M NaCl. Each experiment was conducted in triplicates at a flow rate of 1 mL min^{-1} during all runs and steps of the experiments.

2.2.5. CC700 purification

As a secondary purification, the CC700 resin (readily packed 1 mL columns, GE Healthcare Life Sciences) was tested in the flow-through mode. The general method equals the conditions for the ion exchange membranes (see Section 2.2.2). The SXC-purified material was adjusted to meet the conditions of the equilibration buffer, which was 20 mM TRIS-HCl pH 7.4 and 180 mM NaCl, respectively. After sample loading and washing with the equilibration buffer, the bound material was eluted, using additional 2 M NaCl in the same buffer. All CC700 runs were done in triplicates, using a flow rate of 1 mL min^{-1}.

2.3. Dynamic binding capacity (DBC) determination

DBC experiments were performed for all membranes operated in the bind-and-elute mode. The virus feed of a known concentration was loaded onto the column until a complete breakthrough was observed, based on the light scattering detection. The amount of virus at 10 % breakthrough was subsequently calculated in relation to the maximum signal. Where necessary, sample loading was stopped prior 100 % breakthrough, if the pressure exceeded the maximum operational limit for the tested membrane modules or the system. For a better comparability, capacities were provided in relation to the applied bed volume.

2.4. Characterization of the virus

SXC-purified virus particles were analyzed for their size and isoelectric point. Therefore, SXC virus elutions were subjected to size (diameter) and to surface potential measurements, using a Zetasizer Nano ZS90 (Malvern Panalytical). For the diameter measurements, disposable semi-micro cuvettes (#67.742, Sarstedt) were used at a 90° light scattering angle. The dispersant refractive index and viscosity of the dispersant were set to 1.45 and 0.954 cP, respectively. For the zeta potential measurement, the sample was mixed with 20 mM Tris at pH values between 3 and 13. The pH was checked and adjusted to the respective value prior to the measurement, and reassessed after analysis. Folded capillary zeta cells (#DTS1070, Malvern) were applied to determine the viral zeta potentials at different pH values. The data analysis was conducted with the Malvern Panalytical Zetasizer Software (version 7.12).

2.5. Virus stability evaluation

Additionally, the virus stability was evaluated by using SXC elution fractions (see Section 2.2.1). The samples were supplemented with 0 %, 5 % or 10 % sucrose (Carl Roth) and subjected to up to three freeze/thaw cycles (alternating between -80 and +20 degrees). After each cycle, the infective virus titer was determined (see Section 2.6.1) for each sample composition in triplicates.

2.6. Analytics of chromatographic fractions

Chromatographic fractions were analyzed for their content of infective virus particles as well as with regard to the levels of protein and DNA. The chromatographic fractions considered during analytics included feed, flow-through, wash, and elution for the evaluation of bind-and-elute methods (SXC, IEX-Q, IEX-STPA, HICP and SCMA). In contrast, the flow-through and wash fractions were pooled and analyzed as a single fraction when using IEX-S and CC700.

2.6.1. Flow cytometric titration

Virus quantification was done by flow cytometry. Initially, Vero cells were seeded in a 24-well format with 100,000 cells per well in a culture volume of 1 mL DMEM (Gibco™, Thermo Fisher Scientific), supplemented with 5 % FCS (Capricorn Scientific). Directly after seeding the cells, the infection of each well was performed using 100 µL of the respective chromatographic sample, the medium blank, or standard virus stock (within the range of 1.5×10^5 to 1×10^7 infective units (IU) mL^{-1}). The cells were incubated for 16 h, washed with PBS, and harvested by using Trypsin/EDTA (Gibco™, Thermo Fisher Scientific). Detached cells were supplemented with FCS to stop a trypsin activity, and transferred to a 96-well U-bottom plate (Nunc, Thermo Fisher Scientific). The cells were washed two times by centrifugation at 400 g for 2 min, removing the supernatant, and re-suspending the pellet in 100 µL PBS. Finally, the cells were analyzed using a flow cytometer (Guava® easyCyte HT, Merck). The percentage of GFP positive (equals infected) cells, compared to the total cell number, was determined. The assays' standard deviation was less than 10 %.

2.6.2. Total protein assay

The content of total protein was evaluated using the Pierce™ BCA Protein Assay Kit (#23225; Thermo Fisher Scientific) according to the manufacturer's instructions. Briefly, 25 µL of each sample were mixed with 200 µL of working reagent and incubated at 37 °C for 30 min in a 96-well plate (Nunc, Thermo Fisher Scientific). Afterwards, the absorbance was measured at 562 nm, using a plate reader (BioTek™ Cytation 3™, Fisher Scientific). Bovine gamma globulin (contained in kit) was applied to prepare a standard calibration curve in the range of $20 - 2{,}000$ µg mL^{-1} with a relative standard deviation of about 10 %.

2.6.3. DNA assay

The total double-stranded DNA (referred to as "DNA" in this work) content was quantified, using the Quant-iT™ PicoGreen® dsDNA Kit (#P11496, Thermo Fisher Scientific) according to the manufacturer's

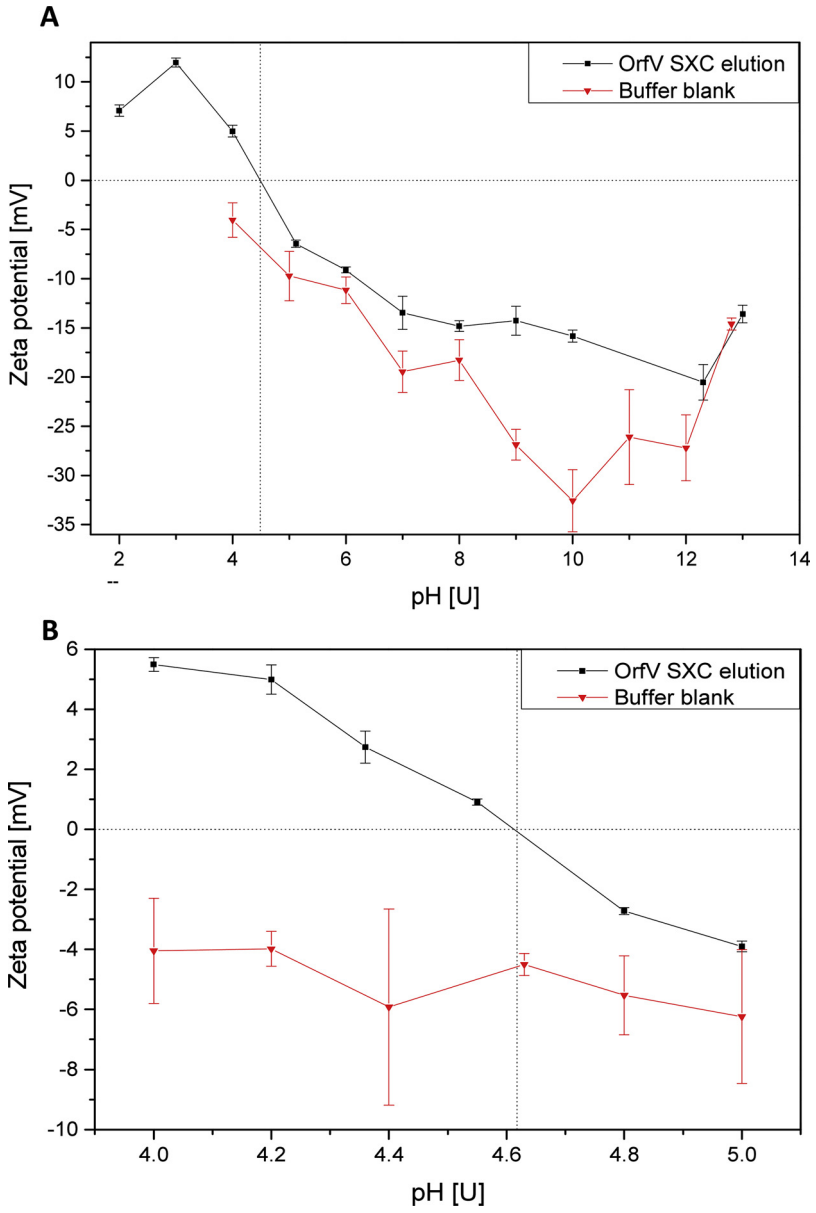

Fig. 1. Determination of the isoelectric point of the Orf virus (ORFV). Zeta potential measurements of virus purified by steric exclusion chromatography (SXC) and the corresponding buffer over a pH range from 2 to 13 (**A**), and more detailed resolution for the apparent transition from positive to negative zeta potential between pH 4 and 5 (**B**). At a pH of 4.61 the net charge is zero. Error bars represent standard deviations of triplicate measurements.

instructions. Samples were analyzed in duplicates in a 96-well format, using black plates (Nunc, Thermo Fisher Scientific) and the same plate reader as for the total protein assay (see Section 2.6.2). Each plate contained two standard calibration curves prepared from λ-DNA contained in the kit in the range of 0.025 ng mL^{-1} to 25 ng mL^{-1} (low-range) and 1 ng mL^{-1} to 1000 ng mL^{-1} (high-range). Fluorescence excitation was at 480 nm, and the emission intensity was measured at 520 nm, with an assay standard deviation of less than 15 %.

3. Results

3.1. Virus characterization

DLS measurements of SXC-purified virus particles showed a size distribution between 130 nm and 370 nm with two main size populations at about 150 ± 14 nm and 250 ± 32 nm. Zeta potential measurements detected a negative viral surface charge above pH values of 5, and a positive surface charge at a pH below or equal to 4 (Fig. 1A). A more detailed analysis of the pH range between 4 and 5 revealed the transition from a positive to a negative surface charge at pH 4.6, which was not detected for the negative control (Fig. 1B). Hence, the viruses' isoelectric point was determined with pH 4.6 under the given environmental conditions.

3.2. Determination of the dynamic binding capacities

The DBC was determined for all bind-and-elute methods at similar conditions, using a clarified harvest. The highest DBC10 % was measured for the SXC, using the 24 mm filter holder with 1.1E + 09 IU mL^{-1} (7.78E + 06 IU cm^{-2}), and for IEX-Q membranes with 5.93E + 08 IU mL^{-1} (1.63E + 07 IU cm^{-2}, Table 1). Compared to the 24 mm device used for SXC, the 13 mm filter holder allowed a DBC10 % of 1.81E + 08 IU mL^{-1} (1.27E + 06 IU cm^{-2}) during SXC, depicting a non-linear correlation between the filter area (volume resp.) and the binding capacity. Comparable results could be determined for the IEX-STPA, HICP and SCMA membranes, with 1.42E + 08, 1.31E + 08, and greater than

Table 1
Overview of the DSP-screening for infective ORFV particles. Different stationary phases were tested for virus and impurity recovery. Capture steps were conducted with clarified virus harvests, whereas SXC-purified material was used for secondary steps. The numbers in brackets show an overall recovery of the respective analyte after secondary chromatography, employing SXC as a capture step. For bind-and-elute methods (SXC, IEX-Q, IEX-STPA, HIC-P, SCMA), the DBC is given in infective units per cm^2. The DBC was not evaluated with regard to methods operated in a flow-through mode, as no binding of the virus was supposed to occur. Recovery values are means of technical triplicates.

		SXC	IEX-Q	IEX-STPA		IEX-S		HICP	CC700	SCMA	
		Capture	SP	Capture	SP	Capture	SP	SP	SP	Capture	SP
Recovery in product fraction [%]	Virus	84	68 (57)	86	57 (48)	39	46 (39)	76 (64)	90 (76)	34	54 (45)
	Total protein	< 1	0	29	0	100	0	0	0	0	0
	DNA	37	100 (37)	64	100 (37)	89	84 (31)	23 (8)	36 (13)	5	80 (30)
$DBC_{10\%}$ [Infective Units mL^{-1}]		**1.81E + 08** (13 mm) **1.1E + 09** (24 mm)	**5.93E + 08**	**1.42E + 08**		Not determined (flow-through method)		**1.31E + 08**	Not determined (flow-through method)	> **1.26E + 08**	

SXC – Steric exclusion chromatography; IEX – Ion exchanger; STPA – Salt tolerant polyamide; HICP – Hydrophobic interaction chromatography with phenyl ligand; CC700 – Capto™ Core 700; SCMA Sulfated cellulose membrane adsorber; $DBC_{10\ \%}$ – dynamic binding capacity (at 10 % breakthrough), SP – Secondary purification.

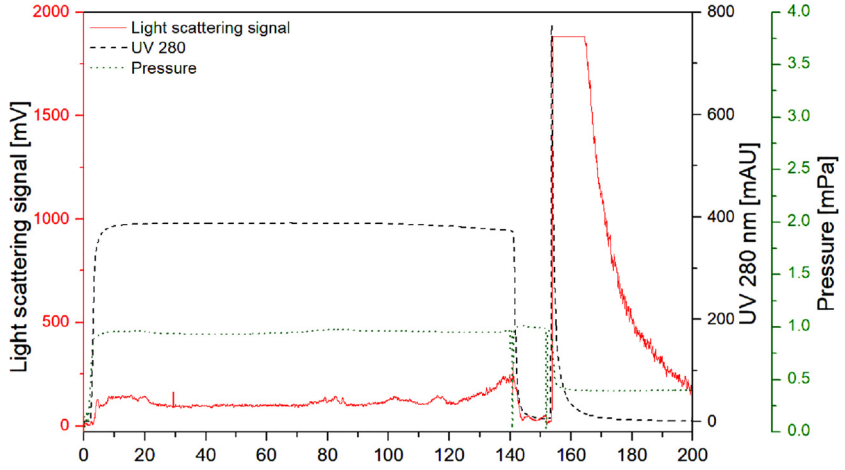

Fig. 2. Determination of the dynamic binding capacity (DBC) during SXC. Representative chromatogram for the SXC using the 25 mm filter holder device, monitoring of UV at 280 nm, light scattering, and pressure. Loading was stopped at 10 % DBC based on light scattering detection.

1.26E + 08 IU mL^{-1} (3.91E + 06, 3.57E + 06 and greater than 8.40E + 05 IU cm^{-2}), respectively. A representative chromatogram is shown in Fig. 2 for the SXC (24 mm membranes), indicating a contaminant breakthrough during sample loading (UV signal), and a virus desorption in the elution fraction (light scattering signal). During loading of the HICP, at 10 % breakthrough, the pressure increased rapidly above 0.5 MPa, which is the operating limit of the HICP according to the manufacturers´ instructions. For the SCMA, a constant breakthrough of 20 % of the maximum signal was observed (data not shown). As a result, a 10 % breakthrough was permanently exceeded during the loading process, and sample loading was stopped once the pressure increased above one MPa.

3.3. Capture step – virus recovery and impurity removal

Of the four tested membranes for the capture step (SXC, IEX-S, IEX-STPA and SCMA), the best virus recovery was achieved by SXC and STPA with viral yields of 84 % and 86 %, respectively (Fig. 3, A). In contrast, using the SCMA or the IEX-S membrane, only 34 % and 39 % of the infective virus particles were collected in the product fraction. Additionally, for the SCMA, only approximately 51 % of the virus could be recovered collectively in all chromatographic fractions, whereas the remaining 49 % could not be accounted for. For the cation exchanger (IEX-S), it has to be noted that the majority of the viruses was found in the elution fraction (56 %) after an application of 2 M NaCl, and not in the flow-through.

Concerning the protein removal, SXC and SCMA performed equally with an almost complete protein depletion (Fig. 3, B). In contrast, almost no protein was removed in the IEX-S flow-through fraction, and about 29 % were found in the STPA elution.

The best unit operation to remove DNA during the capture step is the SCMA, with only 5 % of the initial DNA content to be detected in the product fraction, and 95 % of the DNA being removed during flow-through and wash or remaining bound to the membrane (Fig. 3, C). For the SXC, about 37 % of the DNA were recovered in the elution. Furthermore, most of the contaminating DNA remained in the product fractions of the IEX-S (89 %) and the IEX-STPA membrane (64 %). About 30 % of the DNA was bound to the IEX-STPA membrane and could not be eluted under any of the tested conditions.

3.4. Secondary purification step – virus recovery and impurity removal after SXC

After SXC, a subsequent purification step was evaluated. In the course of these experiments, the highest virus recovery was achieved using CC700 with about 90 % (Fig. 4, A). The second-best performing unit operation was the HICP membrane adsorber, resulting in virus yields of about 76 % (elution fraction) and in about 42 % of losses in the flow-through and wash fractions. Similar to the capture step using the IEX-S purification, approximately half of the virus amount was found in the flow-through product fraction, whereas the other half bound to the membrane and eluted at 2 M NaCl. The tested anion exchange membranes all performed similarly. Approximately 68 % of the virus was found in the product fraction for the Q membrane adsorber, and 57 %

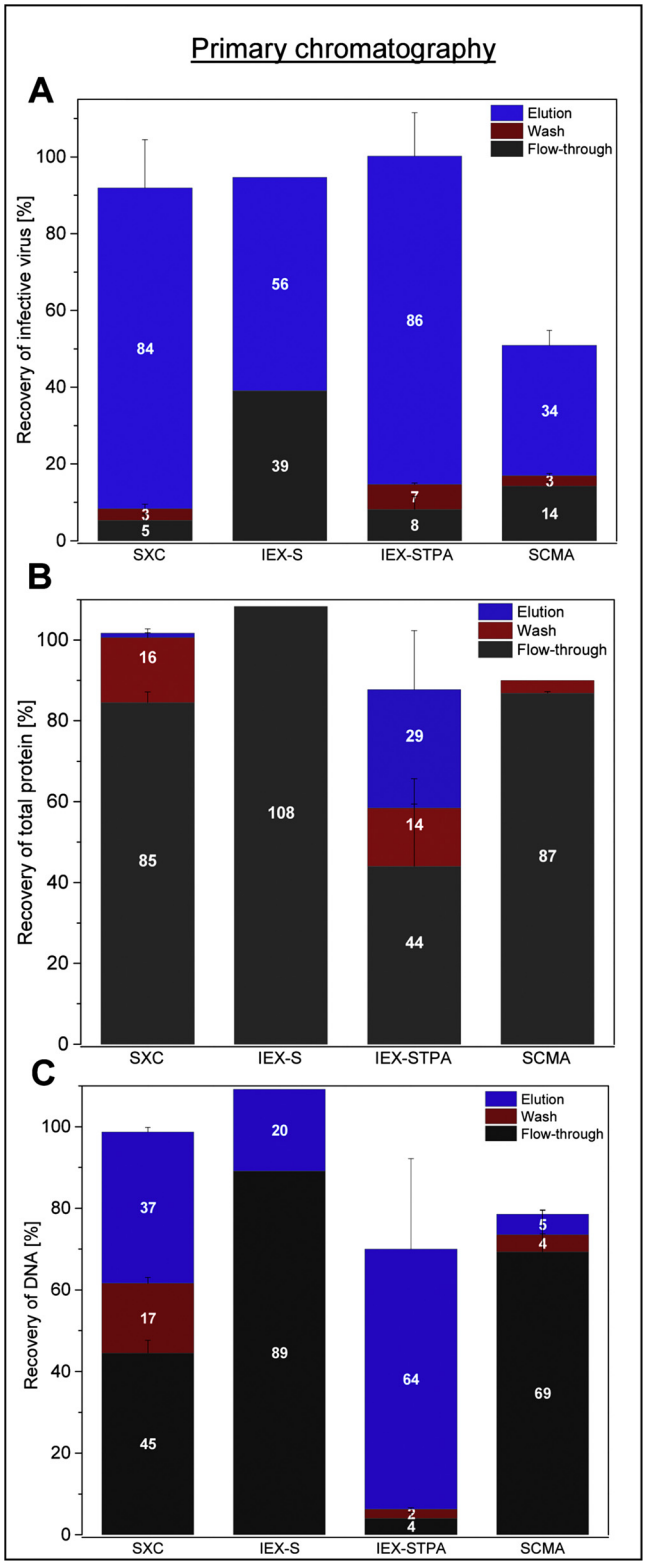

Fig. 3. Virus and impurity recovery for different unit operations during capture. Shown are the relative recoveries for ORFV (**A**), protein (**B**) and DNA (**C**) using SXC, cation exchange membrane adsorbers (IEX-S), anion exchangers (IEX-STPA) and sulfated cellulose membrane adsorbers (SCMA). Depicted are the quantities contained in the flow-through, wash and elution fractions, whereas for the IEX-S (operated in flow-through-mode), flow-through and wash fractions are combined. Error bars reflect the standard deviation of technical triplicates, except for the IEX-S membrane, which was only tested once to show the proof of concept.

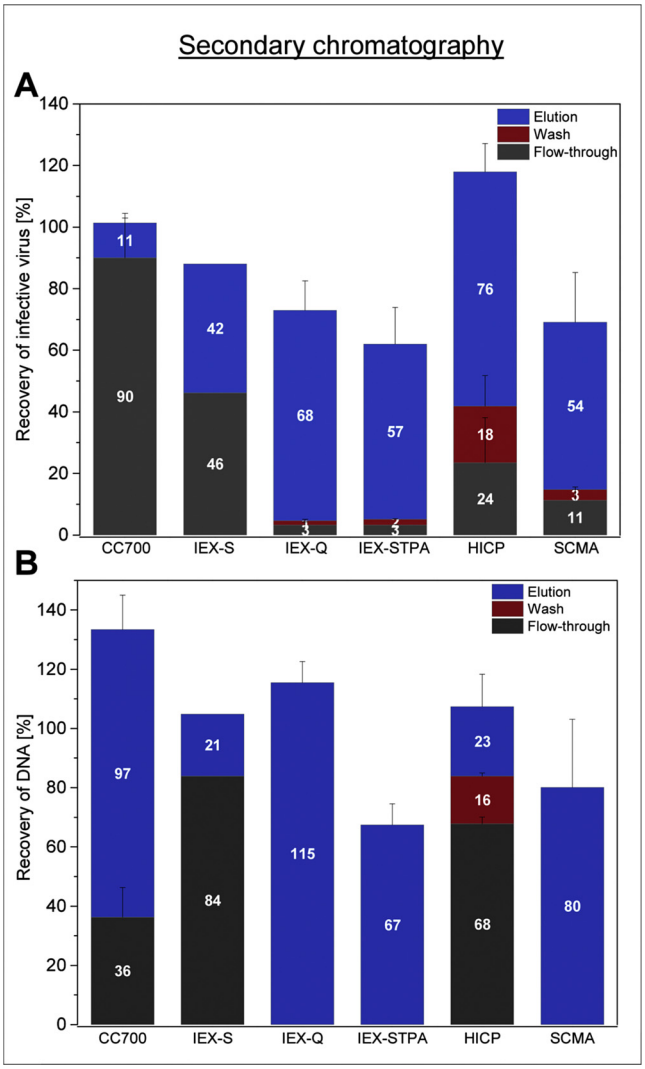

Fig. 4. Virus and impurity recovery for different unit operation during secondary chromatography. Shown are the relative recoveries for ORFV (**A**) and DNA (**B**) during secondary purification, evaluating the Capto™ Core 700 resin (CC700), IEX-S, strong and salt-tolerant anion exchange membrane adsorbers (IEX-Q and IEX-STPA), as well as hydrophobic interaction membrane adsorbers (HICP) and the SCMA. Depicted are the quantities contained in the flow-through, wash and elution fractions, whereas for methods in the flow-through-mode (CC700 and IEX-S), flow-through and wash fractions are combined. Error bars reflect the standard deviation of technical triplicates, (IEX-S membrane was only tested once). Protein recovery is not shown for the secondary purification as already after SXC capture no protein quantities were remaining.

for the STPA membrane adsorber. Notably, a distinct amount of virus could not be eluted at 2 M NaCl, with roughly 30 % and 40 % not being recovered from the IEX-Q and IEX-STPA membranes adsorbers, respectively. The SCMA showed less retained viruses on the device than in the previous capture step. However, the overall recovery of all fractions was at about 70 %, with 54 % of the viruses being detected in the product fraction.

For none of the applications used for the secondary purification, proteins could be determined in any fraction.

The most efficient DNA depletion was achieved using the CC700 and the HICP membrane adsorber, with 36 % and 23 % of the initial DNA amount remaining in the product fraction, respectively, (Fig. 4, B). For all other applications, most of the contained DNA was co-eluted with the product virus, with DNA amounts of 84 % (S-membrane), more than 100 % (IEX-Q), 67 % (STPA), and 80 % (SCMA) being left in the product fraction. Following Q, STPA, and SCMA purification, no DNA

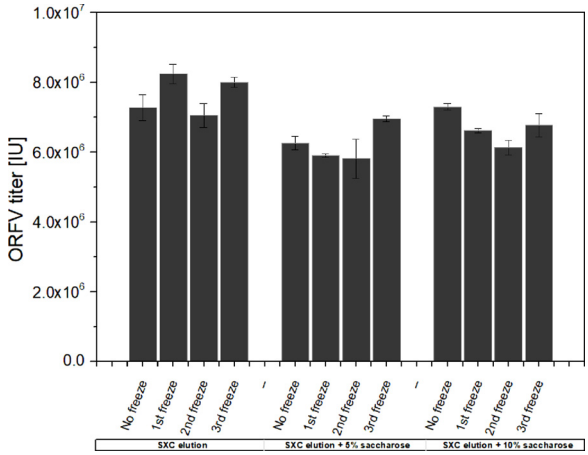

Fig. 5. ORFV stability after freeze/thawing with and without sugar supplementation. Infective ORFV titers in SXC elution buffer (20 mM TRIS-HCL pH 7.4 with 0.4 M NaCl), supplemented with 0 %, 5 % and 10 % sucrose. The quantification was done by flow cytometry, directly after the purification and after each of up to three freeze/thaw cycles. Error bars indicate the standard deviation of technical triplicates.

was found during flow-through and wash. Last it should be noted that for STPA and SCMA the material balance could not be closed with 33 % (STPA), and up to 20 % (SCMA) of the DNA remaining unaccounted for.

3.5. Virus stability

Virus particles after SXC purification were stable for at least four freeze/thaw cycles, without any loss of infectivity (Fig. 5). An additional application of sucrose did not affect the viruses' infectivity during freezing at −80 °C.

3.6. Overview and summary

In summary, the combinations of SXC and CC700 or HICP showed the highest overall virus recovery of approximately 76 % and 64 % after both chromatography steps, respectively. Furthermore, these combinations offered a complete protein removal, and final DNA concentrations of 24 ng mL^{-1} (CC700) and 47 ng mL^{-1} (HICP) at virus titers of 2.0E + 06 IU mL^{-1} and 1.1E + 06 IU mL^{-1}, respectively.

4. Discussion

Medical applications of viral vectors for gene therapy and vaccines are continuously increasing (Shirley et al., 2020). One promising viral vector that is currently undergoing preclinical evaluations, the ORFV, lacks an efficient and economic production process. In this study, we focused on its downstream processing and, in particular, on the development of chromatographic methods for the purification of the cell culture-derived ORFV.

4.1. Virus characterization

So far, the pI has not yet been determined for ORFV strain D1701-V particles. Previously reported values for vaccinia viruses range between 2.3 and 5.9, depending on the analytical method and on the virus strain analyzed (Douglas et al., 1966, 1969; Resch et al., 2007; Taylor and Bosmann, 1981; Wolff and Reichl, 2011). Hence, the determined pI of 4.6 for ORFV is within the expected range. The same applies for the determined main size populations after SXC purification of 150 and 250 nm, representing width and length of the ORFV in accordance with literature (Nanington et al. 1964).

4.2. Determination of the dynamic binding capacities

In general, membrane adsorbers have been widely used for the purification of viruses and virus-like particles due to their superior performance, especially in view of their flow properties and binding capacities for nanoplexes (Hoffmann et al., 2019). In this study, we evaluated ion exchange-, pseudo-affinity-, and hydrophobic interaction chromatography membrane adsorbers, as well as size-dependent techniques such as the CC700 and SXC.

At present, the membrane-based SXC was only described for Influenza A (Marichal-Gallardo et al., 2017) and baculovirus (Lothert et al., 2020) purifications, yielding dynamic binding capacities of up to 1.2E + 07 plaque-forming units cm^{-2}, which exceed our observations for the ORFV (1.63E + 06 IU cm^{-2} to 7.78E + 06 IU cm^{-2}). In the presented study, two membrane holders with a diameter of 13 mm and 25 mm (24 mm membranes) were tested with a corresponding volumetric increase between the two membrane holders by a factor of 3.7. The amount of retained viruses between the two membrane volumes was increased by a factor of approximately 6 (Table 1). The slight deviation between the volumetric increase and the retained amount of virus suggests a potential non-linear behavior when scaling up the SXC. However, this could be explained by the error of the analytical method for virus quantification, and the differences in the membrane housing devices in terms of the assembly and housing materials. For the assembly, both require a sealing ring in order to prevent a leakage. This O-ring is relatively large for the 13 mm device, probably resulting in an inefficient perfusion of the membrane stack. This could reduce the accessible membrane volume, thus reducing the overall capacity compared to the larger filter holder. Additionally, most of the interactions for the SXC occur in the upper layers of the membrane stack (unpublished data), suggesting, that a comparison of the membrane areas accessible for the virus particles might be more appropriate. However, this cannot be reliably determined.

The 4.2-fold higher DBC observed for the Q membrane adsorber, in comparison to the STPA membrane adsorber (Table 1), was not expected. Based on the manufacturer´s product sheet, the ligand density is nearly six times higher for the STPA membrane than for the Q membrane, resulting in BSA binding capacities of 0.8 mg cm^{-2} (Q membrane) and 1.4 mg cm^{-2} (STPA). However, for virus molecules as large as the ORFV particles, an increased ligand density might not affect the binding capacity, but rather the binding strength, as multiple ligands bind to a single virus particle.

Anion exchange membranes were frequently applied for the purification of different viruses with varying results on binding capacities. For example, Grein et al. reported total capacities on similar Q membranes of 1.7E + 08 plaque-forming units per cm^2 using a recombinant baculovirus (Grein et al., 2012) whereas McNally et al. captured retroviral vectors on Mustang Q membranes with 1.2E + 08 IP per mL membrane (McNally et al., 2014). Hence, data on binding capacities is frequently difficult to compare. Reasons for this are differences in virus morphology and surface properties, varying analytical quantification methods, and the deviations between membrane adsorbers from different manufactures. However, the data we obtained can be considered within the same range as described by Grein et al. and McNally et al. For MVA, Wolff et al. achieved binding capacities of greater than 1.2E + 07 fifty-percent tissue culture infective dose ($TCID_{50}$) per cm^2 using Q and D anion exchangers (Wolff et al., 2010b), which were also exceeded for the Q device.

For the SCMA, a constant breakthrough of a small virus fraction was observed by the light scattering detector from the moment that sample loading started (data not shown). This was confirmed by offline analytics, as approximately 10 %–15 % of the viruses were found in the flow-through fraction. Previous publications described the application of SCMA for the purification of the Influenza A virus, Influenza virus-like particles, and MVA (Carvalho et al., 2018; Fortuna et al., 2018, 2019; Opitz et al., 2009; Wolff et al., 2010a), with the virus content

varying between 2.4 % and 30 % in the flow-through fraction during the loading procedure. The precise interaction of different viruses and sulfated cellulose or sulfated dextran is currently not yet fully understood. However, several studies reported antiviral activities (Chattopadhyay et al., 2008; Mitsuya et al., 1988; Nelson and Rosowsky, 2002; Piret et al., 2000) and the binding of viruses to sulfated cellulose (O'Neil and Balkovic, 1993), suggesting that sulfated cellulose can mimic a heparin or heparin sulfate ligand (Gallagher et al., 2020; Paluck et al., 2016). The purification of ORFV via a heparin affinity chromatography has already been described in literature (Scagliarini et al., 2002, 2004), thus, ORFV could be suitable for SCMA purification. Scagliarini and co-workers reported the ORF virus' F1L protein being mainly responsible for heparin binding (Scagliarini et al., 2004). It is located on the viral envelope, presenting a glycosaminoglycan binding motive (Lin et al., 2000; Scagliarini et al., 2002). During the life cycle of the ORFV, different infectious progeny of ORFV exist with altered surface structures and properties (Spehner et al., 2004; Tan et al., 2009), and F1L could not be detected on all progenies (Tan et al., 2009). For a complete virus recovery, the host cells were disrupted after harvesting, releasing all progeny regardless of their maturity level, which might explain the diminished performance during SCMA for these virus particles. Besides, for Influenza virus particles, Fortuna et al. showed a dependency of the SCMA performance on the virus titer of the feed stream and on its ionic strength (Fortuna et al., 2018, 2019). Different virus titers were not examined, therefore no statement can be made on this. However, the conductivity of the tested feed stream (3.5–4 mS cm^{-2}) matched their recommendation, and therefore should not have influenced the adsorption behavior of the virus during the sample loading process.

4.3. Evaluation of the capture step

Due to the estimated isoelectric point of the virus and the applied buffer pH of 7.4, the IEX-S membrane was intended to be used in flow-through mode (contaminant adsorption). In contrast to the expectation, about 50 % were retained in the applied neutral pH process condition and only eluted at higher (2 M NaCl) salt concentrations (Fig. 3). Virus purification, using cation- and anion exchangers under comparable process conditions, has been described repeatedly in the literature for various cell culture-derived viruses (Wolff and Reichl, 2011), such as the Influenza A virus (Opitz et al., 2009), the adeno-associated virus (Okada et al., 2009), and for MVA (Wolff et al., 2010b), where virus particles can be adsorbed up to a certain degree to both types of ion exchangers. Based on the varying protein compositions, it can be assumed that individual patches on the virus surface have different physicochemical properties, leading to a complex adsorption behavior.

The tested anion exchange membrane adsorber resulted in a virus recovery for the IEX-STPA of 86 % during primary chromatography (Fig. 3). Anion exchange chromatography is widely used for virus purifications, such as adenoviruses (Nestola et al., 2015) and the Influenza A virus (Weigel et al., 2016). Generally, the main disadvantage of the method is the co-elution of process-related nucleic acids with the product virus (Wolff and Reichl, 2011). As a result, the obtained virus yield depends on the level of DNA depletion and must be optimized with regard to the economics of the entire production process.

During the capture of the ORFV from the clarified cell culture material by SCMA, the losses, which were observed in the DBC studies throughout column loading, were confirmed (Fig. 3). In the course of the capture experiments, virus losses throughout loading and wash amounted to 17 %. This was also the case for the secondary chromatographic purification via SCMA, where 14 % of the virus was detected in the flow-through and wash fraction (see Sections 3.4 and 4.4). However, during the SCMA capture only 51 % (Fig. 3) of the virus could be recovered in total, excluding this method as a potential capture step. For the SCMA purification of MVA, Wolff et al. described virus yields ranging from 65 % to 75 %, while at the same time achieving a DNA and protein depletion greater than 90 % and 95 %, respectively (Wolff et al., 2010b, a). MVA also belongs to the poxvirus family and, thus, allows a limited basis for comparison despite certain differences in morphology. For the capturing step in the presented study, the protein and DNA depletions are comparable to the studies of Wolff et al. According to the literature (Fortuna et al., 2019; Wolff et al., 2010b) however, the virus recovery is below expectations. This might be attributed to aspects already discussed in 3.2. Besides, it could also be due to the fact, that custom-made membranes with pore sizes of 3 − 5 µm were employed in the cited MVA study. Here, we used commercially available membranes with 0.8 µm pores, leading to an increased filtration effect, and thus, losses in the total virus recovery.

4.4. Evaluation of the secondary chromatographic step after SXC

After the purification of the virus particles by SXC, several membrane adsorbers (IEX-S, IEX-Q, IEX-STPA, HICP and SCMA) as well as the CC700 resin were tested for a subsequent chromatographic step to remove residual contaminants.

For the cation exchange membrane adsorber, a comparable performance of the secondary chromatography and the capture step (see Sections 3.3 and 3.4) was achieved. Nearly half of the total virus amount was not retained, and the product fractions did not show a sufficient contaminant depletion (Fig. 4). Thus, the cation exchange membrane adsorber was not suitable for a purification process of Vero cell culture-derived ORFV under the tested conditions. The use of anion exchangers as a secondary chromatographic step resulted in lower virus yields compared to the capture step. More accurately, the virus yield was reduced by 29 % (Figs. 3 and 4) for the IEX-STPA membrane adsorber. Compared to the IEX-Q membrane adsorber, though, the IEX-STPA membrane adsorber had an increased ligand density and virus losses were insignificantly higher. The yields for the Q membrane adsorber were comparable to values previously described for other virus applications, such as for Influenza A (77–86 %, (Kalbfuss et al., 2007a), Parvovirus-like particles (59 %, (Ladd Effio et al., 2016)) and MVA (77 %, (Wolff et al., 2010b)). Thus, virus losses in the course of anion exchange chromatography have already been described previously. The above-mentioned higher virus losses, using the IEX-STPA in the secondary step compared to the capture step (complete virus recovery, Fig. 3), could not have been caused by an infectivity loss as the process conditions were the same in both approaches. Instead, the effect might be explained by a shielding effect of contaminants in the solution, preventing interactions of viruses with the surface ligands (Weigel et al., 2016), with higher contaminant levels during the primary chromatography. Under the applied elution buffer conditions, the DNA could not be separated from the virus in any of the anion exchange methods, resulting in DNA levels above 120 ng mL^{-1}, thus rendering these methods to be less suitable for the ORFV purification. If possible at all, an extensive method optimization for an appropriate functionality would be required.

While the absence of contaminating proteins reduces the performance of the anion exchangers, the opposite effect is observable for the SCMA membrane. When applied as a secondary step, the total virus recovery is approximately 17 % higher than during capture (Table 1, Figs. 3 and 4). This increase is mainly attributed to a higher amount of virus being eluted from the membrane adsorber, as the amounts in flow-through and wash were unchanged. Possibly, the membrane fouling effect is reduced when performed as a secondary purification in the absence of proteins. As described in 3.3. the membranes' pores are at 0.8 µm, generally leading to higher filtration effects than in previous reports on MVA with larger pore membranes (Wolff et al., 2010b, a). Thus, the filtration effects could be increased at higher protein concentrations during the capture step. Total virus recoveries in all fractions accounted for 68 %, ruling out SCMA for an ORFV purification.

Concerning the HICP membrane, high losses (about 40 %) were observed during sample loading and wash (Fig. 4). HIC processes for

virus purification are less well characterized and applied than the use of anion exchange methods. However, Weigel et al. described a resin-based HIC purification for Influenza A with > 90 % virus yield and about 99 % DNA removal (Weigel et al., 2019). Furthermore, also MVA was previously purified with the HICP membranes as a secondary purification, yielding up to 76 % of the virus (Wolff et al., 2010a), matching the data of 76 % virus in the elution pool that we obtained (Fig. 4). However, the DNA removal was higher in the referred study, with less than 1 % of the initial DNA content being found in the product (23 % in this work). Relative DNA amounts are difficult to compare, and no values on absolute DNA concentrations are given in the published data. In the presented study, the final DNA concentration in the product fraction was about 47 ng mL^{-1} (containing total virus amounts of 1.1E + 06 IU). Thus, when considering this unit operation for process implementation, a further optimization of the buffer composition must be evaluated. The virus recovery in the elution could potentially be increased for higher ammonium sulfate concentrations in the binding buffer, presuming that the virus activity is not affected. The total amount of recovered virus in all fractions can be attributed to the analytical error, accounting up to 15 % for each fraction.

All IEX and HIC methods described here, were performed using elution buffer conditions that support a high virus recovery using high salt concentrations (2 M NaCl). As under these circumstances most of the DNA is co-eluted with the virus, the product purity was not optimized. However, the intention here was the identification of possible chromatographic methods for the purification of ORFV, and optimizations would have exceeded the scope of this study.

Among the techniques tested as secondary chromatographic methods, CC700 allowed the highest DNA removal with only 24 ng mL^{-1} of the DNA remaining in the product fraction at virus titers of 2.0E + 06 IU mL^{-1}. Accordingly, this combination offers the highest potential for a further process optimization in order to comply with a production process in agreement with regulatory guidelines (European Pharmacopoeia, 2020; World Health Organization, 2017). The use of CC700 and HICP both showed a high virus yield (90 % and 76 %) and a high DNA depletion in the product fraction (64 % and 77 %, Fig. 4). The latter is based on a total DNA assay, which needs to be further characterized for a production process in order to discriminate between viral DNA and host cell DNA. Furthermore, the combination SXC and CC700 or HICP allowed a protein depletion below the quantification limit (25 µg/mL) of the applied assay and, thus, meets the requirements of the regulatory guidelines. Nonetheless, it will be necessary for a production process to further characterize the remaining proteins in order to determine their source.

As carried out in the experiments shown here, the final arrangement of the two chromatographic purification methods should start with the SXC. This method is mainly independent of the loading- and the elution buffer, reducing the need for additional buffer exchanges, which would be necessary for HICP (Weigel et al., 2019; Wolff et al., 2010a). Furthermore, SXC allows a concentration of the virus (Marichal-Gallardo et al., 2017), whereas the CC700 rather leads to a sample dilution. Also the polishing effect of the CC700 resin might be reduced, if overburdened with higher contaminant amounts of the clarified feed (James et al., 2016).

The experiments described here were all conducted on a laboratory scale. However, most of the evaluated techniques are membrane-based and available, either commercially in different scales, or can be custom-made from commercial flat sheet membranes (SXC, SCMA) to accommodate the required scale. The only applied resin-based technique, the CC700, is used to bind and remove remaining impurities in a flow-through mode for the virus. It is therefore uncritical for upscaling.

4.5. Evaluation of the virus stability during freeze/thaw cycles

The data suggests that the virus can be stored at −80 °C after the first chromatographic purification, without affecting the virus stability for up to three freeze/thaw cycles (Fig. 5). Additionally, a supplementation of 5% or 10 % sucrose is not required and can be omitted. Previously, the addition of stabilizers, such as sugars, was described to be beneficial for storage and formulation of various viruses (Adebayo et al., 1998; Kumru et al., 2018). In our case, an intermediate storage and freeze/thawing in a SXC elution buffer (20 mM Tris pH 7.4, 180 mM NaCl) was uncritical; for a long term storage, though, additional studies are required.

5. Conclusion

This study evaluates the general performance and applicability of different chromatographic unit operations for the purification of cell culture-derived ORFV. In summary, anion exchangers, HIC, and SXC are suitable possibilities with satisfying product recoveries and contaminant depletions. Cation exchange membrane chromatography and SCMA appeared less eligible for such a process. SXC and IEX-STPA membranes present the most promising capture steps with 84 % and 86 % virus recovery, respectively, whereas the impurity removal was better for SXC (greater than 99 % protein and 67 % DNA reduction). The combination of SXC chromatography with a subsequent CC700 or HIC membrane adsorption chromatography resulted in an overall virus yield in the two combined chromatographic steps in 90 % and 76 %, respectively. Hence, these unit operations or the combination of the SXC capture step with a CC700 or HIC chromatography are promising candidates for a DSP of cell culture-derived ORFV. In addition, the utilized membranes or chromatographic modules are well suited for upscaling and single use applications, providing the possibility for the development of an economic production process, which will be the focus of upcoming experiments.

Funding

The work was supported by the EXIST-Forschungstransfer grand # 03EFKBW171 of the German Federal Ministry for Economic Affairs and Energy.

CRediT authorship contribution statement

Keven Lothert: Conceptualization, Methodology, Data curation, Formal analysis, Writing - original draft. **Felix Pagallies:** Methodology, Investigation, Writing - review & editing. **Thomas Feger:** Methodology, Data curation, Writing - review & editing. **Ralf Amann:** Supervision, Funding acquisition, Writing - review & editing. **Michael W. Wolff:** Supervision, Project administration, Funding acquisition, Writing - review & editing.

Declaration of Competing Interest

None.

Acknowledgements

The authors would like to thank Hanns-Joachim Rziha for scientific advice on the manuscript. Additionally, we want to thank Catherine Meckel-Oschmann and Friederike Eilts for proofreading. This work is part of a dissertation under the aegis of the Justus Liebig University of Giessen, Germany in cooperation with the Technische Hochschule Mittelhessen (University of Applied Sciences), Giessen, Germany.

References

Adebayo, A.A., Sim-Brandenburg, J.W., Emmel, H., Olaleye, D.O., Niedrig, M., 1998. Stability of 17D yellow fever virus vaccine using different stabilizers. Biologicals 26 (4), 309–316. https://doi.org/10.1006/biol.1998.0157.

Amann, R., Rohde, J., Wulle, U., Conlee, D., Raue, R., Martinon, O., Rziha, H.-J., 2013. A

new rabies vaccine based on a recombinant ORF virus (parapoxvirus) expressing the rabies virus glycoprotein. J. Virol. 87 (3), 1618–1630. https://doi.org/10.1128/JVI.02470-12.
Bergqvist, C., Kurban, M., Abbas, O., 2017. Orf virus infection. Rev. Med. Virol. 27 (4). https://doi.org/10.1002/rmv.1932.
Carvalho, S.B., Fortuna, A.R., Wolff, M.W., Peixoto, C.M., Alves, P., Reichl, U., Jt Carrondo, M., 2018. Purification of influenza virus-like particles using sulfated cellulose membrane adsorbers. J. Chem. Technol. Biotechnol. 93 (7), 1988–1996. https://doi.org/10.1002/jctb.5474.
Chattopadhyay, K., Ghosh, T., Pujol, C.A., Carlucci, M.J., Damonte, E.B., Ray, B., 2008. Polysaccharides from Gracilaria corticata: sulfation, chemical characterization and anti-HSV activities. Int. J. Biol. Macromol. 43 (4), 346–351. https://doi.org/10.1016/j.ijbiomac.2008.07.009.
Douglas, H.W., Rondle, C.J., Williams, B.L., 1966. Micro-electrophoresis of cowpox and vaccinia viruses in molar sucrose. J. Gen. Microbiol. 42 (1), 107–113. https://doi.org/10.1099/00221287-42-1-107.
Douglas, H.W., Williams, B.L., Rondle, C.J.M., 1969. Micro-electrophoresis of pox viruses in molar sucrose. J. Gen. Virol. 5 (3), 391–396. https://doi.org/10.1099/0022-1317-5-3-391.
European Pharmacopoeia, 2020. Ed. 10.2.
Fleming, S.B., Wise, L.M., Mercer, A.A., 2015. Molecular genetic analysis of orf virus: a poxvirus that has adapted to skin. Viruses 7 (3), 1505–1539. https://doi.org/10.3390/v7031505.
Fortuna, A.R., Taft, F., Villain, L., Wolff, M.W., Reichl, U., 2018. Optimization of cell culture-derived influenza A virus particles purification using sulfated cellulose membrane adsorbers. Eng. Life Sci. 18 (1), 29–39. https://doi.org/10.1002/elsc.201700108.
Fortuna, A.R., van Teeffelen, S., Ley, A., Fischer, L.M., Taft, F., Genzel, Y., Villain, L., Wolff, M.M., Reichl, U., 2019. Use of sulfated cellulose membrane adsorbers for chromatographic purification of cell cultured-derived influenza A and B viruses. Sep. Purif. Technol. (226), 350–358. https://doi.org/10.1016/j.seppur.2019.05.101.
Friebe, A., Siegling, A., Weber, O., 2018. Inactivated Orf-virus shows disease modifying antiviral activity in a guinea pig model of genital herpesvirus infection. J. Microbiol. Immunol. Infect. 51 (5), 587–592. https://doi.org/10.1016/j.jmii.2017.03.002.
Gagnon, P., Toh, P., Lee, J., 2014. High productivity purification of immunoglobulin G monoclonal antibodies on starch-coated magnetic nanoparticles by steric exclusion of polyethylene glycol. J. Chromatogr. A 1324, 171–180. https://doi.org/10.1016/j.chroma.2013.11.039.
Gallagher, Z.J., Fleetwood, S., Kirley, T.L., Shaw, M.A., Mullins, E.S., Ayres, N., Foster, E.J., 2020. Heparin mimic material derived from cellulose nanocrystals. Biomacromolecules 21 (3), 1103–1111. https://doi.org/10.1021/acs.biomac.9b01460.
Grein, T.A., Michalsky, R., Vega López, M., Czermak, P., 2012. Purification of a recombinant baculovirus of Autographa californica M nucleopolyhedrovirus by ion exchange membrane chromatography. J. Virol. Methods 183 (2), 117–124. https://doi.org/10.1016/j.jviromet.2012.03.031.
Hain, K.S., Joshi, L.R., Okda, F., Nelson, J., Singrey, A., Lawson, S., Martins, M., Pillatzki, A., Kutish, G.F., Nelson, E.A., Flores, E.F., Diel, D.G., 2016. Immunogenicity of a recombinant parapoxvirus expressing the spike protein of Porcine epidemic diarrhea virus. J. Gen. Virol. 97 (10), 2719–2731. https://doi.org/10.1099/jgv.0.000586.
Heyward, J.T., Klimas, R.A., Stapp, M.D., Obijeski, J.F., 1977. The rapid concentration and purification of influenza virus from allantoic fluid. Arch. Virol. 55 (1-2), 107–119. https://doi.org/10.1007/BF01314484.
Hoffmann, D., Leber, J., Loewe, D., Lothert, K., Oppermann, T., Zitzmann, J., Weidner, T., Salzig, D., Wolff, M., Czermak, P., 2019. Purification of new biologicals using membrane-based processes. In: Basile, A., Charcosset, C. (Eds.), Current Trends and Future Developments on (Bio-) Membranes. Elsevier, pp. 123–150. https://doi.org/10.1016/B978-0-12-813606-5.00005-1.
James, K.T., Cooney, B., Agopsowicz, K., Trevors, M.A., Mohamed, A., Stoltz, D., Hitt, M., Shmulevitz, M., 2016. Novel high-throughput approach for purification of infectious virions. Sci. Rep. 6, 36826. https://doi.org/10.1038/srep36826.
Kalbfuss, B., Wolff, M., Geisler, L., Tappe, A., Wickramasinghe, R., Thom, V., Reichl, U., 2007a. Direct capture of influenza A virus from cell culture supernatant with Sartobind anion-exchange membrane adsorbers. J. Membr. Sci. 299 (1-2), 251–260. https://doi.org/10.1016/j.memsci.2007.04.048.
Kalbfuss, B., Wolff, M., Morenweiser, R., Reichl, U., 2007b. Purification of cell culture-derived human influenza A virus by size-exclusion and anion-exchange chromatography. Biotechnol. Bioeng. 96 (5), 932–944. https://doi.org/10.1002/bit.21109.
Kumru, O.S., Wang, Y., Gombotz, C.W.R., Kelley-Clarke, B., Cieplak, W., Kim, T., Joshi, S.B., Volkin, D.B., 2018. Physical characterization and stabilization of a lentiviral vector against adsorption and freeze-thaw. J. Pharm. Sci. 107 (11), 2764–2774. https://doi.org/10.1016/j.xphs.2018.07.010.
Ladd Effio, C., Hahn, T., Seiler, J., Oelmeier, S.A., Asen, I., Silberer, C., Villain, L., Hubbuch, J., 2016. Modeling and simulation of anion-exchange membrane chromatography for purification of Sf9 insect cell-derived virus-like particles. J. Chromatogr. A 1429, 142–154. https://doi.org/10.1016/j.chroma.2015.12.006.
Lee, J., Gan, H.T., Latiff, S.M.A., Chuah, C., Lee, W.Y., Yang, Y.-S., Loo, B., Ng, S.K., Gagnon, P., 2012. Principles and applications of steric exclusion chromatography. J. Chromatogr. A 1270, 162–170. https://doi.org/10.1016/j.chroma.2012.10.062.
Lin, C.L., Chung, C.S., Heine, H.G., Chang, W., 2000. Vaccinia virus envelope H3L protein binds to cell surface heparan sulfate and is important for intracellular mature virion morphogenesis and virus infection in vitro and in vivo. J. Virol. 74 (7), 3353–3365. https://doi.org/10.1128/jvi.74.7.3353-3365.2000.
Loa, C.C., Lin, T.L., Wu, C.C., Bryan, T.A., Thacker, H.L., Hooper, T., Schrader, D., 2002. Purification of turkey coronavirus by Sephacryl size-exclusion chromatography. J. Virol. Methods 104 (2), 187–194. https://doi.org/10.1016/S0166-0934(02)00069-1.
Lothert, K., Sprick, G., Beyer, F., Lauria, G., Czermak, P., Wolff, M.W., 2020. Membrane-based steric exclusion chromatography for the purification of a recombinant baculovirus and its application for cell therapy. J. Virol. Methods 275, 113756. https://doi.org/10.1016/j.jviromet.2019.113756.
Marichal-Gallardo, P., Pieler, M.M., Wolff, M.W., Reichl, U., 2017. Steric exclusion chromatography for purification of cell culture-derived influenza A virus using regenerated cellulose membranes and polyethylene glycol. J. Chromatogr. A 1483, 110–119. https://doi.org/10.1016/j.chroma.2016.12.076.
McNally, D.J., Darling, D., Farzaneh, F., Levison, P.R., Slater, N.K.H., 2014. Optimised concentration and purification of retroviruses using membrane chromatography. J. Chromatogr. A 1340, 24–32. https://doi.org/10.1016/j.chroma.2014.03.023.
Mitsuya, H., Looney, D.J., Kuno, S., Ueno, R., Wong-Staal, F., Broder, S., 1988. Dextran sulfate suppression of viruses in the HIV family: inhibition of virion binding to CD4+ cells. Science 240 (4852), 646–649. https://doi.org/10.1126/science.2452480.
Nagington, J., Newton, A.A., Horne, R.W., 1964. The structure of orf virus. Virology 23 (4), 461–472. https://doi.org/10.1016/0042-6822(64)90230-2.
Nayak, D.P., Lehmann, S., Reichl, U., 2005. Downstream processing of MDCK cell-derived equine influenza virus. J. Chromatogr. B Anal. Technol. Biomed. Life Sci. 823 (2), 75–81. https://doi.org/10.1016/j.jchromb.2005.05.022.
Nelson, R.G., Rosowsky, A., 2002. Dicyclic and tricyclic diaminopyrimidine derivatives as potent inhibitors of cryptosporidium parvum dihydrofolate reductase: structure-activity and structure-selectivity correlations. Antimicrob. Agents Chemother. 46 (3), 940. https://doi.org/10.1128/aac.
Nestola, P., Peixoto, C., Villain, L., Alves, P.M., Carrondo, M.J.T., Mota, J.P.B., 2015. Rational development of two flowthrough purification strategies for adenovirus type 5 and retro virus-like particles. J. Chromatogr. A 1426, 91–101. https://doi.org/10.1016/j.chroma.2015.11.037.
O'Leary, M.P., Choi, A.H., Kim, S.-I., Chaurasiya, S., Lu, J., Park, A.K., Woo, Y., Warner, S.G., Fong, Y., Chen, N.G., 2018. Novel oncolytic chimeric orthopoxvirus causes regression of pancreatic cancer xenografts and exhibits abscopal effect at a single low dose. J. Transl. Med. 16 (1), 110. https://doi.org/10.1186/s12967-018-1483-x.
O'Neil, P.F., Balkovic, E.S., 1993. Virus harvesting and affinity-based liquid chromatography. A method for virus concentration and purification. Biotechnology 11 (2), 173–178. https://doi.org/10.1038/nbt0293-173.
Okada, T., Nonaka-Sarukawa, M., Uchibori, R., Kinoshita, K., Hayashita-Kinoh, H., Nitahara-Kasahara, Y., Takeda, S.'i., Ozawa, K., 2009. Scalable purification of adeno-associated virus serotype 1 (AAV1) and AAV8 vectors, using dual ion-exchange adsorptive membranes. Hum. Gene Ther. 20 (9), 1013–1021. https://doi.org/10.1089/hum.2009.006.
Opitz, L., Lehmann, S., Reichl, U., Wolff, M.W., 2009. Sulfated membrane adsorbers for economic pseudo-affinity capture of influenza virus particles. Biotechnol. Bioeng. 103 (6), 1144–1154. https://doi.org/10.1002/bit.22345.
Paluck, S.J., Nguyen, T.H., Maynard, H.D., 2016. Heparin-mimicking polymers: synthesis and biological applications. Biomacromolecules 17 (11), 3417–3440. https://doi.org/10.1021/acs.biomac.6b01147.
Pastoret, P.-P., Vanderplasschen, A., 2003. Poxviruses as vaccine vectors. Comp. Immunol. Microbiol. Infect. Dis. 26 (5-6), 343–355. https://doi.org/10.1016/S0147-9571(03)00019-5.
Piret, J., Lamontagne, J., Bestman-Smith, J., Roy, S., Gourde, P., Désormeaux, A., Omar, R.F., Juhász, J., Bergeron, M.G., 2000. In vitro and in vivo evaluations of sodium lauryl sulfate and dextran sulfate as microbicides against herpes simplex and human immunodeficiency viruses. J. Clin. Microbiol. 38 (1), 110–119.
Pohlscheidt, M., Langer, U., Minuth, T., Bödeker, B., Apeler, H., Hörlein, H.-D., Paulsen, D., Rübsamen-Waigmann, H., Henzler, H.-J., Reichl, U., 2008. Development and optimisation of a procedure for the production of Parapoxvirus ovis by large-scale microcarrier cell culture in a non-animal, non-human and non-plant-derived medium. Vaccine 26 (12), 1552–1565. https://doi.org/10.1016/j.vaccine.2008.01.032.
Resch, W., Hixson, K.K., Moore, R.J., Lipton, M.S., Moss, B., 2007. Protein composition of the vaccinia virus mature virion. Virology 358 (1), 233–247. https://doi.org/10.1016/j.virol.2006.08.025.
Rintoul, J.L., Lemay, C.G., Tai, L.-H., Stanford, M.M., Falls, T.J., Souza, C.Tde, Bridle, B.W., Daneshmand, M., Ohashi, P.S., Wan, Y., Lichty, B.D., Mercer, A.A., Auer, R.C., Atkins, H.L., Bell, J.C., 2012. ORFV: a novel oncolytic and immune stimulating parapoxvirus therapeutic. Mol. Ther. 20 (6), 1148–1157. https://doi.org/10.1038/mt.2011.301.
Rohde, J., Schirrmeier, H., Granzow, H., Rziha, H.-J., 2011. A new recombinant Orf virus (ORFV, Parapoxvirus) protects rabbits against lethal infection with rabbit hemorrhagic disease virus (RHDV). Vaccine 29 (49), 9256–9264. https://doi.org/10.1016/j.vaccine.2011.09.121.
Rohde, J., Amann, R., Rziha, H.-J., 2013. New Orf virus (Parapoxvirus) recombinant expressing H5 hemagglutinin protects mice against H5N1 and H1N1 influenza A virus. PLoS One 8 (12), e83802. https://doi.org/10.1371/journal.pone.0083802.
Rziha, H.-J., Rohde, J., Amann, R., 2016. Generation and selection of orf virus (ORFV) recombinants. Methods Mol. Biol. 1349, 177–200. https://doi.org/10.1007/978-1-4939-3008-1_12.
Scagliarini, A., Ciulli, S., Battilani, M., Jacoboni, I., Montesi, F., Casadio, R., Prosperi, S., 2002. Characterisation of immunodominant protein encoded by the F1L gene of orf virus strains isolated in Italy. Arch. Virol. 147 (10), 1989–1995. https://doi.org/10.1007/s00705-002-0850-2.
Scagliarini, A., Gallina, L., Dal Pozzo, F., Battilani, M., Ciulli, S., Prosperi, S., 2004. Heparin binding activity of orf virus F1L protein. Virus Res. 105 (2), 107–112. https://doi.org/10.1016/j.virusres.2004.04.018.
Shirley, J.L., de Jong, Y.P., Terhorst, C., Herzog, R.W., 2020. Immune responses to viral gene therapy vectors. Mol. Ther. 28 (3), 709–722. https://doi.org/10.1016/j.ymthe.2020.01.001.
Spehner, D., de Carlo, S., Drillien, R., Weiland, F., Mildner, K., Hanau, D., Rziha, H.-J.,

2004. Appearance of the bona fide spiral tubule of ORF virus is dependent on an intact 10-kilodalton viral protein. J. Virol. 78 (15), 8085–8093. https://doi.org/10.1128/JVI.78.15.8085-8093.2004.

Tan, J.L., Ueda, N., Mercer, A.A., Fleming, S.B., 2009. Investigation of orf virus structure and morphogenesis using recombinants expressing FLAG-tagged envelope structural proteins: evidence for wrapped virus particles and egress from infected cells. J. Gen. Virol. 90 (Pt 3), 614–625. https://doi.org/10.1099/vir.0.005488-0.

Tan, J.L., Ueda, N., Heath, D., Mercer, A.A., Fleming, S.B., 2012. Development of orf virus as a bifunctional recombinant vaccine: surface display of Echinococcus granulosus antigen EG95 by fusion to membrane structural proteins. Vaccine 30 (2), 398–406. https://doi.org/10.1016/j.vaccine.2011.10.079.

Tao, S.-P., Zheng, J., Sun, Y., 2015. Grafting zwitterionic polymer onto cryogel surface enhances protein retention in steric exclusion chromatography on cryogel monolith. J. Chromatogr. A 1389, 104–111. https://doi.org/10.1016/j.chroma.2015.02.051.

Taylor, D.H., Bosmann, H.B., 1981. Measurement of the electrokinetic properties of vaccinia and reovirus by laser-illuminated whole-particle microelectrophoresis. J. Virol. Methods 2 (5), 251–260. https://doi.org/10.1016/0166-0934(81)90023-9.

Transfiguracion, J., Jaalouk, D.E., Ghani, K., Galipeau, J., Kamen, A., 2003. Size-exclusion chromatography purification of high-titer vesicular stomatitis virus G glycoprotein-pseudotyped retrovectors for cell and gene therapy applications. Hum. Gene Ther. 14 (12), 1139–1153. https://doi.org/10.1089/104303403322167984.

van Rooij, E.M.A., Rijsewijk, F.A.M., Moonen-Leusen, H.W., Bianchi, A.T.J., Rziha, H.-J., 2010. Comparison of different prime-boost regimes with DNA and recombinant Orf virus based vaccines expressing glycoprotein D of pseudorabies virus in pigs. Vaccine 28 (7), 1808–1813. https://doi.org/10.1016/j.vaccine.2009.12.004.

Verheust, C., Goossens, M., Pauwels, K., Breyer, D., 2012. Biosafety aspects of modified vaccinia virus Ankara (MVA)-based vectors used for gene therapy or vaccination. Vaccine 30 (16), 2623–2632. https://doi.org/10.1016/j.vaccine.2012.02.016.

Wang, C., Bai, S., Tao, S.-P., Sun, Y., 2014. Evaluation of steric exclusion chromatography on cryogel column for the separation of serum proteins. J. Chromatogr. A 1333, 54–59. https://doi.org/10.1016/j.chroma.2014.01.059.

Wang, R., Wang, Y., Liu, F., Luo, S., 2019. Orf virus: a promising new therapeutic agent. Rev. Med. Virol. 29 (1), e2013. https://doi.org/10.1002/rmv.2013.

Weigel, T., Solomaier, T., Wehmeyer, S., Peuker, A., Wolff, M.W., Reichl, U., 2016. A membrane-based purification process for cell culture-derived influenza A virus. J. Biotechnol. 220, 12–20. https://doi.org/10.1016/j.jbiotec.2015.12.022.

Weigel, T., Soliman, R., Wolff, M.W., Reichl, U., 2019. Hydrophobic-interaction chromatography for purification of influenza A and B virus. J. Chromatogr. B Anal. Technol. Biomed. Life Sci. 1117, 103–117. https://doi.org/10.1016/j.jchromb.2019.03.037.

Wolff, M.W., Reichl, U., 2011. Downstream processing of cell culture-derived virus particles. Expert Rev. Vaccines 10 (10), 1451–1475. https://doi.org/10.1586/ERV.11.111.

Wolff, M.W., Siewert, C., Hansen, S.P., Faber, R., Reichl, U., 2010a. Purification of cell culture-derived modified vaccinia ankara virus by pseudo-affinity membrane adsorbers and hydrophobic interaction chromatography. Biotechnol. Bioeng. 107 (2), 312–320. https://doi.org/10.1002/bit.22797.

Wolff, M.W., Siewert, C., Lehmann, S., Hansen, S.P., Djurup, R., Faber, R., Reichl, U., 2010b. Capturing of cell culture-derived modified Vaccinia Ankara virus by ion exchange and pseudo-affinity membrane adsorbers. Biotechnol. Bioeng. 105 (4), 761–769. https://doi.org/10.1002/bit.22595.

World Health Organization, 2017. WHO Expert Committee on Biological Standardization. Repo, Geneva.

Chapter 4 – Evaluation of the SXC in DSP trains for ORFV and Hepatitis C purification

Up to the date and in the previous chapters, the SXC was only described and referred to as platform technology, with potential applications in the biopharmaceutical industry, allowing for high recoveries and excellent product purities. However, to our knowledge it was not yet shown, if the SXC can be successfully integrated into complete downstream processing schemes to enable pharmaceutical application in humans.

To show this possibility, the following chapter describes the implementation of such processes. Based on the findings in chapter 3, in a second step, the presented purification process for ORFV was complemented by an optimized clarification step, a nuclease treatment and a final polishing using the Capto^{TM} Core 700 resin, in order to intensify the performance of the SXC step. The Capto^{TM} Core 700 was selected as it represents the best option regarding virus integrity and impurity clearance. The resulting process enabled overall product recoveries of 64% with the possibility for human treatment, regarding its purity. The process, and particularly the optimized process conditions during SXC, were robust and reproducible for two different ORFV genotypes and did not require additional adjustments on the tested laboratory scale. This can be mainly attributed to the similar size and equaling isoelectric points of the applied virus genotypes.

Beside the purification of different genotypes of one virus, the next aim was to confirm the benefits of the SXC as a capture step during a purification scheme for a different type of virus with varying physio-chemical properties. Therefor, the method was applied for the purification of whole inactivated hepatitis C virus (HCV). The development had great impact on future SXC development, as it revealed the high pH dependency of the SXC for virus purification with membranes. In this work it was shown for the first time using membrane-based SXC for virus purification, that leaving the optimum pH window at a pH of 8.5 ± 0.5 highly reduces the SXC performance. In the worst case, applying the wrong conditions led to a complete lack of functionality making virus retention impossible or resulted in increased aggregation and blocking of the column. In turn, after adhering to pH conditions near the isoelectric point of the virus, the procedure did not require any additional optimization, but allowed for a complete virus recovery and satisfying impurity removal.

Furthermore, the study was of major interest as up to the date no HCV vaccine and thus, no corresponding DSP process was available. The SXC capture step was accompanied by a preceding filtration train and a subsequent secondary pseudo-affinity purification using sulfated cellulose. Particular attention shall be drawn to the importance of the appropriate pH value

during SXC processing. In combination with an anterior filtration and the inclusion of a nuclease treatment, the chromatographic purification train was able to achieve product qualified for human vaccination. As during the ORFV process, the SXC capture step was responsible for removing most of the protein contaminants (>97%) and a significant amount of host cell DNA (86-94%), whereas the subsequent pseudo affinity chromatography allowed for a further decrease of DNA levels below regulatory limits. Again, the whole process was evaluated for two of the major HCV genotypes and allowed a similar performance for both of them.

Journal of Biotechnology 323 (2020) 221–230

Contents lists available at ScienceDirect

Journal of Biotechnology

journal homepage: www.elsevier.com/locate/jbiotec

A scalable downstream process for the purification of the cell culture-derived Orf virus for human or veterinary applications

Keven Lothert [a], Felix Pagallies [b], Friederike Eilts [a], Arabi Sivanesapillai [a], Martin Hardt [c], Anna Moebus [c], Thomas Feger [b], Ralf Amann [b], Michael W. Wolff [a,d,*]

[a] Institute of Bioprocess Engineering and Pharmaceutical Technology, University of Applied Sciences Mittelhessen (THM), Giessen, Germany
[b] Department of Immunology, University of Tuebingen, Tuebingen, Germany
[c] Imaging Unit, Biomedical Research Centre Seltersberg, Justus Liebig University, Giessen, Germany
[d] Fraunhofer Institute for Molecular Biology and Applied Ecology (IME), Giessen, Germany

ARTICLE INFO

Keywords:
Viral vector vaccine
Orf virus
Downstream process
Steric exclusion chromatography
Nuclease treatment

ABSTRACT

The large demand for safe and efficient viral vector-based vaccines and gene therapies against both inherited and acquired diseases accelerates the development of viral vectors. One outstanding example, the Orf virus, has a wide range of applications, a superior efficacy and an excellent safety profile combined with a reduced pathogenicity compared to other viral vectors. However, besides these favorable attributes, an efficient and scalable downstream process still needs to be developed. Recently, we screened potential chromatographic stationary phases for Orf virus purification. Based on these previous accomplishments, we developed a complete downstream process for the cell culture-derived Orf virus. The described process comprises a membrane-based clarification step, a nuclease treatment, steric exclusion chromatography, and a secondary chromatographic purification step using Capto® Core 700 resin. The applicability of this process to a variety of diverse Orf virus vectors was shown, testing two different genotypes. These studies render the possibility to apply the developed downstream scheme for both genotypes, and lead to overall virus yields of about 64 %, with step recoveries of >70 % for the clarification, and >90 % for the chromatography train. Protein concentrations of the final product are below the detection limits, and the final DNA concentration of about 1 ng per 1E + 06 infective virus units resembles a total DNA depletion of 96–98 %.

1. Introduction

The parapoxvirus Orf virus (ORFV) has been known for decades as a zoonotic pathogen, which mainly affects small ruminants causing skin lesions. The virus, however, can also be transmitted to humans, e.g. via broken skin (Haig and McInnes, 2002; Haig and Mercer, 1998). Recent publications demonstrated the potential of the ORFV as a novel poxviral vector platform (Amann et al., 2013; Rziha et al., 2016, 2019), an immunomodulatory agent (Bergqvist et al., 2017; Fleming et al., 2015), and as an antiviral- and oncolytic treatment (Friebe et al., 2018; O'Leary et al., 2018; Rintoul et al., 2012; Wang et al., 2019). The loss of virulence factors in attenuated ORFV highly reduces its pathogenicity to humans and animals, and offers advantages over common viral vectors like adeno- or adeno associated viruses, lenti-, or retroviruses (Fleming et al., 2017; Scott et al., 2016; Vannucci et al., 2013). In contrast to the highly attenuated Modified Vaccinia Ankara virus (MVA), ORFV are replication–competent, assuring a potent and more effective immune response (Albarnaz et al., 2018; García-Arriaza and Esteban, 2014; Rziha et al., 2019). Among the additional striking vector properties of ORFV are the restricted host range, the lack of systemic spread even in immuno-compromised animals, and the induction of strong B- and T-cell immune responses to expressed antigens (Rziha et al., 2019). Moreover, multiple re-immunizations are possible, due to a short-lived duration of the ORFV-specific immunity (Haig and Mercer, 1998; Rintoul et al., 2012). However, despite the qualification of ORFV for human and veterinary medical applications, literature exclusively focuses on the

Abbreviations: CC700, Capto™ Core 700; DF, depth filtration; DBC, dynamic binding capacity; DLS, dynamic light scattering; IU, infective units; MVA, Modified Vaccinia Ankara virus; NTU, nephelometric turbidity units; ORFV, Orf virus; ORFV-GFP, Orf virus genotype expressing the green fluorescence protein; qPCR, quantitative polymerase chain reaction; RT, room temperature; SCMA, sulfated cellulose membrane adsorber; SXC, steric exclusion chromatography.

* Corresponding author at: Wolff University of Applied Sciences Mittelhessen (THM), Wiesenstr. 14, 35390 Giessen, Germany.
E-mail address: Michael.Wolff@lse.thm.de (M.W. Wolff).

https://doi.org/10.1016/j.jbiotec.2020.08.014
Received 16 June 2020; Received in revised form 6 August 2020; Accepted 23 August 2020
Available online 27 August 2020

upstream of ORFV production processes up to the date (Pohlscheidt et al., 2008; Rziha et al., 2016). So far, no suitable downstream process for a large-scale economic production of cell culture-derived ORFV has been described, and virus purification is currently mainly done by sucrose gradient centrifugation (Rziha et al., 2016). This method is generally uneconomic, underlies a poor scalability and high product losses and, most importantly, an insufficient removal of cellular impurities (Hoffmann et al., 2019; Wolff and Reichl, 2011). In analogy to other poxviridae, such as the MVA application of ion exchange-, hydrophobic interaction- (HIC), or pseudo affinity, chromatography is a reasonable possibility (Wolff et al., 2010b, a). Recently, we screened different chromatographic process conditions and methods for the purification of ORFV (Lothert et al., 2020). In that study, we evaluated ion exchange and hydrophobic interaction membrane adsorbers as well as steric exclusion chromatography (SXC) and the Capto™ Core 700 (named CC700 hereafter) chromatography. According to our findings, the most promising combination of chromatographic purification steps with regard to virus recovery and impurity depletion was the SXC followed by a CC700 chromatography. The SXC is a size-based purification technology, employing the mutual steric exclusion of macromolecules from a polymer-rich solution. The method, initially used for the purification of large proteins and bacteriophages employing monoliths (Gagnon et al., 2014; Lee et al., 2012; Tao et al., 2015; Wang et al., 2014), was later applied for the separation of RNA molecules (Levanova and Poranen, 2018), as well as for membrane-based virus purification (Lothert et al., 2019; Marichal-Gallardo et al., 2017). SXC allows a selective retention of the target molecules by adjusting the polymer (e.g. polyethylene glycol, PEG) concentration, and enables an efficient contaminant removal due to the distinctive size difference between virus and proteins or DNA. CC700, in turn, is a chromatographic resin with bimodal functions. The outer surface is inert, and only components below 700 kDa, which can penetrate the pores, adsorb to the internal mixed mode ligands (James et al., 2016). As Orf virions with a size of about 260 nm x 160 nm (Guo et al., 2003) are excluded from the pores, this method provides a possibility to eliminate residual amounts of DNA and protein. In a previous study (Lothert et al., 2020), however, it was shown that the mere combination of the SCX and CC700 is not sufficient for human applications according to regulatory safety requirements (European Pharmacopoeia, 2020; World Health Organization, 2017), as DNA-levels in the product fraction were still above 24 ng ml^{-1} (~12 ng per 1E + 06 infective units).

Here, we describe the development and optimization of a

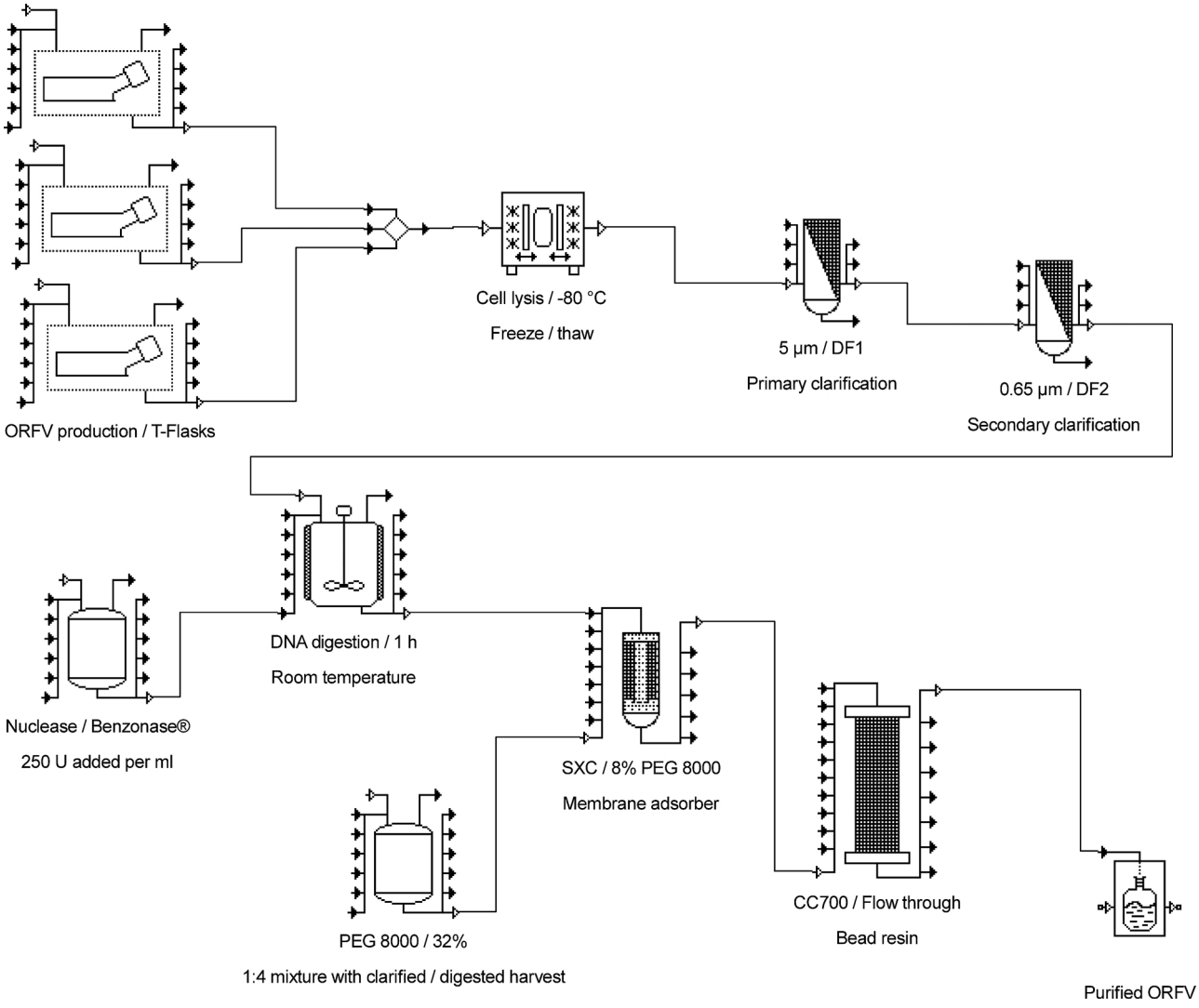

Fig. 1. Process overview. ORFV production divided into virus amplification, harvest, and cell disruption, followed by primary and secondary depth filtration (DF), nuclease digestion, and a two-step chromatographic purification. The first chromatography is a capture step by steric exclusion chromatography (SXC) after a mixing of the clarified and nuclease-treated harvest with polyethylene glycol (PEG), followed by a secondary clarification using the Capto™ Core 700 (CC700) resin and collecting the unbound fraction.

downstream scheme, based on the previous findings for two genotypes of cell culture-derived ORFV. Therefore, the developed purification train comprises a membrane-based clarification, a nuclease treatment, an intermediate chromatographic purification by SXC, and a final purification step using CC700 (Fig. 1).

2. Materials and methods

2.1. Virus production

The virus was propagated in Vero cells (ATCC, CCL-81) as previously described (Rziha et al., 2016), using T-225 CytoOne® flasks (STARLAB International GmbH). The cells were infected at a multiplicity of infection of 0.05 to produce two different genotypes of the ORFV, namely, the ORFV expressing the green fluorescence protein (ORFV-GFP) and the ORFV-Cherry. In addition to the different fluorescence gene (GFP and mCherry, respectively), the ORFV-Cherry genome contains two additional membrane bound proteins. The virus was harvested 120 h post-infection, and remaining intracellular virus was released from the host cells by a freeze/thaw cycle.

The clarification performance (section 2.2) and the nuclease digestion (section 2.3) were evaluated, exclusively using ORFV-GFP, whereas the chromatography (sections 2.4 and 2.5) was done with clarified and nuclease-treated samples of both genotypes.

2.2. Clarification of virus harvests

All filtrations were carried out using a Sartoflow® Smart, operated by the Biopat® MFCS 4 software (Sartorius Stedim Biotech GmbH). Clarification was undertaken using a sequence of depth filters with decreasing pore sizes. For cell and cell debris separation, filters with pore sizes of 5 µm were used, employing either Sartopure® PP3 MidiCaps® (5055342P7-FF-A, Sartorius Stedim Biotech GmbH) or Millistak+® C0HC filters (MC0HC23CL3, Merck). For a secondary clarification, filters of the same membrane material with 0.65 µm pores were applied, being Sartopure® PP3 capsules (5051305P4-SS-B, Sartorius Stedim Biotech GmbH) or Millistak+® D0HC (MD0HC23CL3, Merck). Sartopure® devices had a membrane surface area of 650 cm^2 (5 µm pores) and 130 cm^2 (0.65 µm pores). The Millistak+® filters were applied in the µPod®-format with a total surface area of 23 cm^2. For a recovery evaluation, a cell-free harvest of ORFV was prepared by low-speed centrifugation at 200 x g for 5 min. All runs were performed in triplicates. Additionally, the capacity per filter area was estimated once for each filter, using a non-centrifuged ORFV-GFP harvest in the primary clarification. The filtrate was then used for the secondary clarification until a pressure limitation occurred. The clarification performance was evaluated by calculating the nephelometric turbidity units (*NTU*), using $NTU = 0.191 + 926.194*A$, where A is the absorbance at 750 nm.

2.3. Nuclease treatment

In order to evaluate the efficiency of the nucleic acid digestion, the clarified ORFV-GFP virus broth was supplemented with Benzonase® nuclease (Merck) at final concentrations of 50, 250 and 500 U ml^{-1} and 2 mM $MgCl_2$ (Carl Roth). DNA concentrations (section 2.6.3) and infective virus titers (section 2.6.1) were determined at several time points within 24 h by single measurements for each concentration (Fig. 2). Process samples of ORFV-GFP and ORF-Cherry were supplemented with 250 U ml^{-1} of the nuclease, and incubated for 1 h at room temperature (RT). After incubation, EDTA (Carl Roth) was added to the mixture in a final concentration of 5 mM, in order to block nuclease activity. Chromatographic purification was started directly afterwards without an additional storage of the sample.

2.4. Primary chromatographic purification (capture)

All chromatographic preparations were done using an Äkta™ Pure 25 (GE Healthcare Life Sciences) with an online-monitoring of conductivity and UV (280 nm). The system was operated by the Unicorn™ 7.1 Software. Additionally, a Nano DLS Particle Size Analyzer (Brookhaven Instruments) was integrated into the flow path to allow an online-particle detection. The used buffers were filtered through a 0.2 µm bottle top filter (Corning) and degassed by ultrasonication, before being applied to the system.

With minor adjustments, SXC was performed as previously described (Lothert et al., 2019). Briefly, the clarified and nuclease-treated virus harvest was mixed with 20 mM TRIS (Carl Roth) adjusted to pH 7.4 with HCl (Carl Roth), supplemented with 32 % (w/v) PEG 8000 (Carl Roth) and 180 mM NaCl (Carl Roth) to a final PEG concentration of 8 %, equaling equilibration buffer conditions. The mixture was applied to a stack of 10 layers of regenerated cellulose membranes with a pore size of 1 µm (Whatman). The membranes were punched and assembled in a 13 mm stainless steel filter holder (Pall), covered with support screens on both sides of the stack. Accordingly, the bed volume and membrane surface were about 0.092 mL and 13.3 cm^2, respectively. The system and the membranes were equilibrated prior to sample application, using at least 6 mL equilibration buffer (20 mM TRIS, pH 7.4). After complete loading, the membranes were washed with equilibration buffer for at least 50 column volumes. Elution was done using 10 mL 20 mM TRIS buffer at pH 7.4 without PEG, but supplemented with 400 mM NaCl. For each chromatographic run, a new membrane stack was prepared. Dynamic binding capacities were determined for both genotypes applying the clarified virus broth without an additional nuclease digestion. The breakthrough of virus particles at 10 % and 100 % were judged by light

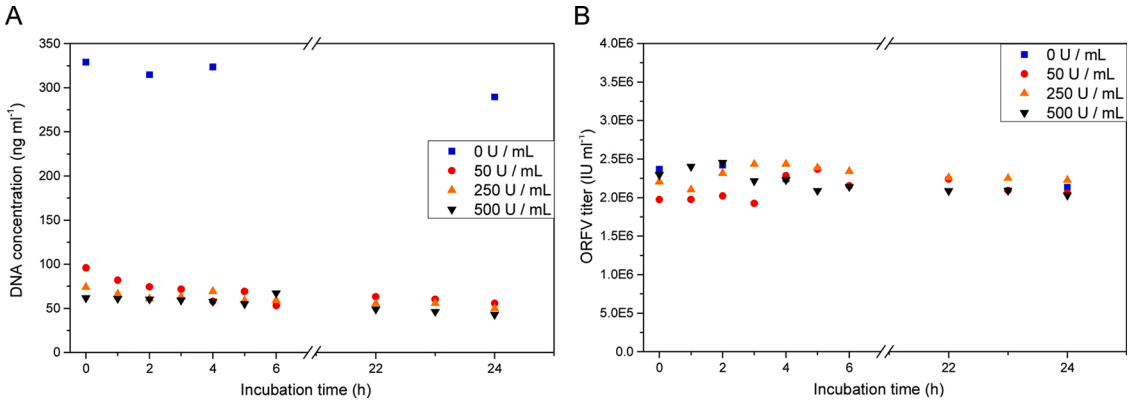

Fig. 2. Evaluation of the nuclease performance. DNA concentrations **(A)** and infective virus titers **(B)** after incubations with 50 (red dots), 250 (orange triangles), and 500 (black triangles) units of the enzyme per ml sample. DNA levels and virus titers of non-treated samples were determined at certain time points as a control (blue squares). (For interpretation of the references to colour in this figure legend, the reader is referred to the web version of this article).

scattering detection.

2.5. Secondary chromatographic purification (CC700)

Secondary purification was done using 1 mL prepacked CC700 columns (GE, Healthcare Life Sciences) at flow rates of 1 mL min^{-1}. The SXC elution was directly applied to equilibrated columns, using 20 mM TRIS buffer, pH 7.4, supplemented with 180 mM NaCl for the equilibration, loading and washing. Flow-through and wash fractions were pooled and considered as the product fraction. Impurities were eluted from the column, using 2 M NaCl in 20 mM Tris at a pH of 7.4. The columns were regenerated by adding 1 M NaOH (Carl Roth) to the elution buffer, as suggested by the manufacturer.

2.6. Analytics

2.6.1. Virus quantification

Infective virus particles were quantified using an automated flow cytometry-based approach, as described previously (Lothert et al., 2020). Briefly, Vero cells were seeded in a 24-well format (Greiner Bio-One) with 100,000 cells per well, in a culture volume of 1 mL DMEM (Gibco™, Thermo Fisher Scientific) supplemented with 5 % fetal calf serum (Capricorn Scientific). Directly after seeding the cells, 100 µL of the respective chromatography sample, the medium blank or the standard virus stock ranging from 1.5E + 05 to 1.0E + 07 infective units (IU) ml^{-1}, was applied to each well for infection. The cells were incubated for 16 h, washed with PBS (Thermo Fisher Scientific), and harvested after detachment with Trypsin/EDTA (Gibco™, Thermo Fisher Scientific). The detached cells were supplemented with FCS (1:4 v/v) to stop the trypsin activity, and transferred to a 96-well U-bottom plate (Nunc, Thermo Fisher Scientific). The cells were washed twice by centrifugation at 400 x g for 2 min, removing the supernatant and re-suspending the pellet in 100 µL PBS. Finally, the cells were analyzed using a flow cytometer (Guava® easyCyte HT, Merck). The percentage of positive/fluorescing cells (i. e. infected) compared to the total number of cells for ORFV-GFP was determined at an emission of 525 nm and an excitation of 488 nm. For the Cherry-genotype, the yellow fluorescence (emission: 583 nm, excitation: 488 nm) was evaluated to quantify the amount of infected cells. The standard deviation of the analysis in both cases was less than 10 % for duplicate measurements.

2.6.2. Protein quantification

The Pierce™ BCA Protein Assay Kit (Thermo Fisher Scientific) was applied for the total protein quantification of chromatographic samples, following the manufacturer's instructions. The standard calibration was prepared using bovine serum albumin, included in the kit, in a range between 25 and 2000 µg ml^{-1}. For all samples and standards, 25 µL were transferred to a 96-well plate and mixed with 200 µL of the reaction mixture. After an incubation of 30 min at 37 °C, the absorbance was measured at 562 nm with a plate reader (BioTek™ Cytation 3™, Fisher Scientific). The sample concentrations were determined from calibration curves prepared in parallel with an average assay deviation of less than 10 % for duplicate measurements.

2.6.3. DNA quantification

The total amount of double-stranded DNA was determined using the Quant-iT™ PicoGreen™ dsDNA Assay Kit (Thermo Fisher Scientific) according to the manufacturers' instruction. In a black 96-well plate (Nunc, Thermo Fisher Scientific), 50 µL of each chromatographic sample were mixed with 50 µL of the assays' 1xTE buffer and 100 µL of the dye mixture. The plates were analyzed for a fluorescence emission at 520 nm, after an excitation at 480 nm, using a plate reader (BioTek™ Cytation 3™, Fisher Scientific). Final concentrations were calculated from standard calibrations in the range of 0.025–25 ng ml^{-1} and 1–1000 ng ml^{-1}, respectively. Standards were freshly prepared for each plate and the assay deviation was below 15 %.

2.6.4. ORFV size determination by dynamic light scattering

Final product fractions were submitted to a dynamic light scattering (DLS) analysis for the verification of the product size. Measurements were performed with a Zetasizer Nano ZS90 (Malvern), using a 90° light scattering detection and a He-Ne laser at 633 nm. Data acquisition was done at RT with settings for a dispersant refractive index and a viscosity value of 1.45 and 0.954 cP, respectively. The latter values were determined by a prior analyzation of the buffers. Undiluted product fractions were characterized in disposable semi-micro cuvettes (Sarstedt). The obtained data was processed by the Zetasizer Software (version 7.12), using multiple narrow modes as option.

2.6.5. Transmission electron microscopy

Electron microscopy was performed as a whole-mount analysis on purified ORFV and stored at −80 °C after the CC700 chromatography. Both genotypes, ORFV-GFP and ORFV-Cherry, were analyzed by negative staining in duplicates, using 2 % ammonium molybdate (Agar Scientific). The stain was freshly prepared, adjusted to pH 7.0 using 5 M NaOH, and finally filtered through 2 µm syringe filters (Carl Roth). Each ORFV sample (20 µL) was incubated for adherence by the on-drop method for 7 min on 300-mesh formvar-coated (1.2 %) copper grids (Plano GmbH), which had been carbonized and glow-discharged immediately before use. Following incubation, the grid was transferred with the virus side pointing towards the drop to the stain (20 µL) for an additional 7 min. Thereafter, the stain was sucked from the grid by a Whatman® filter paper (GE Healthcare Life Sciences) and grids were finally air-dried. The preparations were inspected in an EM912 AB transmission electron microscope (Zeiss) at 120 kV under zero-loss conditions at slight underfocus. Micrographs were recorded using a 2k x 2k slow-scan CCD camera (TRS), and processed using the iTEM software package (Olympus-SIS).

3. Results

3.1. Clarification

Clarification experiments were conducted with low speed (200 x *g, 5 min*) -centrifuged ORFV-GFP culture supernatants. Under these conditions, about 90 % virus recovery was achieved for the primary clarification for both the Sartopure® PP3 capsules (5 µm) and Millistak+® MD0HC devices (Table 1). During the secondary clarification, the Sartopure® PP3 capsules (0.65 µm) and the Millistak+® MC0HC devices resulted in a mean recovery of 77 % and 70 %, respectively. A consecutive clarification with the Millistak+® filters (MD0HC + MC0HC) for the primary and secondary clarification enabled a DNA depletion of 52 % and 68 %, respectively, resulting in a complete DNA depletion of about 75 %. The combination of the PP3 capsules (5 + 0.65 µm) lead to an overall DNA depletion after secondary clarification of about 53 %. The reduction of the total protein content for both tested filter combinations was about 20 %.

The membrane capacity per filter area for the culture broth, which had not been pre-clarified by low speed centrifugation, was about 1.1E + 09 IU for the Millistak+® filters. In a comparable experiment, the PP3 devices resulted in a capacity of about 2.3E + 08 IU per cm^2 filter area (Table 1).

3.2. Evaluation of the nuclease treatment using ORFV-GFP

Initial DNA levels of about 325 ng ml^{-1} after clarification (control sample) were reduced by a factor of 3.3 when using 50 U ml^{-1} of the enzyme, and by 4.3 and 5.4 using 250 and 500 U ml^{-1}, respectively, directly after mixing the sample with nuclease (Fig. 2, A). When using enzyme concentrations of 50 U ml^{-1}, a further decrease of DNA levels was detected for up to six hours. For the other two enzyme concentrations, after an incubation time of one hour, no major changes were observed. Compared to the non-digested control sample, a five- to six-

Table 1
Summary of the clarification results for different filter types after primary and secondary clarification.

Clarification step	Filter	Final turbidity [NTU]	Turbidity reduction [%]	Virus recovery [%]	DNA depletion [%]	Protein depletion [%]	Filter capacity [IU cm^{-2}]
Primary clarification	MD0HC 5 µm	3.2 ± 2	98	89 ± 5	52 ± 6	11 ± 4	1.1E + 09
	PP3 5 µm	4.4 ± 5	97	91 ± 2	39 ± 3	7 ± 6	2.3E + 08
Secondary clarification	MC0HC 0.65 µm	1.8 ± 1	>99	70 ± 6	68 ± 7	20 ± 7	>1.1E + 09
	PP3 0.65 µm	1.7 ± 3	>99	77 ± 2	53 ± 5	20 ± 7	4.4E+08

NTU: Nephelometric turbidity units; IU: Infective units.

fold overall DNA reduction, from a starting concentration of 325 ng ml^{-1}, was observed. The virus infectivity was not impaired by the nuclease treatment for up to an incubation time of 24 h (RT), in relation to the control sample (Fig. 2, B).

3.3. Primary chromatographic purification (SXC capture)

The dynamic binding capacity $DBC_{100\ \%}$ for the ORFV-GFP was about 7.72E + 08 IU ml^{-1} membrane volume and a 5.4E + 06 IU cm^{-2} membrane surface area. The evaluation of the $DBC_{10\ \%}$ for the identical virus sample resulted in 2.01E + 08 IU ml^{-1} and 1.41E + 06 IU cm^{-2}. For ORFV-Cherry, a $DBC_{10\ \%}$ of 4.01E + 08 IU ml^{-1} and 2.8E + 06 IU cm^{-2} was determined. $DBC_{100\ \%}$ could not be reached. In this attempt, loading was stopped after 1.30E + 09 IU ml^{-1} (9.1E + 06 IU cm^{-2}), as the pressure limits of the housing were reached.

Additionally, it was observed that a minor breakthrough of the ORFV-Cherry started immediately after application, whereas the ORFV-GFP was completely retained during early sample loading (Fig. 3, A and C).

Applying the SXC as a capture step for both evaluated ORFV genotypes, more than 90 % of the viruses were recovered in the elution fraction (Fig. 4). Protein removal was above 98 % in both cases. The remaining DNA amount in relation to the feed was 24 % and 19 % for the GFP and Cherry genotype, respectively (Fig. 4, Table 2).

3.4. Secondary chromatographic purification (CC700)

The CC700 was applied in a flow-through mode, and the chromatograms show a direct breakthrough of virus particles during sample loading in the light scattering signal with a negligible UV-signal (Fig. 3 B, D). A virtually complete virus recovery was possible using the CC700 chromatography, with 99 ± 3 % and 95 ± 1 % of the virus being recovered in the product fraction for the ORFV-GFP and the ORFV-Cherry, respectively (Fig. 5). DNA levels were reduced by an additional 75 % (ORFV-GFP) and 72 % (ORFV-Cherry), based on the remaining DNA content after the SXC. Accordingly, this resulted in a final DNA content of approximately 1 ng per 1E + 06 IU for both genotypes. For the secondary chromatographic purification, the overall DNA recovery was incomplete, with a total of 54 %–68 % being recovered in all fractions. Furthermore, the protein concentrations in all of the obtained chromatographic fractions was below the detection limits of the applied assays, while minor signals were observed at the UV and light scattering detector during the column regeneration.

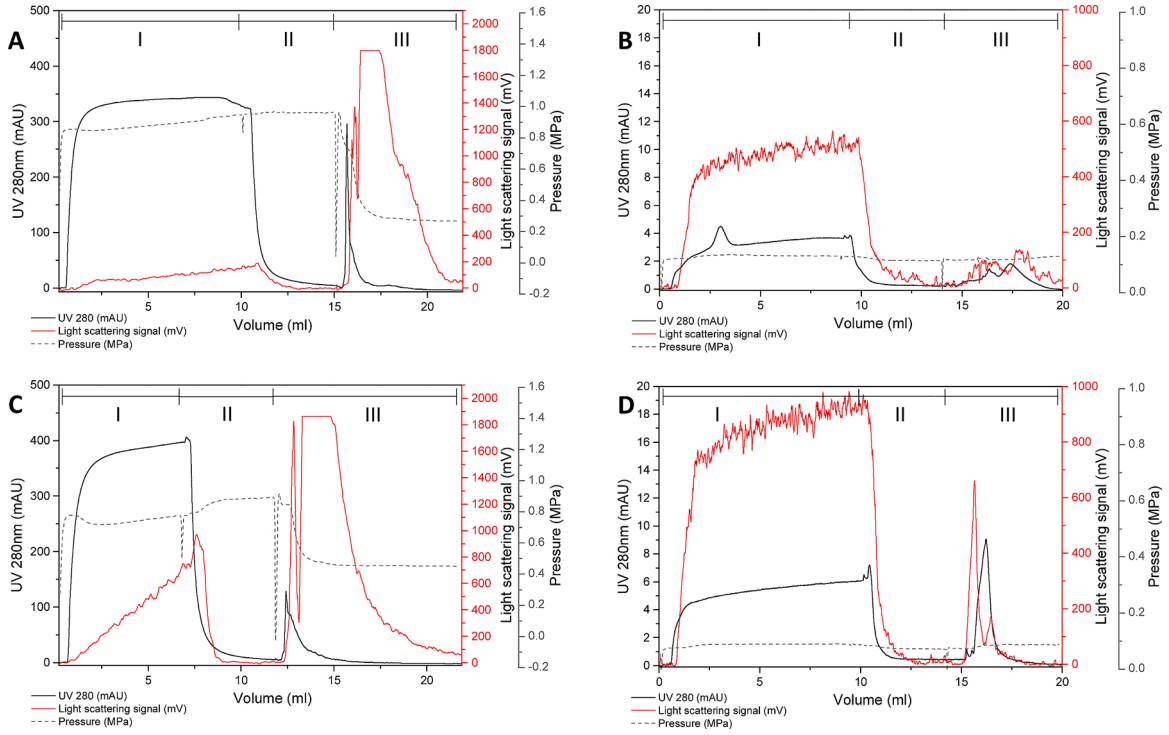

Fig. 3. Chromatograms for the two evaluated genotypes during each process step. SXC chromatograms for ORFV-GFP **(A)** and ORFV-Cherry **(C)** as well as Capto™ Core 700 (CC700) chromatograms for both, the ORFV-GFP **(B)** and the ORFV-Cherry **(D)** genotype. In all chromatograms, the sections are divided into loading (I), wash (II) and elution (III). In each case, the signals for UV at 280 nm (black line), the light scattering signal (red line), and the pre-column pressure (grey dashed line) are plotted. (For interpretation of the references to colour in this figure legend, the reader is referred to the web version of this article).

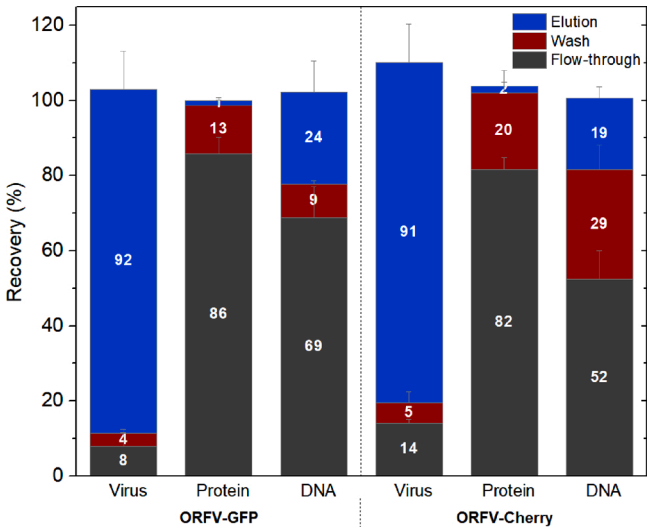

Fig. 4. Relative recoveries of virus, protein, and DNA during SXC purification. Shown are the values for both tested genotypes, ORFV-GFP and ORFV-Cherry, in the different fractions of the capture step: flow-through, wash and elution. Error bars represent technical triplicates.

3.5. Product characterization: ORFV size and morphology after purification

For the purified ORFV, two main size populations at 253.2 ± 35.1 nm and 163.7 ± 23.5 nm, and 261.3 ± 25.6 nm and 172.8 ± 19.8 nm were identified for ORFV-GFP and ORF-Cherry, respectively (Fig. 6A, B) by DLS measurements. Occasionally, however, a third particle population with length values of 368.6 ± 67.6 nm was observed (data not shown). Electron microscopy imaging additionally confirmed the presence of intact viral particles for both evaluated genotypes. Exemplarily, a representative image of ORFV-GFP after CC700 purification is illustrated in Fig. 6C.

4. Discussion

4.1. Clarification

Virus recoveries of about 90 % (Sartopure® PP3 and Millistak+® C0HC filters, both 5 µm membranes) during primary clarification, and 70 % (Millistak+® D0HC 0.65 µm filters) to 77 % (Sartopure® PP3 capsules 0.65 µm) after secondary clarification were achieved (Table 1). These values are comparable to clarification studies previously performed for rotavirus-like particles (3 µm filter with 85 % recovery, Peixoto et al., 2007), Influenza A viruses (0.65 µm polypropylene mesh filter with 85 % virus recovery Kalbfuss et al., 2007), or recombinant baculoviruses (3 µm + 0.65 µm Sartopure® PP2 polypropylene filter with 95 % recovery, Nestola et al., 2015; Vicente et al., 2009). A direct comparison of these filtration performances is rather difficult, as not only the targets vary, but also the applied filters, i.e. filter materials, use of filter aids, etc. However, recoveries >85 % meet current expectations, thus indicating an adequate performance of the herein used clarification strategy. Here, however, the high yield could only be achieved after the removal of the remaining complete cells containing intracellular ORFV by low-speed centrifugation (data not shown). These additional pre-clarifications have already been described in literature. For example, Fernandes et al. reported a poor adenovirus type 2 recovery (30 %) using filtration techniques without prior centrifugation (90 % recovery with preceding centrifugation, Fernandes et al., 2013). Previous studies on MVA also described a three-fold decrease in viral yields after centrifugation at 13,000 x g, and discarding cellular debris (Jordan et al., 2009). A very likely explanation for the observed losses is a potentially incomplete cell disruption. If so, the intracellular virus is present in the feed stream and accounted for by the flow cytometric analysis. Hence, an elevated virus titer, which is only partially accessible, leads to an apparent high virus loss during filtration. Thus, the inclusion of an additional step for cell disruption or the freeze/thaw-cycles in the process scheme might have to be considered for an industrial process. This has, for example, been investigated for MVA by Jordan et al., considering either three subsequent freeze/thaw-cycles or sonification (Jordan et al., 2009, 2011; Jordan et al., 2013). In this context, the degree of virus release and, thus, the improved virus output, must meet the economic considerations in terms of the required resources. In addition, the virus integrity and the

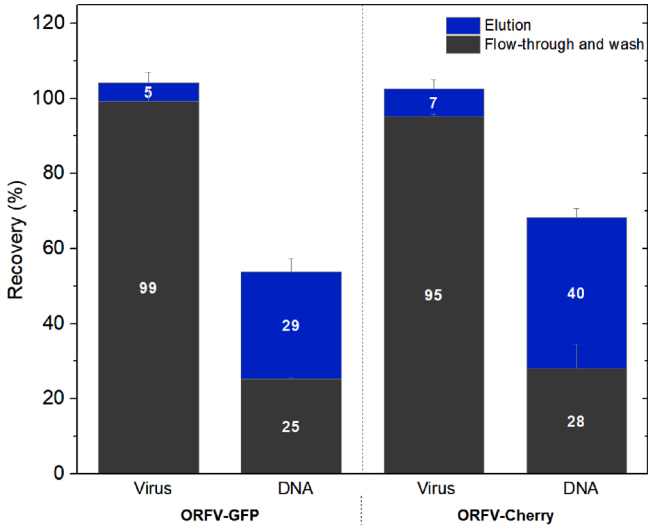

Fig. 5. Relative recoveries of virus and DNA during Capto™ Core 700 (CC700) purification. Values depict the amount of virus found in the individual fractions during the secondary chromatographic step in relation to the amount applied to the CC700 column. The fractions' flow-through and wash were mixed as a combined product fraction. Error bars represent SD of technical triplicates. No protein was found in any of the fractions during CC700 purification.

Table 2
Summary of the overall product yields and contaminant depletions for the ORFV chromatographic purification process.

Virus genotype	Process step	Product yield * [%]	Product concentration [IU ml^{-1}]	Protein depletion* [%]	Final protein concentration [µg ml^{-1}]	DNA depletion * [%]	Final DNA concentration [ng ml^{-1}]
ORFV-GFP	Capture	92	1.6E+06	98	28	76	8.5
	Secondary purification	91	1.1E + 06	>99	<LOD	98	1.2
ORFV-Cherry	Capture	91	4.8E+06	98	21	81	17.3
	Secondary purification	86	4.2E+06	>99	<LOD	96	4.1

* All values are overall yields from using clarified harvest to the product of the respective step. LOD: Limit of detection; IU: Infective units, ORFV-GFP/-Cherry Orf virus genotypes expressing green fluorescence / -mCherry proteins.

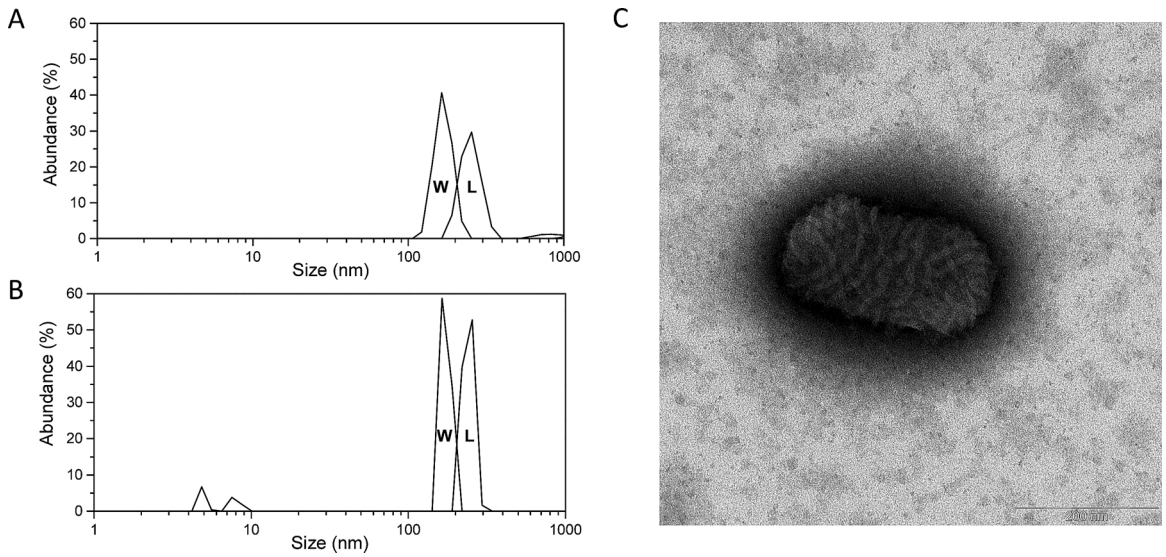

Fig. 6. Investigation on particle integrity after complete purification by size distribution evaluation and electron microscopy. Characteristic curves for the size populations, determined by dynamic light scattering for **(A)** ORFV-GFP and **(B)** ORFV-Cherry after Capto™ Core 700 (CC700) purification. "L" and "W" indicate size populations of the viruses' width and length, respectively. Electron micrograph of purified ORFV-GFP after ammonium molybdate stain, bar resembles 200 nm **(C)**.

increased accumulation of small cell fragments must be taken into account.

For a better impression of the possible throughput of culture harvests with regard to potential loading volumes and membrane capacity, additional filtration experiments were performed without preceding low-speed centrifugation. Here, the capacity per area (cm^2) was up to five times higher for the Millistak+® devices (Table 1), which can presumably be explained by the different capsule geometries, total membrane areas, and the membrane material.

4.2. Nuclease treatment

The nuclease treatment at RT did not affect virus infectivity over a period of up to 24 h (Fig. 2). Using 50 U ml^{-1} of the nuclease, DNA degradation was monitored over a time period of four hours. Any further incubation did not result in a considerable additional DNA reduction. For 250 U ml^{-1} and 500 U ml^{-1}, the DNA degradation was virtually completed in less than one hour, and for 500 U ml^{-1} nuclease a 5.4 fold DNA decrease was observed immediately after enzyme addition (Fig. 2). In literature, a wide range of successful process conditions during nuclease digestion is described. These include treatments with 10 U ml^{-1}, incubated for 24 h at RT (Rabies vaccine, Li et al., 2014), 50 U ml^{-1} incubated for 30 min at 37 °C (Adenovirus, Fernandes et al., 2013), 50 U ml^{-1} for 12 h at 37 °C (Influenza A Virus, Marichal-Gallardo *et al.*, 2017), or 100 U ml^{-1} for 60 min at RT (Canine adenoviral vectors, Segura et al., 2012), to only name a few. The choice of suitable process conditions for a successful DNA degradation depends, among others, on the amount of DNA in the culture broth. This, in turn, is influenced by the upstream conditions, i. e. the harvesting point, the type of bioreactor, the host cells or the culture media, and the positioning of the nuclease treatment step within the process train, e. g. prior or after clarification/concentration (Nestola et al., 2015). Furthermore, it is crucial that the nuclease treatment itself does not affect the virus integrity or infectivity (Hughes et al., 2017). Hence, process conditions such as temperature and incubation time need to be optimized accordingly. In the present study, the use of 250 U ml^{-1} of the enzyme was determined appropriate, to assure an adequate nucleic acid digestion in the sample, while allowing short incubation times (1 h) at mild conditions (RT).

4.3. Primary chromatographic purification (SXC capture)

Dynamic binding capacities of the SXC membranes were at 10 % breakthrough at about 1.41E + 06 IU (ORFV-GFP) and 2.8E + 06 IU (ORFV-Cherry) per cm^2 of the membrane surface. Although these values confirm data previously described for ORFV (Lothert et al., 2020), the values were lower than reported for $DBC_{10\ \%}$ of baculoviruses using membrane-based SXC (1.23E + 07 plague forming units per cm^2, Lothert et al., 2019). One reason for this might be the relatively large size of the ORFV (253 × 133 nm, section 3.5) in combination with a potential virus aggregation during the process, compared to baculovirus particles (Lothert et al., 2019) or Influenza A (Marichal-Gallardo et al., 2017). For the latter, $DBC_{5\ \%}$ values were estimated in terms of a hemagglutination assay and not with regard to infective virus particles. Although the relative amounts determined by the two quantification approaches are comparable, a direct conversion of dynamic binding capacities is not assured. Nonetheless, we recently reported on the evaluation of different chromatographic unit operations for ORFV purification (Lothert et al., 2020). There, we determined comparable $DBC_{10\ \%}$ values to the SXC for commonly used salt tolerant ion exchange (3.9E + 06 IU cm^{-2}) and hydrophobic interaction (3.5E + 06 IU cm^{-2}) chromatography membrane adsorbers, suggesting a similar productivity of the SXC. As mentioned above, DBC values for different viruses are hard to compare due to different physicochemical properties of the particles and varying analytical approaches. Similarly to that, a detailed comparison of DBCs for different chromatographic methods is also not conclusive, as it is highly depending on the individual properties of the membrane adsorbers (e.g. ligand densities and pore size) as well as the buffer and feed composition. Apart from the $DBC_{10\ \%}$ evaluation, no complete virus breakthrough ($DBC_{100\ \%}$) could be detected for ORFV-Cherry, as the sample application was limited by the pressure drop over the column during the loading process. In contrast, this effect was not observed for ORFV-GFP, which supports the idea of aggregation for the ORFV-Cherry. This aggregation of the ORFV-Cherry might be due to the different surface properties of the two investigated virus subtypes. While the GFP genotype represents a rather native surface phenotype, the Cherry genotype encodes for two large membrane-bound proteins in addition to the different fluorescence protein (data not shown). It could be assumed that these proteins modify the physico-chemical properties of the virus surface and, thus, affect the interaction behavior between each other

and the chromatographic stationary phase. This might lead to virus aggregation and, consequently, to a changed size distribution of the virus particles, which, in turn, influences the retention characteristics during SXC. However, this was not shown experimentally. Unpublished data, though, suggests that both genotypes have a similar isoelectric point which is a major influential variable aside from the particles' size (Lee et al., 2012). This would again confirm a robust process performance for similar sizes and isoelectric points, irrespective of specific protein compositions. In summary, the presented studies indicated a two-fold improved binding capacity ($DBC_{10\ \%}$) for the ORFV-Cherry compared to ORFV-GFP that can be caused by a changed retention characteristic. Another possibility, a higher retention due to sterical reasons, is not probable, as DLS measurements showed no distinct size differences between the two genotypes (Sections 3.5, 4.5, Fig. 6). In addition, the increased particle retention might lead to an accelerated pore blocking of the membrane and, thus, explains the enhanced pressure increase.

Based on the results of the dynamic binding capacities, chromatographic runs were performed with loading volumes $\leq DBC_{10\ \%}$. Under these conditions, virus elution and recovery (above 90 %, Fig. 4) were equally efficient for both genotypes with no significant differences (students' T-test, $P < 0.05$) with respect to the analytical error. Impurity depletions were also independent of the ORFV genotype and allowed a protein depletion above 98 % and a DNA removal of 76 % (ORFV-GFP) and 81 % (ORFV-Cherry, Fig. 4). This indicates that the use of other ORF viruses will allow a similar performance. Previous studies already suggested an SXC independency of the virus production batch, as shown for cell culture derived baculovirus (Lothert et al., 2019) as well as for different Influenza A strains (Marichal-Gallardo et al., 2017), confirming the platform technology characteristic of this purification method.

It was shown, that after the nuclease treatment and the capture step, the total DNA amounts were below 10 ng (5.3 ng for ORFV-GFP, 3.6 ng for ORFV-Cherry) related to 1E + 06 IU of virus particles with residual protein amounts of less than 30 µg (Table 2, Fig. 4). Thus, depending on the dosage requirements for the therapeutic treatment and the intended product application, the achieved purity for a dose of up to 1E + 06 IU in respect of the DNA-content is within current regulatory requirements for new cell culture-derived vaccine products (European Pharmacopoeia, 2020; World Health Organization, 2017). However, it is questionable whether these viral dosages are sufficient for a successful treatment. Even though this has already been demonstrated in animal experiments, there are also examples suggesting the contrary. In that regard, it was shown that a treatment against HBV infections with 5.0E + 05 inactivated ORFV particles lead to promising results (Wang et al., 2019; Weber et al., 2003). Furthermore, an anti-tumor activity was successfully shown in transplantable tumor models at doses between 1E + 05 to 1E + 06 median tissue-culture infective dose of ORFV (Fiebig et al., 2011). In turn, Rintoul et al. reported a repeated application of 1E + 07 plague forming units of ORFV to reduce the tumor burden in a mouse cancer model. Regardless of these examples, a further reduction of the DNA contents would be desirable and the remaining size of the DNA-fragments must be monitored in order to develop a robust production process for human applications.

4.4. Secondary chromatographic purification (CC700)

An additional purification, using the CC700 resin for this process step, resulted in a virtually complete virus recovery and protein depletion, regardless of the virus genotype (Fig. 5, Table 2). A further DNA depletion was at 22 % (ORFV-GFP) and 15 % (ORFV-Cherry) during secondary chromatography. This resulted in a nearly complete DNA removal during the entire process for both tested viruses with 98 % for ORFV-GFP and 96 % for ORFV-Cherry and the DNA removal is, thus, comparable with regard to the analytical error. As the remaining protein amounts were completely removed during the CC700 purification, and DNA levels were at 2–4 % of the original content (finally about 1 ng DNA per 1.0E + 06 IU), a successful CC700 performance is indicated. Due to the functionality of the CC700, it is not surprising that no differences were observed between the two genotypes during the secondary purification step. As CC700 is a bifunctional resin comprising hydrophobic and positively charged ligands, only accessible through pores on the particle surface with 700 kDa cut-off, the CC700 is primarily designed for macromolecules and nanoplexes with regard to a flow-through application. While impurities, such as proteins and DNA, can penetrate these pores, no viruses should be retained by the resin (James et al., 2016). Both evaluated genotypes exceeded the pore size (Fig. 6) and are, thus, excluded from the interior of the beads. This is supported by the data, as only about 1–5 % of the initial amount of the product was retained on the column (Fig. 5). The residual levels of DNA in the product fraction might be caused by DNA fragments that adhere to the virus particles as previously described (Marichal-Gallardo et al., 2017). Nevertheless, after an additional DNA depletion, the achieved product purity levels at doses below 1E + 07 IU as considered in 4.1 (Wang et al., 2019) and the amount of protein and DNA contaminants would be below the regulatory limitations for cell culture-derived vaccines (<100 µg total protein and <10 ng DNA per dose, European Pharmacopoeia, 2020; World Health Organization, 2017). Admittedly, some additional considerations are required. Firstly, the ORFV is a DNA virus, hence the remaining DNA levels are not all host cell-derived, but might be caused by the virus particles themselves. Thus, for a final optimization, assays need to be established, which allow to distinguish between the virus and host cell DNA. Unfortunately, there is currently no quantitative polymerase chain reaction (qPCR) method available for the applied cells. Furthermore, the Pico green assay determines DNA fragments of at least 20–100 base pairs (Dragan et al., 2010; Weigel et al., 2014, 2016) while other assays e. g. the Threshold assay or qPCR only take larger DNA fragments into account. Here, the applied samples were nuclease-treated prior to the purification. This leads to an overestimation of the values obtained by the Pico green assay. This effect was already reported by Weigel et al. (Weigel et al., 2016). Nevertheless, if specific applications require a higher dosage, the implementation of a further unit operation, such as the hydrophobic interaction chromatography (Weigel et al., 2019; Wolff et al., 2010a) or sulfated cellulose membrane adsorbers (Carvalho et al., 2018; Fortuna et al., 2018, 2019) should be considered. A selection of feasible unit operations for the ORFV has been published recently (Lothert et al., 2020). These considerations must also take recent regulatory developments into account, where an exceeding of the host cell DNA levels might be acceptable in some cases with respect to individual process and product demands (European Pharmacopoeia, 2020; Vernay et al., 2019).

4.5. Product characterization: ORFV size and morphology after purification

Beside the maintained infectivity confirmed by flow cytometry, further morphologic characteristics were determined to investigate differences between the two genotypes. In that respect, size determination and electron microscopy evaluation suggest particle sizes of about 150 × 250 nm as expected for ORFV (Guo et al., 2003), without variations between the GFP and the Cherry genotype (Fig. 6). The presence of a few larger particles in some of the DLS measurements (~360 nm, data not shown) might indicate a certain particle aggregation, which could be caused by the PEG-induced particle association during SXC and an incomplete dissociation after elution. However, no major aggregates were found during an electron microscopy observation. This is in line with previous observations from Marichal Gallardo et al., who showed for Influenza A, that no aggregations were present after a SXC purification (Marichal-Gallardo et al., 2017). Based on these observations, the absence of aggregates is not certain, however, and if present, then only in negligible amounts. Additionally, the viral particle size and surface structure (criss-cross tubular pattern surrounding the particle, Nagington and Horne, 1962; Zhao et al., 2010) could be

confirmed clearly in the electron micrograph (Fig. 6). In this regard, it should be noted that the residual salt and PEG content of the probe impair the resolution of the protein structures. In combination with the maintained infectivity of the virus confirmed during virus quantification, it can be stated that the process described here allows a gentle processing without considerably affecting the viruses' integrity and infectivity.

The overall impact of the genetic modifications on the process performance between the two tested genotypes of ORFV, with regard to analytical errors, was negligible. Therefore, it can be assumed that the described process is robust for a large variety of different ORFV genotypes. This qualifies the developed process, comprising of clarification, nuclease treatment followed by SXC and CC700 purification, as a platform approach. Furthermore, the process does not only enable the purification of different ORFV genotypes, but is theoretically also applicable to other poxviruses, viruses of further classes or virus-like particles, as the individual process steps have previously been applied for a variety of nanoplexes. Nonetheless, depending on the morphology of the target product and the applied upstream processing conditions, minor adjustments to the process conditions (e.g. nuclease treatment, PEG concentration during SXC) are presumably required.

5. Conclusion

Here, we presented a robust downstream process for the production of parapoxviruses using the ORFV. The process is suitable as a platform technology, enabling the processing of different ORFV. The virus yield during clarification reached 70 %, and a maximum recovery of 91 % was possible for the chromatographic set-up. This resulted in an overall process yield of about 64 %. Due to the implemented nuclease treatment, the final product contained DNA levels of 1 ng per 1E + 06 IU. Additionally, the protein contamination of the processed samples was below the detection limits. Thus, by using this process, purified ORFV are suitable for human or veterinary antiviral and immunomodulatory applications within the regulatory limits for contaminant levels. However, for specific oncolytic therapies, the required dosage levels might be higher and contaminating DNA levels need to be further reduced. Additionally, the utilized materials for the filtration and chromatography allow an easy scalability and single-use applications without the need for cleaning-in-place and sterilization-in-place, reflecting the current trends in pharmaceutical manufacturing processes.

Funding

The work was supported by an EXIST-Forschungstransfer grand (03EFKBW171) of the German Federal Ministry for Economic Affairs and Energy.

CRediT authorship contribution statement

Keven Lothert: Conceptualization, Methodology, Data curation, Formal analysis, Writing - original draft. **Felix Pagallies:** Methodology, Investigation, Writing - review & editing. **Friederike Eilts:** Investigation, Visualization, Writing - review & editing. **Arabi Sivanesapillai:** Investigation, Visualization, Writing - review & editing. **Martin Hardt:** Visualization, Supervision, Writing - review & editing. **Anna Moebus:** Visualization, Writing - review & editing. **Thomas Feger:** Methodology, Data curation, Writing - review & editing. **Ralf Amann:** Supervision, Funding acquisition, Writing - review & editing. **Michael W. Wolff:** Supervision, Project administration, Funding acquisition, Writing - review & editing.

Acknowledgements

Many thanks also to Hanns-Joachim Rziha for scientific advice and to Catherine Meckel-Oschmann for the proof-reading of the manuscript. This work is part of a dissertation under the aegis of the Justus-Liebig-University of Giessen, Germany, in cooperation with the Technische Hochschule Mittelhessen (University of Applied Sciences), Giessen, Germany.

References

Albarnaz, J.D., Torres, A.A., Smith, G.L., 2018. Modulating vaccinia virus immunomodulators to improve immunological memory. Viruses 10 (3). https://doi.org/10.3390/v10030101.

Amann, R., Rohde, J., Wulle, U., Conlee, D., Raue, R., Martinon, O., Rziha, H.-J., 2013. A new rabies vaccine based on a recombinant ORF virus (parapoxvirus) expressing the rabies virus glycoprotein. J. Virol. 87 (3), 1618–1630. https://doi.org/10.1128/JVI.02470-12.

Bergqvist, C., Kurban, M., Abbas, O., 2017. Orf virus infection. Rev. Med. Virol. 27 (4) https://doi.org/10.1002/rmv.1932.

Carvalho, S.B., Fortuna, A.R., Wolff, M.W., Peixoto, C., Alves, P.M., Reichl, U., Jt Carrondo, M., 2018. Purification of influenza virus-like particles using sulfated cellulose membrane adsorbers. J. Chem. Technol. Biotechnol. 93 (7), 1988–1996. https://doi.org/10.1002/jctb.5474.

Dragan, A.I., Casas-Finet, J.R., Bishop, E.S., Strouse, R.J., Schenerman, M.A., Geddes, C. D., 2010. Characterization of PicoGreen interaction with dsDNA and the origin of its fluorescence enhancement upon binding. Biophys. J. 99 (9), 3010–3019. https://doi.org/10.1016/j.bpj.2010.09.012.

European Pharmacopoeia, 2020. Ed. 10.2.

Fernandes, P., Peixoto, C., Santiago, V.M., Kremer, E.J., Coroadinha, A.S., Alves, P.M., 2013. Bioprocess development for canine adenovirus type 2 vectors. Gene Ther. 20 (4), 353–360. https://doi.org/10.1038/gt.2012.52.

Fiebig, H.-H., Siegling, A., Volk, H.-D., Friebe, A., Knolle, P., Limmer, A., Weber, O., 2011. Inactivated orf virus (Parapoxvirus ovis) induces antitumoral activity in transplantable tumor models. Anticancer Res. 31 (12), 4185–4190.

Fleming, S.B., Wise, L.M., Mercer, A.A., 2015. Molecular genetic analysis of orf virus: a poxvirus that has adapted to skin. Viruses 7 (3), 1505–1539. https://doi.org/10.3390/v7031505.

Fleming, S.B., McCaughan, C., Lateef, Z., Dunn, A., Wise, L.M., Real, N.C., Mercer, A.A., 2017. Deletion of the chemokine binding protein gene from the parapoxvirus orf virus reduces virulence and pathogenesis in sheep. Front. Microbiol. 8, 46. https://doi.org/10.3389/fmicb.2017.00046.

Fortuna, A.R., Taft, F., Villain, L., Wolff, M.W., Reichl, U., 2018. Optimization of cell culture-derived influenza A virus particles purification using sulfated cellulose membrane adsorbers. Eng. Life Sci. 18 (1), 29–39. https://doi.org/10.1002/elsc.201700108.

Fortuna, A.R., van Teeffelen, S., Ley, A., Fischer, L.M., Taft, F., Genzel, Y., Villain, L., Wolff, M.W., Reichl, U., 2019. Use of sulfated cellulose membrane adsorbers for chromatographic purification of cell cultured-derived influenza A and B viruses. Sep. Purif. Technol. 226, 350–358. https://doi.org/10.1016/j.seppur.2019.05.101.

Friebe, A., Siegling, A., Weber, O., 2018. Inactivated Orf-virus shows disease modifying antiviral activity in a guinea pig model of genital herpesvirus infection. J. Microbiol. Immunol. Infect. 51 (5), 587–592. https://doi.org/10.1016/j.jmii.2017.03.002.

Gagnon, P., Toh, P., Lee, J., 2014. High productivity purification of immunoglobulin G monoclonal antibodies on starch-coated magnetic nanoparticles by steric exclusion of polyethylene glycol. J. Chromatogr. A 1324, 171–180. https://doi.org/10.1016/j.chroma.2013.11.039.

García-Arriaza, J., Esteban, M., 2014. Enhancing poxvirus vectors vaccine immunogenicity. Hum. Vaccin. Immunother. 10 (8), 2235–2244. https://doi.org/10.4161/hv.28974.

Guo, J., Zhang, Z., Edwards, J.F., Ermel, R.W., Taylor, C., La Concha-Bermejillo, Ade, 2003. Characterization of a North American orf virus isolated from a goat with persistent, proliferative dermatitis. Virus Res. 93 (2), 169–179. https://doi.org/10.1016/s0168-1702(03)00095-9.

Haig, D.M., McInnes, C.J., 2002. Immunity and counter-immunity during infection with the parapoxvirus orf virus. Virus Res. 88 (1-2), 3–16. https://doi.org/10.1016/s0168-1702(02)00117-x.

Haig, D.M., Mercer, A.A., 1998. Ovine diseases. Orf. Vet Res 29 (3-4), 311–326.

Hoffmann, D., Leber, J., Loewe, D., Lothert, K., Oppermann, T., Zitzmann, J., Weidner, T., Salzig, D., Wolff, M., Czermak, P., 2019. Purification of New biologicals using membrane-based processes. In: Basile, A., Charcosset, C. (Eds.), Current Trends and Future Developments on (Bio-) Membranes. Elsevier, pp. 123–150. https://doi.org/10.1016/B978-0-12-813606-5.00005-1.

Hughes, L., Wilkins, K., Goldsmith, C.S., Smith, S., Hudson, P., Patel, N., Karem, K., Damon, I., Li, Y., Olson, V.A., Satheshkumar, P.S., 2017. A rapid Orthopoxvirus purification protocol suitable for high-containment laboratories. J. Virol. Methods 243, 68–73. https://doi.org/10.1016/j.jviromet.2017.01.018.

James, K.T., Cooney, B., Agopsowicz, K., Trevors, M.A., Mohamed, A., Stoltz, D., Hitt, M., Shmulevitz, M., 2016. Novel high-throughput approach for purification of infectious virions. Sci. Rep. 6, 36826. https://doi.org/10.1038/srep36826.

Jordan, I., Vos, A., Beilfuss, S., Neubert, A., Breul, S., Sandig, V., 2009. An avian cell line designed for production of highly attenuated viruses. Vaccine 27 (5), 748–756. https://doi.org/10.1016/j.vaccine.2008.11.066.

Jordan, I., Northoff, S., Thiele, M., Hartmann, S., Horn, D., Höwing, K., Bernhardt, H., Oehmke, S., Horsten, Hvon, Rebeski, D., Hinrichsen, L., Zelnik, V., Mueller, W., Sandig, V., 2011. A chemically defined production process for highly attenuated poxviruses. Biologicals 39 (1), 50–58. https://doi.org/10.1016/j.biologicals.2010.11.005.

Jordan, I., Horn, D., John, K., Sandig, V., 2013. A genotype of modified vaccinia Ankara (MVA) that facilitates replication in suspension cultures in chemically defined medium. Viruses 5 (1), 321–339. https://doi.org/10.3390/v5010321.

Kalbfuss, B., Genzel, Y., Wolff, M., Zimmermann, A., Morenweiser, R., Reichl, U., 2007. Harvesting and concentration of human influenza A virus produced in serum-free mammalian cell culture for the production of vaccines. Biotechnol. Bioeng. 97 (1), 73–85. https://doi.org/10.1002/bit.21139.

Lee, J., Gan, H.T., Latiff, S.M.A., Chuah, C., Lee, W.Y., Yang, Y.-S., Loo, B., Ng, S.K., Gagnon, P., 2012. Principles and applications of steric exclusion chromatography. J. Chromatogr. A 1270, 162–170. https://doi.org/10.1016/j.chroma.2012.10.062.

Levanova, A., Poranen, M.M., 2018. Application of steric exclusion chromatography on monoliths for separation and purification of RNA molecules. J. Chromatogr. A 1574, 50–59. https://doi.org/10.1016/j.chroma.2018.08.063.

Li, S.-M., Bai, F.-L., Xu, W.-J., Yang, Y.-B., An, Y., Li, T.-H., Yu, Y.-H., Li, D.-S., Wang, W.-F., 2014. Removing residual DNA from vero-cell culture-derived human rabies vaccine by using nuclease. Biologicals 42 (5), 271–276. https://doi.org/10.1016/j.biologicals.2014.06.005.

Lothert, K., Sprick, G., Beyer, F., Lauria, G., Czermak, P., Wolff, M.W., 2019. Membrane-based steric exclusion chromatography for the purification of a recombinant baculovirus and its application for cell therapy. J. Virol. Methods, 113756. https://doi.org/10.1016/j.jviromet.2019.113756.

Lothert, K., Pagallies, F., Feger, T., Amann, R., Wolff, M.W., 2020. Selection of chromatographic methods for the purification of cell culture-derived Orf virus for its application as a vaccine or viral vector. J. Biotechnol. https://doi.org/10.1016/j.jbiotec.2020.07.023. In press.

Marichal-Gallardo, P., Pieler, M.M., Wolff, M.W., Reichl, U., 2017. Steric exclusion chromatography for purification of cell culture-derived influenza A virus using regenerated cellulose membranes and polyethylene glycol. J. Chromatogr. A 1483, 110–119. https://doi.org/10.1016/j.chroma.2016.12.076.

Nagington, J., Horne, R.W., 1962. Morphological studies of orf and vaccinia viruses. Virology 16 (3), 248–260. https://doi.org/10.1016/0042-6822(62)90245-3.

Nestola, P., Peixoto, C., Silva, R.R.J.S., Alves, P.M., Mota, J.P.B., Carrondo, M.J.T., 2015. Improved virus purification processes for vaccines and gene therapy. Biotechnol. Bioeng. 112 (5), 843–857. https://doi.org/10.1002/bit.25545.

O'Leary, M.P., Choi, A.H., Kim, S.-I., Chaurasiya, S., Lu, J., Park, A.K., Woo, Y., Warner, S.G., Fong, Y., Chen, N.G., 2018. Novel oncolytic chimeric orthopoxvirus causes regression of pancreatic cancer xenografts and exhibits abscopal effect at a single low dose. J. Transl. Med. 16 (1), 110. https://doi.org/10.1186/s12967-018-1483-x.

Peixoto, C., Sousa, M.F.Q., Silva, A.C., Carrondo, M.J.T., Alves, P.M., 2007. Downstream processing of triple layered rotavirus like particles. J. Biotechnol. 127 (3), 452–461. https://doi.org/10.1016/j.jbiotec.2006.08.002.

Pohlscheidt, M., Langer, U., Minuth, T., Bödeker, B., Apeler, H., Hörlein, H.-D., Paulsen, D., Rübsamen-Waigmann, H., Henzler, H.-J., Reichl, U., 2008. Development and optimisation of a procedure for the production of Parapoxvirus ovis by large-scale microcarrier cell culture in a non-animal, non-human and non-plant-derived medium. Vaccine 26 (12), 1552–1565. https://doi.org/10.1016/j.vaccine.2008.01.032.

Rintoul, J.L., Lemay, C.G., Tai, L.-H., Stanford, M.M., Falls, T.J., Souza, C.Tde, Bridle, B. W., Daneshmand, M., Ohashi, P.S., Wan, Y., Lichty, B.D., Mercer, A.A., Auer, R.C., Atkins, H.L., Bell, J.C., 2012. ORFV: a novel oncolytic and immune stimulating parapoxvirus therapeutic. Mol. Ther. 20 (6), 1148–1157. https://doi.org/10.1038/mt.2011.301.

Rziha, H.-J., Rohde, J., Amann, R., 2016. Generation and selection of orf virus (ORFV) recombinants. Methods Mol. Biol. 1349, 177–200. https://doi.org/10.1007/978-1-4939-3008-1_12.

Rziha, H.-J., Büttner, M., Müller, M., Salomon, F., Reguzova, A., Laible, D., Amann, R., 2019. Genomic characterization of orf virus strain D1701-V (Parapoxvirus) and development of novel sites for multiple transgene expression. Viruses 11 (2). https://doi.org/10.3390/v11020127.

Scott, M.K., Chommanard, C., Lu, X., Appelgate, D., Grenz, L., Schneider, E., Gerber, S.I., Erdman, D.D., Thomas, A., 2016. Human adenovirus associated with severe respiratory infection, Oregon, USA, 2013-2014. Emerging Infect. Dis. 22 (6), 1044–1051. https://doi.org/10.3201/eid2206.151898.

Segura, M.M., Puig, M., Monfar, M., Chillón, M., 2012. Chromatography purification of canine adenoviral vectors. Hum. Gene Ther. Methods 23 (3), 182–197. https://doi.org/10.1089/hgtb.2012.058.

Tao, S.-P., Zheng, J., Sun, Y., 2015. Grafting zwitterionic polymer onto cryogel surface enhances protein retention in steric exclusion chromatography on cryogel monolith. J. Chromatogr. A 1389, 104–111. https://doi.org/10.1016/j.chroma.2015.02.051.

Vannucci, L., Lai, M., Chiuppesi, F., Ceccherini-Nelli, L., Pistello, M., 2013. Viral vectors: a look back and ahead on gene transfer technology. New Microbiol. 36 (1), 1–22.

Vernay, O., Sarcey, E., Detrez, V., Abachin, E., Riou, P., Mouterde, B., Bonnevay, T., Mallet, L., 2019. Comparative analysis of the performance of residual host cell DNA assays for viral vaccines produced in Vero cells. J. Virol. Methods 268, 9–16. https://doi.org/10.1016/j.jviromet.2019.01.001.

Vicente, T., Peixoto, C., Carrondo, M.J.T., Alves, P.M., 2009. Purification of recombinant baculoviruses for gene therapy using membrane processes. Gene Ther. 16 (6), 766–775. https://doi.org/10.1038/gt.2009.33.

Wang, C., Bai, S., Tao, S.-P., Sun, Y., 2014. Evaluation of steric exclusion chromatography on cryogel column for the separation of serum proteins. J. Chromatogr. A 1333, 54–59. https://doi.org/10.1016/j.chroma.2014.01.059.

Wang, R., Wang, Y., Liu, F., Luo, S., 2019. Orf virus: a promising new therapeutic agent. Rev. Med. Virol. 29 (1), e2013 https://doi.org/10.1002/rmv.2013.

Weber, O., Siegling, A., Friebe, A., Limmer, A., Schlapp, T., Knolle, P., Mercer, A., Schaller, H., Volk, H.-D., 2003. Inactivated parapoxvirus ovis (Orf virus) has antiviral activity against hepatitis B virus and herpes simplex virus. J. Gen. Virol. 84 (Pt 7), 1843–1852. https://doi.org/10.1099/vir.0.19138-0.

Weigel, T., Solomaier, T., Peuker, A., Pathapati, T., Wolff, M.W., Reichl, U., 2014. A flow-through chromatography process for influenza A and B virus purification. J. Virol. Methods 207, 45–53. https://doi.org/10.1016/j.jviromet.2014.06.019.

Weigel, T., Solomaier, T., Wehmeyer, S., Peuker, A., Wolff, M.W., Reichl, U., 2016. A membrane-based purification process for cell culture-derived influenza A virus. J. Biotechnol. 220, 12–20. https://doi.org/10.1016/j.jbiotec.2015.12.022.

Weigel, T., Soliman, R., Wolff, M.W., Reichl, U., 2019. Hydrophobic-interaction chromatography for purification of influenza A and B virus. J. Chromatogr. B Analyt. Technol. Biomed. Life Sci. 1117, 103–117. https://doi.org/10.1016/j.jchromb.2019.03.037.

Wolff, M.W., Reichl, U., 2011. Downstream processing of cell culture-derived virus particles. Expert Rev. Vaccines 10 (10), 1451–1475. https://doi.org/10.1586/ERV.11.111.

Wolff, M.W., Siewert, C., Hansen, S.P., Faber, R., Reichl, U., 2010a. Purification of cell culture-derived modified vaccinia ankara virus by pseudo-affinity membrane adsorbers and hydrophobic interaction chromatography. Biotechnol. Bioeng. 107 (2), 312–320. https://doi.org/10.1002/bit.22797.

Wolff, M.W., Siewert, C., Lehmann, S., Hansen, S.P., Djurup, R., Faber, R., Reichl, U., 2010b. Capturing of cell culture-derived modified Vaccinia Ankara virus by ion exchange and pseudo-affinity membrane adsorbers. Biotechnol. Bioeng. 105 (4), 761–769. https://doi.org/10.1002/bit.22595.

World Health Organization, 2017. WHO Expert Committee on Biological Standardization. Repo, Geneva.

Zhao, K., Song, D., He, W., Lu, H., Zhang, B., Li, C., Chen, K., Gao, F., 2010. Identification and phylogenetic analysis of an Orf virus isolated from an outbreak in sheep in the Jilin province of China. Vet. Microbiol. 142 (3-4), 408–415. https://doi.org/10.1016/j.vetmic.2009.10.006.

SCIENTIFIC REPORTS
nature research

Check for updates

OPEN

Development of a downstream process for the production of an inactivated whole hepatitis C virus vaccine

Keven Lothert[1,4], Anna F. Offersgaard[2,4], Anne F. Pihl[2], Christian K. Mathiesen[2], Tanja B. Jensen[2], Garazi Peña Alzua[2], Ulrik Fahnøe[2], Jens Bukh[2], Judith M. Gottwein[2,4]✉ & Michael W. Wolff[1,3,4]✉

There is a large unmet need for a prophylactic hepatitis C virus (HCV) vaccine to control the ongoing epidemic with this deadly pathogen. Many antiviral vaccines employ whole viruses as antigens. For HCV, this approach became feasible following the development of infectious cell culture systems for virus production. However, the lack of efficient downstream processes (DSP) for HCV purification poses a roadblock for the development of a whole virus vaccine. Using cell culture-derived genotype 1a HCV we developed a scalable and efficient DSP train, employing commonly used clarification and ultrafiltration techniques, followed by two membrane-based chromatography steps. For virus capture, steric exclusion chromatography using cellulose membranes was established, resulting in a virtually complete virus recovery with > 99% protein and 84% DNA depletion. Virus polishing was achieved by sulphated cellulose membrane adsorbers with ~ 50% virus recovery and > 99% protein and 90% DNA depletion. Additional nuclease digestion resulted in 99% overall DNA depletion with final DNA concentrations of 2 ng/mL. Process results were comparable for cell culture-derived HCV of another major genotype (5a). This study provides proof-of-concept for establishment of an efficient and economically attractive DSP with potential application for production of an inactivated whole virus vaccine against HCV for human use.

Abbreviations

AEM	Adenovirus expression medium
DAA	Direct-acting antivirals
DBC	Dynamic binding capacity
DMEM	Dulbecco's modified eagle medium
DSP	Downstream process
FFU	Focus forming units
GMP	Good manufacturing practices
HCV	Hepatitis C virus
Huh7.5	Human hepatoma cell line 7.5
IU	International units
NGS	Next generation sequencing
PCR	Polymerase chain reaction
pI	Isoelectric point

[1]Institute of Bioprocess Engineering and Pharmaceutical Technology, Department of Life Science Engineering, University of Applied Sciences Mittelhessen (THM), Giessen, Germany. [2]Copenhagen Hepatitis C Program (CO-HEP), Department of Infectious Diseases, Hvidovre Hospital and Department of Immunology and Microbiology, Faculty of Health and Medical Sciences, University of Copenhagen, Copenhagen, Denmark. [3]Fraunhofer Institute for Molecular Biology and Applied Ecology (IME), Giessen, Germany. [4]These authors contributed equally: Keven Lothert and Anna F. Offersgaard. These authors jointly supervised this work: Judith M. Gottwein and Michael W. Wolff. ✉email: jgottwein@sund.ku.dk; michael.wolff@lse.thm.de

PBS	Phosphate buffered saline
PEG	Polyethylene glycol
qPCR	Quantitative polymerase chain reaction
SCMA	Sulphated cellulose membrane adsorber
SD	Standard deviation
SXC	Steric exclusion chromatography

The hepatitis C virus (HCV) is a small enveloped virus, 30–80 nm in diameter[1,2], with a single positive stranded RNA genome, belonging to the *Flaviviridae* family[3,4]. The RNA genome encodes 3 structural proteins, the capsid protein Core, and the envelope glycoproteins E1 and E2, which are incorporated into the viral particle, as well as 7 nonstructural proteins (p7, NS2, NS3, NS4A, NS4B, NS5A, and NS5B). There are 8 different major genotypes, differing in ~ 30% of their nucleotide and amino acid sequence, with genotype 1 being most frequent worldwide[5,6].

Each year, there are at least 2 million new HCV infections, of which ~ 80% result in chronic infections. There are at least 71 million chronically infected individuals worldwide with an increased risk of liver cirrhosis and hepatocellular carcinoma, resulting in ~ 400,000 deaths per year[7–9].

Only a minor fraction of HCV-infected individuals are treated with recently licensed efficient direct-acting antivirals (DAA). The main reasons for this are that most individuals are not aware of their infection status, as the infection is typically asymptomatic until a severe and often irreversible liver disease has developed, and because of the lack of screening programs and the high cost of DAA. Furthermore, resistance to DAA is increasing and might compromise future treatment efficacy[10,11]. Thus, a vaccine is urgently needed to control HCV on a global scale[12–14].

Many antiviral vaccines are based on viral particles as vaccine antigens[15,16] and protect by their induction of neutralizing antibodies. The proof-of-concept for the immunogenicity of cell culture-derived inactivated HCV has been obtained in animal models[17–19]. However, in these studies, ultracentrifugation-based downstream processes (DSP) were employed for virus concentration and purification. This approach is in general characterized by a relatively low recovery, a limited scalability, and a limited impurity depletion. Thus, as for most other vaccines, the development of an efficient DSP, compatible with industrial requirements, is a major bottleneck for the manufacturing of a whole virus HCV vaccine for human use[20–22].

Here, we evaluated commonly used clarification and ultrafiltration in combination with two membrane-based chromatography technologies, (1) steric exclusion chromatography (SXC), and (2) chromatography based on sulphated cellulose membrane adsorbers (SCMA), for the development of a cost-efficient and scalable DSP, compatible with good manufacturing practices (GMP). SXC was initially described for the purification of bacteriophages and large proteins, using hydrophilic monoliths and starch-coated magnetic nanoparticles[23–25]. With the application of unmodified cellulose membranes, SXC also proved to be a valuable tool for the purification of different viruses with recoveries of 99% (Influenza A[26]) and 91% (Baculovirus[27]). The method is based on the steric exclusion of particles in a solution of an inert polymer, e.g. polyethylene glycol (PEG). This exclusion leads to the formation of polymer-rich and polymer-deficient zones, resulting in thermodynamic instability, which is resolved by an association of the excluded particles with each other, and with the hydrophilic stationary phase, thus, retaining target molecules from the mobile phase. A careful adjustment of the PEG concentration and the molecular weight, with regard to the size of the product and expected process impurities, allows a selective product retention. Retained particles are eluted by the removal of the inert polymer from the mobile phase[26,27]. As the method highly depends on the size of the product, it is important to mention that HCV is thought to be smaller than the viruses used in previous publications on membrane-based SXC. Additionally, it has previously been described, that the retention works best near the isoelectric point (pI) of the target molecule[28].

SCMA was applied for subsequent polishing, employing a pseudo affinity-based orthogonal technique. The method has been described for the purification of the Influenza A virus and the Modified Vaccinia Ankara virus[29–33]. It utilizes the heparin-mimicking effect of sulphated cellulose and should, thus, be widely applicable to viruses with an affinity to heparin. As HCV was successfully purified from infected plasma using a heparin chromatography resin, such an affinity could be expected[34].

The aim of this study was to provide proof-of-concept for the development of an efficient, scalable, and GMP-compatible DSP for the purification of cell culture-derived HCV to eventually facilitate an industrial production of a human HCV vaccine. In summary, the evaluated process unit operations included clarification, ultrafiltration, nuclease treatment as well as SXC and SCMA as chromatographic capture and polishing steps.

Results

Production of high-titre HCV genotype 1a virus stock for DSP development. We first focussed on processing HCV genotype 1 being the most prevalent HCV genotype worldwide. However, to facilitate DSP development, a high-titre variant efficiently producing infectious viruses in cell culture was required. Thus, the previously reported recombinant genotype 1a virus TNcc[35] was serially passaged in naïve human hepatoma cell line 7.5 (Huh7.5) cells for a further adaptation to the cell culture, until HCV infectivity titres of ~ 6 $\log_{10}$ focus forming units (FFU)/mL, were observed for several passages. A passage 19 stock was prepared, serving as the seed for the genotype 1a passage 20 virus production in triple layer culture flasks, which was then used in the DSP development. Next generation sequencing (NGS) revealed that, in addition to the eight cell culture adaptive substitutions in the original 1a virus recombinant, passage 20 viruses had acquired 3 substitutions present in > 50% of the virus population, G1909A in NS4B as well as N2651H and H2986R in NS5B (Supplementary Table S1). Overall, the largest heterogeneity was observed in the nonstructural proteins.

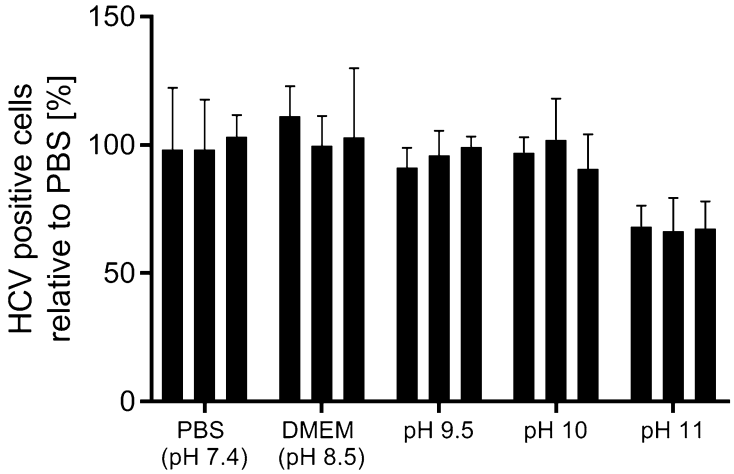

Figure 1. HCV stability at alkaline pH. HCV was incubated at room temperature for 90 min in PBS (pH 7.4), DMEM standard cell culture medium (pH 8.5) and phosphate buffers for alkaline conditions (pH 9.5, 10 and 11). Subsequently, solutions were neutralized with DMEM containing 20 mM HEPES and used to infect cells. The number of infected cells after 48 h of incubation was evaluated relative to the mean of the number of infected cells resulting from infection with virus incubated in PBS. Data from 3 biological replicates are shown as separate bars. Error bars are standard deviations (SD) representing 3 technical replicates.

HCV clarification and ultrafiltration. A two-step filtration, with cut-offs of 5 µm and 0.65 µm, was selected for the clarification of genotype 1a HCV. Subsequently, the clarified material was concentrated in two sequential ultrafiltration steps with a cut-off of 500 kDa from a starting volume of 10.5 L to volumes of 600 mL and 42 mL, respectively. We observed a virtually complete virus recovery for the clarification and the first ultrafiltration step, whereas a 45% recovery was observed for the second ultrafiltration step. For inactivation, the resulting material was treated by UV irradiation, and naïve cell cultures were inoculated and followed for three weeks by regular immunostainings for the HCV NS5A antigen to confirm inactivation.

HCV capture by SXC. When in initial SXC experiments published standard conditions with 8% PEG and physiological pH values were used[26], the majority of the viruses were found in the flow-through fraction. An increase in the PEG concentration to up to 12% did not result in improvements. Based on prior publications, unpublished experiments and theoretical sequence-based calculations provided on viprbrc.org, we hypothesized that the pI of HCV might be alkaline[36]. Thus, prior to testing alkaline SXC conditions, we investigated HCV stability at different pH values. HCV was incubated in phosphate-buffered saline (PBS, pH 7.4), Dulbecco's Modified Eagle Medium (DMEM, standard cell culture medium, pH 8.5), and phosphate buffers for final pH values of ~ 9.5, 10 and 11, prior to inoculation of naïve Huh7.5 cells for the determination of HCV infectivity. Of note, the tested conditions did not result in an impairment of cell viability. HCV was stable when subjected to pH values of up to 10 for 90 min (Fig. 1), which equals the approximate duration of the SXC. Testing alkaline SXC conditions revealed a large virus breakthrough at pH 8 and 10 during loading (Fig. 2A,C) based on light-scattering detection. At pH 11 a strongly increasing back pressure was observed with increasing loading volume during sample application and wash (Fig. 2D). This resulted in a reduced virus breakthrough, a decreased possible loading volume, and nearly no virus recovery in any of the fractions. In contrast, at pH 9, the virus breakthrough was minimized (Fig. 2B). In an additional experiment, the qualitative data based on the light-scattering signal, was verified by quantitative polymerase chain reaction (qPCR) analytics of the recovered viral RNA. Here, at pH 8.5, 9, and 9.5, a virtually full virus retention and recovery in the elution fraction could be achieved, with a product yield in the range of 90% to 105% (Fig. 3, Table 1). An additional nuclease treatment did not affect the SXC and resulted in similar recoveries of 99% (Fig. 3, Table 1) with minor amounts of virus found in the flow-through (2%) and wash (< 1%) fractions.

The dynamic binding capacity (DBC) of the membranes was determined using 3.9E+08 international units (IU)/cm^2 until a pressure limitation occurred and was approximately 2.1E+08 IU/cm^2 until a 10% breakthrough was observed ($DBC_{10\%}$). However, due to an excessive pressure increase, it was not possible to load the virus until a 100% breakthrough occurred, thus $DBC_{100\%}$ could not be determined.

The impurity removal did not depend on the pH value. For the runs without a preceding nuclease treatment as shown in Fig. 3 (pH 8.5, 9 and 9.5), the protein depletion was above 99% and the DNA depletion was 84% (data for pH 9 shown in Table 1, other data not shown). The additional nuclease digestion, followed by SXC at pH 9, did not affect the protein depletion, which was above 99% resulting in a protein concentration of 4 µg/mL (Fig. 4A, Table 1), but resulted in an increased DNA depletion of 94%, and DNA concentrations of 9 ng/mL at viral RNA titres of 9.3E+07 IU/mL after SXC (Fig. 4B, Table 1).

HCV polishing by SCMA chromatography. The SXC elutions, resulting from the SXC experiments done at pH 9 without and with preceding nuclease treatment (Fig. 3), were further processed using SCMA.

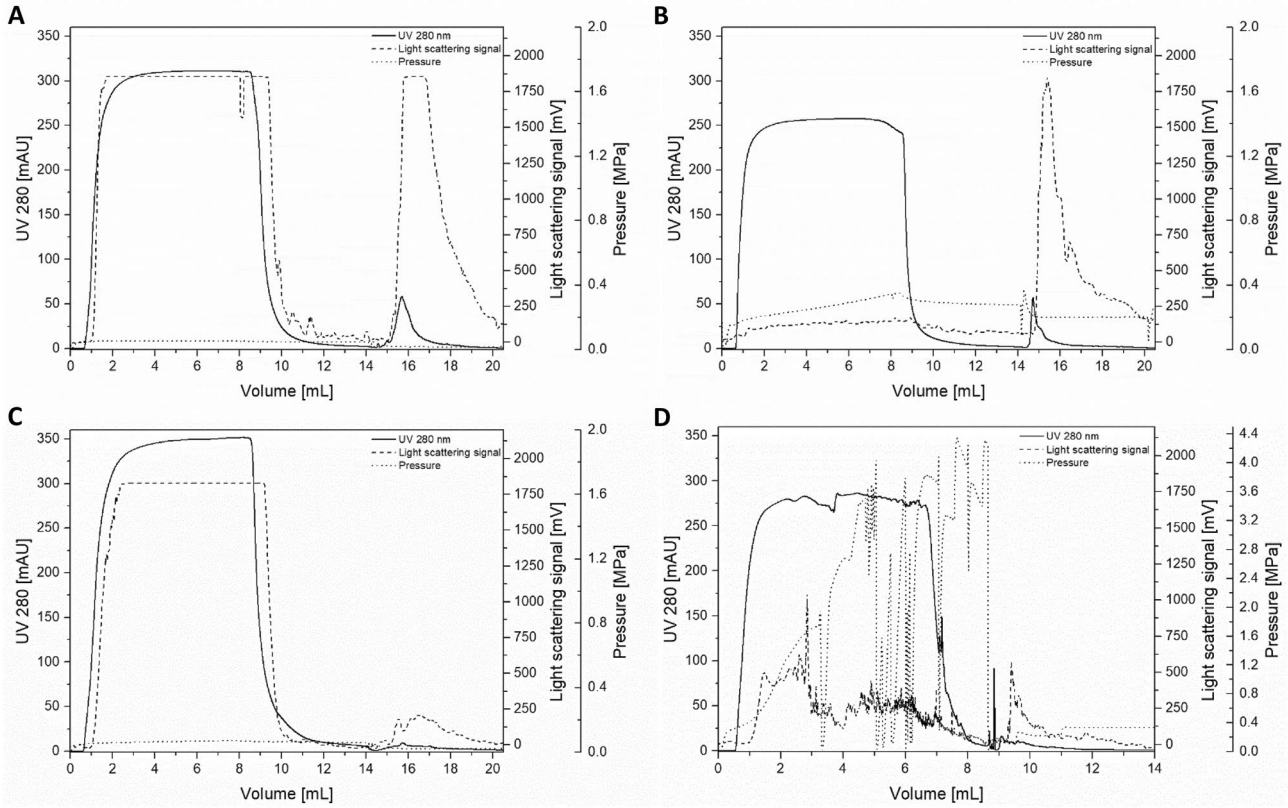

Figure 2. Influence of pH on SXC chromatography. For binding and washing of genotype 1a HCV 20 mM Tris with 180 mM NaCl and 8% PEG 6,000 were used at (**A**) pH 8, (**B**) pH 9 and (**C**) pH 10; loading: 0–9 mL, washing: 9–15 mL, elution (without PEG using 180 mM NaCl): 15–21 mL. (**D**) at pH 11 the flow rate was reduced at about 4 mL as the pressure already increased above 2.5 MPa. Here washing was already initiated after 6 mL.

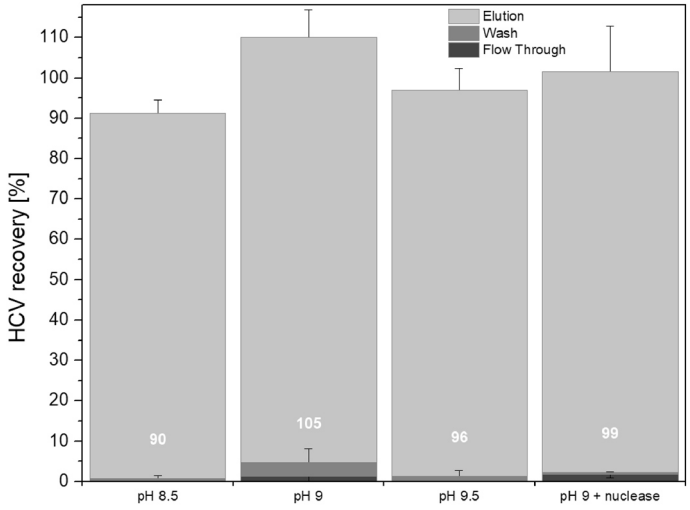

Figure 3. SXC HCV recoveries for different process conditions. Recovery was calculated by relating amounts of genotype 1a HCV RNA in flow through, wash and elution fractions to the total RNA amount in the feed prior to SXC. Variations included changes in the process pH and additional nuclease digestion prior to SXC. Values are means of technical triplicates with error bars reflecting SD.

HCV genotype	Virus in product [IU/mL]	Virus recovery [%]	Protein in product [µg/mL]	Protein depletion [%]	DNA in product [ng/mL]	DNA depletion [%]	DNA per 1.0E+08 IU/mL [ng]
SXC capture							
1a (without nuclease)	2.7E+08	105 ± 7	5 ± 2	> 99	107 ± 42	84 ± 3	~ 39
1a	9.3E+07	99 ± 11	4 ± 1	> 99	9 ± 1	94 ± 2	~ 10
5a	8.1E+07	97 ± 3	15 ± 6	97 ± 2	12 ± 2	86 ± 1	~ 15
SCMA polishing							
1a (without nuclease)	1.7E+08	63 ± 16	< 0.5	> 99	57 ± 17	90 ± 6	~ 33
1a	3.5E+07	50 ± 16	0.9 ± 0.5	> 99	2 ± 0.5	99 ± 0.5	~ 5
5a	3.2E+07	49 ± 5	1.5 ± 0.4	> 99	3 ± 1	98 ± 1	~ 9

Table 1. Overview on viral recovery and impurity depletion for the two chromatography-based process steps and cell culture-derived genotype 1a and 5a HCV. Shown are the values for SXC capture at pH 9 and the SCMA polishing using a TRIS buffer at pH 7.4. Recoveries are step recoveries comparing feed and product fractions of the respective step, and depletions are overall values, related to the initial feed concentrations before nuclease treatment and SXC. For a better overview, normalized DNA contents are given for each step, calculated for virus titres of 1.0E+08. While stated values for protein and DNA concentrations are rounded, values for % protein and DNA depletion as well as DNA per 1.0E+08 IU/ml were calculated using non-rounded values. n = 3 for all steps.

Following SXC without a preceding nuclease treatment, the HCV recovery was 63% in the 0.6 M NaCl elution fraction, when the SXC elution was directly processed without an additional freeze–thaw cycle (Fig. 5). A storage at − 80 °C in between the SXC and SCMA led to a reduction of retained and eluted viruses to 15%, with the majority of viruses found in the flow-through and wash fractions. When testing the implementation of a nuclease treatment prior to SXC, a virus recovery of 50% in the 0.6 M NaCl elution fraction was observed. In this experiment, minor amounts of virus eluted at higher salt concentrations of 1.2 and 2 M NaCl (Fig. 5), whereas 42% of the loaded virus was found in the flow-through and wash fractions.

Due to a breakthrough of about 40–50% of the virus, $DBC_{10\%}$ and $DBC_{100\%}$ could not be reached. However, the sample application was not limited by binding capacity but by pressure, as the pressure after an application of ~ 5.9E+09 IU/cm^2 exceeded the limits.

Considering the removal of impurities, no proteins could be detected in the SCMA flow-through and wash fractions, whereas less than 1 µg/mL was found in the SCMA elution fraction obtained following SXC at pH 9 without or with preceding nuclease treatment, indicating a virtually complete protein depletion (Fig. 4A for nuclease treatment + SXC (pH 9) + SCMA; Table 1 for both datasets). The overall DNA depletion was 90% following SXC (pH 9) and SCMA without a preceding nuclease treatment compared to the initial feed concentration before SXC (Table 1). The introduction of a nuclease digestion followed by SXC (pH 9) and SCMA resulted in an increased DNA depletion of above 99% compared to the initial feed concentration before nuclease treatment and SXC, leading to DNA concentrations of about 2 ng/mL at viral RNA titres of 3.5E+07 IU/mL (Fig. 4B, Table 1).

The developed DSP was equally efficient for different HCV genotypes. In order to investigate the applicability of the developed DSP for different HCV isolates, we applied this strategy to a high-titre cell culture-derived genotype 5a virus[37,38], which was selected due to its efficient growth characteristics in cell culture. Compared to the genotype 1a virus, the genotype 5a structural proteins differ by ~ 20%, while the envelope proteins differ by ~ 26% on the amino acid level.

The 5a virus was produced in cell factories; NGS showed that, in comparison to the published sequence, no additional substitutions were present in > 2% of the viral population. Clarification and ultrafiltration were carried out as for the 1a virus, with a volume reduction from 20.4 L to 420 mL and 63 mL in the first and second ultrafiltration, respectively. During clarification and the first ultrafiltration, we observed a virtually complete virus recovery, whereas a recovery of 87% was observed for the second ultrafiltration step. The resulting 5a material was UV- irradiated and the inactivation was confirmed as described for the 1a material.

With a preceding nuclease digestion, the SXC virus recovery was 97% (Fig. 6A, Table 1). During the SXC, the $DBC_{10\%}$ was determined with 9.8E+07 IU/cm^2 and a sample application was pressure-limited at about 2.7E+08 IU/cm^2. SCMA was carried out directly after SXC and resulted in a virus recovery of 49% in the 0.6 M NaCl elution fraction, whereas 47% of the applied virus was lost in the flow-through (Fig. 6B, Table 1). As for the 1a virus, $DBC_{10\%}$ or $DBC_{100\%}$ could not be determined during SCMA. The whole process led to a virtually complete protein removal with a protein depletion of 97% after SXC and > 99% after SCMA, resulting in protein concentrations of ~ 15 µg/mL after SXC and < 2 µg/mL after SCMA (Fig. 6A,C, Table 1). The DNA depletion was 86% after SXC and 98% after SCMA compared to the initial feed concentration before nuclease treatment and SXC (Fig. 6A,B,D Table 1). In the SCMA eluate, the DNA concentration was 3 ng/mL at viral RNA titres of 3.2E+07 IU/mL (Fig. 6B,D, Table 1).

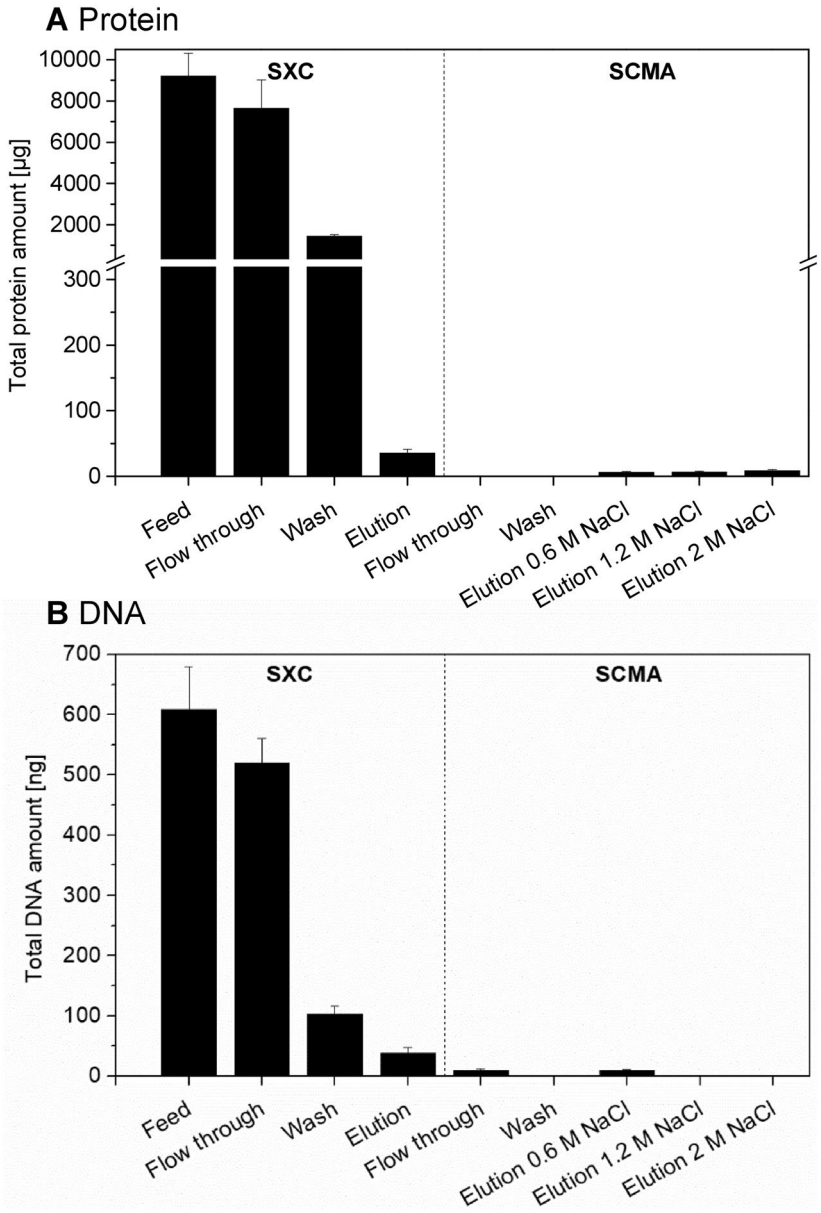

Figure 4. Impurity removal during SXC and SCMA with preceding nuclease treatment. Shown is the total amount of (**A**) protein and (**B**) DNA in individual fractions resulting from SXC (pH 9) of nuclease treated 1a HCV (material shown in Fig. 3) and consecutive SCMA. In the cases where no bars are visible, protein and DNA amounts were below the limit of detection of the assays (25 pg/mL for the DNA and 0.5 µg/mL for the protein assay).

Discussion

The DSP developed in this study consisted of clarification, ultrafiltration, nuclease treatment, and SXC and SCMA steps. While filtration-based clarification and concentration are commonly used initial process steps for the production of viral vaccines, a major rationale for using SXC for the virus capture was the predominant dependency on the size of the target species[28]. This promised an independence with regard to the specific HCV genotype and the robust depletion of smaller impurities. SCMA was selected for virus polishing, based on the heparin affinity of HCV[31,34]. Additionally, both methods allowed to fully exploit the advantages of membrane adsorbers, such as a higher capacity and convective flow properties, compared to packed-bed resins[20]. Another benefit of the chosen methodology is the possibility to directly load the SXC eluent to the SCMA—if necessary, by an inline dilution. Importantly, the described DSP showed a similar performance for two major HCV genotypes (1a and 5a), potentially facilitating the development of vaccines targeting different HCV genotypes.

Filter-based HCV clarification resulted in virtually complete virus recovery. For ultrafiltration, we observed that recovery varied between 50 and 100% with mean recovery of approximately 70% (numbers are based on described and additional unpublished experiments). According to these data, recovery was neither depending on the genotype of the processed virus nor on the size of the hollow fibre. This variation is likely due to suboptimal

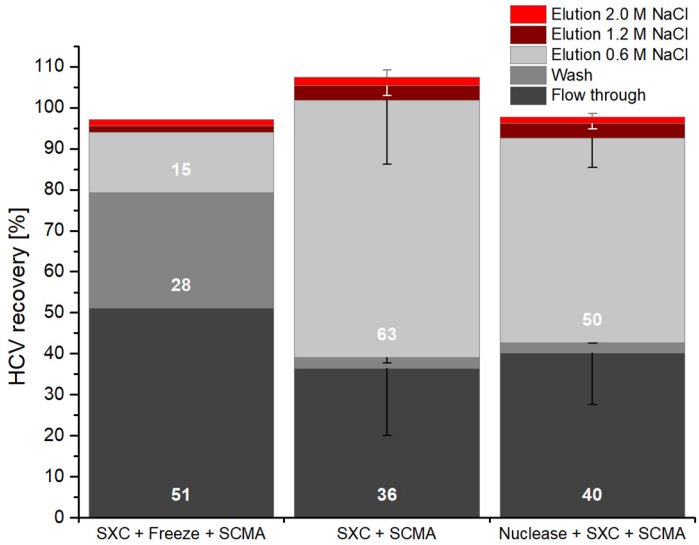

Figure 5. SCMA HCV recoveries for different process conditions. Recovery was calculated by relating amounts of genotype 1a HCV RNA in flow through, wash and elutions at 0.6, 1.2, and 2.0 M NaCl to the total RNA amount prior to SCMA. All preceding SXC runs were performed at pH 9 (eluate fractions of Fig. 3), without nuclease treatment prior to SXC (left and middle bar), including intermediate freezing (left bar) and with nuclease treatment preceding SXC (right bar). Bar captions state the order, in which steps were performed. Error values are means of technical triplicates with error bars reflecting SD.

process control. In the laboratory facilities where infectious virus was handled no ultrafiltration system was available, and thus optimal control of pressure and flow rate was not possible. As ultrafiltration resulted in virtually complete HCV recovery in several experiments and as high recoveries for other viruses have been described using this methodology[39,40], we anticipate that consistently high HCV ultrafiltration recoveries could be achieved given the possibility for optimal process control.

For SXC, the initial application of published process conditions[26] did not result in a successful virus retention. It was previously described, that the SXC performance is optimal at pH conditions near the pI[28]. For HCV, no characterization of the pI of the complete virus has been published so far. However, Prasetyo et al. reported a pI of 9.3 for HCV virus-like particles comprised of HCV Core (protein specific pI: 11.5) and envelope proteins (protein specific pI 8.1)[36]. Further, for genotype 1a, Viprbrc.org provided a theoretical pI of ~ 12, 7.4 and 7.8 for the structural proteins Core, E1 and E2, respectively, based on computation from GenBank sequences. Testing alkaline pH conditions, we defined a small operating window for an optimal SXC performance at pH 9 ± 0.5. It has not yet been described how pH alterations affect SXC of other virus particles, such as the Influenza A virus[26] and the Baculovirus[27], which have neutral to acidic pI and a > 90% recovery in SXC at pH 7.4. For HCV, the intense pressure increase observed during SXC at pH 11 suggested severe membrane fouling, resulting in a nearly complete virus retention, which hampers elution. This might be caused by the precipitation of proteins, medium components, or virus particles under these conditions. It is not surprising that an impurity removal during the SXC was independent of the applied pH, as the chosen PEG concentrations were too low to sterically exclude the DNA and protein molecules[27]. At these conditions, a protein retention does not occur, and the observed DNA retention may be due to DNA attachment to the virus or to DNA co-purified inside extracellular vesicles as previously described by Marichal-Gallardo *et al*[26]. The membrane capacity during SXC was slightly higher than previously reported for the Baculovirus[27], which could be explained by the smaller size of HCV. The pressure increase during DBC determination may be due to the possible aggregation potential of the virus, leading to increased membrane fouling for higher loading volumes. It is not likely that an increased pore blockage is caused by protein impurities, as these are mostly washed out during sample application, with mainly virus particles remaining on the column. On a process scale, the pressure limitations might be additionally reduced as well as the binding capacity increased by using a different type of membrane housing, offering an altered angle of the incident flow.

Our data highlights the importance of avoiding a freeze–thaw cycle in an SXC elution buffer preceding SCMA, which resulted in a large decrease in recovery, possibly due to a degradation of HCV particles, or changes in the surface protein composition or structure. The decreased virus stability during freeze-thawing might be caused by removal of the proteins during SXC, which might stabilize the virus and prevent degradation. Although, in general, storage times using freeze–thaw cycles are unusual during a production process, this information may support similar trials in other laboratories. With regard to virus recovery, no significant differences (according to a students' T-test, data not shown) were observed for samples that had been subjected to a nuclease treatment + SXC prior to SCMA (50% for 1a and 49% for 5a HCV) compared to samples that had been processed by SXC only prior to SCMA (63% for 1a HCV), with respect to the analytical error. Thus, SCMA appeared to be unaffected by a preceding nuclease treatment and independent of the virus genotype. However, SCMA recoveries were below the values previously described for the Influenza A virus[31]. Fortuna et al. reported 75–81% recovery

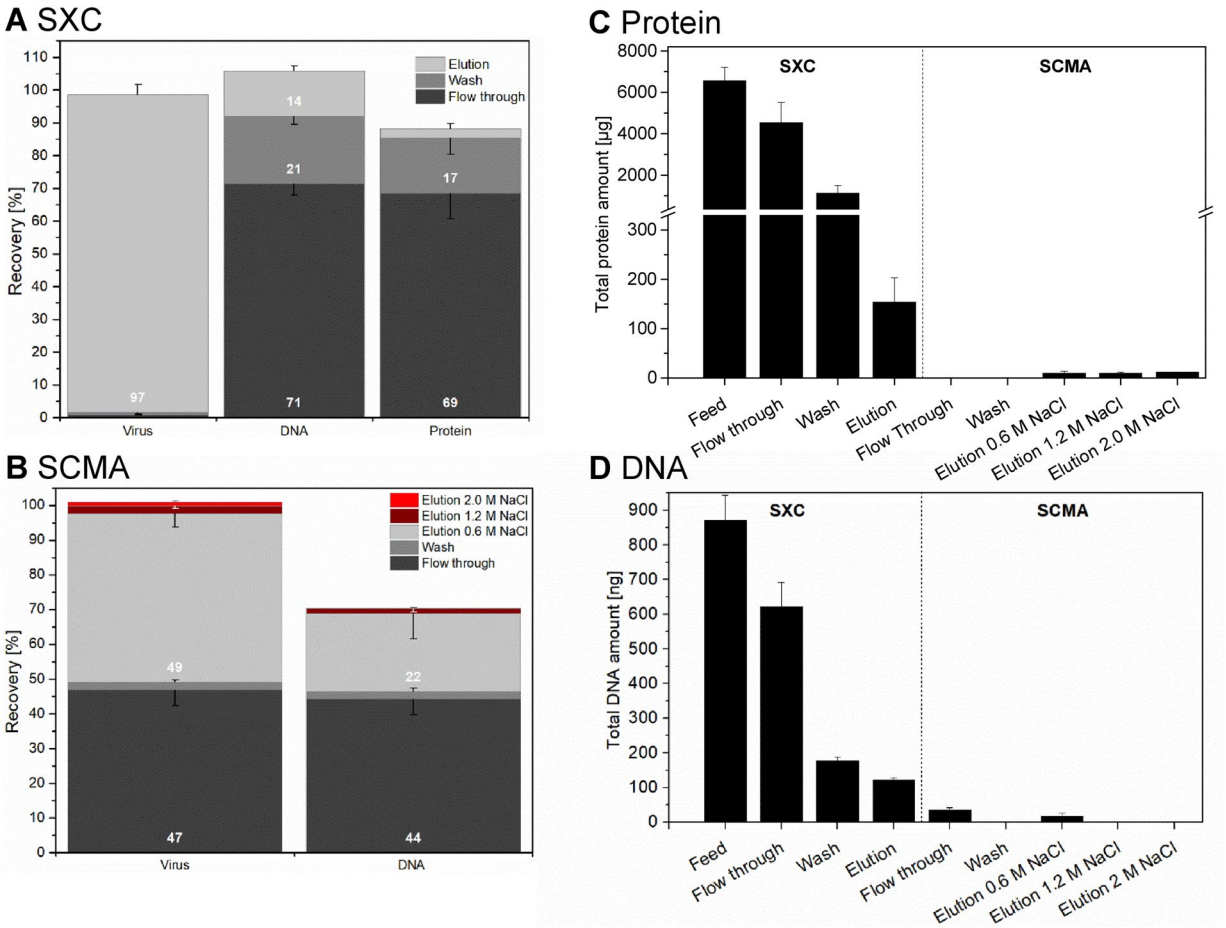

Figure 6. Process performance for a different HCV genotype. Shown is (**A**) the recovery of virus, DNA and protein during SXC and (**B**) the recovery of virus and DNA in the different SCMA fractions. Furthermore, (**C**) the total protein amounts and (**D**) the total DNA amounts throughout the process are depicted. All recovery values are step-recoveries, correlated to the quantities in the loading sample of the respective step. For the SCMA, no protein and DNA recoveries and amounts are depicted in case the concentration was below the limit of detection of the assay (0.5 µg/mL and 25 pg/mL for protein and DNA, respectively). Error bars indicate technical triplicates with error bars reflecting SD.

for the Influenza A virus, using the same type of membranes. Furthermore, a low conductivity and a high virus titre of the virus feed were reported to be required for an optimal SCMA performance[32]. While we maintained the conductivity during sample application below 5 mS/cm, the virus was diluted 10 times after SXC in order to obtain these conditions. Thus, the SCMA recovery may be further increased by interposing a concentration and diafiltration step, reducing both the sample volume and the conductivity, which might also allow a reduction of the processing time. Furthermore, an optimization of the membrane ligand density as previously done for Influenza A virus-like particles could improve the virus retention and reduce losses during loading[33].

We observed a highly efficient protein depletion. Within the analytical error, a virtually full protein depletion could be achieved by SXC, with a protein removal of > 99% for 1a HCV and 97% for 5a HCV. Using the Micro BCA assay, following SXC protein concentrations of 4 µg/mL (1a HCV) and 15 µg/mL (5a HCV) were determined with a further reduction to 0.9 µg/mL (1a HCV) and 1.5 µg/mL (5a HCV) following SCMA. These results were verified using silver staining of SDS-PAGE gels, also suggesting efficient protein depletion in SXC and removal of residual protein in SCMA (data not shown). The fact that protein could not be detected in the SCMA flow-through and wash fractions might be due to the sample dilution preceding the SCMA. Since the SCMA elution resulted in a sample concentration, the low concentration of proteins in the final HCV product (< 2 µg/mL) suggested a successful depletion of the remaining proteins during SCMA.

A comparable DNA depletion of at least 98% was achieved for both viruses of both HCV genotypes following a nuclease treatment, SXC, and SCMA. Of this overall DNA depletion, 5–12% were achieved by SCMA, whereas the nuclease treatment allowed an additional removal of about 10% of the total DNA. At present, it is not known, which amount of HCV particles a vaccine should contain to induce an efficient immune response. If required, an additional DNA reduction may be achieved by optimizing the nuclease treatment regarding the enzyme concentration and the incubation time. Most likely, the remaining DNA represents fragments attached to the virus as described above, or DNA being co-eluted with the virus particles using 0.6 M NaCl as SCMA elution buffer. For the latter, a further optimization of the SCMA procedure, including the evaluation of the virus elution using

buffers with lower conductivity, is conceivable. Additionally, it should be mentioned, that the entire amount of DNA in the SCMA feed could not be recovered in the subsequent fractions. This might be caused by the DNA remaining on the column, and by an inhomogeneous error distribution between the varying salt concentrations.

We provide proof-of-concept for a novel DSP for purification of cell culture-derived HCV facilitating development of a whole virus vaccine. In future studies it will be important to demonstrate scalability of this DSP. Purification of larger amounts of HCV will facilitate more detailed studies of the potential vaccine antigen including analysis of virus structure by electron microscopy and quantification of HCV structural proteins.

Further, chromatographic experiments were carried out using inactivated HCV, as preferable for an industrial vaccine production. In future studies it would be of interest to process non-inactivated HCV to confirm that SXC and SCMA do not have a negative impact on HCV infectivity, implying a preservation of structural integrity. Importantly, it has previously been reported for other virus particles, that neither of the methods affected virus infectivity[26,27,31].

We showed process robustness for two different HCV genotypes with significant sequence difference in the structural proteins Core, E1 and E2, which are incorporated in the viral particle. As all cell culture viable HCV recombinants, genotype 1a and 5a viruses used in this study contained cell culture adaptive substitutions. While for genotype 5a an early passage virus was used recapitulating the sequence of the most cell culture adapted clone available[41], for genotype 1a a passage 20 virus was used showing a higher degree of genetic heterogeneity and differing at several amino acid positions compared to the less cell culture adapted original clone[35]. However, for the genotype 1a passage 20 virus most sequence heterogeneity was found in the nonstructural proteins, which are thought not to be incorporated in the HCV particle. The influence of cell culture adaptive substitutions in the structural proteins on immunogenicity remains to be determined in future studies.

Finally, in future studies it would be of interest to evaluate applicability of the developed DSP to the purification of HCV virus-like particles consisting of HCV structural proteins. During clarification different filter pore sizes and for SXC, an adjustment of the PEG concentration might be required in case of varying product sizes. The use of SCMA will require that virus-like particles maintain pseudo-affinity to sulfated cellulose.

For HCV vaccine development an inactivated whole virus approach is attractive, given the intricate conformation of the envelope proteins, which is difficult to mimic in subunit envelope vaccines. Further, given the higher immunogenicity of whole viruses compared to viral envelope proteins[17], and the historic success of whole virus vaccines[16], whole viruses are attractive vaccine antigens. This approach has only become feasible due to the relatively recent development of cell culture systems for the production of HCV[42]. However, further studies are needed to elucidate which HCV genotypes, possibly with certain envelope modifications for exposure of conserved epitopes, have the highest immunogenicity.

Materials and methods

Huh7.5 cell culture. Huh7.5 cells (obtained from Apath, LLC; New York, USA) were maintained in DMEM (Gibco) with 10% fetal bovine serum (Sigma) and penicillin (100 U/mL) / streptomycin (100 µg/mL) (Sigma) and were incubated at 37 °C and 5% CO_2. Adenovirus Expression Medium (AEM) (Gibco), supplemented with penicillin (100 U/mL) and streptomycin (100 µg/mL), was used for HCV production under serum-free conditions[38].

The percentage of HCV infected cells was evaluated by immunostainings[38,43]. In brief, cells were seeded in a chamber slide (Thermo Fisher Scientific) for a confluent cell layer, fixed with acetone (Merck) the next day, and stained with primary antibody 9E10 diluted 1:3,000[44], followed by secondary antibody Alexa Flour 488 goat anti-mouse IgG diluted 1:500 (Invitrogen), and Hoechst 33342 (Molecular Probes) diluted 1:1,000.

HCV-infectivity titres were determined with three technical replicates as FFU/mL in a cell-based assay in 96-well plates as described[45,46]. The immunostaining of 96-well plates was carried out with primary antibody 9E10 diluted 1:5,000, secondary antibody ECL Anti-mouse IgG Horseradish Peroxidase linked from sheep (Amersham Biosciences) diluted 1:500, and visualized with Pierce DAB Substrate Kit (Thermo Scientific). 96-well plates were imaged and automatically counted for FFU quantification.

Serial passage for generation of high-titre genotype 1a HCV. For the production of genotype 1a HCV, the cell culture infectious recombinant TNcc[35] was further adapted to cell culture by serial passage in Huh7.5 cells. Following a transfection of HCV RNA transcripts, 18 viral passages to naïve cells were carried out in T80 cell culture flasks (Nunc). Naïve cells were inoculated with cell culture supernatant derived from the previous culture at the peak of infection according to immunostainings as described[41]. A passage 19 virus seed stock was prepared in T500 triple layer flasks (Nunc TripleFlask Treated Cell Culture Flask); supernatants from two time points at the peak of infection were pooled.

Production of genotype 1a and 5a HCV for DSP development. For genotype 1a HCV, T175 flasks, seeded with 6×10^6 cells in DMEM on the previous day, were inoculated at a multiplicity of infection of 0.003 with the passage 19 virus seed stock. Cultures were expanded to T500 triple layer flasks. When 80% of cells were estimated to be infected by immunostaining in a replicate T25 culture, the cultures were washed with PBS (Sigma) and subsequently maintained in AEM under serum-free conditions. The supernatant was harvested five times every 2–3 days, yielding 10.5 L, which was stored at − 80 °C until further processing.

For genotype 5a HCV, 18×10^6 cells, seeded the previous day in DMEM, were infected at a multiplicity of infection of 0.003 in T500 triple layer cell culture flasks with a 3rd passage seed stock of the further adapted SA13/JFH1 recombinant[37,41]. The following day, cells were transferred to cell factories (Nunc Cell Factory). When 80% of cells were expected to be infected as indicated by immunostaining in a replicate T25 culture, the cells

were washed with PBS and cultured in AEM. The harvesting of the supernatant was carried out five times every 2–3 days, yielding 20.4 L total, stored as described above.

Sequence analysis. NGS of the virus populations was carried out as described[47,48]. Briefly, RNA was extracted with Trizol LS and the RNA Clean & Concentrator-5 (Zymo research) kit. The reverse transcription was carried out with Maxima H Minus Reverse Transcriptase (ThermoScientific), the whole open reading frame was amplified with polymerase chain reaction (PCR) Q5 Hot start High-Fidelity DNA Polymerase (New England Biolabs), and the PCR product was purified (DNA Clean & Concentrator-25 and Zymoclean Large Fragment DNA Recovery Kit, Zymo research). The NEBNext ultra II FS DNA Library Prep Kit (New England Biolabs) was used for library preparation, and sequencing was performed with an Illumina Miseq platform.

The alignment of amino acid sequences of structural proteins (Core, envelope proteins E1 and E2) of 1a and 5a HCV was done in BLAST (database version 5; https://blast.ncbi.nlm.nih.gov/Blast.cgi)[49,50].

Evaluation of infectious HCV stability at alkaline pH values. The HCV genotype 5a seed stock described above, was concentrated using Ultra-15 Centrifugal Filter Unit-100 K (Amicon) and diluted by a factor 17 in PBS (for pH 7.4 reference), DMEM (standard cell culture medium, pH 8.5) or phosphate buffer (KH_2PO_4 (Sigma) and K_2HPO_4 (Sigma), adjusted with NaOH for pH values of 9.5, 10 and 11) in triplicate Eppendorf tubes, and incubated for 90 min at room temperature. After incubation, the virus/buffer solutions were diluted 1:40 in DMEM containing 20 mM HEPES (HEPES solution 1 M, Sigma), and added to triplicate wells seeded with 7×10^3 cells/well in 96-well poly-D lysine plates (Thermo Scientific) the previous day. The infected cell plates were incubated for six hours at 37 °C and 5% CO_2 before the medium was exchanged to DMEM without HEPES. The cell plates were fixed, stained, and evaluated as described above, in order to quantify HCV infected single cells. The cell viability was evaluated after the experimental read-out had been obtained in a replicate experiment with the CellTiter 96 AQueous One Solution Cell Proliferation Assay (Promega) according to the manufacturer's protocol. The pH effect on virus stability was evaluated as the number of HCV-positive cells in a well, relative to the average number of HCV-positive cells obtained from the virus incubated at a pH value of 7.4.

Virus clarification, ultrafiltration and inactivation. The genotype 1a and 5a virus material was passed over 5 µm and 0.65 µm Sartopure PP3 (Sartorius) capsule filters for a two-step clarification by peristaltic pumping (Masterflex L/S 7554–95 Cole-Parmer, Masterflex L/S Easy Load pump head, and Extended Lifetime Silicone Tubing size 17 (Repligen)). Subsequently, the clarified 1a and 5a viruses were concentrated 249 and 325 times, respectively, in two sequential ultrafiltration steps with hollow fibre filters (MINIKROS SAMPLER 65CM 500 K MPES 0.5MM 3/4TC X 3/4TC STERILE followed by MINIKROS SAMPLER 20CM 500 K MPES 0.5MM 3/4TC X 3/4TC STERILE, both Repligen). The HCV infectivity titres and RNA titres were determined for samples from each step of clarification and concentration. The virus recovery was calculated from the HCV RNA titres.

The virus was inactivated by UV exposure (UVP Handheld UV lamp, UVG-54 254 nm in lamp stand) in 6-well plates (Nunc) with 1.5–2.5 mL per well for eight hours. The 6-well plate was kept on ice with frequent agitation. To confirm inactivation, naïve Huh7.5 cells were seeded in triplicate T25 flasks (1×10^6 cells/flask) the previous day, and inoculated with 20 µL of UV-treated material. Inoculated cultures were passaged for 21 days and monitored for HCV positive cells by immunostaining as described above. In replicate samples, it was confirmed that a similar incubation without UV irradiation did not inactivate HCV.

Nuclease treatment. The nuclease treatment was performed in triplicates for both genotypes. The clarified virus was subjected to 250 U/mL Benzonase nuclease (Merck) at a final concentration of 2 mM $MgCl_2$. The incubation was done overnight at 4 °C, and the nuclease activity was blocked afterwards, using a final concentration of 5 mM EDTA. Subsequently, the chromatography was performed, using nuclease–digested, clarified HCV.

Chromatographic purification. The chromatographic experiments were done with an Äkta Pure 25 system, operated by Unicorn (version 7.1, GE Healthcare Life Sciences). Online monitoring was done by system-integrated UV (280 nm) and conductivity detectors, and additionally light-scattering was detected with a Nano DLS Particle Size Analyzer (Brookhaven Instruments). All chromatographic experiments were done in technical triplicates, unless stated otherwise.

Virus capture using SXC. SXC was performed using regenerated cellulose membranes with 1 µm pore size (Whatman), as previously reported[26,27]. In brief, for preparing the column, 10 membranes were punched and stacked into a 13 mm filter holder (Pall), yielding a total membrane area of 13.3 cm^2. All steps were performed at a flow rate of 2 mL/min. The stack was equilibrated using 5–10 mL of 20 mM Tris at the specified pH value, supplemented with 180 mM NaCl, and 8% PEG 6,000. Clarified, concentrated, and inactivated HCV was mixed 1:4 with the above stated buffer and supplemented with 32% PEG to yield final concentrations of 8% PEG to match the equilibration conditions. After sample application, the stack was washed with equilibration buffer until the detector signals decreased to baseline (> 5 mL). Elution was achieved using 20 mM Tris at pH 7.4 without PEG, but supplemented with 0.4 M NaCl. Initial screening SXC runs were tested at pH 7.4 to pH 11 for genotype 1a HCV, while final process conditions were at pH 9, and tested for robustness at pH 8.5 and 9.5. Following optimization, the SXC performance was verified for the genotype 5a HCV at pH 9 with a preceding nuclease treatment.

Virus polishing using SCMA. Sartobind Sulphated Cellulose membranes with a nominal pore size of 0.8 µm (Sartorius Stedim Biotech GmbH) were punched to disks of 13 mm diameter. As for SXC, the disks were

stacked to layers of 10 membranes (13.3 cm^2 total membrane area). All steps were performed at a flow rate of 0.8 mL/min. Membranes were equilibrated using 20 mM Tris pH 7.4 prior to sample application. For the purification, SXC elution fractions were diluted 1:10 with equilibration buffer in order to reduce the conductivity of the solution below 5 mS/cm. After complete sample loading, the membranes were washed with equilibration buffer until UV- and light scattering signals returned to baseline. Bound components were subsequently eluted in 3 fractions, using increasing NaCl concentrations (0.6, 1.2 and 2 M). The SCMA was evaluated for genotype 1a HCV, using SXC elutions with and without an interim storage at − 80 °C, as well as with and without additional nuclease treatment before SXC. Finally, the SCMA performance was confirmed, using a nuclease-treated and SXC-purified genotype 5a HCV.

Determination of dynamic binding capacities. For SXC and SCMA, the DBC was determined in order to optimize the virus load on the membrane stacks. Stationary and mobile phase compositions were the same as described above. A clarified, concentrated, and inactivated virus feed of a known concentration was prepared and applied to the column, until detected breakthrough of 10% and 100% of the particles, based on the evaluation of the light-scattering detector signal. Depending on the loaded volume, the total amount of virus particles, at which breakthrough rates of 10% or 100% (DBC_{10} and DBC_{100}) occurred, was calculated and related to the area of the membrane. All process runs were performed at or below DBC_{10}.

HCV quantification. The virus amount was evaluated using an in-house qPCR as described previously, with minor modifications[43]. Briefly, viral RNA was extracted from 200 µL sample and eluted in 50 µL water, using the High Pure Viral Nucleic Acid Kit (Roche) according to the manufacturer´s instructions. Afterwards, a mixture comprising TaqMan Fast Virus 1-step Mastermix (Thermo Fisher Scientific), nuclease-free water, probe (containing a FAM dye and an MGB quencher) and primers (Sigma-Aldrich) was prepared. 12 µL of that mixture were added to 8 µL of the extracted RNA in a 96-well PCR plate (twin.tec, Eppendorf) preparing duplicates for each sample. The amplification was done using a Mastercycler Ep gradient S realplex (Eppendorf) after a pre-incubation period at 50 °C for 300 s. A total of 53 cycles of 95 °C for 20 s, followed by 62 °C for 60 s, were performed. An HCV standard panel, containing 10^2 to 10^6 IU/mL in 1-log increments, was prepared and included in each run, in addition to negative control samples. HCV RNA titres (IU/mL) were calculated using a standard curve generated from values obtained for the standard panel and corresponding cycle threshold values. The standard deviation of triplicate measurements was below 20%.

Protein determination. For a quantification of the total protein amount contained in the chromatographic samples, the Pierce BCA Protein Assay Kit (Thermo Fisher Scientific) was applied according to the manufacturer's instructions. In brief, 25 µL of sample were transferred into a clear 96-well plate; duplicates were prepared for each sample. The standard panel (in the range of 25 to 2,000 µg/mL) was prepared from gamma globulin according to the manufacturer's instructions. To each well, 200 µL of the reaction mix were added, and absorbance at 562 nm was measured after 30 min of incubation at 37 °C using the Cytation 3 plate reader (BioTek). Additionally, product fractions of the two purification steps (SXC and SCMA elutions) were analysed using the Pierce Micro BCA Protein Assay Kit, offering a lower calibration range between 0.5 and 200 µg/mL. Sample preparation was done as instructed by the manufacturer in a 96-well format and measurements were obtained using the same equipment and absorbance as described above. For both approaches, the values obtained from a blank sample (buffer) were subtracted before interpolating the sample concentrations. Results given are from duplicate measurements with less than 10% standard deviation.

DNA determination. The total amount of double stranded DNA (referred to as "DNA" in this work) was determined, using the Quant-iT PicoGreen dsDNA Kit according to the manufacturers´ instructions. The assay was performed in a 96-well format, using black microtiter plates (Nunc). Chromatographic samples, including the feed, were mixed 1:4 (SXC samples) or 1:2 (SCMA samples) with the assay's 1 × TE buffer to a final volume of 100 µL. For each plate, blank samples (buffer) and two standard panels were prepared from kit-contained lambda-DNA in the range of 1 to 1,000 ng/mL and 0.025–25 ng/mL, using a tenfold dilution series. After adding 100 µL of the reaction dye, the plate was incubated for 5 min in the dark, and a fluorescence emission at 520 nm (excitation: 485 nm) was subsequently determined, using the Cytation 3 plate reader (BioTek). All measurements were done in duplicates with a general standard deviation of less than 10%.

Received: 26 May 2020; Accepted: 26 August 2020
Published online: 01 October 2020

References

1. Merz, A. *et al.* Biochemical and morphological properties of hepatitis C virus particles and determination of their lipidome. *J. Biol. Chem.* **286**, 3018–3032. https://doi.org/10.1074/jbc.M110.175018 (2011).
2. Yuasa, T. *et al.* The particle size of hepatitis C virus estimated by filtration through microporous regenerated cellulose fibre. *J. Gen. Virol.* **72**(Pt 8), 2021–2024. https://doi.org/10.1099/0022-1317-72-8-2021 (1991).
3. Simmonds, P. *et al.* ICTV virus taxonomy profile: flaviviridae. *J. Gen. Virol.* **98**, 2–3. https://doi.org/10.1099/jgv.0.000672 (2017).
4. Dubuisson, J. & Cosset, F.-L. Virology and cell biology of the hepatitis C virus life cycle: an update. *J. Hepatol.* **61**, S3–S13. https://doi.org/10.1016/j.jhep.2014.06.031 (2014).
5. Bukh, J. The history of hepatitis C virus (HCV): Basic research reveals unique features in phylogeny, evolution and the viral life cycle with new perspectives for epidemic control. *J. Hepatol.* **65**, S2–S21. https://doi.org/10.1016/j.jhep.2016.07.035 (2016).

6. Borgia, S. M. *et al.* Identification of a novel hepatitis C virus genotype from Punjab, India: expanding classification of hepatitis C virus into 8 genotypes. *J. Infect. Dis.* **218**, 1722–1729. https://doi.org/10.1093/infdis/jiy401 (2018).
7. WHO. *Global Hepatitis Report* (World Health Organization, Geneva, 2017).
8. Manns, M. P. *et al.* Hepatitis C virus infection. *Nat. Rev. Dis. Primers* **3**, 17006. https://doi.org/10.1038/nrdp.2017.6 (2017).
9. Blach, S. *et al.* Global prevalence and genotype distribution of hepatitis C virus infection in 2015: a modelling study. *Lancet Gastroenterol. Hepatol.* **2**, 161–176. https://doi.org/10.1016/S2468-1253(16)30181-9 (2017).
10. Pawlotsky, J.-M. Hepatitis C virus resistance to direct-acting antiviral drugs in interferon-free regimens. *Gastroenterology* **151**, 70–86. https://doi.org/10.1053/j.gastro.2016.04.003 (2016).
11. Sarrazin, C. The importance of resistance to direct antiviral drugs in HCV infection in clinical practice. *J. Hepatol.* **64**, 486–504. https://doi.org/10.1016/j.jhep.2015.09.011 (2016).
12. Bartenschlager, R. *et al.* Critical challenges and emerging opportunities in hepatitis C virus research in an era of potent antiviral therapy: considerations for scientists and funding agencies. *Virus Res.* **248**, 53–62. https://doi.org/10.1016/j.virusres.2018.02.016 (2018).
13. Bailey, J. R., Barnes, E. & Cox, A. L. Approaches, progress, and challenges to hepatitis C vaccine development. *Gastroenterology* **156**, 418–430. https://doi.org/10.1053/j.gastro.2018.08.060 (2019).
14. Maticic, M., Lombardi, A., Mondelli, M. U. & Colombo, M. Elimination of hepatitis C in Europe: can WHO targets be achieved?. *Clin. Microbiol. Infect.* **26**, 818–823. https://doi.org/10.1016/j.cmi.2020.01.014 (2020).
15. Fauvelle, C. *et al.* Hepatitis C virus vaccine candidates inducing protective neutralizing antibodies. *Expert Rev. Vaccines* **15**, 1535–1544. https://doi.org/10.1080/14760584.2016.1194759 (2016).
16. Plotkin, S. A. & Plotkin, S. L. The development of vaccines: how the past led to the future. *Nat. Rev. Microbiol.* **9**, 889–893. https://doi.org/10.1038/nrmicro2668 (2011).
17. Akazawa, D. *et al.* Neutralizing antibodies induced by cell culture-derived hepatitis C virus protect against infection in mice. *Gastroenterology* **145**, 447-55.e1–4. https://doi.org/10.1053/j.gastro.2013.05.007 (2013).
18. Gottwein, J. M. & Bukh, J. Viral hepatitis: cell-culture-derived HCV–a promising vaccine antigen. *Nat. Rev. Gastroenterol. Hepatol.* **10**, 508–509. https://doi.org/10.1038/nrgastro.2013.136 (2013).
19. Yokokawa, H. *et al.* Induction of humoural and cellular immunity by immunisation with HCV particle vaccine in a non-human primate model. *Gut* **67**, 372–379. https://doi.org/10.1136/gutjnl-2016-312208 (2018).
20. Wolf, M. W. & Reichl, U. Downstream processing of cell culture-derived virus particles. *Expert Rev. Vaccines* **10**, 1451–1475. https://doi.org/10.1586/erv.11.111 (2011).
21. Nestola, P. *et al.* Improved virus purification processes for vaccines and gene therapy. *Biotechnol. Bioeng.* **112**, 843–857. https://doi.org/10.1002/bit.25545 (2015).
22. Effio, C. L. & Hubbuch, J. Next generation vaccines and vectors. Designing downstream processes for recombinant protein-based virus-like particles. *Biotechnol. J.* **10**, 715–727. https://doi.org/10.1002/biot.201400392 (2015).
23. Gagnon, P., Toh, P. & Lee, J. High productivity purification of immunoglobulin G monoclonal antibodies on starch-coated magnetic nanoparticles by steric exclusion of polyethylene glycol. *J. Chromatogr. A.* **1324**, 171–180. https://doi.org/10.1016/j.chroma.2013.11.039 (2014).
24. Tao, S.-P., Zheng, J. & Sun, Y. Grafting zwitterionic polymer onto cryogel surface enhances protein retention in steric exclusion chromatography on cryogel monolith. *J. Chromatogr. A.* **1389**, 104–111. https://doi.org/10.1016/j.chroma.2015.02.051 (2015).
25. Wang, C., Bai, S., Tao, S.-P. & Sun, Y. Evaluation of steric exclusion chromatography on cryogel column for the separation of serum proteins. *J. Chromatogr. A.* **1333**, 54–59. https://doi.org/10.1016/j.chroma.2014.01.059 (2014).
26. Marichal-Gallardo, P., Pieler, M. M., Wolff, M. W. & Reichl, U. Steric exclusion chromatography for purification of cell culture-derived influenza A virus using regenerated cellulose membranes and polyethylene glycol. *J. Chromatogr. A* **1483**, 110–119. https://doi.org/10.1016/j.chroma.2016.12.076 (2017).
27. Lothert, K. *et al.* Membrane-based steric exclusion chromatography for the purification of a recombinant baculovirus and its application for cell therapy. *J. Virol. Methods* **275**, 113756. https://doi.org/10.1016/j.jviromet.2019.113756 (2019).
28. Lee, J. *et al.* Principles and applications of steric exclusion chromatography. *J. Chromatogr. A.* **1270**, 162–170. https://doi.org/10.1016/j.chroma.2012.10.062 (2012).
29. Wolff, M. W., Siewert, C., Hansen, S. P., Faber, R. & Reichl, U. Purification of cell culture-derived modified vaccinia ankara virus by pseudo-affinity membrane adsorbers and hydrophobic interaction chromatography. *Biotechnol. Bioeng.* **107**, 312–320. https://doi.org/10.1002/bit.22797 (2010).
30. Opitz, L., Lehmann, S., Reichl, U. & Wolff, M. W. Sulfated membrane adsorbers for economic pseudo-affinity capture of influenza virus particles. *Biotechnol. Bioeng.* **103**, 1144–1154. https://doi.org/10.1002/bit.22345 (2009).
31. Fortuna, A. R. *et al.* Use of sulfated cellulose membrane adsorbers for chromatographic purification of cell cultured-derived influenza A and B viruses. *Sep. Purif. Technol.* **226**, 350–358. https://doi.org/10.1016/j.seppur.2019.05.101 (2019).
32. Fortuna, A. R., Taft, F., Villain, L., Wolff, M. W. & Reichl, U. Optimization of cell culture-derived influenza A virus particles purification using sulfated cellulose membrane adsorbers. *Eng. Life Sci.* **18**, 29–39. https://doi.org/10.1002/elsc.201700108 (2018).
33. Carvalho, S. B. *et al.* Purification of influenza virus-like particles using sulfated cellulose membrane adsorbers. *J. Chem. Technol. Biotechnol.* **93**, 1988–1996. https://doi.org/10.1002/jctb.5474 (2018).
34. Zahn, A. & Allain, J.-P. Hepatitis C virus and hepatitis B virus bind to heparin. Purification of largely IgG-free virions from infected plasma by heparin chromatography. *J. Gen. Virol.* **86**, 677–685. https://doi.org/10.1099/vir.0.80614-0 (2005).
35. Li, Y.-P. *et al.* Highly efficient full-length hepatitis C virus genotype 1 (strain TN) infectious culture system. *PNAS* **109**, 19757–19762. https://doi.org/10.1073/pnas.1218260109 (2012).
36. Prasetyo, A. A. VLPs of HCV local isolates for HCV immunoassay diagnostic approach in Indonesia. *AIP Conf. Proc.* **1788**, 30100. https://doi.org/10.1063/1.4968353 (2017).
37. Pihl, A. F. *et al.* High density Huh7.5 cell hollow fiber bioreactor culture for high-yield production of hepatitis C virus and studies of antivirals. *Sci. Rep.* **8**, 17505. https://doi.org/10.1038/s41598-018-35010-5 (2018).
38. Mathiesen, C. K. *et al.* Production and characterization of high-titer serum-free cell culture grown hepatitis C virus particles of genotype 1–6. *Virology* **458–459**, 190–208. https://doi.org/10.1016/j.virol.2014.03.021 (2014).
39. Cooper, A. R. *et al.* Highly efficient large-scale lentiviral vector concentration by tandem tangential flow filtration. *J. Virol. Methods* **177**, 1–9. https://doi.org/10.1016/j.jviromet.2011.06.019 (2011).
40. Wickramasinghe, S. R., Kalbfuß, B., Zimmermann, A., Thom, V. & Reichl, U. Tangential flow microfiltration and ultrafiltration for human influenza A virus concentration and purification. *Biotechnol. Bioeng.* **92**, 199–208. https://doi.org/10.1002/bit.20599 (2005).
41. Mathiesen, C. K. *et al.* Adaptive mutations enhance assembly and cell-to-cell transmission of a high-titer hepatitis C virus genotype 5a core-NS2 JFH1-based recombinant. *J. Virol.* **89**, 7758–7775. https://doi.org/10.1128/JVI.00039-15 (2015).
42. Ramirez, S. & Bukh, J. Current status and future development of infectious cell-culture models for the major genotypes of hepatitis C virus: essential tools in testing of antivirals and emerging vaccine strategies. *Antiviral Res.* **158**, 264–287. https://doi.org/10.1016/j.antiviral.2018.07.014 (2018).
43. Gottwein, J. M. *et al.* Robust hepatitis C genotype 3a cell culture releasing adapted intergenotypic 3a/2a (S52/JFH1) viruses. *Gastroenterology* **133**, 1614–1626. https://doi.org/10.1053/j.gastro.2007.08.005 (2007).

44. Lindenbach, B. D. *et al.* Complete replication of hepatitis C virus in cell culture. *Science* **309**, 623–626. https://doi.org/10.1126/science.1114016 (2005).
45. Gottwein, J. M. *et al.* Novel infectious cDNA clones of hepatitis C virus genotype 3a (strain S52) and 4a (strain ED43): genetic analyses and in vivo pathogenesis studies. *J. Virol.* **84**, 5277–5293. https://doi.org/10.1128/JVI.02667-09 (2010).
46. Scheel, T. K. H., Gottwein, J. M., Mikkelsen, L. S., Jensen, T. B. & Bukh, J. Recombinant HCV variants with NS5A from genotypes 1–7 have different sensitivities to an NS5A inhibitor but not interferon-α. *Gastroenterology* **140**, 1032–1042. https://doi.org/10.1053/j.gastro.2010.11.036 (2011).
47. Jensen, S. B. *et al.* Evolutionary pathways to persistence of highly fit and resistant hepatitis C virus protease inhibitor escape variants. *Hepatology* **70**, 771–787. https://doi.org/10.1002/hep.30647 (2019).
48. Fahnøe, U. & Bukh, J. Full-length open reading frame amplification of hepatitis C virus. *Methods Mol. Biol.* **85–91**, 2019. https://doi.org/10.1007/978-1-4939-8976-8_5 (1911).
49. Altschul, S. F. *et al.* Gapped BLAST and PSI-BLAST: a new generation of protein database search programs. *Nucl. Acids Res.* **25**, 3389–3402. https://doi.org/10.1093/nar/25.17.3389 (1997).
50. Altschul, S. F. *et al.* Protein database searches using compositionally adjusted substitution matrices. *FEBS J.* **272**, 5101–5109. https://doi.org/10.1111/j.1742-4658.2005.04945.x (2005).

Acknowledgements

We thank Lotte Mikkelsen, Anna-Louise Sørensen, and Pia Pedersen (Copenhagen University Hospital, Hvidovre) for laboratory assistance and Bjarne Ø. Lindhardt (Copenhagen University Hospital, Hvidovre) and Carsten Geisler (University of Copenhagen) for their support. Furthermore, we want to thank Udo Reichl and Anja Bastian (Max Plank Institute for Dynamics of Complex Technical Systems, Magdeburg) for additional analytics and support on the manuscript. Reagents were provided by C.M. Rice (The Rockefeller Center, USA). Parts of this work are part of dissertations under the supervision of the Justus Liebig University Giessen in cooperation with the University of Applied Sciences Mittelhessen (THM Giessen) (K.L.) and under the supervision of the University of Copenhagen (A.F.O.).

Author contributions

K.L. and A.F.O. were responsible for study design, data acquisition, analysis and manuscript drafting. A.F.P. did data acquisition. C.K.M. and T.B.J. performed data analysis. G.P.A. did data acquisition. U.F. and J.B. did data analysis; J.M.G. and M.W. supervised the study design, data acquisition, analysis and manuscript drafting. All authors reviewed the manuscript.

Funding

Open Access funding provided by Projekt DEAL. This work was supported by PhD stipends from the Candys foundation (A.F.O. and A.F.P.) and from the University of Copenhagen (A.F.O., A.F.P., C.M., T.J., G.P.), grants from the Novo Nordisk Foundation (J.B., J.M.G.), the Lundbeck Foundation (J.B.), the Danish Cancer Society (J.B., J.M.G.), the Independent Research Fund Denmark (J.B., J.M.G.), the Danish Innovation Foundation (J.B., J.M.G.), The Region H Foundation (J.B., J.M.G.), and The Toyota Foundation (A.F.O., J.M.G).

Competing interests

The authors declare no competing interests.

Additional information

Supplementary information is available for this paper at https://doi.org/10.1038/s41598-020-72328-5.

Correspondence and requests for materials should be addressed to J.M.G. or M.W.W.

Reprints and permissions information is available at www.nature.com/reprints.

Publisher's note Springer Nature remains neutral with regard to jurisdictional claims in published maps and institutional affiliations.

Chapter 5 – Accomplishments and pitfalls: An overview on the obtained results, remaining hurdles, and future perspectives

Summary of the presented findings

Within the scope of this work, the feasibility of the SXC in DSP processes for pharmaceutical applications was clearly demonstrated. Whereas the early work concerning the chromatography on the basis of PEG induced macromolecular crowding was mainly focusing on a general proof-of-principle, this work is aiming to bridge the gap between general applicability and actual benefit for the development of production processes. Basis of this project were the descriptions of high recovery rates and an efficient impurity removal during the application of the SXC. This was confirmed within the presented studies for the additionally evaluated viruses of different types. By using the baculovirus, HCV and the ORFV not only viruses with entirely differing physico-chemical properties, such as size, isoelectric point and surface composition, were used, but also representatives of different pharmaceutical application fields, like viral vectors for gene transfer, vaccine candidates for human or veterinary immunization or for oncolytic treatment. In all laboratory scale applications, the SXC performed well, delivering virus recoveries above 90%, virtually full protein depletion, and satisfying DNA depletions above 85%. Although some aspects of the process parameters had to be fine-tuned, e.g., the pH value during HCV purification or the PEG concentration in general depending on the product size, the overall basis of the process conditions was highly comparable and overlapping for the different products. This once more underlines the platform character of the SXC and answers the demand for fast in place and flexible platform processing techniques. The integration of the SXC into two production schemes, HCV and ORFV, displays its capability of being a backbone and major building block of these DSP procedures. That is depicted by the fact that the SXC is primarily responsive for impurity removal and additionally allows a simultaneous concentration of the product. This results in a DSP process comprising of only four technical unit operations and a nuclease treatment, which reaches acceptable impurity levels for pharmaceutical applications. Further reduction of process units is unlikely as the initial clarification train is required to remove the larger cell debris. Furthermore, a final polishing step is necessary to remove residual protein and DNA levels and to reduce process-related impurities, such as nuclease and PEG. However, this final polishing after the SXC is flexible and can be selected on product characteristics.

During process development various polishing steps after the SXC were evaluated for ORFV purification and showed one crucial advantage of the SXC itself, namely its highly customizable elution conditions. Any PEG-free buffer might theoretically be applied, omitting the need for an

intermediate buffer exchange step. Although the obtained results indicate a beneficial influence of elevated salt levels during the elution, depending on the polishing step a buffer with low salt concentrations, e.g. for SCMA or IEX, or with increased salt levels, e.g. for HIC, might be selected.

Another advantage of integrating the SXC into DSP production processes is its superior performance over commonly applied chromatographic methods regarding the combination of recovery and contaminant depletion. Although similarly high recovery rates may be achieved using for example AEX techniques, the impurity removal, especially in terms of DNA, is more problematic for the ion exchanger. This was shown within the scope of this study, as a co-elution of DNA and product during AEX is likely and can only be diminished by rigorous method optimization. This includes a multi-dimensional optimization including various types and amounts of salts or even adjustments in the pH and the conductivity. Next to possibly affecting the virus stability and activity, this approach also limits the selection of subsequent processing steps, probably resulting in an additionally required diafiltration and buffer exchange.

In this work, membranes were used mainly in single-use, hence a sterilization and regeneration procedure was dispensable. For industrial applications this is particularly beneficial as it reduces buffer consumption, process times and thereby overall costs. Further on, it is advantageous to use disposable membranes instead of monoliths due to higher cost of goods for the latter ones. In addition, for aseptic large-scale purifications, monolithic columns are no choice as these cannot be sterilized by radiation and autoclaving is difficult due to their weight. In contrast to that, there are already several membrane devices for other chromatographic techniques, such as IEX, that are commercially available sterilized on an industrial scale.

Current limitations for an industrial application of the SXC

Despite the positive outcome of the presented studies, meaning the successful implementation of the SXC into laboratory-scale DSP procedures and its superior performance over commonly applied unit operations, major limitations and yet open questions require consideration.

First, all experiments performed within the scope of this work were undertaken in a laboratory scale. This includes the use of a custom-made stationary SXC phase, as these are so far commercially not available. The applied membranes were manually punched and the resulting discs assembled into stainless steel housings. This represents a major hurdle for a good manufacturing practice (GMP) production process as the required material certificates can not be provided. For this, membrane manufacturers must be identified who can provide respective modules that are scalable and in a GMP grade.

To overcome that limitation, monoliths and membrane prototypes provided by Sartorius Stedim Biotech GmbH were evaluated subsequently to these studies. Both devices promised a standardized material supply and a linear scalability over a broad range. Accordingly, the herein described process for ORFV purification was afterwards transferred to a contract development and manufacturing organization (CDMO) production site, processing up to 200 L of STR harvests of a Covid-19 second generation vaccine candidate. However, under scale-up conditions the recovery rates were not reproducible. Without changing the overall process conditions, recoveries either drastically decreased to below 30% or were occasionally as high as 80%. Up to the date no conclusive explanation could be determined, what causes the lack of process robustness and further investigation will be required.

Additionally, during the process transfer problems arose, which were not considered at the time of the laboratory development. This includes the high viscosity of the PEG-containing buffer. For one thing the stock solution must be filtered prior to use. On laboratory scale the filtration of one liter of the highly viscous solution is conceivable. Preparing hundreds of liters of buffer, increasing filtration times and appropriately large filters must be considered. Apart from the filtration during buffer preparation, the viscosity of the buffer might also hinder a precise inline mixing during the actual chromatography. However, for larger volumes and scales inline mixing is preferred to avoid possible aggregation during long holding times of product-PEG-solutions. Further on, pressure limits must be examined and evaluated in detail during the SXC. As the method employs viscous polymer solutions and is based on molecular crowding, in general higher pressures are observed compared to common IEX procedures. Hence, laboratory flow rates are not linearly transferable. Depending on the scale and the applied pump system, limitations in the pumpability might occur as well as pressure constraints due to the tubing and the housing.

Another point of consideration is the remaining PEG concentrations in the product, which must be carefully observed, especially considering the dead volume of the column and the tubing in regard to the volume of the elution fraction. Although PEG itself has GRAS status, an influence on the product must be considered, if for example stored in a combined formulation buffer. Depending on the product application, potentially a PEG clearance must be verified.

Finally, a major drawback of implementing the SXC in industrial scale purification processes is the acceptability and tolerance of both regulatory authorities and manufacturers for novel approaches. Compared to standardized and established processes, the knowledge on the SXC mechanism is yet limited and actual process data is scarce. Thus, regarding risk assessments and for the reduction of unexpected events, the decision for one or the other

method is rather driven in favor of the well understood method, even if that means a significantly reduced productivity.

Future perspectives to overcome yet unanswered questions

Starting from the presented data, future work should be focusing on four major aspects: i.) enabling a robust method performance for increasing scales, which was here only shown on a laboratory scale ii) standardization of SXC processes and stationary phases over a range of scales in order to be compliant with the GMP guidelines while at the same time keeping up the method performance iii.) the fundamental characterization of the methods principle by means of mechanistic modeling or deep learning procedures to enlighten the adsorption and desorption kinetics and the multi-layer binding during SXC, which is likely, but currently not well characterized; iv.) the analysis of dynamic kinetics of the particles in solution, including their aggregation behavior in the presence of PEG and other salts and the impacts on viral activity and integrity, especially concerning rather long processing times with increasing scale.

Concluding remarks

In summary this work provides a key step for the SXC to be implemented into scalable pharmaceutical production schemes. As a capture step, linking the initial clarification and the final polishing, it enables concentration and impressive impurity clearance, while at the same time allowing high viral yields. According to this, the SXC has in our studies outperformed common membrane purification approaches and allowed a minimum of process unit operations within the process train. By knowing the size and the pI of the product molecule, the method optimization is straightforward. Only a few parameters, such as PEG concentration and buffer pH need to be considered and adjusted. However, although successfully working on laboratory scale, a process transfer and its scale-up is not trivial and will require further effort, optimization and adjustments in order to enable a robust and reproducible performance.